SESM 68-9

STRUCTURES AND MATERIALS RESEARCH
DEPARTMENT OF CIVIL ENGINEERING

STATIC AND DYNAMIC ANALYSIS OF SANDWICH SHELLS WITH VISCOELASTIC DAMPING

by

JOHN F. ABEL

Report to
National Aeronautics and Space Administration
NASA Research Grant No. NsG 274 S-3

AUGUST 1968

STRUCTURAL ENGINEERING LABORATORY
UNIVERSITY OF CALIFORNIA
BERKELEY CALIFORNIA

Structures and Materials Research
Department of Civil Engineering

STATIC AND DYNAMIC ANALYSIS OF SANDWICH SHELLS WITH VISCOELASTIC DAMPING

by

John F. Abel
Graduate Student

E. P. Popov
Faculty Investigator

Report to

National Aeronautics and Space Administration
NASA Research Grant No. NsG 274 S-3

Structural Engineering Laboratory
University of California
Berkeley, California

August 1968

ABSTRACT

The finite element technique is extended to the refined analysis of multilayer beams, plates and shells with no restriction placed upon the ratios of the layer thicknesses and properties. The method is applicable to structures wherein shearing deformations are significant, including sandwich-type structures.

Element stiffnesses developed are based on polynomial displacement models and are for the linear elastic analysis of beams, circular plates, and thin, axisymmetric shells of arbitrary meridian. Although stiffnesses derived are for three-layered construction with similar facings, the proposed theory is applicable to any flexural elements and to any arrangement of laminations, provided the total thickness is moderate. Here, doubly-curved elements have been used to represent rotational shells. Computer programs have been written both for static analysis and for free and forced steady-state vibration analysis. Inclusion of rotatory as well as translational inertia allows determination of natural thickness-shear frequencies and mode shapes in addition to flexural vibration characteristics.

Finally, the use of viscoelastic layers for the damping of flexural vibrations is discussed. To determine the effective damping due to such layers, the analysis method is extended by means of the correspondence principle for linear dynamic viscoelasticity.

Several examples are presented to illustrate the efficacy of the method. Listings of the computer programs for axisymmetric shells are given in the appendices.

ACKNOWLEDGMENTS

The author wishes to express his deep gratitude to Professor E. P. Popov for his interest and encouragement during the course of this research. His continuing concern for his students has been an inspiration. The writer would also like to express his gratitude to the other member of his dissertation committee, Professors J. L. Sackman and M. C. Williams, for reading the manuscript and making helpful suggestions. In addition, the author is also indebted to many faculty members and graduate students at the University of California for their advice and assistance. These individuals include Dr. C. A. Felippa, Dr. M. Khojasteh-Bakht and Messrs. S. Yaghmai, B. Pinkney and S. Pawsey.

During the early stages of this research, the author was sponsored by a National Science Foundation Graduate Fellowship. Thereafter, support was provided by the National Aeronautics and Space Administration under Research Grant NsG 274 S-3. Computer facilities and time were provided by the Computer Center of the University of California at Berkeley. All of this support is gratefully acknowledged.

The final report was typed by Mrs. Carmella Bryant and the appendices by Mrs. Arlene Martin. Donna Margaret Wilcox did the drawings.

Finally, the author wishes to express his appreciation to his wife, Lynne. Her patience and encouragement throughout the course of the writer's graduate studies has been invaluable. In addition, she typed most of the draft manuscripts for this dissertation.

TABLE OF CONTENTS

		PAGE
ABSTRACT		ii
ACKNOWLEDGMENTS		iii
TABLE OF CONTENTS		iv
NOMENCLATURE		vi
I.	INTRODUCTION	1
	I.1. General Objective	1
	I.2. Survey of Previous Work	3
	I.3. Outline and Assumptions	15
II.	GENERAL THEORY AND THE FINITE ELEMENT METHOD	18
	II.1. General Theory	18
	II.2. Stiffness Analysis of Elements for the Displacement Method	34
	II.3. The Direct Stiffness Method	41
III.	STATIC ANALYSIS OF ELASTIC SANDWICH STRUCTURES	45
	III.1. Sandwich Beams and Cylindrical Bending of Plates	45
	III.2. Axisymmetric Sandwich Plates	54
	III.3. A Doubly-Curved Axisymmetric Shell Element	59
	III.4. Axisymmetric Sandwich Shells	63
	III.5. Examples of Static Analysis	69
IV.	FREE VIBRATION OF ELASTIC SANDWICH STRUCTURES	98
	IV.1. Lumped Translatory and Rotatory Inertia	98
	IV.2. Formulation of the Eigenvalue Problem	102
	IV.3. Vibration Modes	106
	IV.4. Examples of Free Vibration Analysis	110

V. DAMPING BY THE INCLUSION OF VISCOELASTIC LAYERS 120

V.1. The Complex Modulus Representation 120

V.2. Correspondence Principle for Linear Dynamic Viscoelasticity 124

V.3. Viscoelastic Properties of Polymers 125

V.4. Measures of Effective Damping 133

V.5. Complex Algebraic Eigenvalue Problems 135

V.6. Damped Response to Steady-State Harmonic Loading 138

V.7. Examples of Damped Vibrations 144

VI. SUMMARY AND CONCLUSIONS 160

REFERENCES 163

APPENDICES 174

A. Matrices for Sandwich Beams 174

B. Matrices for Axisymmetric Sandwich Plates 184

C. Matrices for Axisymmetric Sandwich Shells 194

D. Computer Program, Static Analysis of Elastic Axisymmetric Shells 208

E. Computer Program, Free Vibrations of Elastic Axisymmetric Shells 227

F. Computer Program, Free Vibrations of Viscoelastic Axisymmetric Shells 248

NOMENCLATURE

$\{\ \}$ = column vector

$\langle\ \rangle$ = row vector

$[\ ]$ = rectangular matrix

$[\ ]$ = diagonal matrix

$*$ = superscript indicating a complex quantity

1,2 = subscripts indicating the principal directions of the shell reference surface; subscripts indicating the real and imaginary parts of a complex quantity, respectively

$[A]$ = transformation matrix relating local nodal displacements to local generalized displacements

a = area of reference surface over which stresses are specified; radius of cylinder or sphere

$[B]$ = matrix relating element strain components to element generalized co-ordinates

b = superscript indicating the bottom (or inside) facing of sandwich construction

$[C]$ = matrix relating total element stresses to total element strains

c = subscript indicating core layer of sandwich construction

$[D]$ = matrix product $[Z]^T[C][Z]$; diagonal matrix of pivots resulting from symmetric Gaussian elimination

D = energy dissipated in a single cycle of vibration

d = thickness distance between middle surfaces of facing layers for symmetric sandwich construction

ds = element of arc length

E = Young's modulus

$E^*(\omega)$ = complex modulus

$E(t)$ = relaxation modulus

$\{e_i\}$ = vector which has all elements zero except the i^{th} which is unity

$[F]$ = flexibility matrix of overall assemblage of elements

$\{f_i\}$ = i^{th} column of the flexibility matrix $[F]$

f = subscript indicating the face layers of sandwich construction

$[G]$ = matrix of layer bending, extensional and shear stiffness (Eq. II.27)

G = shear modulus

h = total thickness of shell

h_k = thickness of the k^{th} layer

i = subscript indicating the i^{th} node of an element

$J^*(\omega)$ = complex compliance

$J(t)$ = creep compliance function

j = subscript indicating the j^{th} node of an element

$[K]$ = stiffness matrix for overall assemblage of elements

$[k]$ = element stiffness matrix

k = subscript indicating the k^{th} layer

$[L]$ = lower unit triangular matrix of multipliers resulting from symmetric Gaussian elimination

L = total number of layers; span length of beam or cylinder

ℓ = length of beam or plate element; chord length of shell element

$[M]$ = mass matrix for overall assemblage of elements

M = moment stress resultant

N = extensional stress resultant

$\{P\}$ = vector of nodal force amplitudes for steady-state forced vibrations

$\{p\}$ = vector of loads

p_z = transverse load intensity for a beam or plate

$\{Q\}$ = vector of element nodal forces in local co-ordinates

Q = shear stress resultant

$\{q\}$ = vector of element nodal displacements in local co-ordinates

$\{R\}$ = vector of element nodal forces in global co-ordinates

R = principal radius of curvature of shell reference surface

$\{r\}$ = vector of element nodal displacements in global co-ordinates

r = radial co-ordinate for a circular plate or rotational shell

$\{S\}$ = vector of layer stress resultants

s = meridional co-ordinate in curvilinear co-ordinates

$[T]$ = transformation matrix relating local co-ordinates to global co-ordinates

$[\underline{T}]$ = matrix product $[A^{-1}][T]$

T = superscript indicating the transpose of a matrix

T_g = glass transition temperature of a polymer

T_m = melt temperature of a polymer

t = time; superscript indicating the top (or outside) facing of sandwich construction

U = strain energy

$\{u\}$ = vector of element displacements in local co-ordinates

u = tangential displacements of the shell

u_1, u_2 = local translations of substitute shell element

u_r, u_z = translations of a rotational shell in cylindrical co-ordinates

$\{V\}$ = vector of nodal forces for the overall assemblage of elements

V = potential energy of loads

$\{v\}$ = vector of nodal displacement for the overall assemblage of elements

v = volume of an element

W = total energy associated with the vibrating structure

$\{w\}$ = vector of displacement amplitudes for vibrations

w = normal displacements of the shell

$[X]$ = symmetric matrix for the eigenvalue problem in standard form

$\{x\}$ = eigenvector of the matrix $[X]$

x = general local co-ordinate (Section II.2); axial co-ordinate of a beam (Section III.1)

$[Z]$ = matrix relating total element strains to element strain components

z = thickness co-ordinate for beam or plate; cylindrical co-ordinate for rotational shell

$\{\alpha\}$ = vector of element generalized co-ordinates

α = metrics of the shell reference surface

β = free index; angle indicated in Figure III.5

γ = shear strain

δ = index; logarithmic decrement of a damped structure

$\{\epsilon\}$ = vector of total layer strains for an element

$\{\varepsilon\}$ = vector of layer strain components for an element

ε = extensional strain

ζ = co-ordinate normal to the shell surface

η = local rectilinear co-ordinate (Figure III.5); loss factor of a damped structure

θ = circumferential co-ordinate; angle by which strain lags behind stress (Figure V.1)

κ = change in curvature (Eqs. (II.10)); shear stress correction factor (Section II.1.3)

λ = root of eigenvalue problem in standard form

ν = Poisson ratio

ξ = Gaussian orthogonal curvilinear co-ordinates for the shell surface (Figure II.1); local normalized co-ordinate for a particular finite element (Chap. III)

π = total potential energy of an element

ρ = density

$\{\sigma\}$ = vector of total layer stresses for an element

σ = extensional stress

τ = shear stress

$[\Phi]$ = matrix relating element displacements to element generalized displacements

ϕ = angle indicated in Figures II.5 and II.6

χ = rotation of the tangent to the reference surface (total rotation)

χ_b = rotation of the normal to the reference surface (bending rotation)

χ_s = rotation due to shearing deformation only

ψ = angle indicated in Figure III.5

Ω = frequency of steady-state forced vibration

ω = frequency of free vibration

CHAPTER I: INTRODUCTION

I.1. General Objective

Multilayer construction has become an increasingly important form in structural engineering as one means of achieving a beneficial combination of the properties of two or more materials. Perhaps the best known examples of this type are the widespread "sandwich" structures used in the aerospace industry. These combine thin, high-strength facing layers with a thicker, light-weight core. Recently, layered structures have also incorporated laminations of materials selected for their energy dissipation characteristics or their heat conduction properties. As new materials are being developed and as the technology of composite construction advances, there is a growing variety of versatile, multiply layered configurations available.

The theory of stress analysis of multilayer structures is well established. In general, two classifications of such structures can be identified: (1) "laminates" in which layers of materials with similar properties are bonded together and for which the Kirchhoff-Love hypothesis is applied and (2) "sandwiches" in which some layers may be significantly weaker than others and for which transverse shear deformation is taken into account. Theory for the laminates [1-6]* has been successfully applied to the analysis of general plates and shells using, for example, the approximate methods of finite differences [7] and finite elements [8]. However, despite the availability of sandwich theories of various

*Numbers in brackets refer to references at the end of the paper.

degrees of refinement in the literature, there have been relatively few solutions published that include the effects of transverse shear. Moreover, these solutions have been restricted to the simpler geometries such as rectangular and circular plates and cylindrical and spherical shells.

The purpose of the present work is to extend the finite element method to the analysis of sandwich plates and shells. Although specific solutions are to be presented here only for axisymmetric cases, the same general approach, using existing standard finite element techniques, will permit the analysis of arbitrary configurations and boundary conditions. In addition to the study of static and dynamic elastic problems, this paper shall also consider the structural damping due to the inclusion of viscoelastic layers. The damping characteristics can be obtained as a natural adjunct of the ordinary procedures of structural analysis.

I.2. Survey of Previous Work

This dissertation is based upon material from three areas of structural engineering, namely, sandwich theory, the finite element method, and structural damping. These topics are now briefly reviewed.

I.2.1. Sandwich Theory

Extensive reviews and bibliographies of the theory of sandwich structures are presented in References [9-12], and the reader is referred to these for a more complete survey than the one given here.

The earliest application of sandwich construction was in the British aircraft industry. Consequently, some of the first published materials on the topic are the works of Williams, Legget and Hopkins [13, 14]. These authors accounted for shear by assuming that material lines originally straight and normal to the middle surface remain straight, but do not remain normal. Among the increasing volume of literature published in the postwar period are papers by E. Reissner [15, 16], Hoff and Mautner [17], Hoff [18], and Eringen [19]. Reissner approximated the sandwich as thin facings acting as membranes and a core with significant stresses only in the transverse direction. The transverse behavior includes both shear and normal deformation. With these simplifications, the equations of sandwich plates and shells are analogous to those of homogeneous structures for which the transverse effects are taken into account [15, 20]. Reissner also studied the large deflections of sandwich plates using the same assumptions [21]. Hoff's work on plates included the flexural rigidity of the facings in addition to the effects considered by Reissner. Finally Eringen added the influence of the flexural rigidity of the core, neglecting only the shearing of the plate facings.

It has become customary to designate sandwiches described by theories which neglect the flexural and stretching effects of the core (e.g., Reissner [15] and Hoff [18]) as having a "weak" or "soft" core and those which include these effects (Eringen [19]) a "stiff" or "strong" core. An example of a shell theory for weak orthotropic cores is that developed by Schmidt [22], whereas Grigolyuk and Kiryukhin [23] have derived the shell equations for orthotropic facings and a stiff orthotropic core. Non-linear shell theories for large deflections of sandwiches with dissimilar facings for the case of a weak core have been published by Wempner and Baylor [24], Wempner [25] and Fulton [26]. Schmidt and Wempner included the effect of the transverse normal deformation of the core, but Grigolyuk and Fulton assumed that the transverse displacement of all layers is the same.

Reissner [16, 21] showed that the assumption of transverse incompressibility is valid for beams and plates, but that this pinching effect could become important for curved structures under some circumstances, such as uniform bending stress states of soft-core shells. However, Raville's work [27-29] indicated that for some purposes pinching may be neglected, and recently developed sandwich theories have tended to assume an infinite transverse core modulus [12]. Other studies on the effects of various approximations in sandwich theories have been conducted by Koch [30] and Cook [31]. These two papers provide quantitative evaluations of several common assumptions, including those of soft cores and membrane facings.

In 1959, Yu [32] presented a new sandwich theory which includes the bending and stretching effects and the transverse shear flexibility of all layers. This theory places no restriction on the ratios of layer thicknesses and material properties and has been extensively applied to

vibration problems of sandwich structures including both shear and rotatory inertia [33 - 41]. In addition, a similar approach has been used for two-layered plates and shells [42]. Throughout these works the transverse displacements of all layers are assumed to be the same. Free vibrations of various types of sandwich structures have also been studied by Kimel et al. [43], Raville et al. [44], Bolotin [45] and Chu [46]. Bieniek and Fruedenthal [47] have investigated the forced vibrations of cylindrical sandwich panels. Finally, non-linear vibrations have received the attention of Yu [48, 49] and Chu [50].

There is not a large body of published solutions for static problems of sandwich shells, although beam and plate problems have been more widely considered. Reissner [16] has included some solutions of special cases and has emphasized the similarity between the equations of sandwich theory and those for homogeneous shells with or without transverse effects. Thus closed form and approximate solutions of the types available for ordinary shells are also applicable to sandwiches under the assumptions of Reissner's theory. For instance, Naghdi [51] discussed the method of asymptotic integration as applied to homogeneous shells of revolution including shear. Some examples of more specific problems are those treated by Rossettos [52], who considered shallow spherical sandwich shells, and Kao [53], who solved multilayer circular cylindrical sandwiches.

I.2.2 The Finite Element Method

The finite element method has developed concurrently with the increasing use of high-speed electronic digital computation and its concommitant emphasis on discretized techniques in structural analysis. In brief, this method consists of idealizing the structure as an

assemblage of geometrically simple domains (elements). Simple, but relatively complete, displacement or equilibrium fields are assumed over each domain; and a variational principle of mechanics is employed to obtain a set of influence coefficients for the element. A set of linear algebraic equations for the overall assemblage is obtained by combining the coefficients for the individual elements so that continuity of the assumed quantities is preserved at the interconnecting nodes. These equations are modified for the boundary conditions and solved to obtain the response of the structure. If displacement models are assumed, the approach is called the "displacement method," and the resulting stiffness coefficients are an upper bound. Conversely, the "equilibrium method" (assumed equilibrium or stress models) results in a lower bound [64]. A combination of assumed equilibrium and displacement models over each domain is called the "mixed method." The vast majority of work in the finite element method as applied to structural mechanics has employed the displacement method, and the present work also follows this approach. Also, for ease in mathematical manipulations, models are generally of polynomial form and that, too, is the case here.

In general, the finite element method has proved to be a successful tool for the systematic analysis of complex structures and the approximate solution of difficult problems in continuum mechanics.

A large number of papers has been published during the last decade on the finite element method, particularly on its applications to structural mechanics. Comprehensive reviews and bibliographies, as well as a survey of the basic methods, can be found in References [54 - 60]. The following review is confined to formative works and to literature on the analysis of plates and shells by the displacement method.

A primary stimulus to the development of the finite element analysis of structures was the formalization of the theory of matrix transformation of structures by Argyris [61]. An early statement of the displacement approach was given by Turner et al. [62]; and, in a later paper, Turner [63] further systematized the analysis technique by formulating an efficient assembly process for the direct stiffness method. Finally, the mathematical foundations of the finite element approach were described by Felippa and Clough [60]. This Reference includes a statement of necessary requirements on the displacement model functions in order to obtain convergence to proper stiffness coefficients. These requirements, which are also given in References [65, 57 - 59], are that the displacement model must provide (1) compatibility between elements and continuity within the element and (2) completeness in the sense that rigid body modes and constant strain states must be included. It should be noted that in some cases useable results may be obtained with element displacement models which do not satisfy these requirements [66, 76]. However, it is known that displacements will not converge to correct values as the mesh size is decreased, if the models fail to fulfill the requirements.

A comprehensive study of early plate bending elements was conducted by Clough and Tocher [66]. They concluded that the best elements then available were their own compatible triangular element [66] and the incompatible rectangular elements derived by Adini and Clough [67] and Melosh [68, 69]. A compatible rectangle [70] was found less favorable mainly because it was lacking in completeness. Since then, improved results have been obtained by Felippa [57, 59] using compatible and complete triangles and arbitrary quadrilaterals composed of four such triangles. He formalized a procedure for developing triangular elements of various degrees of refinement, i.e., various higher order elements that

not only satisfy the minimum conditions, but also provide extra degrees of freedom which permit a better solution with a coarser mesh. Felippa [59] also developed a bending element for plates of moderate thickness which accounts for transverse shear in a fashion analogous to Timoshenko beam theory [71, 72] and Mindlin's plate theory [73].

Most finite element analyses of arbitrary shell structures have employed flat triangular elements. In representing a curved surface by an assemblage of flat surfaces, the membrane and bending behavior are uncoupled within the individual elements, but are coupled by the discontinuities of slope at the interelement nodes. Clough and Johnson [74] used a system employing five degrees of freedom at each corner node and achieved satisfactory results except in cases having complex membrane states. Carr [75] developed a refined element with nine degrees of freedom per node, obtaining better results at the expense of a more complicated formulation. Finally, Johnson [76] combined four flat triangles into a non-planar quadrilateral with five degrees of freedom at each corner. This last technique provides superior solutions even for the troublesome cases.

A greater amount of attention has been devoted to the less difficult class of shell problems, the axisymmetric case. The conical frustrum element has been widely used, although recently three axisymmetric types of doubly curved elements have been introduced. Two early approaches by Meyer and Harmon [77] and Popov et al. [78] utilize exact shell theory bending displacements due to edge loading rather than simple displacement models for each conical segment. Consequently, for membrane type problems some rather large inaccuracies are introduced. However, some useful results are obtainable with this approach, particularly for edge effect influence coefficients. Grafton and Strome [79] used conical elements

in a true finite element technique and Percy et al.[80] provided an important correction to Grafton and Strome's strain energy integration. In addition, Percy et al. extended the application to asymmetric loading cases by use of Fourier expansions in the circumferential directional. Although the results provided by References [79 and 80] are an improvement over previous work, for predominately membrane solutions there are still inaccurate moments introduced through the approximation of a doubly curved structure by singly curved elements, particularly because of the discontinuity of slope at the nodes of the substitute structure. Jones and Strome [81] studied this problem and developed a doubly curved element [82] which matched both the location and slopes of the original shell at the nodal circles, thus avoiding unwanted discontinuities of slope at these locations. Despite a marked improvement of solutions achieved through the use of this new element, the geometric formulation causes some difficulty where the latitude angle of the shell is small. Stricklin et al. [83] also formulated a curved element which duplicates both slope and position at the nodes, but which removes the geometrical difficulties.

Representation of the meridian of the original shell by a series of straight segments or simple curved segments, an approximation first evaluated by Jones and Strome [81], was further investigated by Khojasteh-Bakht [84]. He compared solutions obtained from two different doubly curved elements satisfying completeness and compatibility, one which matched position and slopes at the nodes and another which additionally duplicated curvatures at these circles. Although both solutions converged well, remarkably accurate results were obtained with very few elements using the latter approach. For example, with only three elements, near-perfect displacements and stress resultants were

attained for a hemisphere under pure membrane loading. In addition, Khojasteh-Bakht contrasted solutions based on displacement models formulated in both local curvilinear and local rectilinear coordinate systems. The first was unable to accomodate certain constant strain states and thus the second proved to be clearly superior. It should be noted that for arbitrary shells the use of a local rectilinear system for the displacement models makes it difficult to satisfy compatibility at the nodes, but for rotational shells this is not a problem.

The central problem in applying the finite element method to dynamic problems is the representation of the inertial properties of the structure. There are two principal approaches, one being the simple lumping of masses at the nodes. Archer [85] has proposed the second, the "consistent mass" matrix which is derived from expressing the kinetic energy in terms of the assumed displacement models. The consistent approach preserves the mass distribution and the coupling between the various inertial effects, whereas the lumped approach leads to an uncoupled (diagonal) mass matrix. Felippa [59] has compared the two techniques and concluded that the lumped mass system is more practical since its diagonal form reduces the computational effort and permits reduction of the degree of the eigenvalue problem. However, one advantage to the consistent mass is that it gives a true upper bound on the frequencies.

I.2.3 Structural Damping

The prevention of near-resonant fatigue has long been a concern of structural engineers. In addition, vibration control is important in reducing noise transmission or re-rediation, in attenuating oscillations

associated with external turbulence of aircraft, and in preventing malfunctions of components and instruments [91]. With the increasing use of lightweight structures subject to intense excitation, particularly in aerospace applications, damping has been recognized as an important property in the overall performance of the structure. Because many structures are subject to random vibrations over a broad spectrum, it is no longer sufficient or even possible merely to identify the natural frequencies and attampt to separate them from the exciting frequencies. For example, jet and rocket engines may excite a large proportion of the natural frequencies of the craft. Consequently, it is advantageous to employ materials that have a capacity to dissipate energy and thus to reduce resonant amplitudes. This type of energy dissipation is known as "structural" or "internal" damping.

Since there are few metals (one example, certain magnesium alloys [87]) or other structural materials that possess both sufficient strength and damping capacity, the emphasis in vibration control methods has been on adding dissipative layer. mping treatments to the basic structures. These added materials are usually lightweight polymer plastics which have a negligable effect on the strength of the structure. However, when a damping material is used as the core filler of sandwich-type structures, the dissipative layer is directly involved in the load resisting mechanism as well as in vibration attenuation. Some practical examples of damping due to dissipative layers are damping tapes applied to the inside of airplane fusilages, coatings on the inside of automobile hoods [89], and viscoelastic layers incorporated into ship structures [93]. The same principles have even been applied to vibration control in buildings and large structures [90]. As this dissertation is concerned with layered construction, the following

survey of work in the field of structural damping concentrates on approaches in which dissipative layers are employed.

Lazan [87, 94] and Blanchflower [91] have considered the damping properties of materials. Two categories of mechanical damping are distinguished, that which is amplitude dependent and that which is not. Amplitude-dependent energy dissipation becomes appreciable only in conjunction with large strains and deflections. Hence for small deflection theories, such as will be used herein, the amplitude-independent energy dissipation is of the greatest significance. This type of damping is characteristic of materials which have rate-dependent stress-strain laws and elliptical hysteresis loops. Therefore, the complex modulus representation of linear viscoelasticity is usually a good approximation to the dissipative behavior [94]. Various specific polymers that can be so characterized and that have proved useful for vibration control were described by Ungar and Hatch [95] and by Oberst et al. [96]. In addition, new synthetics for damping applications are steadily being developed [e.g., 97, 98]. The viscoelastic and dissipative properties of such polymers will be discussed in Chapter V.

Two major structural damping mechanisms of multilayer composite structures were discussed by Ross et al. [88] and by Kerwin [92]. The first is the "free layer" mechanism in which the viscoelastic material is a surface coating. Thus, during flexural behavior, this damping layer acts primarily in extension. The second mechanism is the "constrained layer" where the dissipative material occurs between two stiffer laminations. This configuration causes the softer layer to deform mostly by shearing. Ross et al. [88] pointed out that, on an equal weight basis, damping treatments that deform primarily in shear

are likely to be more effective than those deforming in extension.

The earliest investigations into structural damping due to viscoelastic layers were carried out by Oberst [99, 100] and by Liénard [101]. These authors developed expressions for the effective damping of plates due to the addition of a free layer of viscoelastic damping material. Schwarzl [102] considered the coupled and uncoupled bending and extensional vibrations of a two-layered viscoelastic beam. Finally, Hertelendy [89] has used exact elasticity solutions to study the effect of viscoelastic membrane coatings on plates. In addition, he treated general vibration problems of homogeneous bodies made of dissipative material.

Much greater attention has been given to the constrained layer mechanisms, particularly in view of the development of "damping tapes" [103]. These tapes are two-layer treatments in which one layer is both adhesive and dissipative and the other is a thin foil which serves as a constraining layer. Ross et al. [88], Ungar and Ross [104] and Kerwin [105] have developed the theory of these tapes and have obtained reasonable verification with experiments. Constrained layer damping in sandwich plates were studied by Plass [106] using a standard solid model for the viscoelastic behavior of the core. The complex modulus representation has been applied to sandwich beams and plates by Ungar [107] and Mead [108]. Among other authors who have also considered the effective damping of flat sandwich structures are DiTaranto and Blasingame [109 - 112] and Bert et al. [113]. Design considerations were discussed by Ruzicka et al. [114].

Yu has applied his theory for sandwich behavior to the study of damped vibrations by using the complex modulus approach [115]. An evaluation of the approximations of Yu's theory in this application is

provided by Hertelendy and Goldsmith [118], who compare the approach with an exact extended Rayleigh-Lamb solution. In addition, Yu has considered the damping of sandwich shells [116] and, together with Ren [117], the damping of two-layer plates and shells. Bieniek and Freudenthal [47] also included structural damping in their study of the forced vibrations of sandwich shells.

Finally, it is interesting to note that vibration experiments with layered specimens are an important means of determining the dynamic viscoelastic properties of materials. Nicholas and Heller [119] employed cantilever sandwich beams with cores made of elastomers in order to determine the complex shear modulus of these polymers. Nashif [120] has advocated the use of specimens with symmetric viscoelastic coatings to ascertain the damping properties of the applied material.

I.3. Outline and Assumptions

As stated previously, the objective of this dissertation is to extend the finite element method of analysis to multilayer beams, plates and shells having layers flexible in transverse shear. A generalized theory analogous to Yu's sandwich theory [32] is adopted for this purpose. In Chapter II it is pointed out how this formulation can be applied to one- and two-dimensional finite element discretizations. However, for the sake of simplicity, specific derivations are carried out only for the case of three-layered construction symmetric about the middle surface and, only for configurations that may be represented by a one-dimensional finite element mesh. Thus, in Chapter III, the stiffness matrices and consistent load vectors for beams, axisymmetric circular plates and rotational shells are derived and applied to the static analysis of elastic structures. For the axisymmetric shells, the doubly curved element due to Khojasteh-Bakht [84] is employed. Throughout this work, assumed polynomial displacement fields and the direct stiffness method are used.

The free vibration analysis of elastic sandwich structures is the subject of Chapter IV. Masses are lumped along a normal to the middle surface in order to represent both the rotatory and translational inertia in uncoupled form. In this manner it is possible to obtain the thickness-shear as well as the flexural natural frequencies. In the former mode, shear deformations predominate over the flexural waves. This type of behavior is important for some types of soft-core sandwiches. The dynamic analysis has not yet been extended to initial value problems because it is felt that the free vibration investigation is a satisfactory test of this approach to discretization. Given the ability to obtain reasonable natural frequencies and mode shapes, it is possible

to apply mode superposition or numerical integration techniques with some confidence.

In Chapter V, damping by the inclusion of viscoelastic layers is studied using the complex modulus representation of linear viscoelasticity. Since polymers are the most widely-used damping materials in composite structures, a discussion of the viscoelastic properties of these materials is included. Special attention is devoted to the temperature and frequency dependence of the properties and an attempt is made to account for frequency dependence in calculating the effective damping of multilayer structures. It should be noted that procedures used in Chapter V are not restricted to layered structures; rather, they can be applied to any finite element representation of a linear viscoelastic continuum subject to steady state oscillations.

The following assumptions apply throughout this paper. Other assumptions of lesser importance will be introduced in the applicable sections.

1. Displacements and strains are sufficiently small so that the linear theories of elasticity and dynamic viscoelasticity apply.

2. Perfect bonding occurs between adjacent layers of the structure.

3. The transverse displacement of all layers is the same at a given location of the middle surface of the structure. In other words, there is no pinching deformation.*

4. Shells are thin in the sense that products of thickness with curvature are much smaller than unity ($\zeta/R \ll 1$).

5. Material lines in each layer originally straight and normal to

---

*See the discussion of this assumption in Section II.1.1.

the middle surface remain straight after deformation, but no longer remain normal. The difference in shear strain in the several layers manifests itself in warping of the cross-section at the interfaces.

6. The materials of each layer are linearly elastic and isotropic. However, the procedure can be easily modified for anisotropic behavior by substituting the appropriate matrix of material properties.

7. All layers are "stiff" in that tangential effects are taken into account. However, this assumption can be relaxed for a particular layer by assigning a zero Young's modulus.

8. All layers are flexible in shear (see 5 above) but this assumption can be relaxed for a particular layer by assigning an infinite shear modulus.

CHAPTER II: GENERAL THEORY AND THE FINITE ELEMENT METHOD

II.1. General Theory

Consider an arbitrary multilayered shell with individual laminations of constant thickness. Let a reference surface within the shell be parallel to the layer interfaces and let ξ_1 and ξ_2 be Gaussian orthogonal curvilear co-ordinates for the surface. Moreover, let the co-ordinate lines coincide with the lines of principal curvature of the surface and let ζ be a co-ordinate normal to the surface (See Figure II.1). With these assumptions a line element in the space surrounding the reference surface can be expressed in terms of the differentials of the orthogonal curvilinear co-ordinates as follows:

$$ds^2 = \alpha_1^2\left(1 - \frac{\zeta}{R_1}\right)^2 d\xi_1^2 + \alpha_2^2\left(1 - \frac{\zeta}{R_2}\right)^2 d\xi_2^2 + d\zeta^2 \qquad \text{(II.1)}$$

where α_1 and α_2 are the surface metrics and R_1 and R_2 are the principal radii of curvature. Displacements of the reference surface corresponding to the co-ordinates ξ_1, ξ_2 and ζ are defined by

$$\begin{aligned} u_1^o &= u_1^o(\xi_1,\xi_2) \\ u_2^o &= u_2^o(\xi_1,\xi_2) \\ w^o &= w^o(\xi_1,\xi_2) \end{aligned} \qquad \text{(II.2)}$$

respectively. Hereafter, Love's first approximation [121] for thin shells will be adopted. That is, the thickness of the shell is considered small as compared to the radii of curvature and thus

$$\zeta/R_\beta \ll 1 \ , \ \beta = 1,2 \ . \qquad \text{(II.3)}$$

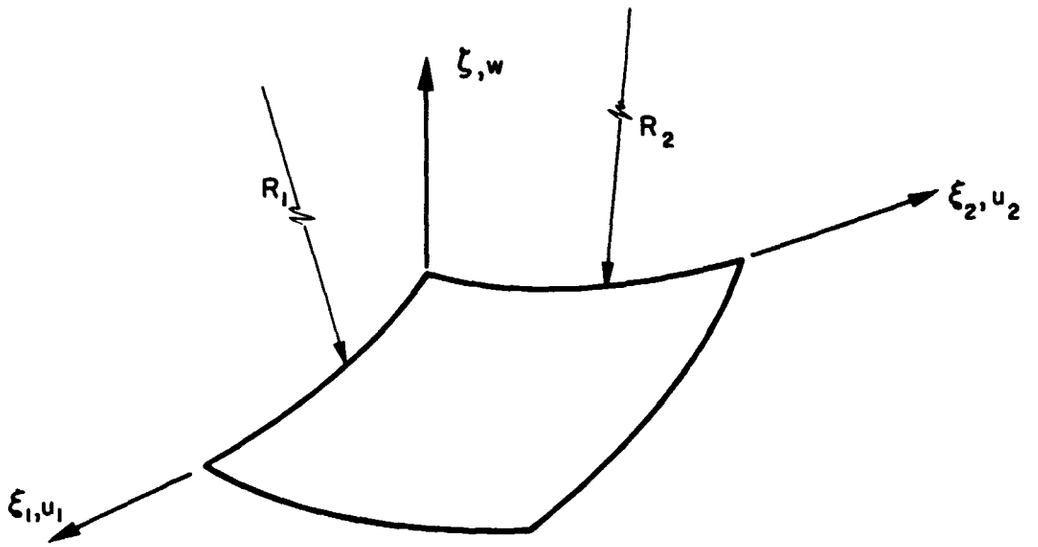

FIGURE II.1 ARBITRARY SHELL REFERENCE SURFACE

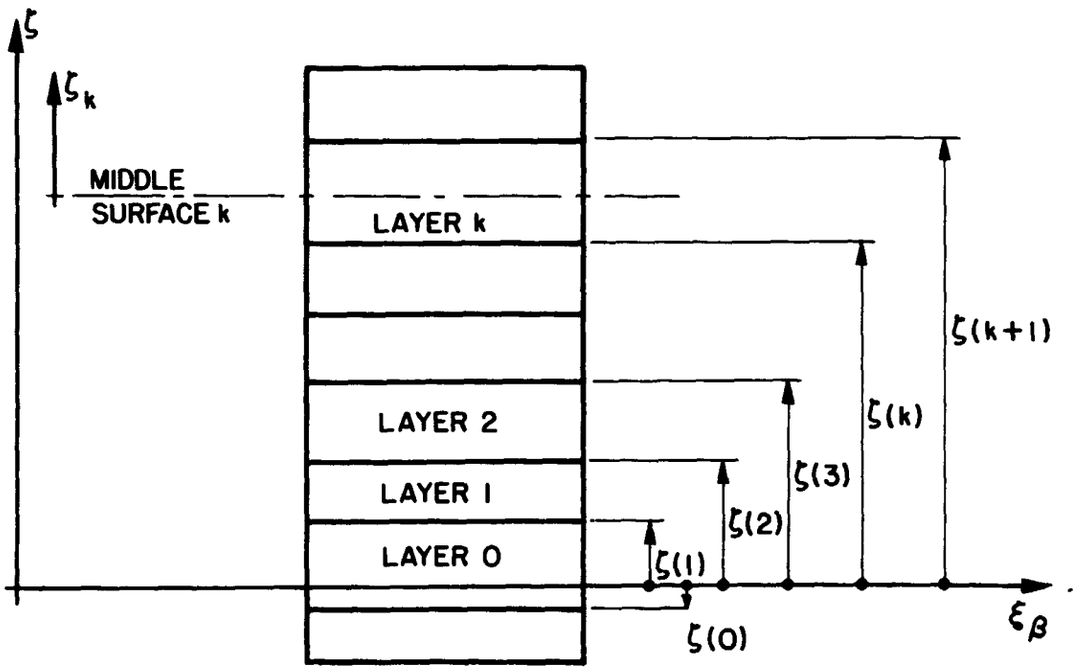

FIGURE II.2 THICKNESS GEOMETRY OF MULTILAYER SHELL

In effect, this means that the variation of curvature through the thickness of the shell is neglected. Finally, the rotations of the tangents to the reference surface are:

$$\chi_\beta = \chi_\beta(\xi_1,\xi_2) = \frac{1}{\alpha_\beta}\frac{\partial w^o}{\partial \xi_\beta} + \frac{u_\beta^o}{R_\beta}\,, \qquad \beta = 1,2\,. \qquad \text{(II.4)}$$

In the following, the subscript β may take the values 1 or 2, and the subscript δ will then take the opposite value. The summation convention does not apply.

II.1.1. Kinematic Assumptions

To represent the behavior of the shell layers, a generalized theory similar to Yu's sandwich theory [32] is adopted. No restriction is placed on the relative layer thicknesses or properties, provided only that the total thickness is sufficiently small so that Equations (II.3) apply. In the following, consider the k^{th} layer as identified by the subscript k. A normal thickness co-ordinate colinear with ζ, but with its origin at the middle surface of the k^{th} layer is designated ζ_k. In other words, the reference surface is given by $\zeta = 0$ and the middle surface of layer k is given by $\zeta_k = 0$. Displacement quantities at the middle surface of the k^{th} layer are referenced by the subscript k and the superscript o. In addition, the value of ζ at the face of layer k closer to the reference surface is indicated by $\zeta(k)$ (See Figure II.2).

First, it is assumed that the transverse displacements of all layers are the same, i.e., that the transverse Young's moduli of the layers are effectively infinite.

$$w_k = w_k^o = w^o \qquad \text{(II.5)}$$

Reissner [16] has shown that this assumption can cause appreciable error for certain cases such as the uniform bending-stress states of shells with very soft layers. However, there are several classes of problems for which the hypothesis of Equation(II.5) is admissable. These include (1) beam and plate problems [16], (2) free vibration problems, provided thickness pinching modes are not important, and (3) edge, concentrated, and partial loading problems where pinching effects remain localized [16]. In addition, since all layers are assumed "stiff" (Section I.3), it is not unreasonable to accept Equation (II.5) if one is aware of the potential inaccuracies in applying the theory to composite structures with very soft layers [16, 27-29, 12].

Next, it is assumed that material lines originally straight and normal to the middle surface of each layer remain straight but do not necessarily remain normal to the deformed surface. This implies that the transverse shearing deformation of each layer is independent of the normal co-ordinate. Hence, the shear rotation of the k^{th} layer is represented by some average value of the shear strain which is a function only of the surface co-ordinates ξ_1 and ξ_2 :

$$\gamma_{\beta k} = \gamma_{\beta k}(\xi_1, \xi_2) \qquad \text{(II.6)}$$

Another implication is that the tangential displacements of the k^{th} layer may be represented by the displacements of the middle surface of the layer and by the rotation of the normals to the middle surface as follows:

$$u_{\beta k} = u_{\beta k}^o - \zeta_k(\chi_\beta - \gamma_{\beta k}) \qquad \text{(II.7)}$$

Note that the difference between this formulation and the Kirchhoff-Love hypothesis is the fact that the rotation of the normal is no longer equal to the rotation of the tangent to the middle surface. Thus the present theory is analogous to the theories for homogeneous structures which include the effects of transverse shear [71-73, 59, 21].

Finally, since perfect bonding between layers is assumed, the tangential displacements must be continuous across the interfaces of the composite shell. This condition leads to the following expressions for the tangential displacements of the middle surface of the k^{th} layer, where $k \geq 0$. If there be $k - 1$ layers between the k^{th} layer and the 0-th (zero-th) layer which contains the reference surface.

$$u^{o}_{\beta k} = u^{o}_{\beta} - \frac{\zeta(k+1) + \zeta(k)}{2} \chi_{\beta} + \zeta(1)\, \gamma_{\beta o} + \sum_{m=1}^{k-1} [\zeta(m+1) - \zeta(m)]\, \gamma_{\beta m} + \\ + \frac{\zeta(k+1) - \zeta(k)}{2} \gamma_{\beta k} = u^{o}_{\beta k}(\xi_1, \xi_2) \ . \qquad \text{(II.8)}$$

For $k = 0$ or 1 , the summations drop out and the Equations (II.8) still apply, where $\zeta(1)$ and $\zeta(0)$ are the interfaces of the zero-th layer.

II.1.2. Strain-Displacement Equations

The strain-displacement equation from classical linear shell theory, (e.g., Reference [122]) are applied. For the k^{th} layer, the equations are:

$$\varepsilon_{\beta k} = \frac{1}{\alpha_\beta}\frac{\partial u_{\beta k}}{\partial \xi_\beta} - \frac{w_k}{R_\beta} + \frac{u_{\delta\beta}}{\alpha_\beta\alpha_\delta}\frac{\partial \alpha_\beta}{\partial \xi_\delta}$$

$$\gamma_{12k} = \frac{\alpha_2}{\alpha_1}\frac{\partial}{\partial \xi_1}\left(\frac{u_{2k}}{\alpha_2}\right) + \frac{\alpha_1}{\alpha_2}\frac{\partial}{\partial \xi_2}\left(\frac{u_{1k}}{\alpha_1}\right) \qquad \text{(II.9)}$$

$$\gamma_{\beta\zeta k} = \frac{1}{\alpha_\beta}\frac{\partial w_k}{\partial \zeta_\beta} + \frac{\partial u_{\beta k}}{\partial \zeta} + \frac{u_{\beta k}}{R_\beta}$$

The in-surface strains may be written in the following form by substituting Equations (II.5), (II.6) and (II.7) into Equations (II.9):

$$\varepsilon_{\beta k} = \varepsilon^o_{\beta k} + \zeta_k \kappa_{\beta k}$$
$$\gamma_{12k} = \gamma^o_{12k} + \zeta_k \kappa_{12k} \qquad \text{(II.10a)}$$

In these equations the middle surface strains are given by

$$\varepsilon^o_{\beta k} = \frac{1}{\alpha_\beta}\frac{\partial u^o_{\beta k}}{\partial \xi_\beta} - \frac{w^o}{R_\beta} + \frac{u^o_{\delta k}}{\alpha_\beta\alpha_\delta}\frac{\partial \alpha_\beta}{\partial \xi_\delta}$$
$$\gamma^o_{12k} = \frac{\alpha_2}{\alpha_1}\frac{\partial}{\partial \xi_1}\left(\frac{u^o_{2k}}{\alpha_2}\right) + \frac{\alpha_1}{\alpha_2}\frac{\partial}{\partial \xi_2}\left(\frac{u^o_{1k}}{\alpha_1}\right) \qquad \text{(II.10b)}$$

and the changes in curvature are given by

$$\kappa_{1k} = \frac{1}{\alpha_\beta}\frac{\partial}{\partial \xi_\beta}(\chi_\beta - \gamma_{\beta k}) - \frac{(\chi_\delta - \gamma_{\delta k})}{\alpha_\beta\alpha_\delta}\frac{\partial \alpha_\beta}{\partial \xi_\delta}$$
$$\kappa_{12k} = -\frac{\alpha_2}{\alpha_1}\frac{\partial}{\partial \xi_1}\left(\frac{\chi_2 - \gamma_{2k}}{\alpha_2}\right) - \frac{\alpha_1}{\alpha_2}\frac{\partial}{\partial \xi_2}\left(\frac{\chi_1 - \gamma_{1k}}{\alpha_1}\right) \qquad \text{(II.10c)}$$

In order to consider the transverse shear strains, the tangential displacements of the k^{th} layer must be written in terms of the reference surface displacements. For example, Equations (II.7) and (II.8) can be combined to give

$$u_{\beta k} = u_\beta^o - \zeta(\chi_\beta - \gamma_\beta) - \frac{\zeta(k+1) + \zeta(k)}{2}\gamma_{\beta k} + \zeta(1)\,\gamma_{\beta o} +$$

$$+ \sum_{m=1}^{k-1} [\zeta(m+1) - \zeta(m)]\gamma_{\beta m} + \frac{\zeta(k+1) - \zeta(k)}{2}\gamma_{\beta k}$$

Substitution of this and Equations (II.5) and (II.6) into the appropriate equation from (II.9) results in

$$\gamma_{3\zeta k} = \frac{1}{\alpha_\beta}\frac{\partial w^o}{\partial \xi_\beta} + \frac{u_\beta^o}{R_\beta} - (\chi_\beta - \gamma_\beta) - \frac{\zeta}{R_\beta}\cdot(\chi_\beta - \gamma_\beta) + \frac{\zeta(k)}{R_\beta}\gamma_{\beta k} +$$

$$+ \frac{\zeta(1)}{R_\beta}\gamma_{\beta o} + \sum_{m=1}^{k-1}\frac{[\zeta(m+1) - \zeta(m)]}{R_\beta}\gamma_{\beta m}$$

The last four terms of this equation are negligible in comparison to the first three terms under the thin shell assumptions of Equations (II.3). Hence, using the Equations (II.4), the transverse shear strains are given by

$$\gamma_{\beta\zeta k} = \frac{1}{\alpha_\beta}\frac{\partial w^o}{\partial \xi_\beta} + \frac{u^o}{R_\beta} - (\chi_\beta - \gamma_{\beta k}) = \gamma_{\beta k} \qquad \text{(II.11)}$$

which is consistent with the kinematic assumptions.

II.1.3. Stress-Strain Relations

Assuming that the in-surface stresses and strains can be represented by a state of generalized plane stress, the stress-strain equations for the k^{th} layer and an isotropic material are given by

$$\begin{Bmatrix} \sigma_{1k} \\ \sigma_{2k} \\ \tau_{12k} \end{Bmatrix} = \begin{bmatrix} E_k/(1-\nu_k^2) & \nu_k E_k/(1-\nu_k^2) & 0 \\ \nu_k E_k/(1-\nu_1^2) & E_k/(1-\nu_k^2) & 0 \\ 0 & 0 & G_k \end{bmatrix} \begin{Bmatrix} \varepsilon_{1k} \\ \varepsilon_{2k} \\ \gamma_{12k} \end{Bmatrix} \qquad \text{(II.12)}$$

For an anisotropic material the appropriate constitutive equations would be used in place of Equations (II.12). The 3 x 3 matrix would depend upon both the particular constitutive law and the orientation of material property axes in relation to the co-ordinate lines (lines of principal curvature). For example, where a material is orthotropic within the surface and has axes of orthotropy coincident with the co-ordinate lines, the stress-strain equations are

$$\begin{Bmatrix} \sigma_{1k} \\ \sigma_{2k} \\ \tau_{12k} \end{Bmatrix} = \begin{bmatrix} E_{1k}/(1 - \nu_{1k}\nu_{2k}) & \nu_{1k}E_{2k}/(1 - \nu_{1k}\nu_{2k}) & 0 \\ \nu_{2k}E_{1k}/(1 - \nu_{1k}\nu_{2k}) & E_{2k}/(1 - \nu_{1k}\nu_{2k}) & 0 \\ 0 & 0 & G_{12k} \end{bmatrix} \begin{Bmatrix} \varepsilon_{1k} \\ \varepsilon_{2k} \\ \gamma_{12k} \end{Bmatrix} \quad \text{(II.13)}$$

where $\nu_{2k}E_{1k} = \nu_{1k}E_{2k}$.

Since the transverse shear strain has been assumed to be constant across the thickness of each layer, the corresponding shear stress is likewise constant and is directly proportional to the shear strain. However, the average shear strain which may provide a good approximation to the shear rotation does not necessarily provide an adequate representation of the transverse shear-stress resultant. Therefore, a shear-stress correction factor is used in conjunction with the transverse stress-strain equations for the k^{th} layer as follows:

$$\tau_{\beta\zeta k} = \kappa_k G_k \gamma_{\beta\zeta k} \quad \text{(II.14)}$$

The shear-stress correction factor, κ_k , is analogous to that used in the theory for homogeneous structures [71-73, 123, 124]. One method of assigning a value to this factor is to compare the approximate theory with exact theory for some aspect of behavior. For example, Mindlin [73] has chosen $\kappa = \pi^2/12$ for homogeneous plates so

that the simple thickness-shear frequency from both theories match. Bert et al. [113] have pointed out that one value for a dynamic correction factor may permit good estimates of natural frequencies, whereas a different value may produce better approximations to mode shapes. It is difficult to make a definitive recommendation for a specific value or expression for κ_k because it is apparent that this factor is dependent upon both the configuration of the multilayer construction (number of layers, ratios of thicknesses and properties) and the specific application (static or dynamic analysis). Additional factors may also influence the selection. For the dynamic analysis of three-layered sandwich construction with thin, heavy facings and a light, weak core, Yu [32, 33] has suggested values very close to unity. Other investigators [113] have derived similar magnitudes; some recommendations range as high as 2.2 [125]. Since most of the applications later in this paper are to three-layered structures with relatively thin facings and a relatively flexible core, a value of unity will be used herein.

In discussing the transverse shear stress, it should be noted that the present approximate theory does not provide for continuity of this stress at the interfaces, nor does the shear stress vanish at the free surfaces.* However, the assumption of a constant shear strain (and thus a constant shear stress) for each layer is consistent with the philosophy of the finite element method. That is, an approximate simple displacement pattern which satisfies compatibility is hypothesized and then a variational theorem is used to obtain an optimal

*See footnote on next page.

approximation of equilibrium.* (See Section I.2.2.)

II.1.4. Stress Resultants

The stress resultants for the k^{th} layer can be obtained by integrating the stresses over the thickness.

$$\begin{Bmatrix} (N_{\beta k}, M_{\beta k}) \\ (N_{\zeta k}, M_{12k}) \end{Bmatrix} = \int_{-h_k/2}^{h_k/2} (1, \zeta_k) \begin{Bmatrix} \sigma_{\beta k} \\ \tau_{12k} \end{Bmatrix} d\zeta_k \qquad \text{(II.15a)}$$

$$Q_{\beta k} = h_k G_k \kappa_k \gamma_{\beta \zeta k} \qquad \text{(II.15b)}$$

where $h_k = |\zeta(k+1) - \zeta(k)|$ is the thickness of the layer. By using Equation (II.12), it is possible to express the first set of resultants in terms of the middle surface strains and the changes of curvature of Equations (II.10). Then the integrations can be evaluated in terms of the extensional, bending and shear stiffnesses of the layer.

The total stress resultants for the shell are obtained from the individual resultants of Equations (II.15) by summing with respect to the reference surface. Let L be the total number of layers.

---

*During the early stages of this investigation, a finite element was developed for sandwich beams using a quadratic variation of shear through the depth such that the shear strain and stress vanished at the free surfaces. This variation was derived on the basis of a linear variation of bending stresses over the depth. Because of the more complex nature of the warping in this case, the formulation was restricted to beams having a continuous shear diagram. That is, interelement compatibility was maintained for all the layer shears. A linear variation of shear strain over the length was used. For beams with dimensions and properties typical of sandwich construction, results using this element were practically indistinguishable from those using a constant shear strain across the thickness. Hence the more complex formulation was discarded in favor of the approximate one.

$$\begin{Bmatrix} N_\beta \\ N_{12} \\ Q_\beta \end{Bmatrix} = \sum_{k=1}^{L} \begin{Bmatrix} N_{\beta k} \\ N_{12k} \\ Q_{\beta k} \end{Bmatrix} \qquad \text{(II.16a)}$$

$$\begin{Bmatrix} M_\beta \\ M_{12} \end{Bmatrix} = \sum_{k=1}^{L} \left(\begin{Bmatrix} M_{\beta k} \\ M_{12k} \end{Bmatrix} + \frac{\zeta(k+1) + \zeta(k)}{2} \begin{Bmatrix} N_{\beta k} \\ N_{12k} \end{Bmatrix} \right) \qquad \text{(II.16b)}$$

The sign conventions for these stress resultants are shown in Figure (II.3).

II.1.5. Application to the Finite Element Method

For the theory presented above, the following displacements are necessary to describe completely the behavior of the shell:

1. The normal displacement of the reference surface, w^o .

2. The tangential displacements of the reference surface, u_1^o and u_2^o .

3. The rotations of the tangents to the reference surface, χ_1 and χ_2 .

4. The shear rotations of each of the layers, γ_{1k} and γ_{2k} for $k = 1,2, \ldots, L$.

For one-dimensional cases, such as axisymmetric shells, the number of displacements in 2 through 4 is halved. Another special case is that of symmetry about the reference surface, for which the number of each of the displacements in 4 are reduced by L/2 if L is even, or by (L-1)/2 if L is odd.

In the finite element method, the deformations of an element are continuous functions in the local co-ordinate system and are expressed in terms of the nodal values of the displacements. In general, for each

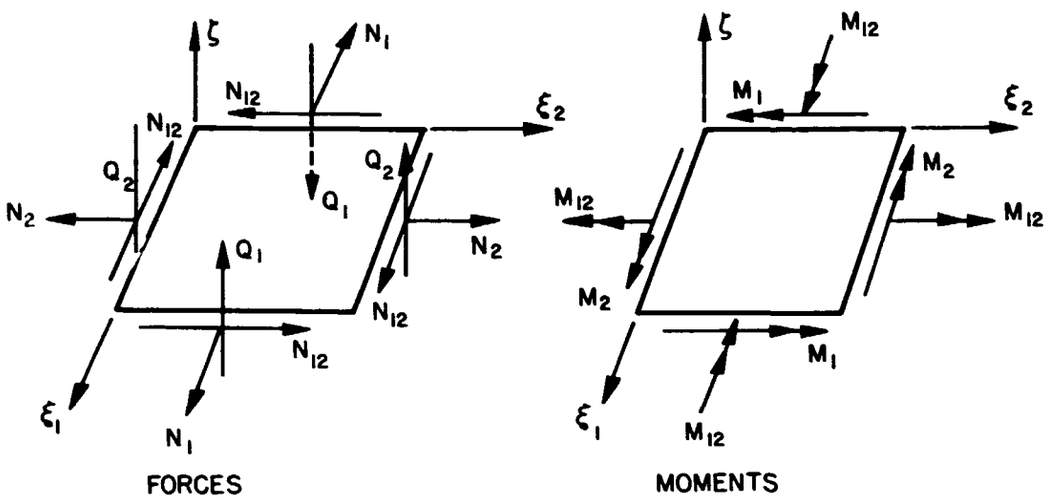

FIGURE II.3 SHELL STRESS RESULTANT SIGN CONVENTIONS

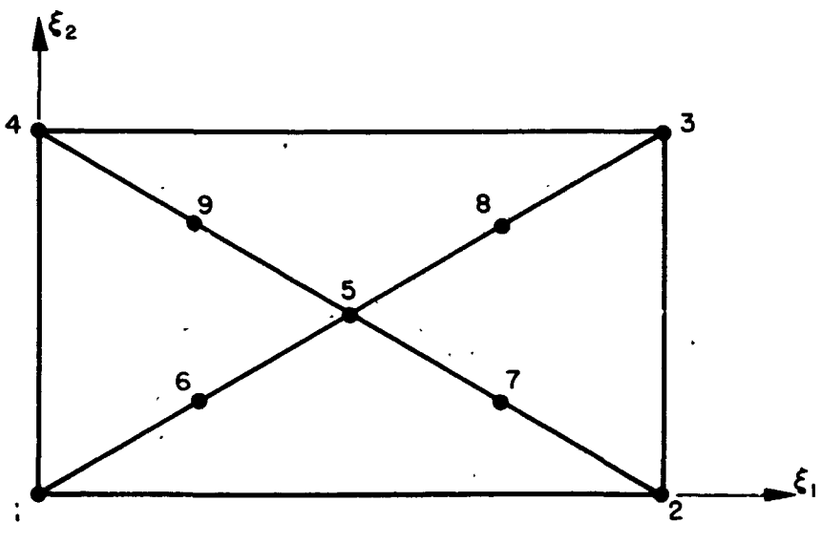

FIGURE II.4 PLANAR QUADRILATERAL ELEMENT
AFTER JOHNSON [76]

primary external node*, all of the above displacements are selected as unknowns. Depending upon the level of refinement of the displacement models, some of the displacements may also be chosen as additional degrees of freedom at internal nodes or at secondary external nodes.* As an example, consider the planar quadrilateral assembled from four triangles used by Johnson [76] for the analysis of singly curved shells (See Figure II.4). For such structures, the nodal lines are coincident with lines of principal curvature. The bending is represented by a cubic normal displacement model after Hsieh, Clough and Tocher [66] whereas the membrane behavior is approximated by a quadratic variation of tangential displacements (linear strain triangles of Reference [58]) with the external boundaries constrained to deform linearly. If the layer shear strains are modeled in the same way as the membrane displacements, a total of 33 + 18L degrees of freedom would be required: (1) at nodes 1 to 5, displacements of type 1,2,3, and 4 contributing 5 + 2L degrees of freedom per node; (2) at nodes 6 to 9, displacements of type 2 and 4 contributing 2 + 2L degrees of freedom per node.

In assembling the elements into a representation of the overall shell, compatibility usually must be maintained for all the displacement degrees of freedom occurring at the interelement nodes. However, when the transverse shear behavior is included, some continuity conditions must be removed in order to permit the "kinking" associated with discontinuities of the shear stress resultant. These discontinuities occur at transverse line loads. Thus, the necessary and sufficient requirement for compatibility of the assemblage is interelement continuity on the following nodal displacements:

---

*A primary external node is, for example, a node occurring at a corner of a two-dimensional element. A secondary external node occurs at mid-side of such an element.

A. The normal displacement of the reference surface, w^o .

B. The tangential displacements of the reference surface, u_1^o and u_2^o .

C. The rotations of the normals to the reference surface (i.e., the rotations associated with bending), χ_{b1} and χ_{b2} .

D. The shear warping angles at each of the layer interfaces, $(\gamma_{1(k+1)} - \gamma_{1k})$ and $(\gamma_{2(k+1)} - \gamma_{2k})$ for $k = 1,2, \ldots, L-1$. The reduction of the number of these displacements for the special cases is similar to that for the basic displacements 1 to 4 above.

Comparing displacements A to D with 1 to 4, it is apparent that, in addition to modifying the character of some of the quantities, the total number of displacements per node has been reduced by two. That is, the number of continuity conditions has been decreased by two. The extra displacement in each of the two directions is any one of the layer shear rotations which may now be considered as an internal degree of freedom for the element. If these extra displacements and the shear warping angles (D) are known, all the layer shear rotations are recoverable. Furthermore, the rotations of the normals to the reference surface may be written as

$$\chi_{b\beta} = \chi_{\beta} - \chi_{s\beta} \qquad \text{(II.17)}$$

where the subscripts b and s represent bending and shearing respectively. The rotations due to shearing may be expressed in terms of the shear rotations and layer thicknesses

$$\chi_{s\beta} = \chi_{s\beta}(h_k, \gamma_{\beta k}) \qquad \text{(II.18)}$$

Hence the rotations χ_{β} are also recoverable. A specific version of

Equation (II.18) will be derived in Section III.1.

At each interelement node there are $5 + 2(L-1)$ degrees of freedom and thus the total number of equations necessary for the overall discretized structure is the product of this quantity and the total number of nodes. The additional internal degrees of freedom are not directly involved in these equations; rather, the element stiffness matrix is condensed with respect to the loads on these internal nodes [62]. This process, called static condensation, is described in Section II.2.6. For example, in the Johnson-type quadrilateral discussed above, the total number of internal degrees of freedom is $2 + 10L$: (1) $2 + 2L$ contributed from each of the internal nodes 6 to 9; (2) $5 + 2L$ contributed from the internal node 5; (3) 2 contributed from each of the nodes 1 to 4, corresponding to the nodal displacements for which continuity is not enforced. As a result, the size of the stiffness matrix for this element after condensation would be $(12 + 8L)$ by $(12 + 8L)$.

It should be emphasized that the generalized theory in this chapter is formulated only in terms of co-ordinates which are coincident with the lines of principal curvature. Thus, when applying the theory to finite elements with curved surfaces, the displacements and their derivatives must be taken in the principal directions. For axisymmetric shells, the application involves no difficulties since the principal co-ordinates are the natural choice. Furthermore, arbitrary shells are usually represented by planar elements [74 - 76] for which the bending and stretching are uncoupled. Hence the choice of the "principal" directions of the substitute structure is open.

II.1.6. Boundary Conditions

In the previous section, it has been shown that the external nodal displacements at any node are

$$w \ , \ u_\beta \ , \ \chi_\beta \ , \ (\gamma_{3(k+1)} - \gamma_{\beta k}) \ , \qquad k = 1,2, \ldots, L$$

Hence, at the boundary of a structure, kinematic constraints can be applied by specifying any or all of the above displacements. In practice, if a displacement quantity is specified to be zero, all the elements of the corresponding row and column of the overall stiffness matrix are set to zero with the exception of the element on the principal diagonal, which is set to one. In addition, the load corresponding to the restrained displacement is set to zero. Elastic constraints and skewed boundaries are also admissable, and their treatment is covered in the literature on matrix analysis and the finite element method [56].

For this particular formulation, it is possible to provide for a support fixed against rotation in two ways. Either bending rotation alone may be prevented or both bending rotation and warping may be constrained. The latter is probably a more accurate representation of a classical "fixed edge," although both possibilities have applications. In either case, rotation of the tangent to the middle surface due to shearing, χ_s , must occur at fixed supports, and this is true for the above formulation.

II.2. Stiffness Analysis of Elements for the Displacement Method

Following is a brief summary of the standard stiffness analysis [126, 127] which will be applied to three different elements later in this chapter. This derivation is the key step in the direct stiffness method outlined in Section II.3. Let $N = n + m$ be the total number of degrees of freedom for a single element, where n and m are the numbers of external and internal degrees of freedom, respectively. Also, let a local co-ordinate system for the element be designated by x.

II.2.1. Displacement Models

The displacements over the domain of the element are expressed in terms of generalized displacements as follows:

$$\{u(x)\} = [\Phi(x)]\{\alpha\} \tag{II.19}$$

Here $[\Phi(x)]$ is the matrix of polynomial displacement models and $\{\alpha\}$ is the $N \times 1$ vector of generalized displacements. $\{\alpha\}$ can be considered to be the amplitudes of the displacement shapes $[\Phi(x)]$. Note that if $[\Phi(x)]$ is expressed directly in terms of the interpolation polynomials for the particular element, $\{\alpha\}$ is replaced by the vector of nodal displacement, $\{q\}$. The displacement models are simple, but relatively complete, fields chosen to satisfy, if possible, the requirements of completeness and compatibility (Section I.2.2). In addition, for an arbitrary two-dimensional structure, the models must provide a stiffness which is invariant with respect to the relative orientation of the local and global co-ordinate systems.

II.2.2. Element Strains

Using the strain-displacement equations and the displacements of Equation (II.19), the element strains may be written in terms of the generalized co-ordinates.

$$\{\varepsilon(x)\} = [B(x)]\{\alpha\} \tag{II.20}$$

In this dissertation, the strain vector $\{\varepsilon\}$ shall be comprised of the middle surface strains and the changes of curvature as given in Equations (II.10b and c) and the transverse shears of Equation (II.11). The total strains may be found from Equations (II.10a) and may be written as

$$\{\boldsymbol{\epsilon}(x,\zeta)\} = [Z(\zeta)]\{\varepsilon(x)\} \tag{II.21}$$

II.2.3. Stress-Strain Relations

Employing submatrices of the type given in Equation (II.12), the total stresses may be expressed in terms of the total strains by

$$\{\sigma(x,\zeta)\} = [C]\{\boldsymbol{\epsilon}(x,\zeta)\} \tag{II.22}$$

II.2.4. Application of the Principle of Minimum Potential Energy

In the absence of body forces, the total potential [128] of an element is given by

$$\pi = U - V = \frac{1}{2}\int_{v} \{\boldsymbol{\epsilon}\}^{T}\{\sigma\}\, dv - \int_{a} \{u\}^{T}\{\bar{\tau}_1\}\, da \tag{II.23}$$

Here the barred quantities are prescribed and the following definitions apply:

v = volume of the element

a = area of reference surface of the element over which stresses specified

$\{\bar{p}_u\}$ = vector of loads corresponding to the displacements $\{u\}$ and distributed over the surface of the element.

Substituting Equations (II.19 - 22) into (II.23) gives

$$\pi = \{\alpha\}^T \left(\frac{1}{2} \int_v [B]^T[Z]^T[C][Z][B]\, dv\{\alpha\} - \int_a [\Phi]^T\{\bar{p}_u\}\, da\right) \quad (II.24)$$

Application of the variational principle [128] to Equation (II.24) results in variation of the generalized co-ordinates only to give

$$\delta\pi = \{\delta\alpha\}^T \left(\int_v [B]^T[D][B]\, dv\{\alpha\} - \int_a [\Phi]^T\{\bar{p}_u\}\, da\right) = 0 \quad (II.25)$$

where the matrix [D] has been defined as

$$[D] = D(\zeta) = [Z(\zeta)]^T[C][Z(\zeta)] \quad (II.26)$$

The integral of [D] over the thickness of the shell is given by

$$[G] = \int_{-h/2}^{h/2} [D]\, d\zeta \quad (II.27)$$

The equilibrium equations which result from Equation (II.25) are

$$\{Q_\alpha\} = [k_\alpha]\{\alpha\} \quad (II.28)$$

where

$$[k_\alpha] = \int_v [B]^T[G][B]\, dv$$

$$\{Q_\alpha\} = \int_a [\Phi]^T\{\bar{p}_u\}\, da \qquad \text{(II.29)}$$

are the element stiffness and consistent generalized loads respectively.

II.2.5. Transformation to Global Co-ordinates

The nodal displacements in local co-ordinates can be obtained in terms of the generalized displacements by evaluating Equation (II.19) at the nodes of the element.

$$\underset{Nx1}{\{q\}} = \begin{bmatrix} \Phi(\text{node 1}) \\ \Phi(\text{node 2}) \\ \text{etc.} \end{bmatrix}\{\alpha\} = \underset{NxN}{[A]}\ \underset{Nx1}{\{\alpha\}}$$

This system of equations can be inverted to obtain

$$\{\alpha\} = [A^{-1}]\{q\} \qquad \text{(II.30)}$$

Had $[\Phi]$ originally been chosen as interpolation functions, then $\{\alpha\}$ and $\{q\}$ would be synonomous and this step would be unnecessary.

Let $\{r\}$ be the vector of nodal displacements in global co-ordinates. Then the relation between $\{q\}$ and $\{r\}$ is given by

$$\{q\} = [T]\{r\} \qquad \text{(II.31)}$$

where the matrix $[T]$ is a simple transformation matrix relating the two co-ordinate systems.

Equations (II.30) and (II.31) may be combined to give

$$\{\alpha\} = [A^{-1}][T]\{r\} = [\underline{T}]\{r\} \qquad \text{(II.32)}$$

Using the transformation matrix of Equation (II.32), it is apparent from Equation (II.24) that the element stiffness and consistent load vector in global co-ordinates are

$$[K] = [\underline{T}]^{T}\{k_{\alpha}\}[\underline{T}]$$
$$\{R\} = [\underline{T}]^{T}\{Q_{\alpha}\} \qquad \text{(II.33)}$$

II.2.6. Static Condensation

The equilibrium equations for the element in global co-ordinates

$$\underset{Nxl}{\{R\}} = \underset{NxN}{[k]}\ \underset{Nxl}{\{r\}} \qquad \text{(II.34)}$$

can be partitioned to distinguish the external and internal degrees of freedom as follows:

$$\begin{Bmatrix} R_1 \\ \hline R_2 \end{Bmatrix} = \left[\begin{array}{c|c} k_{11} & k_{12} \\ \hline k_{21} & k_{22} \end{array}\right] \begin{Bmatrix} r_1 \\ \hline r_2 \end{Bmatrix} \qquad \text{(II.35a)}$$

$$\begin{matrix} nxl \\ mxl \end{matrix} \quad \begin{matrix} nxn \\ mxn \end{matrix} \quad \begin{matrix} nxm \\ mxm \end{matrix} \quad \begin{matrix} nxl \\ mxl \end{matrix}$$

Equations (II.35a) can also be written

$$\{R_1\} = [k_{11}]\{r_1\} + [k_{12}]\{r_2\}$$
$$\{R_1\} = [k_{21}]\{r_1\} + [k_{22}]\{r_2\} \qquad \text{(II.35b)}$$

by solving the second of these equations for $\{r_2\}$

$$\{r_2\} = [k_{22}]^{-1}\{R_2\} - [k_{22}]^{-1}[k_{21}]\{r_1\}$$

and by substituting this result into the first of Equations (II.35b), there is obtained upon regrouping

$$\underset{n\bar{x}1}{\{\underline{R}\}} = \underset{}{[\underline{k}]}\{r_1\} = \underset{n\bar{x}n}{[\underline{k}]}\ \underset{n\bar{x}1}{\{r\}} \tag{II.36a}$$

where

$$\begin{aligned} \{\underline{R}\} &= \{R_1\} - [k_{12}][k_{22}]^{-1}\{R_2\} \\ [\underline{k}] &= [k_{11}] - [k_{12}][k_{22}]^{-1}[k_{21}] \end{aligned} \tag{II.36b}$$

In practice, the condensation is carried out by a symmetric backward Gaussian elimination process [58]. The matrices of Equations (II.36) are in suitable form for employment of the direct stiffness assembly procedure (See Section II.3 below).

II.2.7 Element Stress Resultants

Stress resultants of the type given in Equations (II.15) can be expressed in terms of the nodal displacements of the element. By using Equations (II.20-22) and (II.32), the element stresses may be written

$$\{\sigma(x,\zeta)\} = [C][Z(\zeta)][B(x)][\underline{T}]\{r\} \tag{II.37}$$

Moreover, the complete set of Equations (II.15) may be written in matrix form as

$$\{S(x)\} = \int_{-h/2}^{h/2} [Z(\zeta)]^T\{\sigma(x,\zeta)\}d\zeta \ . \tag{II.38}$$

where $\{S\}$ is the vector of all layer stress resultants. Upon combining Equations (II.37) and (II.38) and using the definition given by Equation (II.27), the element stress resultants at any location within the element are given by

$$\{S(x)\} = [G][B][\underline{T}]\{r\} \ . \tag{II.39}$$

It is a simple matter to assemble the total stress resultants according to Equations (II.16) once $\{S\}$ has been determined at a particular point on the reference surface.

II.3. The Direct Stiffness Method

The direct stiffness method is the most efficient and systematic approach to the stiffness analysis of structures [63]. It has become the basic technique of the finite element method and is described in several of the References, e.g., [126, 127]. The following sequence of steps summarizes the direct stiffness method as applied to the displacement method of solution:

1. Discretization of the structure.
2. Discretization of the displacements and selection of displacement models.
3. Derivation of the element stiffnesses.
4. Assembly of the element stiffnesses into the stiffness of the complete structure.
5. Solution for the displacement amplitudes.
6. Computation of the stress resultants.

Steps 2, 3, and 6 are discussed in Section II.2 above and the remaining steps are briefly described below.

When discretizing the structure, there are certain natural locations for interelement nodes. Line loads and discontinuities in geometric or material properties are examples of such locations. Beyond this, considerable judgment must be exercized in selecting a nodal mesh. In general, a finer grid is required where there are steeper gradients of behavior. For two-dimensional structures, attention should also be devoted to choosing a systematic mesh pattern so that the final equations can be ordered to give a minimum band width.

[illegible] element stiffness has been derived and transformed to a [illegible] system (global co-ordinates), the interelement

compatibility conditions can be applied to assemble the structure stiffness. The element nodes can be identified with nodes of the overall structure. The element influence coefficients are merely added to their proper locations in the overall stiffness, using the cross-identification of nodes. The element consistent loads are similarly assembled into the structure load vector. Another way of interpreting the direct stiffness assembly process is to consider the variational theorem of Equation (II.25) as being applied to the entire structure. Because the displacement fields are separately assumed over each element, the integral over the structure can be taken as the sum of the integrals over the elements. Hence, the $n \times n$ element stiffness can be considered a compact form of an $M \times M$ contribution to the structure stiffness, where M is the total number of degrees of freedom of the structure.

The equilibrium equations for the overall structure are

$$\underset{Mx1}{\{V\}} = \underset{MxM}{[K]} \underset{Mx1}{\{v\}} \tag{II.40a}$$

and may be partitioned according to the structure nodes as

$$\begin{Bmatrix} V_1 \\ V_2 \\ \cdot \\ \cdot \\ \cdot \end{Bmatrix} = \begin{bmatrix} K_{11} & K_{12} & \cdots \\ K_{21} & K_{22} & \\ & & \end{bmatrix} \begin{Bmatrix} v_1 \\ v_2 \\ \cdot \\ \cdot \\ \cdot \end{Bmatrix} \tag{II.40b}$$

If all of the equations of type (II.36a) are partitioned on the same basis as (II.40b), then the compatibility equations for the p-th node are given by

$$\{v_p\} = \{\underline{r}\}_p^{(1)} = \{\underline{r}\}_p^{(2)} = \ldots = \{\underline{r}\}_p^{(E)} \tag{II.41}$$

Here the subscript indicates the node; the superscript, the element; and there are E elements adjacent to the p-th node. The assembly process is then given by

$$\{V_p\} = \sum_{i=p}^{E} \{\underline{R}\}_p^{(i)}$$

$$[K_{pp}] = \sum_{i=1}^{E} [\underline{k}]_{pp}^{(i)} \qquad \text{(II.42)}$$

$$[K_{pq}] = \sum_{j=1}^{F} [\underline{k}]_{pq}^{(j)}$$

where F is 2 for two-dimensional meshes and 1 for one-dimensional grids. The final step in the assembly process is to modify the structure equilibrium equations for the geometric boundary conditions, i.e., the kinematic constraints.

The resulting stiffness matrix is symmetric and sparse. With the proper ordering of equations, it is also narrowly banded about the principal diagonal and thus can be efficiently stored. Provided the boundary conditions are sufficient to prevent rigid body motion, the matrix is positive-definite and well-conditioned. In practice, only the upper half of the banded symmetric matrix is stored in the computer, and a symmetric Gaussian composition is used [60].

$$[K] = [L][D][L]^T \qquad \text{(II.43)}$$

where [L] is a lower unit triangular matrix of multipliers and [D] is a diagonal matrix of pivots. Without pivoting, the banded nature of the stiffness is maintained in the decomposition and $[D][L]^T$ may be overwritten on the upper band of [K].

When the stress resultants are computed as suggested in Section II.2.7, some discontinuities in stress occur at the element interfaces. These arise from (1) the approximation of the true displacements by the superposition of the simple displacements assumed over each element and (2) the fact that interelement continuity is not maintained on deformation gradients. An averaging process is carried out to obtain a single value for the stress resultants at the nodes. It should be noted that as the mesh is refined and the solution converges monotonically, these nodal stress discontinuities decrease in magnitude.

CHAPTER III: STATIC ANALYSIS OF ELASTIC SANDWICH STRUCTURES

III.1. Sandwich Beams and Cylindrical Bending of Sandwich Plates

For the one-dimensional case of beam analysis, the parameters used in Section II.1 take the following values:

$$R_1 = R_2 = \infty \ , \ \xi_1 = x \ , \ \alpha_1 = 1 \ , \ \zeta = z$$

$$u_1^o = u^o \ , \ w^o = w \ , \ \chi_1 = \chi = \frac{dw}{dx} \ , \ \gamma_{1k} = \gamma_k \qquad \text{(III.1)}$$

$$\varepsilon_{1k} = \varepsilon_{xk} \ , \ \gamma_{1\zeta k} = \gamma_{xzk}$$

The remaining parameters (ξ_2, α_2, u_2^o, χ_2 , γ_{2k} , γ_{12k} , $\gamma_{2\zeta k}$) vanish from the formulation. Furthermore, attention is restricted to three-layer sandwich beams with facings of equal thickness and composed of the same material (Figure III.1). Hence the bending and stretching is uncoupled and only the flexural behavior is considered:

$$u^o = 0 \ . \qquad \text{(III.2)}$$

The thickness of the core layer is taken to be h_c and that of the facings h_f . The total thickness is h and the distance between the middle surfaces of the facings is designated d . The reference surface is selected to be identical with the core middle surface and a normalized co-ordinate is defined

$$\xi = (x - x_i)/(x_j - x_i) = (x - x_i)/\ell \qquad \text{(III.3)}$$

where the subscripts identify the i-th and j-th nodes of the beam element of length ℓ (Figure III.1). In all cases, the width of the beam section is taken to be unity. Sign conventions are indicated in Figures III.1 and III.2.

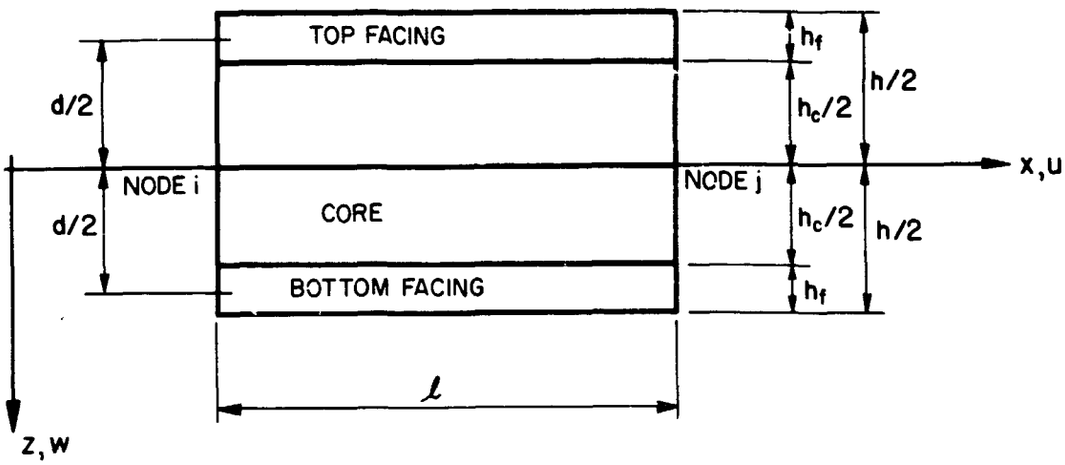

FIGURE III.1 TYPICAL BEAM ELEMENT

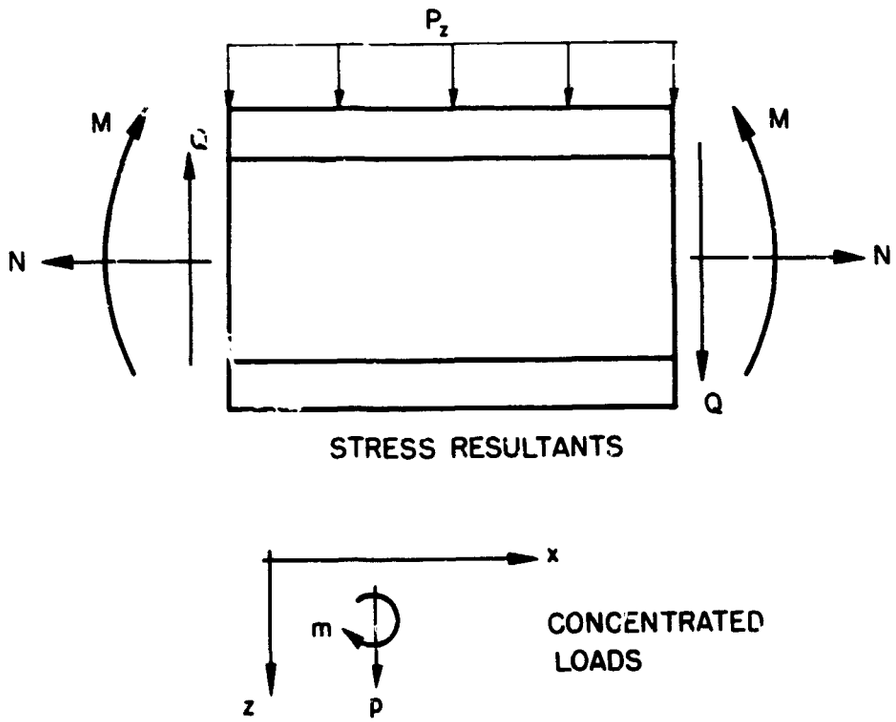

FIGURE III.2 BEAM ELEMENT SIGN CONVENTIONS

III.1.1. Slope Due to Transverse Shear

In equations (II.17) and (II.18) it was indicated that separate components of the slope, χ, could be identified. The expression for the contribution due to shear is derived in this section. Figure III.3 shows a differential element deforming under pure shearing of the core and the facings. With this type of loading, there is no net extension of the layers so the tangential displacement of each middle surface is zero. The tangential displacement of the interface must be the same when computed with reference to the middle surface of either the face or core. For the case of constant shear carried entirely by the core, this condition gives

$$u(z = h_c/2) = (\gamma_c - \chi_{sc})h_c/2 = \chi_{sc}\, h_f/2$$

and for the case of face shearing it gives

$$u(z = -h_c/2) = (\gamma_f - \chi_{sf})h_f/2 = \chi_{sf}\, h_c/2$$

Adding the two equations and using $d = h_c + h_f$, one obtains

$$\gamma_s = \chi_{sc} + \chi_{sf} = \gamma_c h_c/d + \gamma_f h_f/d \qquad \text{(III.4)}$$

χ_{sc} and χ_{sf} are defined in Figure III.3.

III.1.2. Stress-Strain Equations

The constitutive matrix is diagonal for the beams and the stress-strain equations are given by

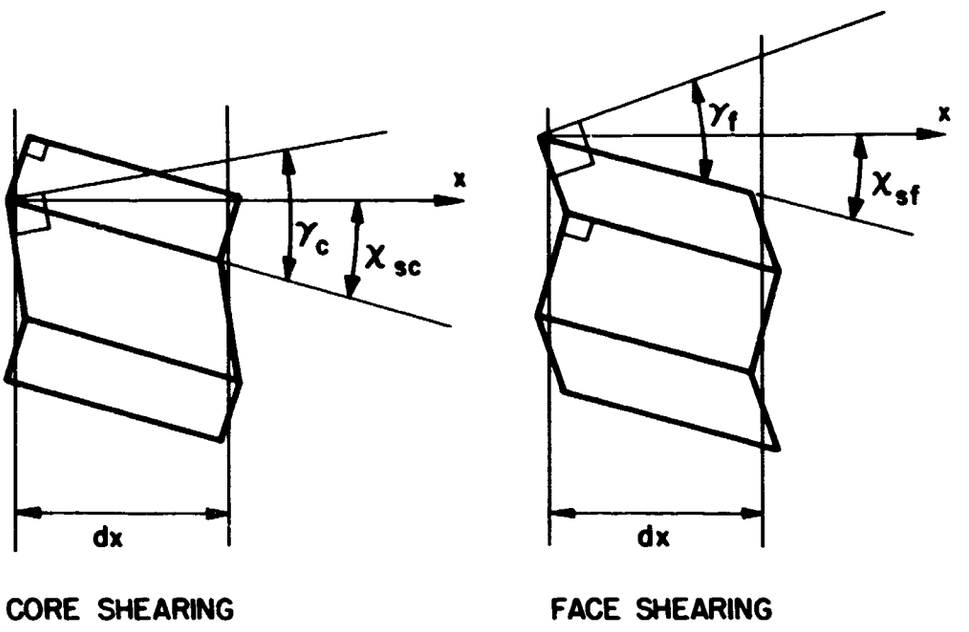

FIGURE III.3 SLOPE DUE TO SHEARING

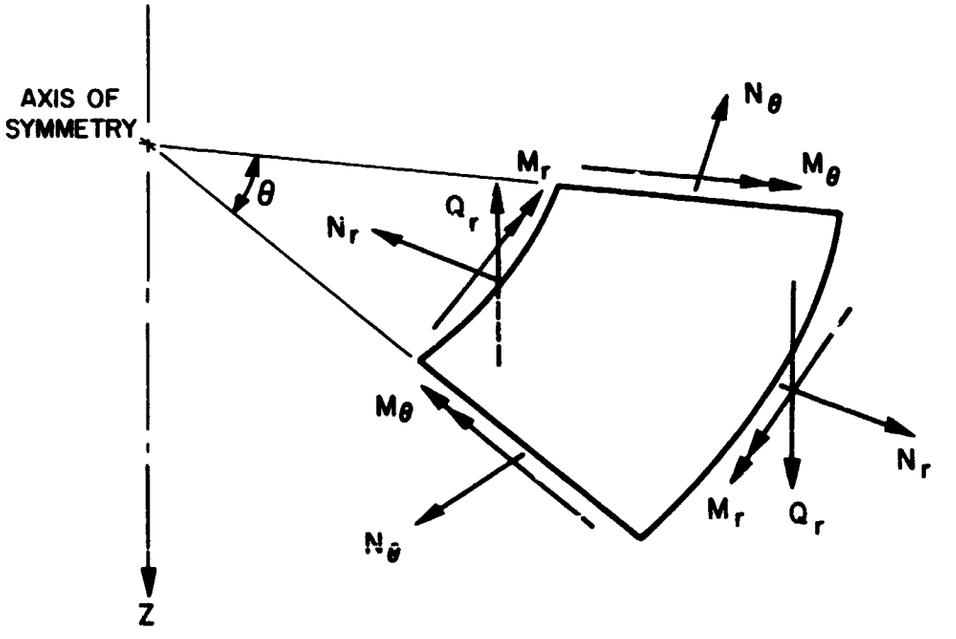

FIG. III.4 AXISYMMETRIC PLATE STRESS RESULTANTS

$$\begin{Bmatrix} \sigma_{xc} \\ \tau_{xzc} \\ \sigma_{xf} \\ \tau_{xzf} \end{Bmatrix} = \begin{bmatrix} E_c & 0 & 0 & 0 \\ 0 & \kappa_c G_c & 0 & 0 \\ 0 & 0 & E_f & 0 \\ 0 & 0 & 0 & \kappa_f G_f \end{bmatrix} \begin{Bmatrix} \varepsilon_{xc} \\ \gamma_{xzc} \\ \varepsilon_{xf} \\ \gamma_{xzf} \end{Bmatrix} \qquad \text{(III.5a)}$$

To modify this for the cylindrical bending of plates, the lateral constraint is taken into account to give

$$\begin{Bmatrix} \sigma_{xc} \\ \tau_{xzc} \\ \sigma_{xf} \\ \tau_{xzf} \end{Bmatrix} = \begin{bmatrix} E_c/(1-\nu_c^2) & 0 & 0 & 0 \\ 0 & \kappa_c G_c & 0 & 0 \\ 0 & 0 & E_f/(1-\nu_f^2) & 0 \\ 0 & 0 & 0 & \kappa_f G_f \end{bmatrix} \begin{Bmatrix} \varepsilon_{xc} \\ \gamma_{xzc} \\ \varepsilon_{xf} \\ \gamma_{xzf} \end{Bmatrix} \qquad \text{(III.5b)}$$

As usual, there is a complete analogy between the two problems.

III.1.3. Stiffness Matrix for Beam Elements

The beam element stiffness matrix is derived in this section following the procedures outlined in Section II.2. A cubic transverse displacement field and a linear variation of shear rotation are assumed. Moreover, interpolation functions are used in order to express the displacement models directly in terms of the nodal displacements. Hence Equation (II.19) may be written

$$\{u(\xi)\} = [\Phi(\xi)]\{q\} , \qquad 0 \leq \xi \leq 1 \qquad \text{(II.19)}$$

Here the vectors are chosen as

$$\begin{aligned} \{u\}^T &= < w \;\; \chi \;\; \gamma_c \;\; \gamma_f > \\ \{q\}^T &= < u(0) \;\vdots\; u(1) > \end{aligned} \qquad \text{(III.6)}$$

The matrix $[\Phi(\xi)]$ is given in Appendix A.1.1.

The kinematic assumptions of Section II.1.1 as applied to the beam are

$$\begin{aligned} u_c &= -z_c(\chi - \gamma_c) \\ u^{t,b} &= -z_f(\chi - \gamma_f) \pm \frac{d}{2}\chi \mp \frac{h_c}{2}\gamma_c \mp \frac{h_f}{2}\gamma_f \\ w_c &= w_f^t = w_f^b = w \end{aligned} \tag{III.7}$$

where the superscripts t and b indicate the top and bottom facings respectively. From Equations (II.9) it is then clear that the strain components of Equation (II.10) are given by

$$\begin{aligned} \varepsilon_{xc}^o &= 0 \\ \varepsilon_{xf}^{o\ t,b} &= \pm \frac{d}{2}\frac{d\chi}{dx} \mp \frac{h_c}{2}\frac{d\gamma_c}{dx} \mp \frac{h_f}{2}\frac{d\gamma_f}{dx} \\ \kappa_{xc} &= -\frac{d\chi}{dx} + \frac{d\gamma_c}{dx} \\ \kappa_{xf}^{t,b} &= -\frac{d\chi}{dx} + \frac{d\gamma_f}{dx} \end{aligned} \tag{III.8}$$

By applying Equations (III.8) to Equations (II.19) and (III.6), the strains may be expressed in terms of the nodal displacements.

$$\{\varepsilon(\xi)\} = [B(\xi)]\{q\} \tag{II.20}$$

When the strain-component vector is defined

$$\{\varepsilon\}^T = < \kappa_{xc}\ \gamma_{xzc}\ \varepsilon_{xf}^{o\,t}\ \kappa_{xf}^t\ \gamma_{xzf}^t\ \varepsilon_{xf}^{o\,b}\ \kappa_{xf}^b\ \gamma_{xzf}^b >$$

then the matrix B is as given in Appendix A.1. Note that

$$\frac{d}{dx} = \frac{d}{d\xi}\frac{d\xi}{dx} = \frac{1}{\ell}\frac{d}{d\xi}$$

Also given in Appendix A.1 are the matrices [Z] , [C] and [F] from Equations (II.21), (II.22) and (II.27), consistent with the definitions

$$\{\epsilon\}^T = < \varepsilon_{xc} \ \gamma_{xzc} \ \varepsilon^t_{xf} \ \gamma^t_{xzf} \ \varepsilon^b_{xf} \ \gamma^b_{xzf} >$$

$$\{\sigma\} \ = < \sigma_{xc} \ \tau_{xzc} \ \sigma^t_{xf} \ \tau^t_{xzf} \ \sigma^b_{xf} \ \tau^b_{xzf} >$$

When the principle of minimum potential energy is applied as in Equations (II.25-29), it is possible to identify the separate contributions to the element stiffness due to shear, bending and axial force:

$$[k_q]_{8\times 8} = [k^Q_c] + [k^M_c] + [k^Q_f] + [k^M_f] + [k^N_f] \qquad \text{(III.9)}$$

The integrations have been carried out in closed form and the stiffness contributions are given in Appendix A.1. The distinction between the various components proves useful in obtaining quantitative evaluations of various approximations; e.g., the effect of neglecting the bending of the facings about their own middle surfaces can be ascertained by omitting $[k^M_f]$ (See example in Section III.5.6).

Although the global and local co-ordinate systems are identical, the stiffness $[k_q]$ still must be transformed so that it is expressed in terms of the following nodal displacements

$$\{r\}^T = < w_i \ \chi_{bi} \ \gamma_i \ w_j \ \chi_{bj} \ \gamma_j \ \gamma_{fi} \ \gamma_{fj} > .$$

These co-ordinates were not the original choice because the use of $\{q\}$ as given in Equation (III.6a) allowed a much simpler closed-form integration for the stiffness matrix. The transformation $[T]$ is quite simple and can be constructed from the definitions

$$\gamma = \gamma_c - \gamma_f$$
$$\chi_b = \chi - h_c\gamma_c/d - h_f\gamma_f/d \qquad \text{(III.10)}$$

The latter is obtained from Equation (III.4). The matrix is given in Appendix A.1.

III.1.4. Consistent Load Vector for Uniform Loads

By substituting the matrix $[\Phi]$ from Equation (II.19) into Equation (II.29) and using the load vector

$$\{\bar{p}_u\}^T = < p_z(\xi)\ 0\ 0\ 0 >$$

where $p_z(\xi) = p_z$ is a uniform transverse load, the consistent loads are found to be

$$\{Q\}^T = \frac{p_z\ell}{2} < 1 \quad \frac{\ell}{6} \quad 0 \quad 0 \quad 1 \quad -\frac{\ell}{6} \quad 0 \quad 0 >$$

These can be transformed to correspond to the $\{r\}$ displacements. The result is

$$\{R\}^T = \frac{p_z\ell}{2} < 1 \quad \frac{\ell}{6} \quad \frac{h_c\ell}{6d} \quad 1 \quad -\frac{\ell}{6} \quad -\frac{h_c\ell}{6d} \quad \frac{\ell}{6} \quad -\frac{\ell}{6} >$$

III.1.5 Element stiffness for Quadratic Variation of Shear Strain

An element stiffness may be derived for a quadratic variation of shear strain by utilizing an internal nodal point at $\xi = \frac{1}{2}$. If this node is designated by the subscript o, the interpolation functions for the shear strains are

$$\gamma_k = (1 - 3\xi + 2\xi^2)\gamma_1 + 4\xi(1 - \xi)\gamma_o + \xi(2\xi - 1)\gamma_j \qquad \text{(III.11)}$$

where $k = c,f$. The details of the derivation are the same as for the linear variation of shear and will not be carried out here. The relevant matrices are given in Appendix A.2, including the contributions to the 10 x 10 stiffness.

III.2 Axisymmetric Sandwich Plates

For the cylindrical co-ordinates used to describe this case, the parameters in Section II.1 take the following forms:

$$R_1 = R_2 = \infty \ , \ \zeta = z$$
$$\xi_1 = r \ , \ \alpha_1 = 1 \ ; \ \xi_2 = \theta \ , \ \alpha_2 = r \qquad \text{(III.12a)}$$

In addition, since only axisymmetric loading is considered:

$$u_1^o = u^o \ , \ u_2^o = u_2 = 0 \ , \ w^o = w$$
$$\chi_1 = \chi = \frac{dw}{dr} \ , \ \gamma_{1k} = \gamma_k \qquad \text{(III.12b)}$$
$$\varepsilon_{1k} = \varepsilon_{rk} \ , \ \varepsilon_{2k} = \varepsilon_{\theta k} \ , \ \gamma_{1\zeta k} = \gamma_{rzk}$$
$$\gamma_{2k} = \gamma_{2\zeta k} = \chi_2 = \gamma_{12k} = 0$$

Attention is again restricted to three-layered construction symmetric about the middle surface of the core. As a consequence, the uncoupled stretching may be neglected in the flexural problem:

$$u^o = 0 \ . \qquad \text{(III.2)}$$

The geometry and terminology will be completely analogous to that for the beam (Figure III.1). Here the normalized co-ordinate in the radial direction is defined as

$$\xi = (r - r_i)/(r_j - r_i) = (r - r_i)/\ell \qquad \text{(III.13)}$$

Sign conventions for the stress resultants are indicated in Figure III.4. The slope due to shearing is also the same as for the beam and the expression is repeated here.

$$\chi_s = \chi - \chi_b = \gamma_c h_c/d + \gamma_f h_f/d \qquad \text{(III.4)}$$

The limitation of axisymmetric loading allows a one-dimensional finite element representation which is more complicated than the beam problem that circumferential stresses and strains are present.

III.2.1. Stiffness Matrix for Annular Plate Elements

The first step in deriving the stiffness matrix is the selection of the assumed displacement field. A cubic transverse displacement model (linear curvatures) is again assumed. In terms of generalized co-ordinates, this field is given by

$$w(\xi) = \alpha_1 + \alpha_2\xi + \alpha_3\xi^2 + \alpha_4\xi^3 , \quad 0 \leq \xi \leq 1 . \tag{III.14}$$

The basic shear strain model is a linear field as follows:

$$\begin{aligned} \gamma_c(\xi) &= \alpha_5 + \alpha_6\xi \\ \gamma_f(\xi) &= \alpha_7 + \alpha_8\xi . \qquad 0 \leq \xi \leq 1 \end{aligned} \tag{III.15a}$$

In addition, a more refined element with respect to shear may be obtained by using a quadratic shear strain field

$$\begin{aligned} \gamma_c(\xi) &= \alpha_5 + \alpha_6\xi + \alpha_9\xi^2 \\ \gamma_f(\xi) &= \alpha_7 + \alpha_8\xi + \alpha_{10}\xi^2 \quad 0 \leq \xi \leq 1 \end{aligned} \tag{III.15b}$$

The kinematic assumptions applied to the axisymmetric plate are the same as those for the beam:

$$\begin{aligned} u_c &= -z_c(\chi - \gamma_c) \\ u_f^{t,b} &= -z_f(\chi - \gamma_f) \pm \frac{d}{2}\chi \mp \frac{h_c}{2}\gamma_c \mp \frac{h_f}{2}\gamma_f \end{aligned} \tag{III.7}$$

However, now there are non-zero strain components in both the radial and circumferential directions. The components are

$$
\begin{aligned}
\varepsilon^{o}_{rc} &= \varepsilon^{o}_{\theta c} = 0 \\
\kappa_{r-} &= -\frac{d\chi}{dr} + \frac{d\gamma_c}{dr} \\
\kappa_{\theta c} &= -\frac{(\gamma - \gamma_c)}{r} \\
\varepsilon^{o\,t,b}_{rf} &= \pm\frac{d}{2}\frac{d\chi}{dr} \mp \frac{h_c}{2}\frac{d\gamma_c}{dr} \mp \frac{h_f}{2}\frac{d\gamma_f}{dr} \\
\varepsilon^{o\,t,b}_{\theta} &= \pm\frac{1}{r}\left(\frac{d}{2}\chi - \frac{h_c}{2}\gamma_c \frac{h_f}{2}\gamma_f\right) \\
\kappa^{t,b}_{rf} &= -\frac{d}{dr} + \frac{d\gamma_f}{dr} \\
\kappa^{t,b}_{\theta f} &= -\frac{(\chi - \gamma_f)}{r}
\end{aligned}
\qquad \text{(III.16)}
$$

These may be applied to the assumed displacement fields in terms of the generalized co-ordinates by using

$$\frac{d}{dr} = \frac{d}{d\xi}\frac{d\xi}{dr} = \frac{1}{\ell}\frac{d}{d\xi}$$

The stiffness analysis is a straightforward application of the techniques outlined in Section II.2. The matrices that result are given in Appendices B.1 and B.2 for the linear and quadratic shear models, respectively. However, the integration to obtain the stiffness matrix is not carried out in closed form. Rather numerical integration using Gauss's formula [131] is incorporated into the computer program for the integral

$$[k_\alpha] = 2\pi\ell \int_0^1 [B(\xi)]^T [G][B(\xi)]\, r\, d\xi \qquad \text{(III.17)}$$

Finally, with the selection of the vector $\{q\} = \{r\}$ as given in the Appendices, the global and local co-ordinates do not differ and the total transformation matrix is given by $[T] = [A^{-1}]$.

II.5.2. Stiffness Matrix for Disc Elements

In the limiting case $r_i = 0$ the annular plate elements described in the previous section and in Appendices B.1 and B.2 become discs. Because the center of the disc occurs on the axis, there are certain constraints that must be introduced to maintain axial symmetry. From the outset, concentrated loads at the center of the plate are excluded in order to avoid the corresponding singularity. Hence the symmetry requirements result in the following "internal" boundary conditions" [84]:

$$\chi = \gamma_c = \gamma_f = 0 \quad \text{at} \quad r = 0 \tag{III.18}$$

These conditions, in effect, remove three generalized co-ordinates and the assumed displacement fields become

$$\begin{aligned} w(\xi) &= \bar{\alpha}_4 + \bar{\alpha}_5\xi^2 + \bar{\alpha}_6\xi^3 \\ \gamma_c(\xi) &= \bar{\alpha}_7\xi \\ \gamma_f(\xi) &= \bar{\alpha}_8\xi \qquad 0 \leq \xi \leq 1 \end{aligned} \tag{III.19a}$$

for linear shear strains and

$$\begin{aligned} w(\xi) &= \bar{\alpha}_4 + \bar{\alpha}_5\xi^2 + \bar{\alpha}_6\xi^3 \\ \gamma_c(\xi) &= \bar{\alpha}_7\xi + \bar{\alpha}_9\xi^2 \\ \gamma_f(\xi) &= \bar{\alpha}_8\xi + \bar{\alpha}_{10}\xi^2 \qquad 0 \leq \xi \leq 1 \end{aligned} \tag{III.19b}$$

for quadratic shear strains. The kinematic assumptions and the strain-displacement equations for annular elements also apply to the disc as long as the new displacement fields are used. In Appendices B.3 and B.4 the matrices arising from the stiffness analysis of disc elements

with linear and quadratic shears are given.. These matrices are derived in the same dimensional format as those for the annular element so that they need no special treatment in the assembly procedure.

III.2.3. Consistent Generalized Load Vector

If the distributed loads are assumed to be linearly varying along the radius, it is an easy matter to perform the integration to obtain the generalized loads, $\{Q_\alpha\}$, of Equation (II.29). Given the transverse load intensity at the nodes, linearly varying loads may be expressed using the interpolation equation

$$p_z = p_{zi} + \xi(p_{zj} - p_{zi}) \qquad \text{(III.20)}$$

Then the generalized loads are obtained from

$$\{Q_\alpha\} = 2\pi\ell \int_0^1 [\Phi]^T\{p\}(r_i + \ell\xi)d\xi \ . \qquad \text{(III.21)}$$

The results of this integration and of the subsequent transformation to global co-ordinates are given in Appendix B. It should be noted that, in the discretized representation, load distributions of an order higher than linear can be approximated by a linear variation over each individual element.

III.3. A Doubly Curved Axisymmetric Shell Element

Various doubly curved elements and local co-ordinate systems for axisymmetric shells were studied by Khojasteh-Bakht [84]. Of the possibilities he considered, he was able to obtain best results from (1) an element which matched the position, slope and curvature of the shell meridian at the nodes and (2) a representation of the element geometry and displacements in local rectilinear co-ordinates. This formulation, which Khojasteh-Bakht designated FDR(2), results in an element which satisfies the completeness and compatibility conditions given in Section I.2.2. It is adopted for use in this paper.

Let the local rectilinear co-ordinate system be $\xi - \eta$ and the displacements in the corresponding directions be u_1 and u_2. Choose the meridional and radial displacements of the shell reference surface to be u and w and the radius of meridional curvature to be R_1. Then the geometry shown in Figure III.5 is substituted for that of an arbitrary rotational shell. The angles are positive as shown in the figure and the following relation applies

$$\phi + \psi + \beta = \pi/2 \ . \qquad \text{(III.22)}$$

Note that ξ is a normalized co-ordinate which takes the values 0 and 1 at nodes i and j, respectively. The meridian of the substitute element is given by

$$\eta = \xi(1 - \xi)\ (a_1 + a_2\xi + a_3\xi^2 + a_4\xi^3) \qquad \text{(III.23a)}$$

where Khojasteh-Bakht has shown that the constants are given by

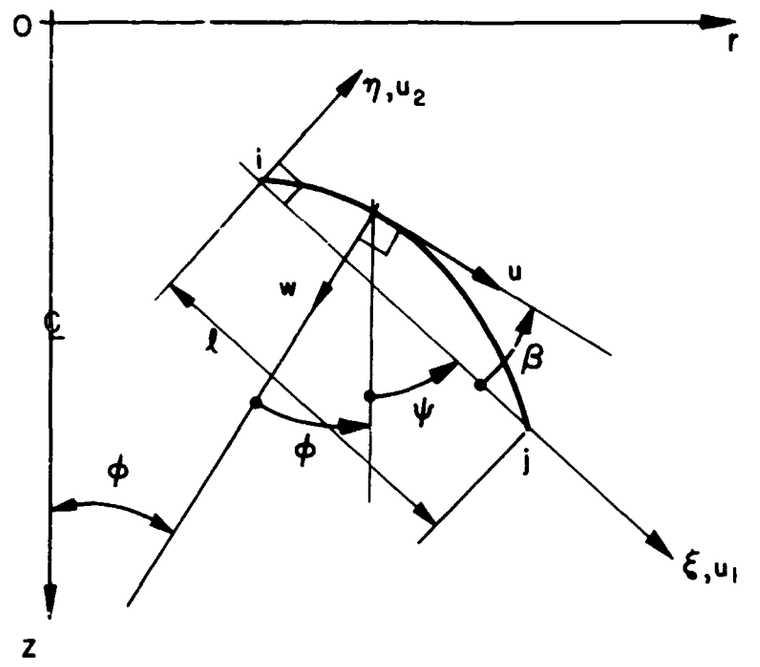

FIGURE III.5 DOUBLLY CURVED ELEMENT AFTER KHOJASTEH [84]

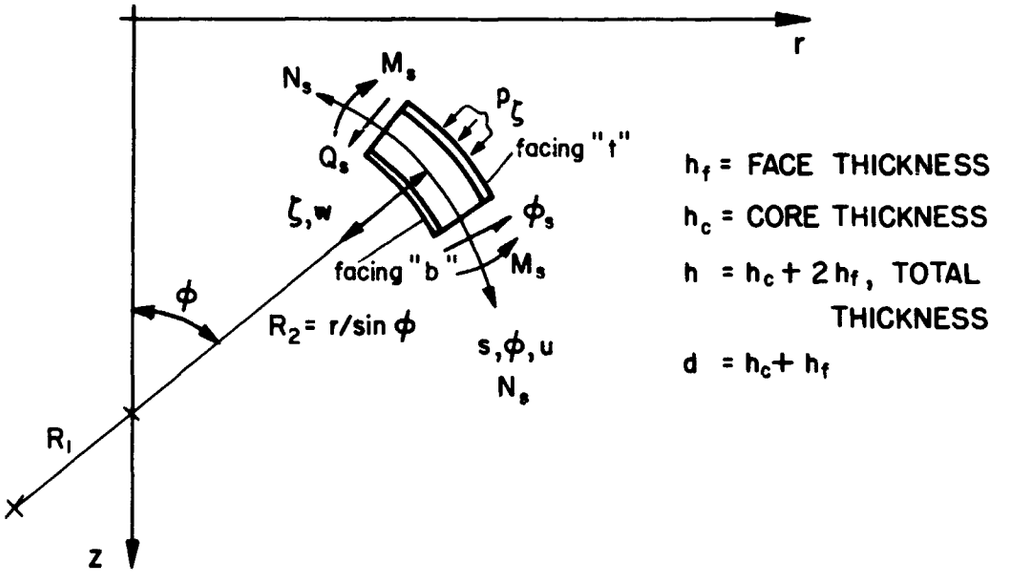

FIGURE III.6 AXISYMMETRIC SANDWICH SHELL GEOMETRY

$$a_1 = \tan \beta_i$$

$$a_2 = \tan \beta_i + \eta_i''/2$$

$$a_4 = 3(\tan \beta_i + \tan \beta_j) - (\eta_j'' - \eta_i'')/2$$

$$a_3 = -(5\tan \beta_i + 4\tan \beta_j) + (\eta_j''/2 - \eta_i') \qquad \text{(III.23b)}$$

$$\eta'' = \frac{d^2\eta}{d\xi^2} = - \frac{\ell}{R_1 \cos^3 \beta}$$

$$\tan \beta = \eta' = \frac{d\eta}{d\xi}$$

The parameters in Equations (III.23) are obtained from

$$\Delta r = r_j - r_i \ , \Delta z = z_j - z_i$$

$$\Delta s = [\overline{\Delta r}^2 + \overline{\Delta z}^2]^{\frac{1}{2}}$$

$$\sin \psi = \Delta r/\Delta s \ , \ \cos \psi = \Delta z/\Delta s \qquad \text{(III.24)}$$

$$\sin \beta_n = \cos \phi_n \cos \psi - \sin \phi_r \sin \psi \qquad n = i,j$$

$$\cos \beta_n = \sin \phi_n \cos \psi + \cos \phi \sin \psi$$

In order to apply a stiffness analysis to this substitute element, the following additional relationships are needed:

$$r = r_i + \ell(\xi \sin \psi + \cos \psi)$$

$$\frac{d\xi}{ds} = \frac{\cos \beta}{\ell} \ , \frac{d\beta}{d\xi} = - \frac{\ell}{R_1 \cos} = \eta'' \cos^2 \beta$$

$$\cos \phi = \cos \beta \ (\tan \beta \cos \psi + \sin \psi) \qquad \text{(III.25)}$$

$$\sin \phi = \cos \beta \ (\cos \psi - \tan \beta \sin \psi)$$

$$\cos \beta = \frac{1}{(1 + \tan^2 \beta)^{\frac{1}{2}}}$$

The displacement transformation equations are also necessary:

$$u = u_1 \cos \beta + u_2 \sin \beta$$
$$w = u_1 \sin \beta - u_2 \cos \beta \qquad \text{(III.26)}$$

In the next section, this doubly curved element is applied to arbitrary rotational sandwich shells. The assumed translational displacement fields are expressed in terms of the local displacements u_1 and u_2 and the local co-ordinate ξ .

III.4. Axisymmetric Sandwich Shells

The geometry of the shell reference surface is described in terms of the following definitions for the parameters in Section II.1:

$$\xi_1 = s \ , \ \alpha_1 = 1 \ ; \ \xi_2 = \theta \ , \ \alpha_2 = r$$
$$R_2 = r/\sin \phi \qquad \text{(III.27a)}$$

where R_1 and ζ remain unchanged. Only axisymmetric loading is considered; therefore, the following apply:

$$u_1^o = u \ , \ u_2^o = u_2 = 0 \ , \ w^o = w$$
$$\chi_1 = \chi = \frac{dw}{ds} + \frac{u}{R_1} \ , \ \gamma_{1k} = \gamma_k \qquad \text{(III.27b)}$$
$$\varepsilon_{1k} = \varepsilon_{sk} \ , \ \varepsilon_{2k} = \varepsilon_{\theta k} \ , \ \gamma_{1\zeta k} = \gamma_{s\zeta k}$$
$$\gamma_{2k} = \gamma_{2\zeta k} = \chi_2 = \gamma_{12k} = 0$$

See Figures III.5, III.6 and II.3 for the geometry and sign conventions. Like the beam and plate analyses above, only the three-layered case symmetric about the reference surface is considered in detail here.

III.4.1. Kinematic Assumptions and Strain-Displacement Equations

The rotation of the shell meridian due to shear remains the same as for the beam and plate

$$\chi_s = \frac{dw}{ds}_s = \chi - \chi_b = \gamma_c h_c/d + \gamma_f h_f/d \qquad \text{(III.4)}$$

The kinematic assumptions are taken from Section II.1.1 and modified in light of Equations (III.27) to obtain

$$u_c = u - \zeta_c(\chi - \gamma_c)$$

$$u_f^{t,b} = u - \zeta_f(\chi - \gamma_f) \pm \frac{d}{2}\chi \mp \frac{h_c}{2}\gamma_c \mp \frac{h_f}{2}\gamma_f \qquad \text{(III.28)}$$

$$w_c = w_f^t = w_f^b = w$$

Furthermore, the strain components of Equations (II.10) for the present notation and loading case are given by:

$$\varepsilon_{sc}^o = \frac{du}{ds} - \frac{w}{R_1}$$

$$\varepsilon_{\theta c}^o = \frac{1}{r}(u \cos\phi - w \sin\phi)$$

$$\kappa_{sc} = -\frac{d\chi}{ds} + \frac{d\gamma}{ds} c$$

$$\kappa_{\theta c} = -\frac{\cos\phi}{r}(\chi - \gamma_c)$$

$$\varepsilon_{sf}^{o\,t,b} = \frac{du}{ds} - \frac{w}{R_1} \pm \frac{d}{2}\frac{d\chi}{ds} \mp \frac{h_c}{2}\cdot\frac{\gamma_c}{ds} \mp \frac{h_f}{2}\frac{d\gamma_f}{ds} \qquad \text{(III.29)}$$

$$\varepsilon_{sf}^{o\,t,b} = \frac{1}{r}(u \cos\phi - w \sin\phi) + \frac{\cos\phi}{r}\left(\frac{d}{2}\chi - \frac{h_c}{2}\gamma_c - \frac{h_f}{2}\gamma_f\right)$$

$$\kappa_{sf}^{t,b} = -\frac{d\chi}{ds} + \frac{d\gamma_f}{ds}$$

$$\kappa_{\theta f}^{t,b} = -\frac{\cos\phi}{r}(\chi - \gamma_f)$$

However, in order to employ the substitute element described in Section III.3, the strains must be expressed in terms of the displacements in local rectilinear co-ordinates. By substituting the transformation of Equations (III.26) into Equations (III.29) and by using

the relationships given in Equations (III.25), one obtains

$$\chi = \frac{\cos^2 \beta}{\ell} \left(\frac{du_1}{d\xi} \tan \beta - \frac{du_2}{d\xi} \right)$$

$$\varepsilon^o_{sc} = \frac{\cos^2 \beta}{\ell} \left(\frac{du_1}{d\xi} + \frac{du_2}{d\xi} \tan \beta \right)$$

$$\varepsilon^o_{\theta c} = \frac{1}{r} (u_1 \sin \psi + u_2 \cos \psi)$$

$$\kappa_{sc} = - \frac{\cos^3 \beta}{\ell^2} \left[\frac{du_1}{d\xi} \eta'' \cos^2 \beta \ (1 - \tan^2 \beta) + \frac{d^2 u_1}{d\xi^2} \tan \beta + \right.$$

$$\left. + 2 \frac{du_2}{d\xi} \eta'' \tan \beta \cos^2 \beta - \frac{d^2 u_2}{d\xi^2} \right] + \frac{\cos \beta}{\ell} \frac{d\gamma_c}{d\xi} =$$

$$= \kappa^{(1)}_{sc} + \kappa^{(2)}_{sc}$$

$$\kappa_{\theta c} = - \frac{1}{r} \left[\frac{\cos^3 \beta}{\ell} \left(\frac{du_1}{d\xi} \tan \beta - \frac{du_2}{d\xi} \right) - \gamma_c \cos \beta \right] (\sin \psi +$$

$$+ \cos \psi \tan \beta) = \kappa^{(1)}_{\theta c} + \kappa^{(2)}_{\theta c}$$

$$\varepsilon^{o\,t,b}_{sf} = \varepsilon^o_{sc} \pm \frac{d}{2} \kappa^{(1)}_{sc} \mp \frac{\cos \beta}{\ell} \left(\frac{h_c}{2} \frac{d\gamma_c}{d\xi} + \frac{h_f}{2} \frac{d\gamma_f}{d\xi} \right)$$

$$\varepsilon^{o\,t,b}_{\theta f} = \varepsilon^o_{\theta c} \pm \frac{d}{2} \kappa^{(1)}_{\theta c} \mp \frac{\cos \beta}{r} \left(\frac{h_c}{2} \gamma_c + \frac{h_f}{2} \gamma_f \right) (\sin \psi + \cos \psi \tan \beta)$$

$$\kappa^{t,b}_{sf} = \kappa^{(1)}_{sc} + \frac{\cos \beta}{\ell} \frac{d\gamma_f}{d\xi}$$

$$\kappa^{t,b}_{\theta f} = \kappa^{(1)}_{\theta c} + \gamma_f \frac{\cos \beta}{r} (\sin \psi + \cos \psi \tan \beta)$$

where terms with the superscript 1 involve only the terms with derivatives of u_1 and u_2 and those with superscript 2 involve only the γ_c terms.

III.4.2. Stiffness Matrix for Fractrum Elements

For a linear variation of shear strain, the assumed local displacements in the rectilinear co-ordinate system are

$$\begin{aligned} u_1 &= \alpha_1 + \alpha_2\xi \\ u_2 &= \alpha_3 + \alpha_4\xi + \alpha_5\xi^2 + \alpha_6\xi^3 \\ \gamma_c &= \alpha_7 + \alpha_8\xi \\ \gamma_f &= \alpha_9 + \alpha_{10}\xi \qquad 0 \leq \xi \leq 1 \end{aligned} \tag{III.31a}$$

Only the last two equations change for the quadratic variation of shear strain

$$\begin{aligned} \gamma_c &= \alpha_7 + \alpha_8\xi + \alpha_{11}\xi^2 \\ \gamma_f &= \alpha_9 + \alpha_{10}\xi + \alpha_{12}\xi^2 \end{aligned} \tag{III.31b}$$

The stiffness analysis follows directly from Equations (III.30) and (III.31). The resulting matrices for the linear and quadratic shear strain models are given in Appendices C.1 and C.2 respectively. Since the integrals for the stiffness matrix and generalized loads,

$$\begin{aligned} [k_\alpha] &= 2\pi\ell \int_0^1 [B]^T[G][B] \frac{r(\xi)}{\cos\beta}\, d\xi \\ \{Q_\alpha\} &= 2\pi\ell \int_0^1 [\Phi]^T\{\bar{p}_u\} \frac{r(\xi)}{\cos\beta}\, d\xi \ , \end{aligned} \tag{III.32}$$

cannot be readily solved in closed form, numerical integration is necessary to evaluate these quantities. Gauss's formula [131] is used in this case, just as for the plate elements.

III.4.3. Stiffness Matrix for Cap Elements

The case in which $r_i = 0$ is analogous to the disc specialization for the plate elements (Section III.2.2). A cap element is shown in Figure III.7. The internal boundary conditions in this case are

$$u_r = \chi = \gamma_c = \gamma_f = 0 \quad \text{at} \quad r = 0 \tag{III.33}$$

where the case of a concentrated load at the apex has been excluded. The first two of the parameters can be expressed in terms of the local displacements and co-ordinates as follows:

$$\begin{aligned} u_r &= u_1 \sin\psi + u_2 \cos\psi \\ \chi &= \frac{\cos^2\beta}{\ell}\left(\frac{du_1}{d\xi}\tan\beta - \frac{du_2}{d\xi}\right) \end{aligned} \tag{III.34}$$

Hence to be consistent, the assumed displacement fields must take the form [84]

$$\begin{aligned} u_1 &= -\bar{\alpha}_5 \cos\psi + \bar{\alpha}_6\xi \\ u_2 &= \bar{\alpha}_5 \sin\psi + \bar{\alpha}_6 \tan\beta_i\xi + \bar{\alpha}_7\xi^2 + \bar{\alpha}_8\xi^3 \\ \gamma_c &= \bar{\alpha}_9\xi \\ \gamma_f &= \bar{\alpha}_{10}\xi \qquad 0 \leq \xi \leq 1 \end{aligned} \tag{III.35.a}$$

for linear shear strain. For quadratic shear strain, the last two of the equations become

$$\begin{aligned} \gamma_c &= \bar{\alpha}_9\xi + \bar{\alpha}_{11}\xi^2 \\ \gamma_f &= \bar{\alpha}_{10}\xi + \bar{\alpha}_{12}\xi^2 \end{aligned} \tag{III.35b}$$

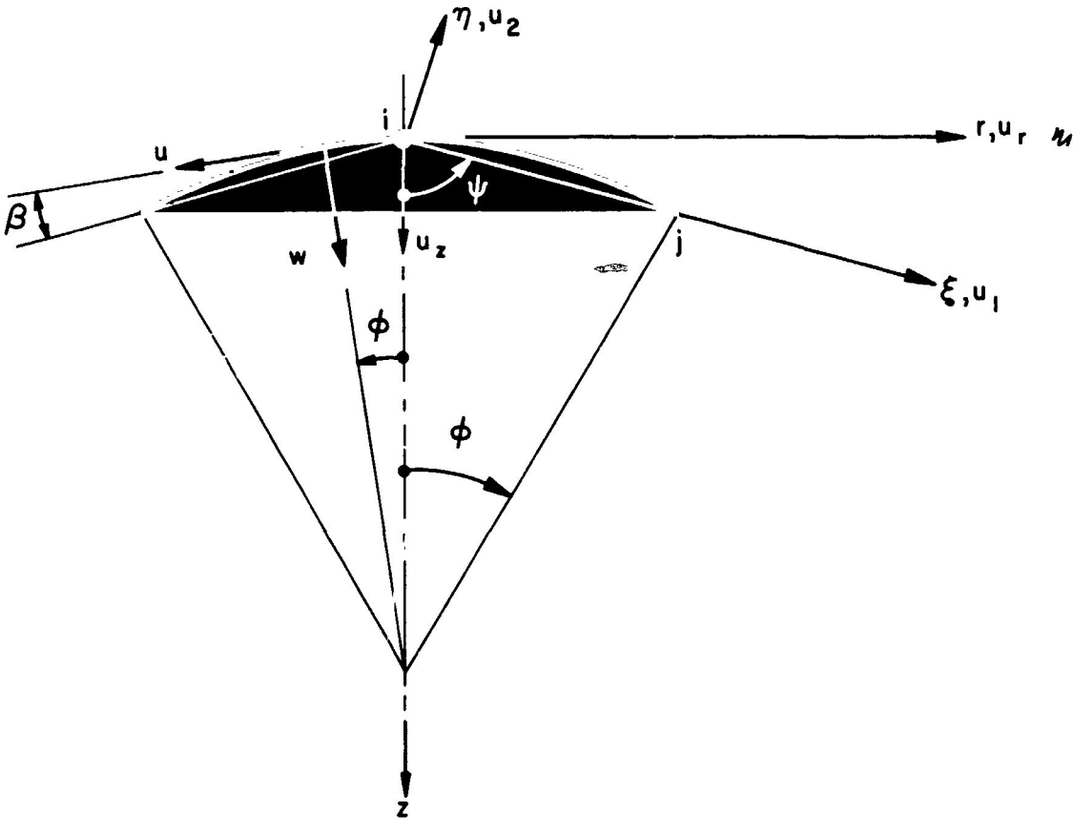

FIGURE III.7 – CAP ELEMENT AFTER KHOJASTEH [84]

The matrices for the cap element for linear and quadratic shear are given in Appendices C.3 and C.4 respectively.

III.4.4. Choice of Global Co-Ordinates for the Shell

There are at least two possible global co-ordinate systems in which to express the displacements of the axisymmetric shell. These are curvilinear surface co-ordinates (s, θ , ζ) and cylindrical co-ordinates (r , θ , z). In shell theory, the former co-ordinate system is usually favored. However, it is possible to apply the finite element method to shells with discontinuities of meridional slope. At the locations of such discontinuities, the "radial" and "meridional" directions are no longer uniquely defined. Hence it is not possible to use surface co-ordinates in the assembly process for these shells. In Appendix C, transformation matrices [T] are given for both curvilinear and cylindrical global co-ordinate systems. The proper transformation is selected according to the nature of the shell meridian.

III.5. Examples of Static Analysis

The above finite element formulation has been applied to various sandwich beam, plate and shell problems and the results compared to solutions from other methods and sandwich theories. A sampling of these problems is presented in this section to demonstrate the efficacy of the method. In general, both the displacement and stress resultants from the finite element method compare favorably to corresponding quantities obtained by established theories. Among the references from which theories were adapted in order to verify the finite element solutions were Yu [32], Plantema [12], March [120], Reissner [16], Kao [53] and Rossettos [52].

III.5.1. End-Loaded Cantilever Beam

A cantilever sandwich beam of unit width with a unit load at the free end illustrates the effect of a constraint on the warping. The dimensions and properties are selected as follows:

$$h_c = 0.5" \ , \ h_f = 0.04" \ , \ h = 0.58"$$
$$E_f = 10^7 \text{ psi} \ , \ G_f = 4 \times 10^6 \text{ psi} \ , \ \kappa_f = 1$$
$$E_c = 2 \times 10^4 \text{ psi} \ , \ G_c = 10^4 \text{ psi} \ , \ \kappa_c = 1$$
$$\text{span} \quad L = 10" \ , \ \text{load} \quad P = 1.0 \text{ lb.}$$

Evenly spaced meshes of 5 and 10 elements as well as uneven meshes are used for both linear shear strain (L elements) and quadratic shear strain (Q elements).

The displacement solution for 5-L elements is shown in Figure III.8; the displacements from a 5-Q analysis fall about midway between the 5-L result and the solution of Reference [ ]. For all meshes and elements used, the overall stress resultants are correct to about five significant

figures, so these results are not shown graphically. Of interest, however, is the distribution of shear force between the facings and core. The fraction of the shear assumed by the core is shown in Figure III.9. The theory from Section 1.2 of Reference [12] does not take into account either the warping behavior or the bending stiffness of the facings; it assumes that all shear is taken by the core. The refinement to take into account the restraint on warping and the consequent flexure of the facings about their own middle surfaces is given in Section 1.3 of that Reference. This formulation is due to van der Neut. Finally, Yu's theory [32] considers both the warping and the shearing of the facings and thus gives the distribution of shear among the various layers. Figure III.9 demonstrates that with a proper mesh refinement, the finite element method gives an adequate representation of this phenomenon. Moreover, the quadratic shear-strain elements enable a satisfactory representation with fewer elements. The constraint against warping causes most of the shear to be carried by the facings. The approximate mechanism of this redistribution is shown in Figures III.10b and III.10c. In these figures, the shear force carried by each layer is the area under the stress diagram.

Failures have been found to occur in the facings near fixed supports of aerospace sandwich structures. For this reason, the facing layers are usually doubled in thickness in these regions. The above results give an insight into the shear redistribution which necessitates the use of such doubler plates. In fact, the finite element method is suited for design of doubler plates since the computer program is readily modified to account for elements with differing face thicknesses. Hence it is possible to include these reinforcing layers in the analysis. As an alternative, it is possible to assume that doubler plates

effectively create a section at their cut-off point which is very stiff with respect to bending rotation, but which is free to warp. Hence one could assume that the boundary of the structure occurs at the cut-off point of the plates and could apply boundary conditions that prevent bending rotation but not warping.

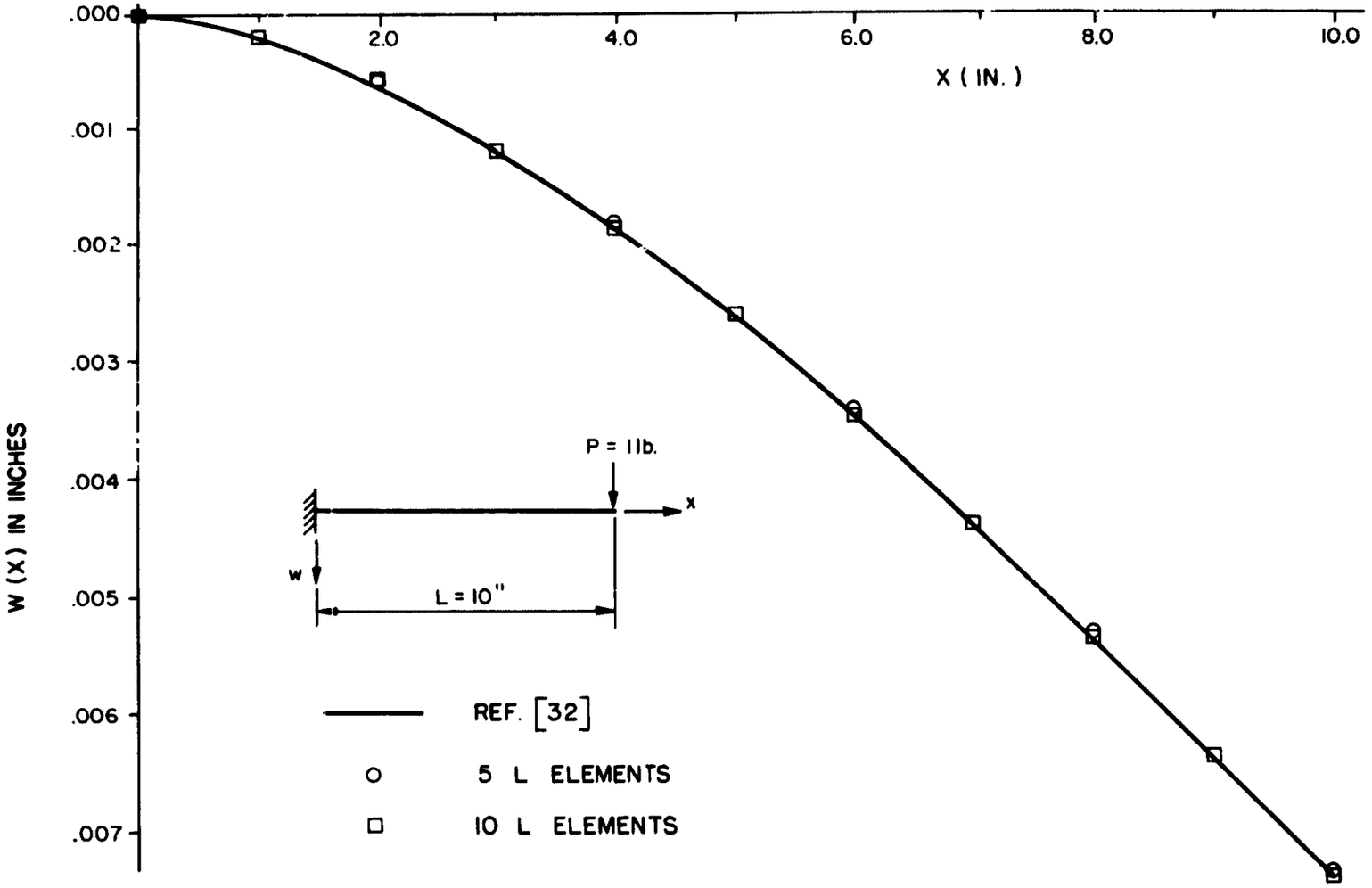

FIGURE III.8 DEFLECTION OF A CANTILEVER BEAM

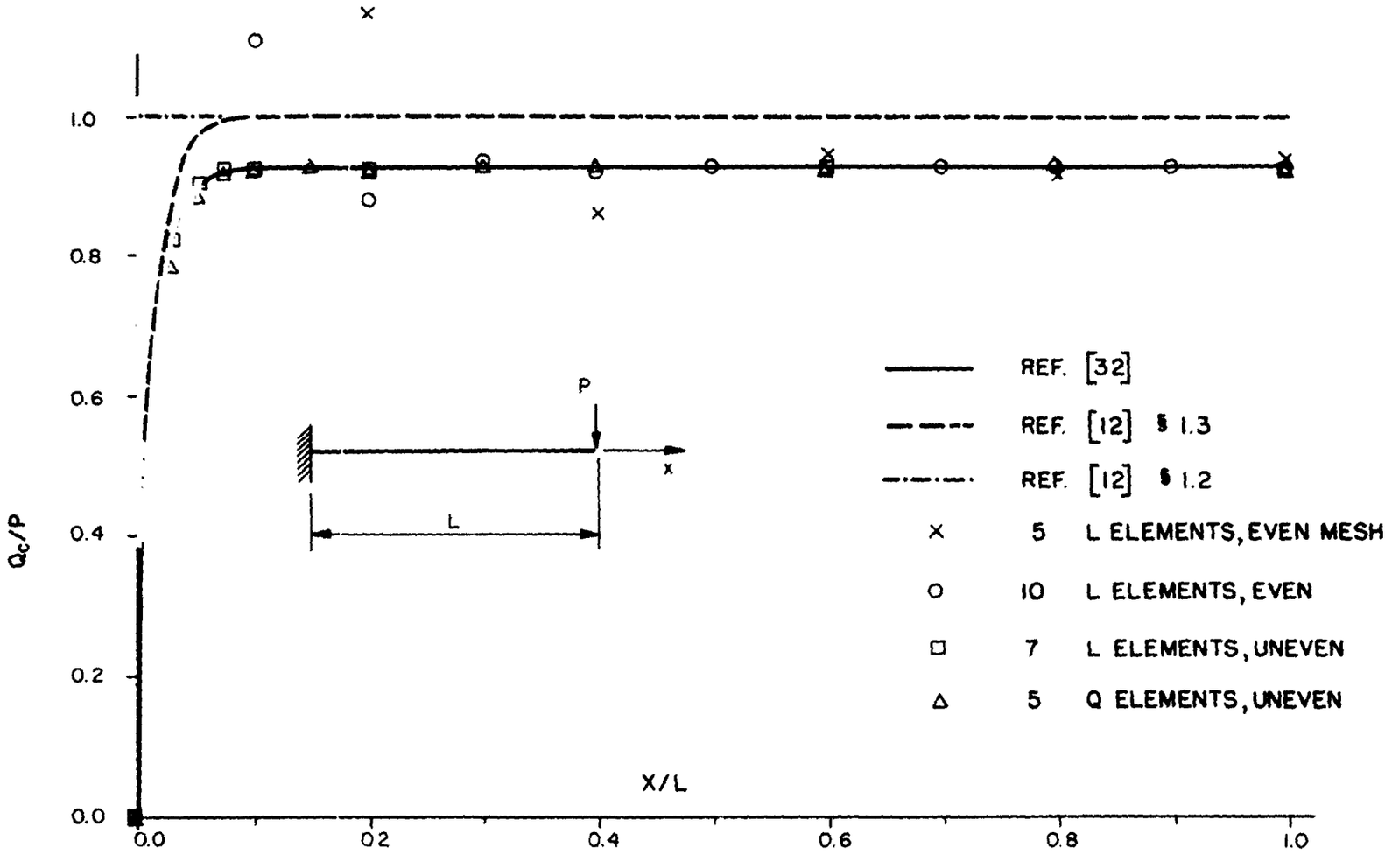

FIGURE III.9 SHEAR DISTRIBUTION BETWEEN FACE AND CORE

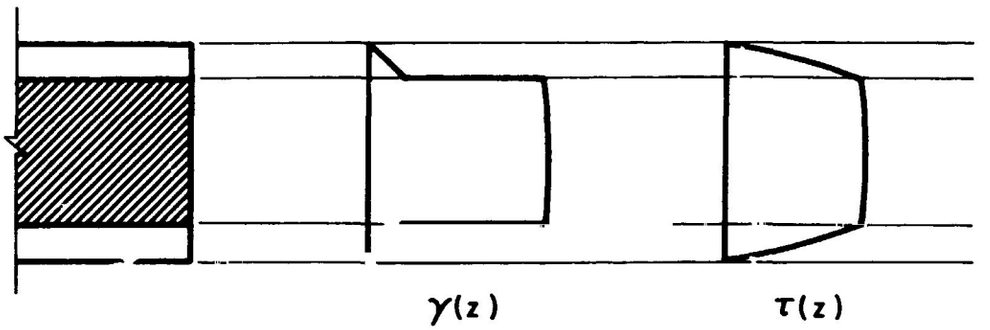

(a) NAVIER - KIRCHHOFF THEORY

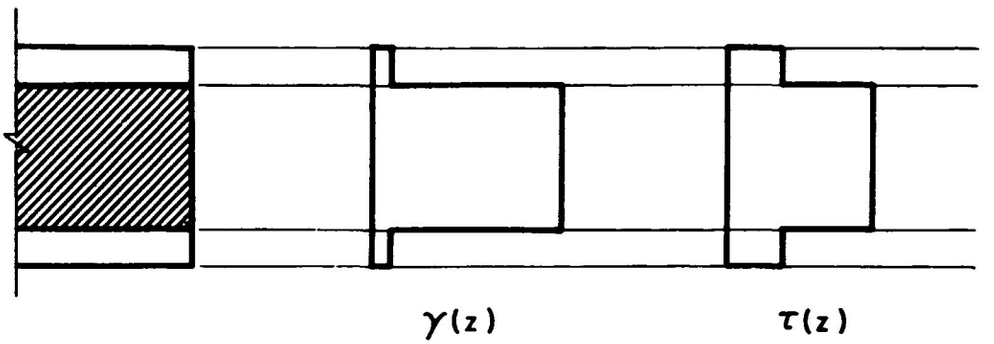

(b) PRESENT APPROXIMATE THEORY - SECTION FREE TO WARP

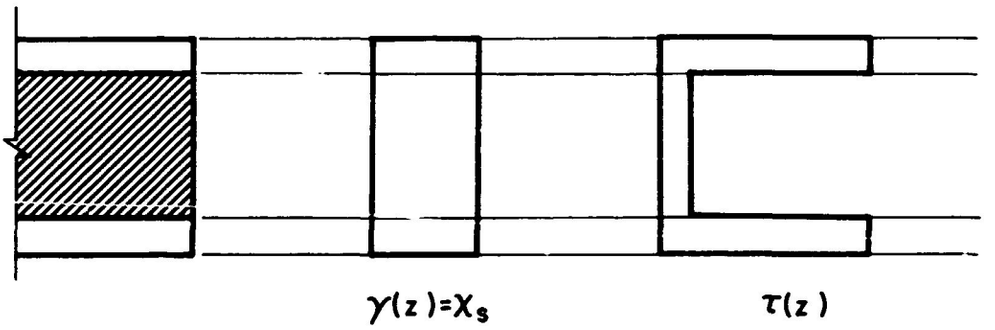

(c) PRESENT APPROXIMATE THEORY - UNWARPED SECTION

FIGURE III.10 APPROXIMATE SHEAR STRAIN AND STRESS DISTRIBUTIONS ($G_c << G_f$)

III.5.2 Uniformly Loaded Clamped Circular Plate

A circular plate with a relatively large ratio of the thickness to the radius is chosen so that the effect of shearing on the deflections is substantial. When the dimensions and properties of the plate are taken to be

$$h_c = 0.75" \ , \ h_f = 0.025" \ , \ h = 0.8"$$
$$E_f = 10^7 \text{ psi} \ , \ \nu_f = 0.3 \ , \ G_f = 3.85 \times 10^6 \text{ psi} \ , \ \kappa_f = 1$$
$$E_c = 2.6 \times 10^4 \text{ psi} \ , \ \nu_c = 0.3 \ , \ G_c = 10^4 \text{ psi} \ , \ \kappa_c = 1$$
$$\text{radius} \quad a = 5" \ , \ \text{load} \quad p_z = 1.0 \text{ psi}$$

the shear flexibility accounts for about 85% of the center deflection. The solution used for a comparison is a superposition of shear deflections after Plantema [12] and bending deflections after Timoshenko [132]. This solution does not take into account prevention of warping at the fixed circumference.

Finite element results are obtained using even meshes of 5, 10, and 20 elements with both linear (L) and quadratic (Q) shear models. Each representation is solved using the two possible fixed-edge boundary conditions, i.e., with warping prevented (U) and with warping allowed (W). In all cases, the shear stress resultants are correct to nine significant figures, so they are not shown graphically. This accuracy is to be expected since the true shear distribution is linear and thus can be represented exactly by either shear model. The bending moments do not differ significantly for the two representations of the boundary conditions or for the two shear models. However, there is some difference in the deflections for the various cases. When warping is prevented, the Q elements converge more rapidly to a final value than do the L elements. Figure III.11 shows that this value is within about 2% of

the deflections for the unwarped case. Thus linear-shear elements with boundary conditions that permit warping are probably sufficient to obtain the gross behavior. However, if one wishes to consider the distribution of the shear between core and facings, one must include the restraint on warping. In this case, the refined Q elements give more rapid convergence for displacements and shears (see Figures III.9 and III.11).

The radial moments for the clamped plate are shown in Figure III.12. Results of about the same quality, or slightly better, are obtained for the circumferential moments.

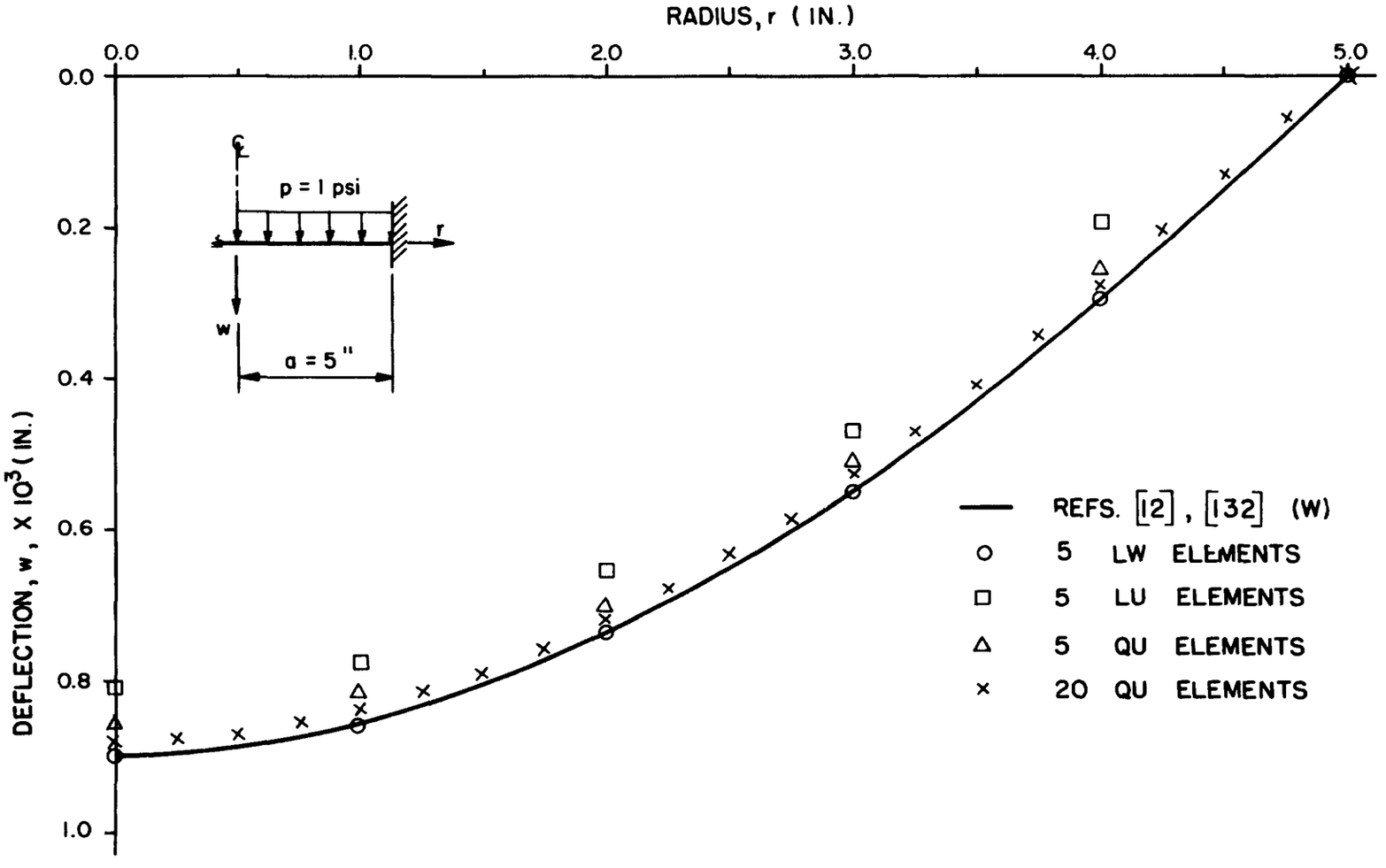

FIGURE III.11 DEFLECTIONS OF A CLAMPED CIRCULAR PLATE

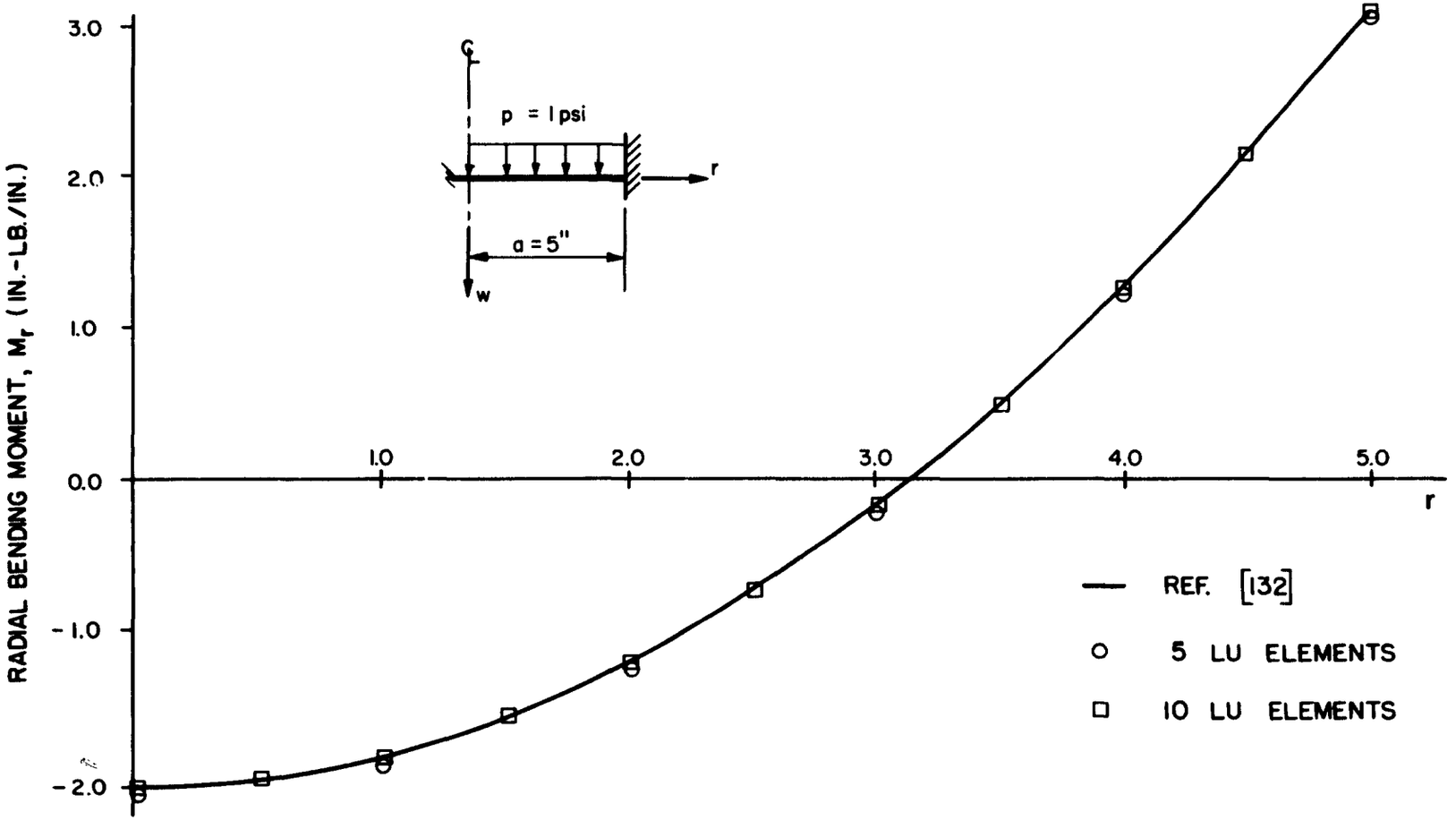

FIGURE III.12 RADIAL BENDING MOMENTS OF A CLAMPED CIRCULAR PLATE

III.5.3. Hemispherical Shell Under Membrane Load

In order to check the effectiveness of the basic element and of the computer program for shells, the membrane states of both cylindrical and spherical shells have been investigated. Generally, the results are satisfactory in that both deflections and stress resultants agree with theoretical values. A typical example is presented here. The sandwich hemisphere has the following properties:

$$h_c = 0.5" \ , \ h_f = 0.04"$$

$$E_f = 10^7 \text{ psi} \ , \nu_f = 0.3 \ , \ G_f = 3.85 \times 10^6 \text{ psi} \ , \ \kappa_f = 1.0$$

$$E_c = 2.6 \times 10^4 \text{ psi} \ , \ \nu_c = 0.3 \ , \ G_c = 10^4 \text{ psi} \ , \ \kappa_c = 1.0$$

$$\text{radius} \quad a = 100" \ , \ \text{load} \quad p_z = -1.0 \text{ psi}$$

Three- and nine-element representations are used with both linear shear and quadratic shear. Results are essentially the same for the two shear-strain models, so only the solution using the less refined model is presented here.

When roller supports that restrict only the meridional displacements at the free edges are used, the theoretical solution [132, 133] is given by

$$w = (1-\nu)\frac{p_z a^2}{2(Eh)_{eff.}} \ , \ u = 0$$

$$N_s = N_\theta = -\frac{p_z a}{2} \ , \ M_s = M_\theta = 0 \ , \ Q_s = 0$$

$$(Eh)_{eff.} = E_c h_c + 2E_f h_f$$

Substituting the proper values, one obtains

$$N_s = N_\theta = 50 \text{ lb./in.}$$

$$w = -0.004305"$$

The finite element solution for three elements is shown in Figure III.13. It is seen that the results agree very closely with the theoretical answers. The nine-element solution is even better, and is not shown since it does not differ significantly from the exact solution.

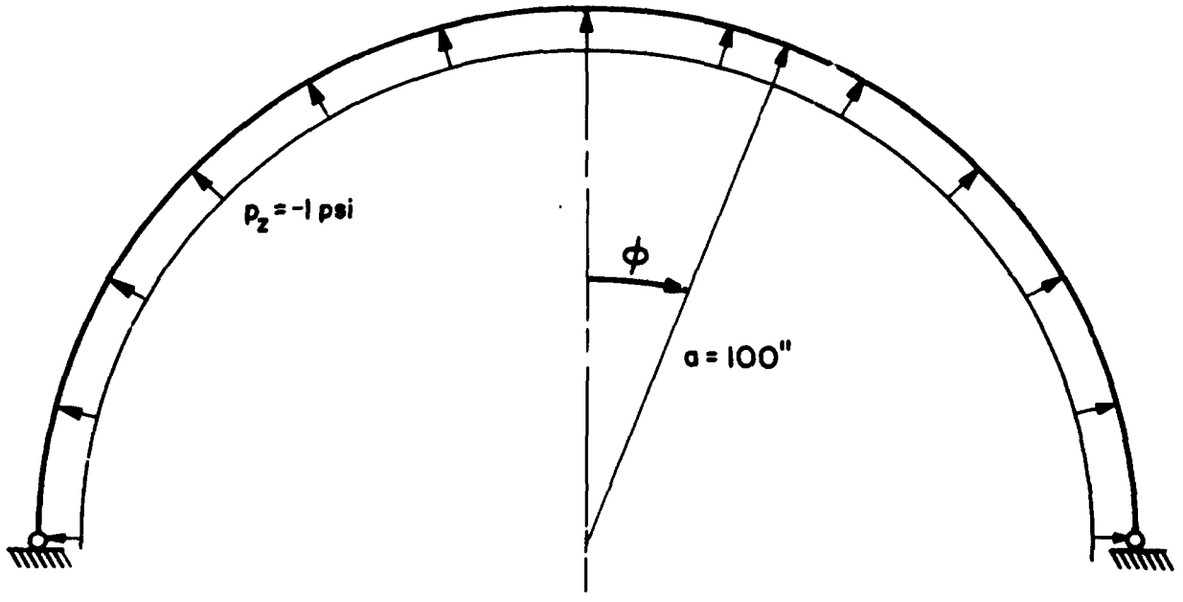

$\phi°$	$-w \times 10^2$ in.	$u \times 10^7$ in.	N_s lb./in.	N_θ lb./in.	Q_s lb./in.	M_s lb.	M_θ lb.
0	0.4306	0.0	49.993	49.993	0.0	0.0018	0.0018
30	0.4303	-0.46	49.987	49.981	0.0008	0.0020	0.0007
60	0.4303	0.69	49.978	49.974	0.0007	0.0022	0.0007
90	0.4302	0.0	50.023	49.981	0.0015	0.0011	0.0003

FIGURE III.13 HEMISPHERICAL SHELL UNDER MEMBRANE LOAD (THREE ELEMENTS)

III.5.4. Edge-Loaded Cylindrical Shell

A sandwich cylinder with the following properties is examined next:

$$h_c = 0.5" \ , \ h_f = 0.04" \ , \ h = 0.58"$$

$$E_f = 10^7 \text{ psi} \ , \ \nu_f = 0.3 \ , \ G_c = 10^4 \text{ psi} \ , \ \kappa_c = 1$$

$$\text{radius} \quad a = 20"$$

$$\text{end shear} = 1.0 \text{ lb./in.} \ , \ \text{end moment} = 1.0 \text{ in-lb./in.}$$

The core bending and extension and the face shearing are neglected by taking

$$E_c = 0 \ , \ G_f = 10^{20} \text{ psi} \ , \ \kappa_f = 1$$

These effects have been omitted in order to compare the results to Reissner's solution for a semi-infinite cylinder [16].

In approximating a semi-infinite cylinder by a finite one, two different types of boundary conditions at the unloaded edge are possible. Constraint on both meridional translation and bending rotation at this edge provides a better approximation than constraint on meridional translation alone. The cylinder is represented by even meshes of 10 and 20 elements with element lengths of one inch and one-half inch. Linear shear-strain elements are used. Results are shown in Figures III.14 through III.17. It is seen that the total length of the finite element representation is an important consideration. Despite a fine mesh, the representation using 10 one-half inch elements for a total length-radius ratio of 1/4 is inadequate. Satisfactory results are obtained with 10 one-inch elements and the other two meshes provide further refinement.

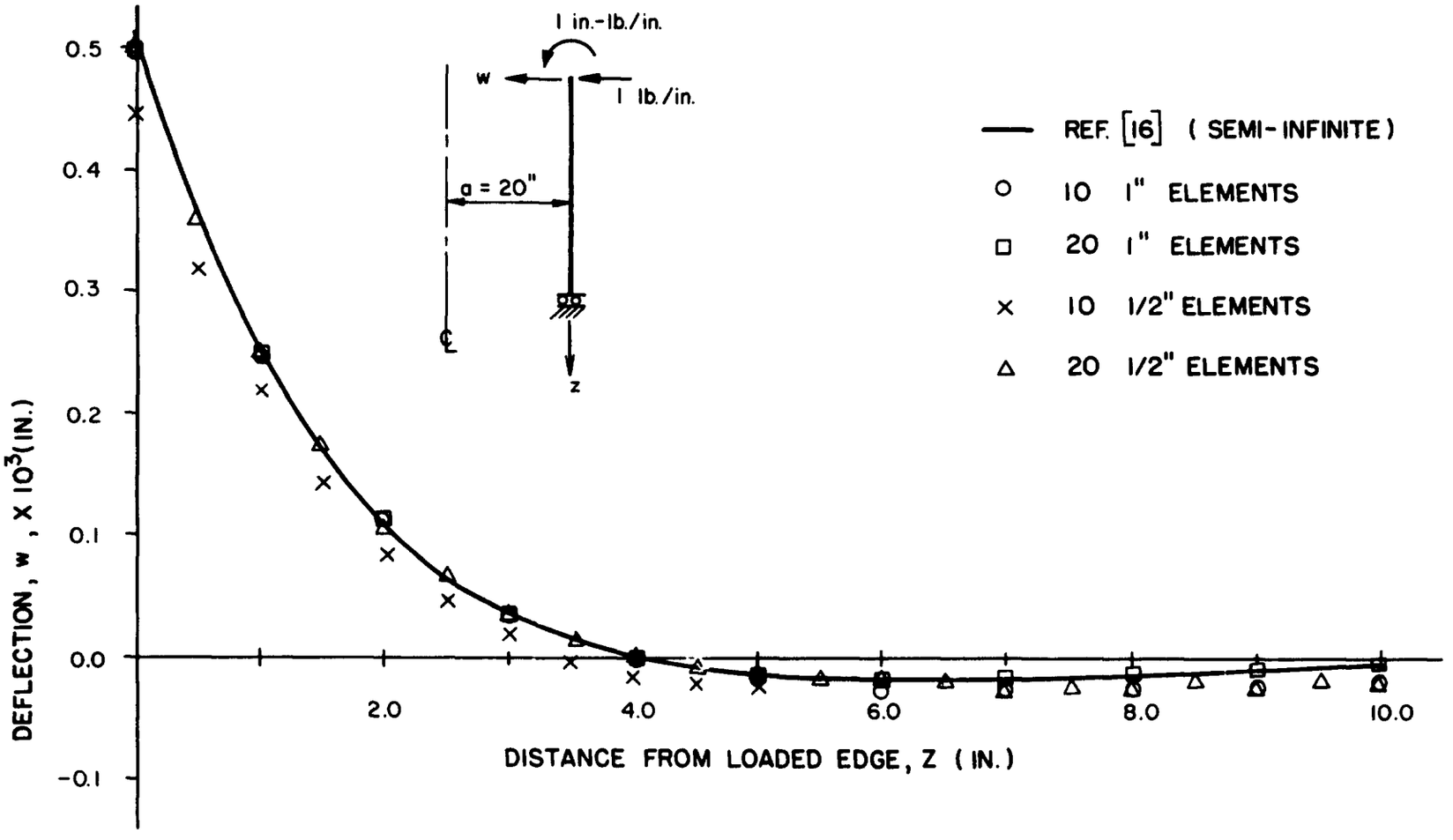

FIGURE III.14 DEFLECTIONS OF AN EDGE LOADED CYLINDER

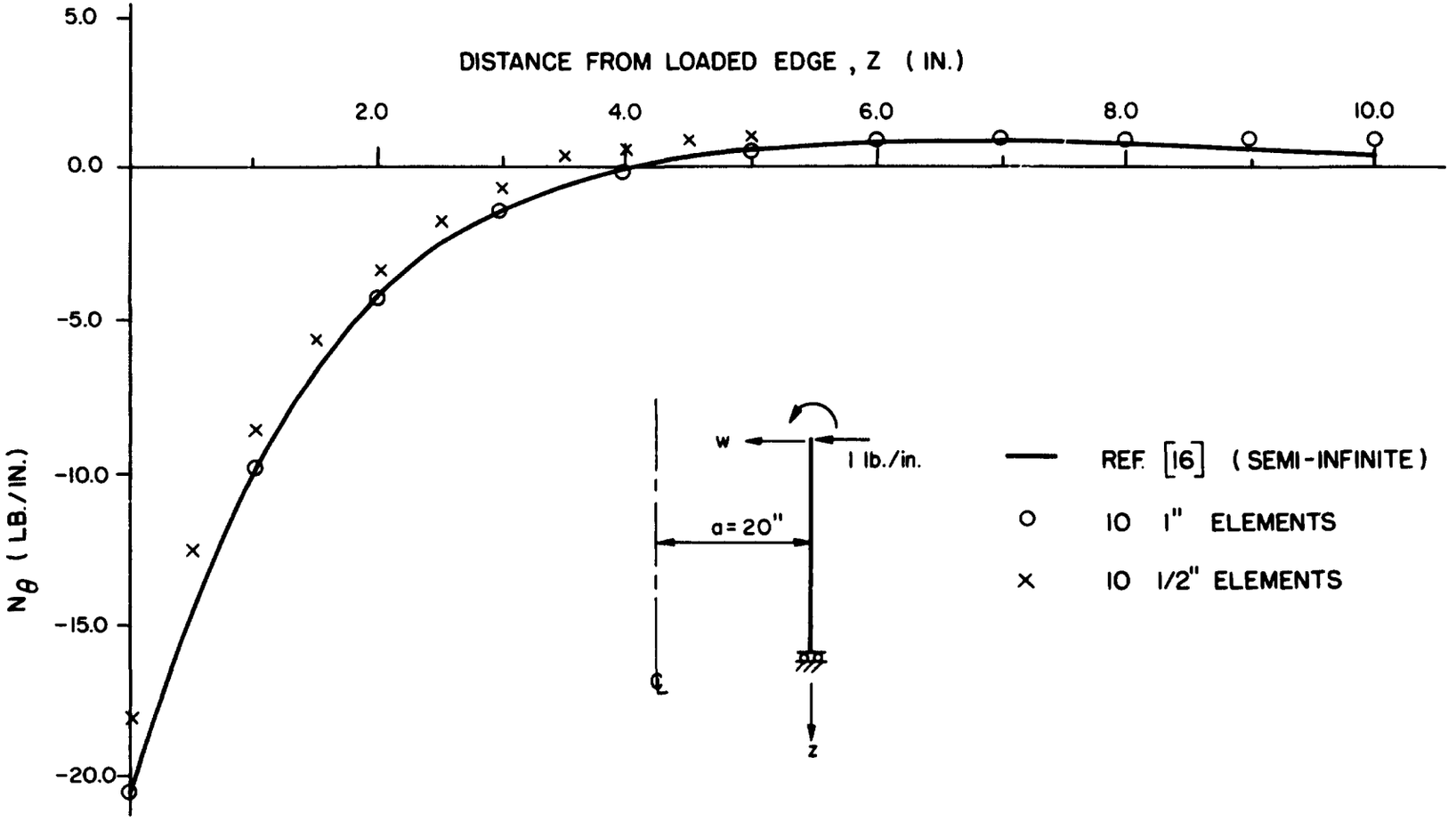

FIGURE III. 15 CIRCUMFERENTIAL STRESS RESULTANT OF AN EDGE LOADED CYLINDER

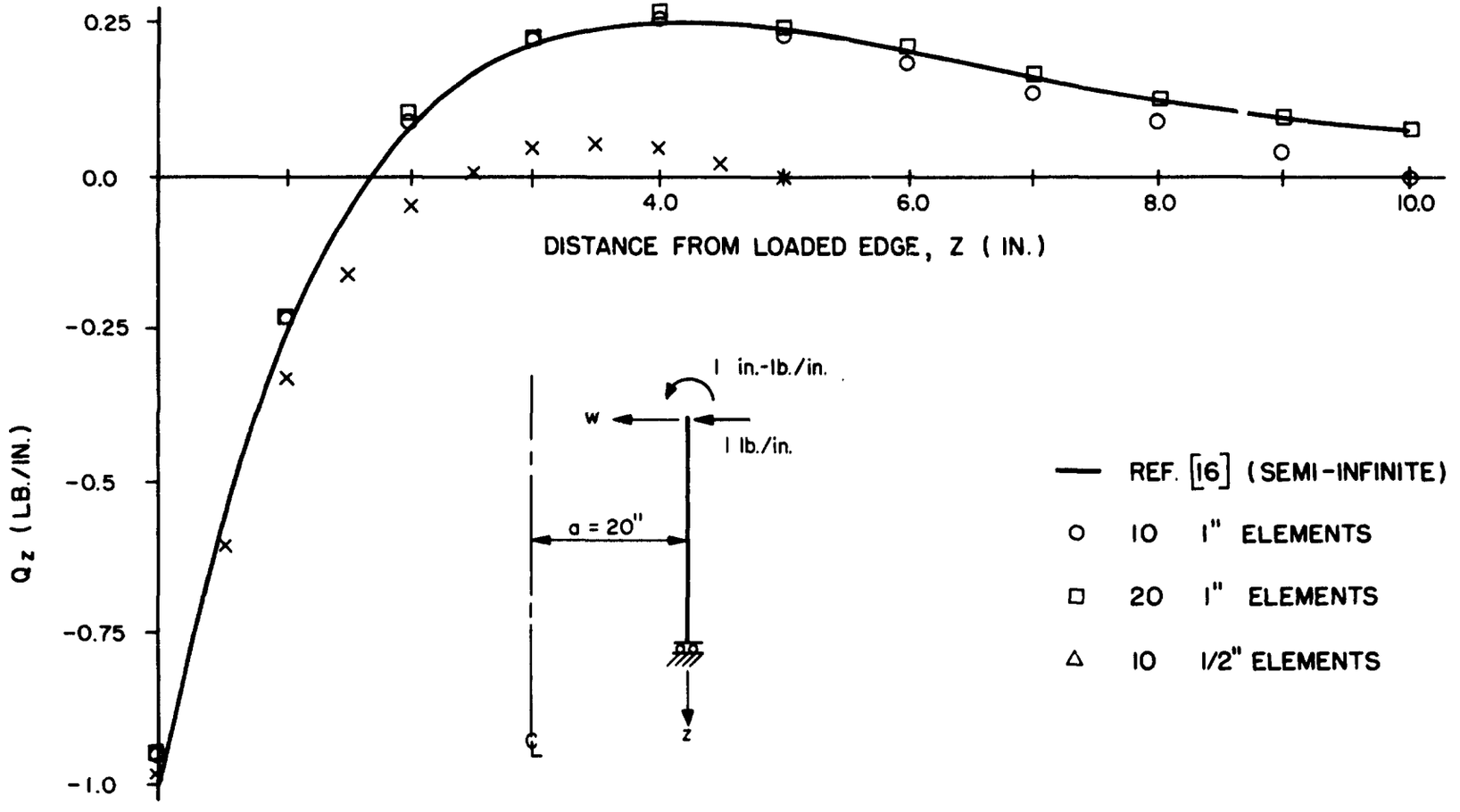

FIGURE III.16 SHEAR STRESS RESULTANT OF AN EDGE LOADED CYLINDER

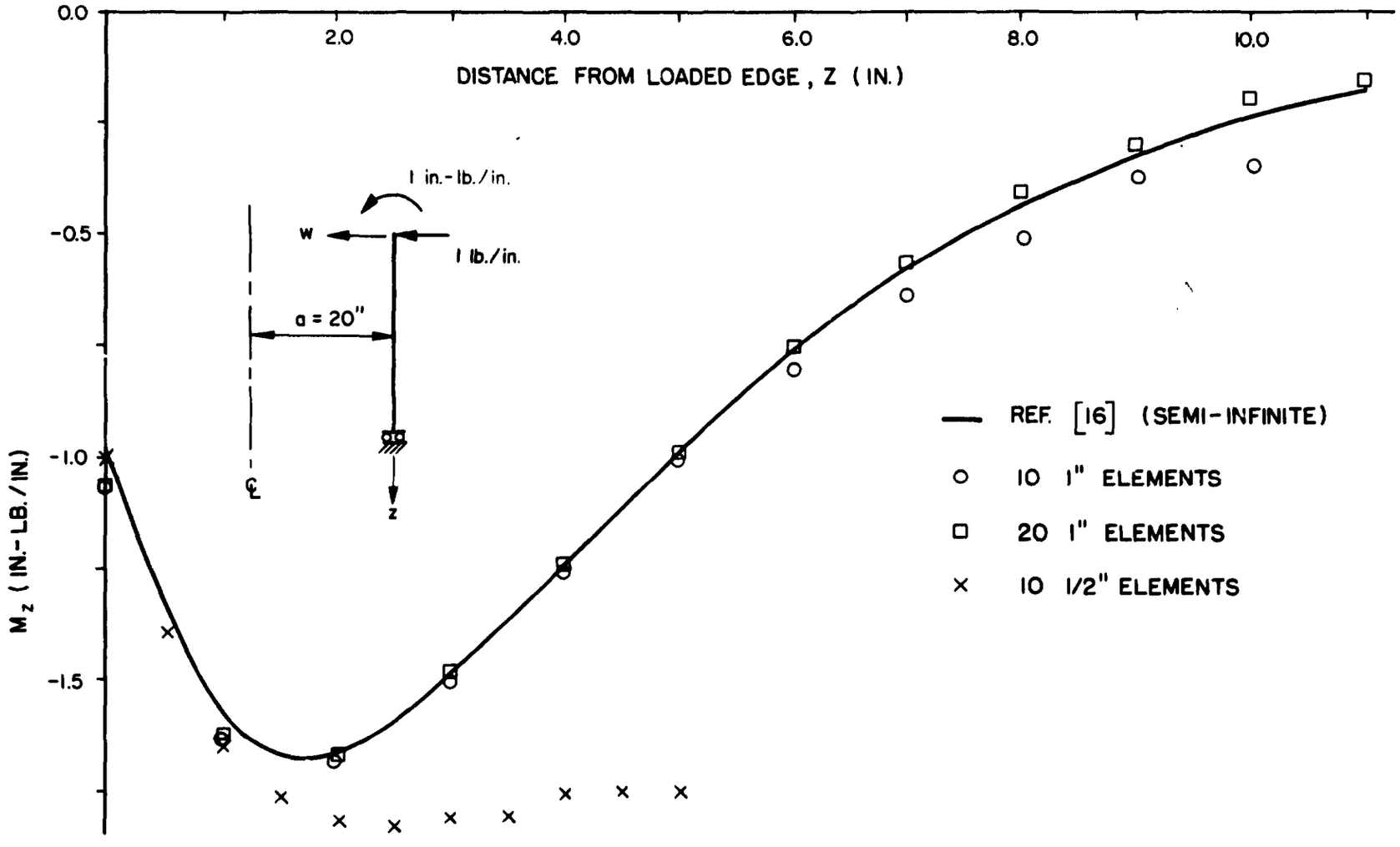

FIGURE III.17 MERIDIONAL MOMENTS OF AN EDGE LOADED CYLINDER

III.5.5. Shallow Spherical Cap with Partial Distributed Loading

The final shell problem presented here is a simply supported shallow spherical cap subject to distributed loading over a portion of its surface. The closed-form solution for this problem in terms of Thomson functions has been given by Rossettos [52]. He neglects the shearing of the facings and the bending and extension of the core, so the following properties are selected:

$$h_c = 0.95" \ , \ h_f = 0.025" \ , \ h = 1"$$

$$E_f = 10^7 \text{ psi} \ , \ \nu_f = 0.3 \ , \ G_f = 10^{20} \text{ psi} \ , \ \kappa_f = 1$$

$$E_c = 0 \ , \ G_c = 10^5 \text{ psi} \ , \ \kappa_c = 1$$

$$\text{radius} \quad a = 20" \ , \ \text{supported edge at} \ \phi = 15^\circ$$

A uniform load of 1 psi is applied in the axial direction over that portion of the surface given by $0 \leq \phi \leq 3^\circ$.

The cap is analyzed using 5 and 10 linear-shear elements. Deflection results are presented in Figures III.18 and III.19, and stress resultants are plotted in Figures III.20 to III.22. In general, satisfactory results are obtained from the 5-element representation. The small difference between the 5- and 10-element results indicates that the finite element solution has effectively converged.

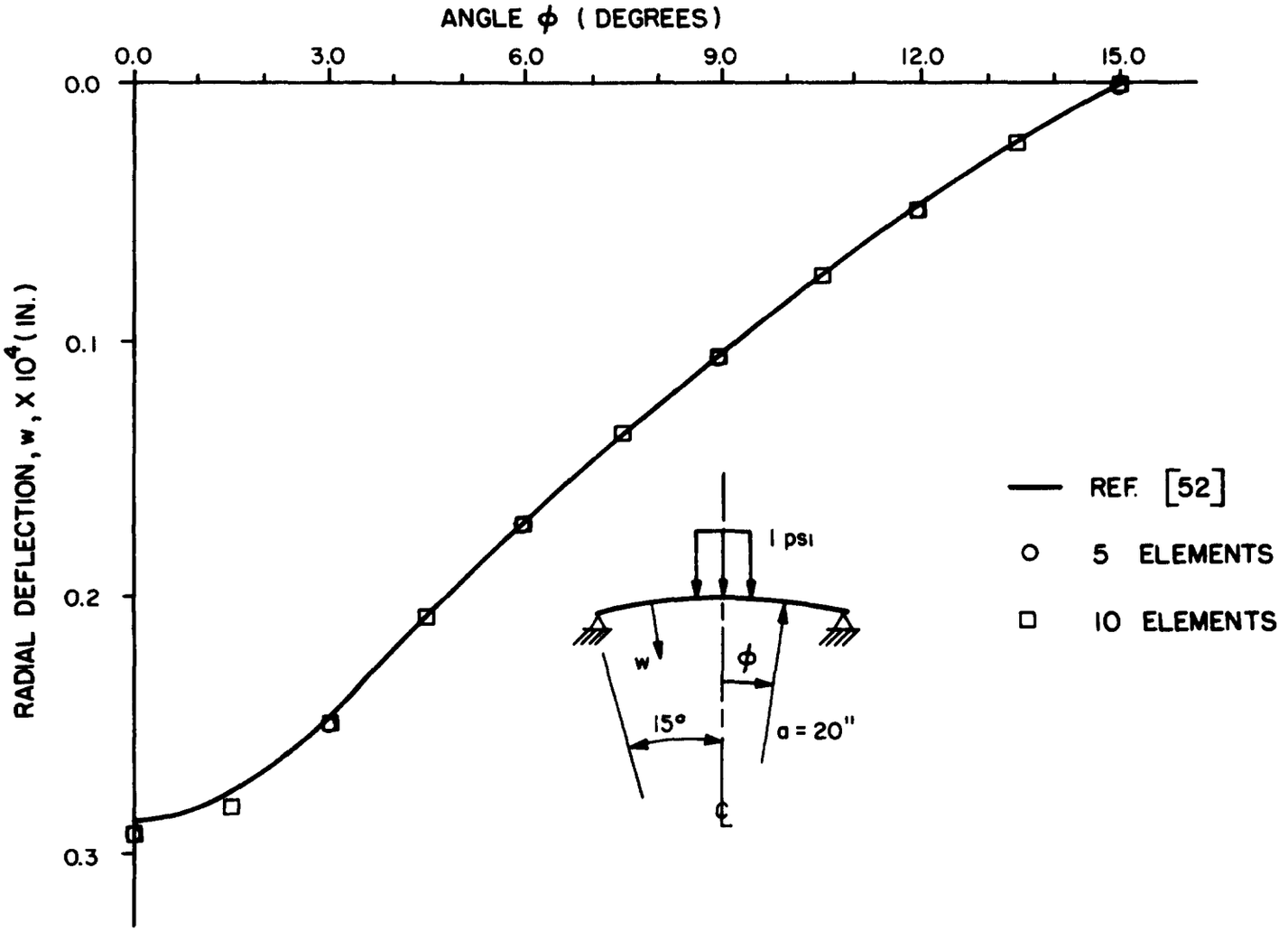

FIGURE III.18 RADIAL DISPLACEMENT OF A SHALLOW SPHERE

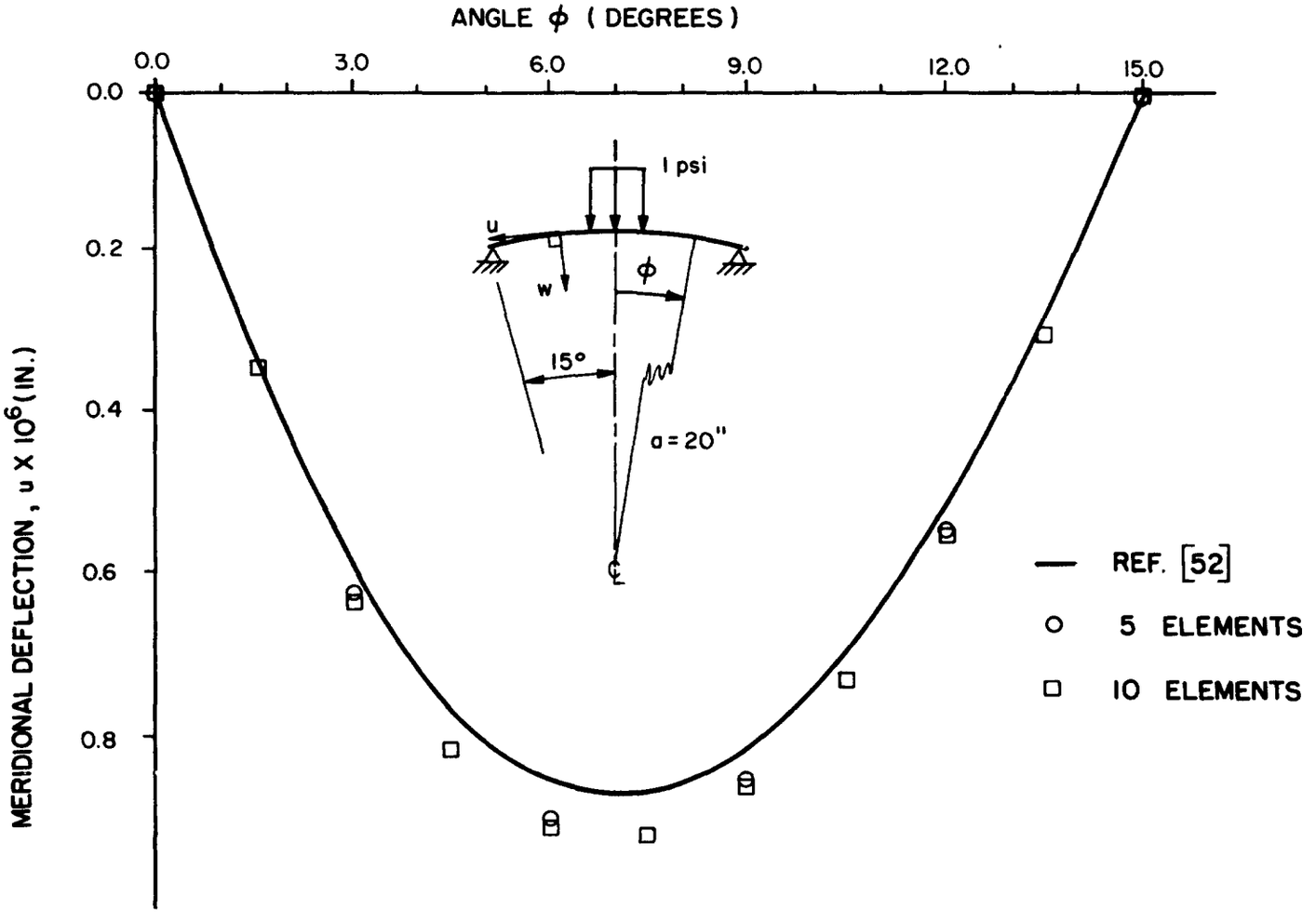

FIGURE III.19 MERIDIONAL DISPLACEMENT OF A SHALLOW SPHERE

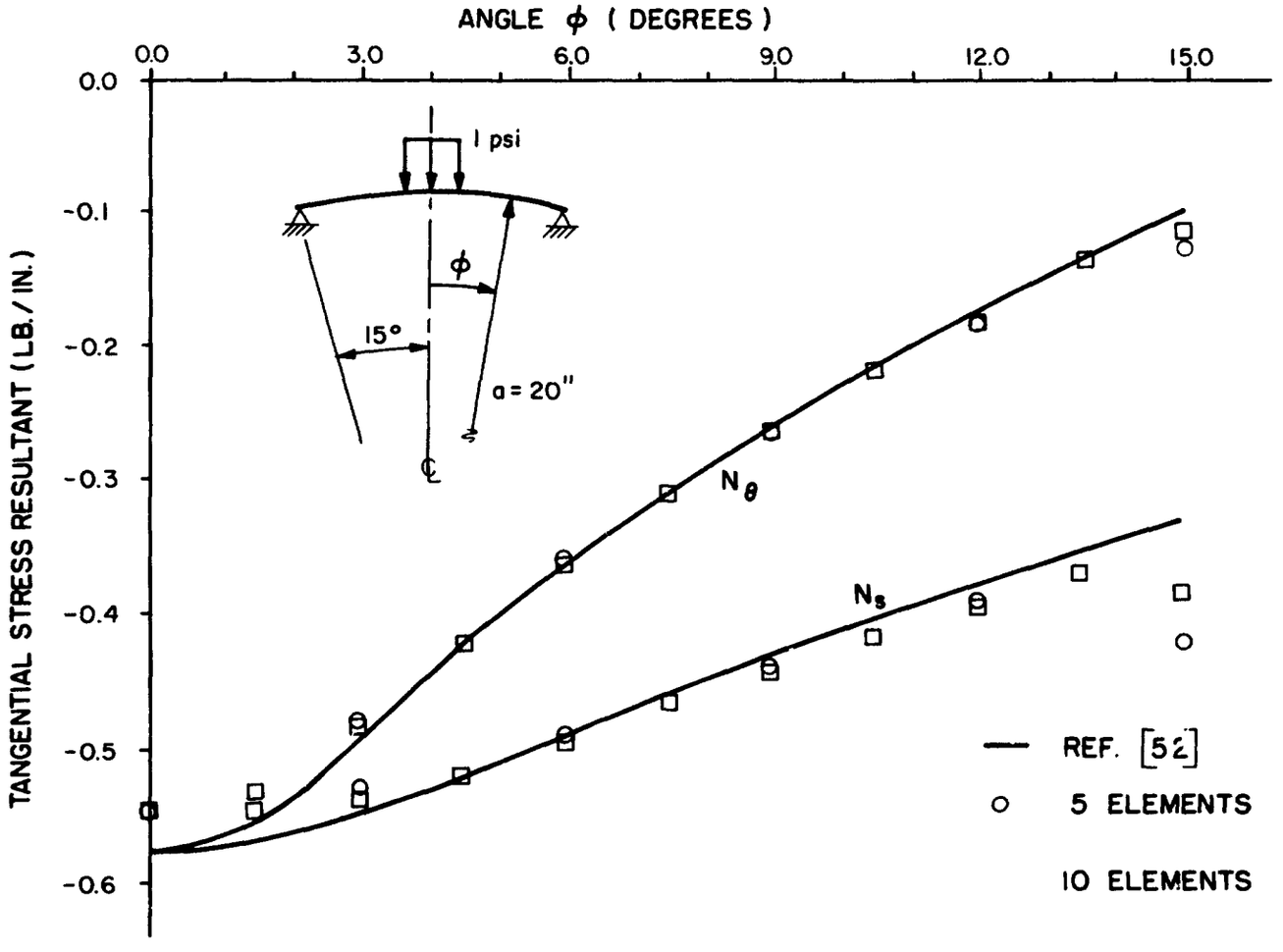

FIGURE III.20 TANGENTIAL STRESS RESULTANTS OF A SHALLOW SPHERE

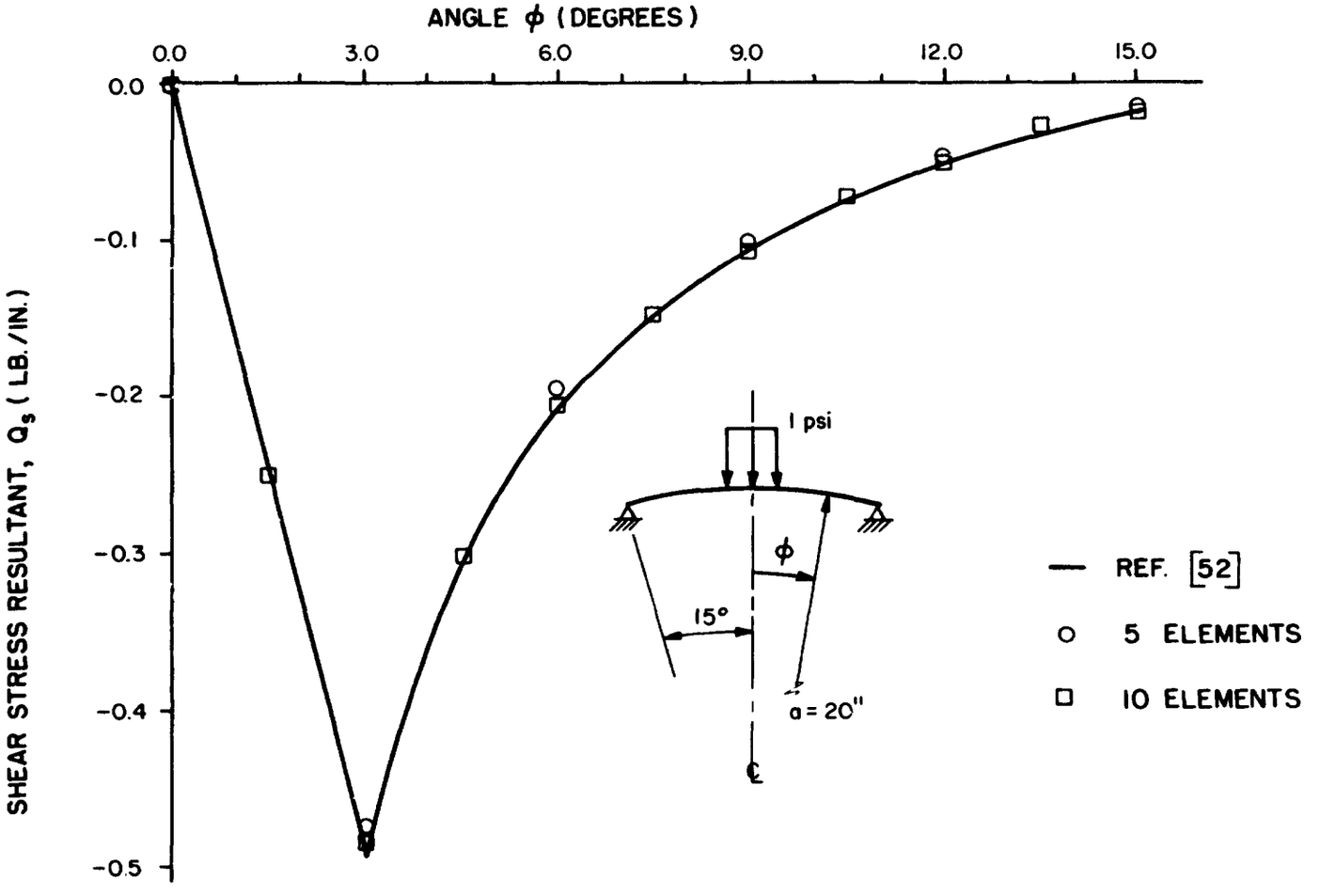

FIGURE III.21 SHEAR STRESS RESULTANT OF A SHALLOW SPHERE

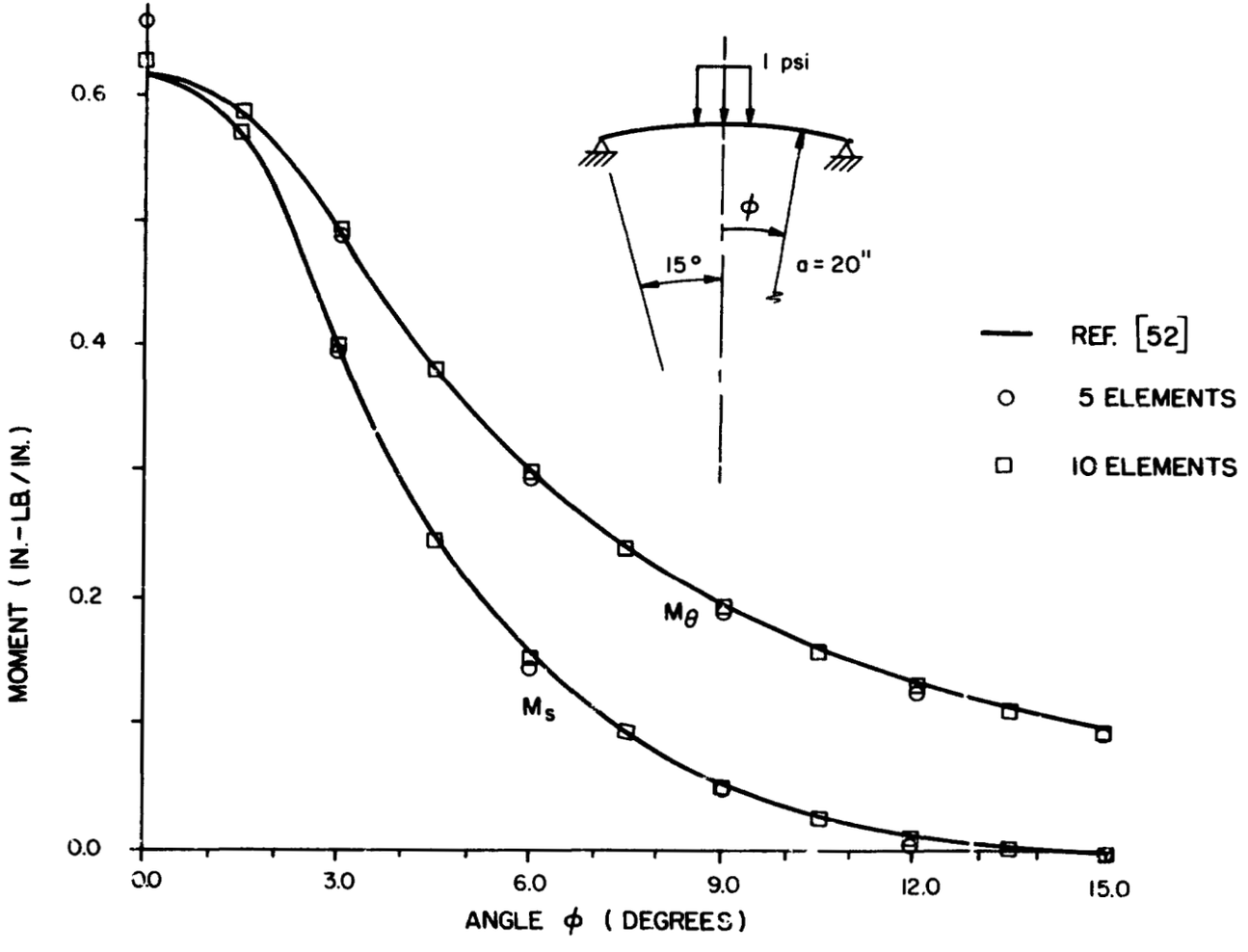

FIGURE III.22 MOMENTS OF A SHALLOW SPHERE

III.5.6. Effect of Various Contributions to Beam Stiffness Matrix

Various approximations are possible in analyzing sandwich structures. Any one or combinations of the following may be neglected: (1) shearing of the facings, (2) bending of the facings about their own middle surface, (3) bending of the core about its middle surface and stretching of the core, and (4) shearing of the core. Generally, the stretching of the facings is not neglected. In addition, approximation (4) would not be valid for sandwich construction with the typical properties used in the preceding examples. However, since the present theory places no restriction on the ratios of layer thicknesses and properties, the approximation may be applied to other configurations. The effect of each of these approximations can be evaluated with the finite element method by choosing an appropriate value of the modulus when computing a contribution to the stiffness matrix. For approximations (1) and (4) the shear modulus of the corresponding layer is set to a very large value (e.g., 10^{20} psi) and for approximations (2) and (3) the Young's modulus of the proper layers is set to zero. The resulting solutions are compared to the case for which none of the effects in question are neglected.

This process is now applied to a simply supported beam subject to a uniformly distributed load and represented by ten linear-shear elements. The basic beam has a unit width and depth, a face modulus of $E_f = 10^7$ psi and a Poisson ratio of 1/3 for both face and core. It is assumed that the shear stress correction factors are unity. Various values of the following ratios are selected in order to vary the parameters that affect the solution:

$$r_h = h_f/h_c$$

$$r_L = h/L$$

$$r_g = G_f/G_c = E_f/E_c$$

where L is the span length and the other parameters have been defined previously. A set of curves for fixed values of r_h and r_L and a variation of r_g is shown in Figure III.23. The ordinates, which are percent errors, are based upon the average value of the ratio of the displacements for the approximate and "exact" cases. Families of such curves could be generated if desired. Koch [30] has already published several such curves for beams and plates using certain simplifying assumptions.

Although the errors due to approximations for different specific configurations (e.g., simply supported beams vs. cantilever) may be somewhat different, the trend is the same; and some generalizations may be made from curves for simple structures. For example, in Figure III.23, increasing values of r_g correspond to cores which are increasingly weak with respect to the facings. As the curves indicate, large errors may be expected from neglecting the bending of a strong core or the shearing of the weak core. A further interesting conclusion is that the bending of the facings about their own middle surface is significant for very weak cores, despite the fact that the facings themselves are very thin. This may be explained by the fact that for high values of r_g, the bending stiffness of the facings plays an important role in causing the core to deform in shear. Hence the face bending is significant because of its effect on another mechanism of the flexural action.

FIGURE III.23 EFFECTS OF CONTRIBUTIONS TO BEAM ELEMENT STIFFNESS

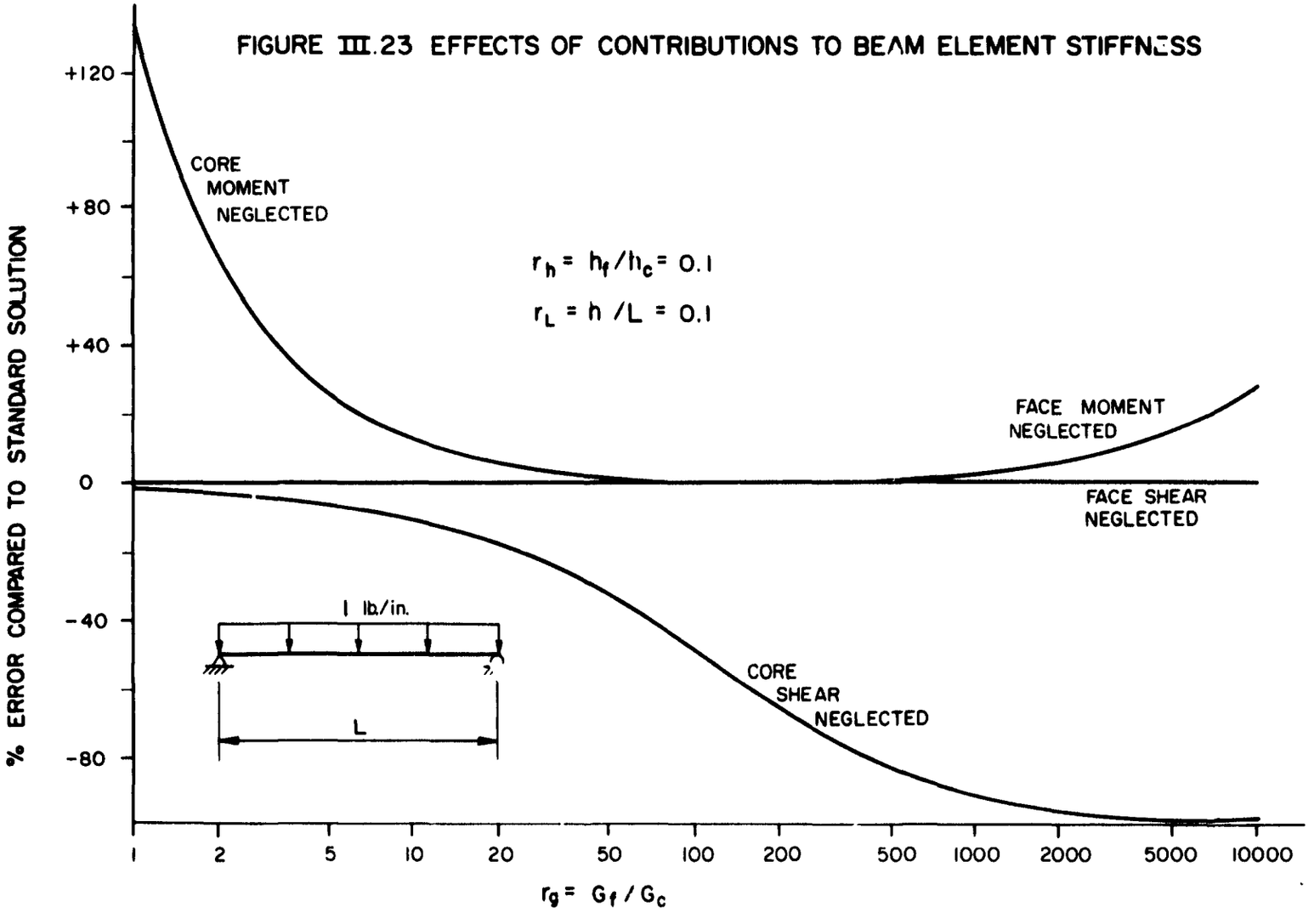

III.5.7. Discussion of Examples

The above results demonstrate the potential of the finite element method of analysis for sandwich structures. Although no examples are presented for closed shells which are not shallow, the computer program is capable of solving them. The reason such examples are not included is the absence of published solutions with which to compare them. The main purpose the examples has been to demonstrate that the finite element analysis converges to known solutions.

Insofar as the warping phenomenon due to shear is approximated, the finite element results are superior to those from some approximate sandwich theories which neglect this effect. In particular, the shearing stiffness of the facings becomes important at fixed supports where warping is prevented and at concentrated transverse loads. A common assumption for sandwich construction is that all the shearing is taken by the core [12]. Hence the facings are assumed to be infinitely stiff in shear. However, if the core carries all of the shear at a section where warping is prevented, the facings must be considered infinitely flexible at such sections. Unless this inconsistency is eliminated by recognizing that the facings must carry a significant portion of the shear at these locations, the resulting deflections will be too large. This difficulty has been recognized by Plantema [12]. (The corresponding phenomenon for homogeneous beams is discussed by Timoshenko [129]). The present finite element formulation permits determination of the distribution of shear between the facings and the core. This is illustrated by the first two examples above.

The relative advantages of linear and quadratic shear models are also illustrated in the examples. For the one-dimensional problems considered here, the use of quadratic shear introduces two extra equations in the

static condensation for each element. The advantage of the refinement is that, where there is a rapid variation of shear, the quadratic shear representation will produce satisfactory results with a coarser mesh. On the other hand, the moments may only vary linearly along the length when a cubic transverse displacement and a quadratic shear strain are used. With this limitation on the variation of the moments, it is perhaps inconsistent to have a more refined model for the shear because a relatively fine mesh may be needed to obtain accurate moments. However, for structures which cannot warp freely in shear, the variation of the distribution of shear between core and facings is very rapid near restrained sections. Indeed, this variation is exponential [12] and is usually more pronounced than the variation of moment over the same length. Thus for some problems the refined shear model seems justified.

The deflection of homogeneous beams including the effect of shear was studied by using the same properties for facings and core and by making the facing thickness very small in relation to the core thickness. Then with the value of $\kappa_c = 2/3$, which is appropriate for rectangular cross-sections, the deflections are identical with those given by Timoshenko [129].

When the shear is neglected by setting the shear modulus to an extremely large value, the finite element solutions for homogeneous structures (same material properties for core and facings) reduce to the classical solutions. For rotational shells, this means the results become exactly the same as those obtained by Khojasteh-Bakht's finite element analysis for elastic problems [84]. For beams and circular plates, the solutions closely approximate those of elementary theory [129, 132].

CHAPTER IV: FREE VIBRATION ANALYSIS OF ELASTIC SANDWICH STRUCTURES

IV.1. Lumped Translational and Rotatory Inertia

The mass of the structure is concentrated at the nodal points so that the inertial properties can be represented by a diagonal mass matrix. Felippa [57, 59] has demonstrated that this lumped mass procedure provides satisfactory fundamental frequencies and mode shapes with less computational effort than the consistent (or distributed) mass approach. For the same number of nodal points, the former method results in fewer equations for the eigenvalue problem. When meshes are arranged so there are the same number of eigenproblem equations for both techniques, Felippa's results for homogeneous plates indicate that the lumped mass approach produces the more accurate frequencies. The consistent mass method is less efficient than the lumped mass scheme for two main reasons. First, static condensation (Section I.2.6) cannot be applied to consistent mass systems. Second, additional condensation can be carried out for the lumped mass representation on the external degrees of freedom which do not correspond to concentrated masses. This process is prescribed in Section IV.2.

IV.1.1. Arrangement of Lumped Masses

Rotatory inertia has been shown to be a more important factor in the vibration of sandwich plates [34] than in the dynamics of homogeneous plates [72]. The effects of this type of inertia is discussed in Section IV.3. In this section a physical interpretation of the lumping process is given.

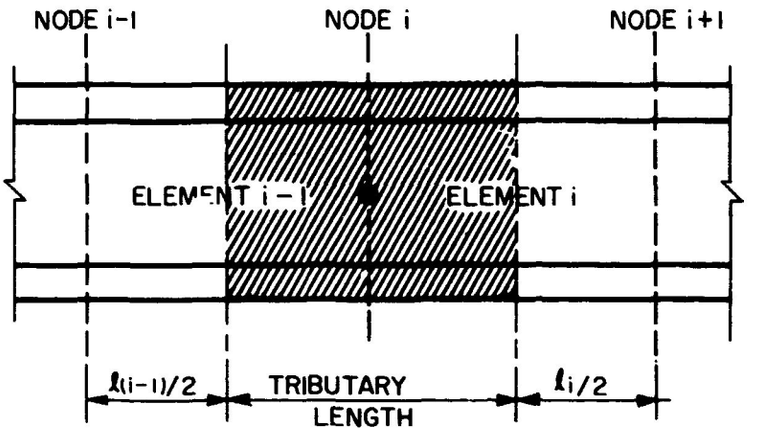

(a) LUMPED MASS FOR TRANSLATIONS

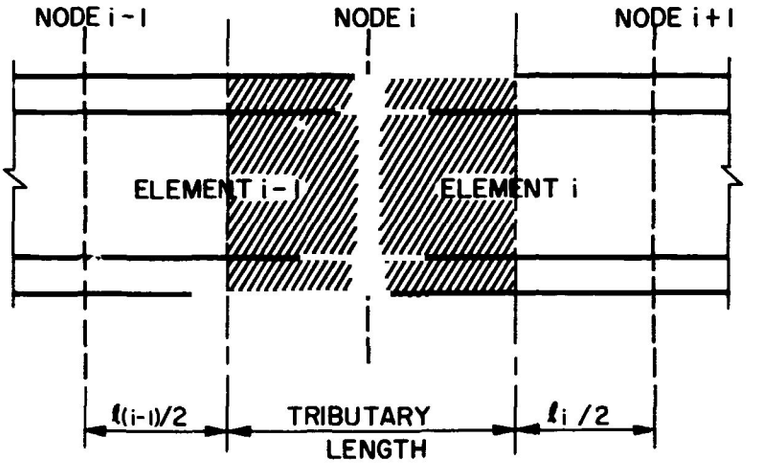

(b) LUMPED MASS FOR ROTATION

FIGURE IV.1 ARRANGEMENT OF LUMPED MASSES

For translational displacements it is sufficient to idealize the lumped mass as a point on the reference surface (Figure IV.1a). However, for rotatory effects, the distribution of the mass through the depth of the beam must be maintained. This is especially true for sandwich structures where the outer-most layers, the facings, may be much denser than the core. Hence, one can visualize the mass as being lumped along the material line originally normal to the reference surface, with no concentration of the mass across the depth (Figure IV.1.b). In effect, this is the same as multiplying the mass moment of inertia of the cross section by the tributary area.

It should be noted that the rotatory inertia is associated with the rotation of the normal to the reference surface, i.e., χ_b . This displacement is chosen as an external degree of freedom at each node (Section II.1.5). The lumped rotatory inertia thus corresponds to this degree of freedom in assembling the equations of motion.

IV.1.2. Determination of Tributary Area

For beams the determination of the tributary area is elementary. It is merely the product of the width and the length of half of each of the adjacent elements (Figure IV.1). For rotational shells of arbitrary meridian, the calculation is more difficult. A logical procedure would be to divide the area of each element at a circumference which is equivalent to the centroid of the area. However, the determination of this centroid would require more information than is needed to construct the substitute element (Section III.3). Hence the tributary area for each node is taken as that area of the two adjacent substitute elements between the node and the points on the meridian where the local co-ordinates ξ are $\frac{1}{2}$. This representation will be

most accurate for shells approaching a cylindrical configuration and least accurate for very flat shells and circular plates. Nevertheless, as the mesh is refined, the difference between the centroid and the point $\xi = \frac{1}{2}$ diminishes. Therefore, this approximate approach is consistent with the other approximations in geometry that are used for the finite element method.

The element of area of the shell reference surface is given by

$$da = 2\pi r(\xi)\, ds = 2\pi \ell \frac{r(\xi)}{\cos \beta}\, d\xi$$

This is integrated over the appropriate range of ξ using Gauss' integration formula simultaneously with the similar numerical integrations for the element stiffness. Whereas a ten-point integration is used for the stiffness for $0 \leq \xi \leq 1$, five-point summation is employed for each of the areas $0 \leq \xi \leq \frac{1}{2}$ and $\frac{1}{2} \leq \xi \leq 1$.

IV.2. Formulation of the Eigenvalue Problem

In the absence of velocity-dependent damping, the equations of motion in matrix form may be written

$$[M]\{\ddot{v}(t)\} + [K]\{v(t)\} = \{V(t)\} \qquad \text{(IV.1)}$$

where $\{V(t)\}$ are the nodal forces, $\{v(t)\}$ are the nodal displacements, $[M]$ is the mass matrix and $[K]$ is the stiffness matrix for the overall structure. Following the usual procedure for free vibrations, the displacements of the unloaded structure are assumed to be harmonic with frequency ω

$$\{v(t)\} = \{w\}\cos \omega t$$

$$\{V(t)\} = \{0\}$$

where $\{w\}$ is the vector of displacement amplitudes. As a result, the accelerations are proportional to the displacements

$$\{\ddot{v}(t)\} = -\omega^2\{v(t)\} = -\omega^2\{w\}\cos \omega t$$

and the eigenvalue problem is stated as

$$[K]\{w_i\} = \omega_i^2[M]\{w_i\} \qquad \text{(IV.2)}$$

However, standard computer subprograms for determining eigenvalues and eigenvectors of a symmetric matrix are based upon the formulation

$$[X]\{x_i\} = \lambda_i\{x_i\} \ . \qquad \text{(IV.3)}$$

Therefore, the vibration problem of Equation (IV.2) must be reduced to the standard form (IV.3)

Felippa [57, 59] advocates a technique which simultaneously transforms the equations to standard form and condenses the degree of the problem. This method is efficient in that it gives numerically accurate results and also uses and preserves the banded nature of $[K]$. Felippa's approach is adopted here and is now described.

With the lumped mass procedure, the mass matrix is diagonal and is thus designated $[\bar{M}]$. Moreover, non-zero elements occur on the diagonal only in positions corresponding to degrees of freedom which are associated with concentrated masses. For the problem under consideration, these degrees of freedom are the translations and, if rotatory inertia is included, the rotations due to bending. Conversely, there are no masses associated with the warping. Only the equations that involve the non-zero elements need be retained in the eigenvalue problem. If the total number of equations is N and the number of lumped masses is $N_r < N$, the following sets of equations are solved

$$[K]\{f_i\} = \{e_i\} \ , \ i = 1, \ \ldots, \ N_r \qquad \text{(IV.4)}$$

The stiffness $[K]$ has already been triangularized by the method given in Section II.3, so the solutions (IV.4) are efficiently achieved. The vector $\{e_i\}$ is a unit vector with zeros at all locations except the one corresponding to the i^{th} lumped mass. As a result, $\{f_i\}$ is the column of the flexibility matrix

$$[F] = [K]^{-1}$$

and, specifically, is the column associated with the i^{th} lumped-mass degree of freedom. It is possible to select the N_r elements of each of the $\{f_i\}$ vectors which correspond only the concentrated masses and thus to construct the $N_r \times N_r$ flexibility $[\bar{F}]$. In effect, the N^{th} degree eigenvalue problem of Equation (IV.2) has now been reduced to

the N_r^{th} degree eigenvalue problem

$$[\bar{F}][\bar{M}]\{\bar{w}_i\} = \frac{1}{\omega_i^2}\{\bar{w}_i\} \quad , \; i = 1, \ldots, N_r \qquad \text{(IV.5)}$$

This equation is readily transformed to standard form (IV.3) by premultiplying by $[\bar{M}]^{\frac{1}{2}}$, the diagonal matrix whose elements are the square root of those of $[\bar{M}]$. Hence

$$[X]\{x_i\} = \lambda_i\{x_i\} \quad , \; i = 1, \ldots, N_r \qquad \text{(IV.3)}$$

where

$$\begin{aligned} [X] &= [\bar{M}]^{\frac{1}{2}}[\bar{F}][\bar{M}]^{\frac{1}{2}} \\ \{x_i\} &= [\bar{M}]^{\frac{1}{2}}\{\bar{w}_i\} \\ \lambda_i &= 1/\omega_i^2 \end{aligned} \qquad \text{(IV.6)}$$

An advantage of this formulation of the problem is that the smallest frequencies ω_i correspond to the largest eigenvalues λ_i . Because eigenvalue programs generally compute roots to within an absolute tolerance, the largest λ_i will have the smallest relative error.* In the computer program, the flexibility matrix $[\bar{F}]$ is not separately computed in its entirety. As each column of $[\bar{F}]$ is obtained from

---

*An alternate approach to formulating the reduced eigenvalue problem in standard form would be to perform a static condensation (Section II.2.6) on the degrees of freedom not corresponding to lumped masses. Then the reduced problem

$$[\bar{K}]\{\bar{w}_i\} = \omega_i^2[\bar{M}]\{\bar{w}_i\}$$

can be transformed by premultiplying by $[\bar{M}]^{-\frac{1}{2}}$. However, the disadvantages of this procedure are that (1) the banded nature of [K] is destroyed in rearranging rows and columns for the condensation and (2) lowest frequencies correspond to lowest eigenvalues.

Equations (IV.4), it is modified using Equation (IV.6a) to construct the corresponding portion of $[X]$.

Once the eigenvectors $\{\ _i\}$ have been found for the standard form, the complete mode shapes can be recovered using the triangularized stiffness matrix. Inertial loads of the form

$$\underset{N_r x 1}{\{\bar{p}_i\}} = \omega_i^2[\bar{M}]\{\bar{w}_i\} = \omega_i^2[\bar{M}]\bar{\bar{2}}\{x_i\} \qquad \text{(IV.7)}$$

are expanded to $N \times 1$ by the addition of zero elements corresponding to the condensed degrees of freedom. When these are applied to the structure using

$$[K]\{w_i\} = \{p_i\} \qquad \text{(IV.8)}$$

the solution of the equations gives the desired mode shape.

IV.3. Vibration Modes

Like the dynamic analysis of homogeneous shells and plates, the study of the free vibrations of sandwich structures is primarily concerned with the most fundamental modes of deformation. These modes correspond to the lowest branches of the frequency equation for three-dimensional theory. However, the relative importance of the various types of behavior is different for homogeneous and sandwich structures. In particular, the thickness shearing modes are of lesser importance for the homogeneous case since they occur at extremely high frequencies in relation to the pure flexural deformations. This is not necessarily true for sandwiches because they are more flexible in shear. Depending upon the nature of the vibration environment and upon the properties and configuration of the sandwich structure, the thickness-shear modes may be quite significant.

Thickness-shear deformations are those in which the shearing across the depth of the structure is predominant. Thus, for the three-layered construction used in the examples of this dissertation, the mode is characterized by a tangential displacement of one facing relative to the other. In terms of the displacement parameters of the finite element method, for thickness-shear behavior the slope due to bending, χ_b , and that due to shear, χ_s , are of opposite sign at any location on the reference surface. Because the shearing deformation is so closely related to the rotation of the structure cross-sections, it is necessary to include the rotatory inertia. Otherwise the mode will not appear in the free vibration analysis.

The importance of thickness-shearing modes has been discussed by Yu [33, 34, 37] and Chu [46]. It will be further emphasized in the

examples of Section IV.4 below. However, a brief qualitative review of the relationship of the various vibration modes is now given. Figures IV.2 and IV.3 demonstrate this relationship. It should be emphasized that these two Figures are merely qualitative sketches to illustrate the modal behavior. They do not represent results calculated for a particular structure. Moreover, the use of continuous curves for each mode implies an infinity of possible wave lengths and hence a structure of infinite length. For a simply supported, finite-length structure, the wave lengths must be integer fractions of the structure length. Hence a finite structure would be represented only by points on the modal curves corresponding to admissible abscissas.

Figure IV.2 shows the two primary modes of a one-dimensional, flat sandwich structure, i.e., a beam or an axisymmetric plate. Point A is known as the "thickness-shear cut-off frequency" or the "simple thickness-shear mode." It corresponds to an infinite wave length and thus represents pure shearing deformation. If the ordinate OA is sufficiently small, the shearing mode becomes significant in analysis and design. For example, if the points F_1 and F_2 indicate the two lowest flexural frequencies, the thickness-shear cut-off becomes the second lowest natural frequency of the structure.

For the axisymmetric vibrations of a sandwich cylinder, the three lowest branches of the frequency equation are shown in Figure IV.3.* Here, point A has the same significance as for the plate. Moreover, for an isotropic cylinder the simple thickness-shear frequencies are the same for the longitudinal and circumferential direction, so some

---

*Wilkinson [134] has described a similar three-branch theory for spherical sandwich shells.

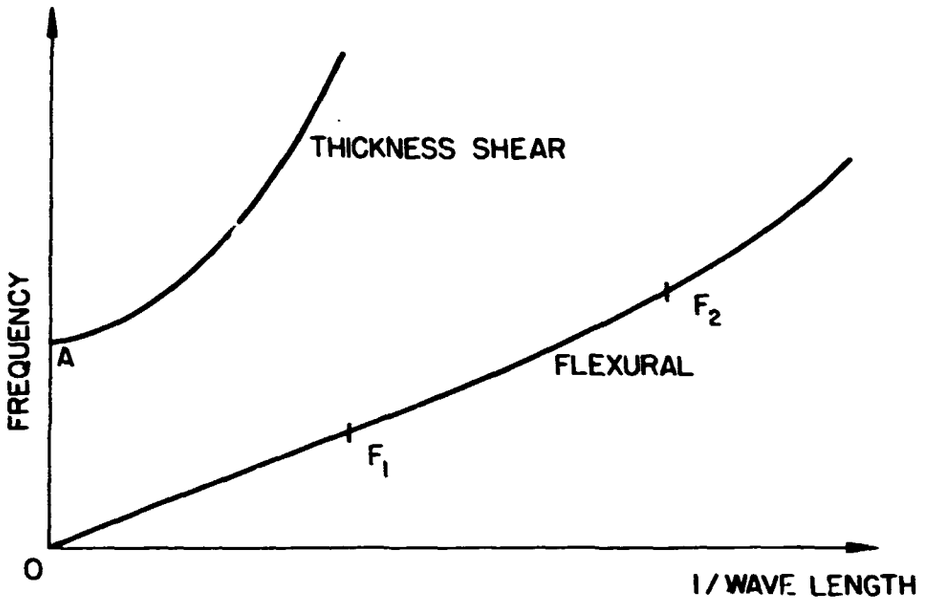

FIGURE IV.2 VIBRATION MODES OF A BEAM OR PLATE

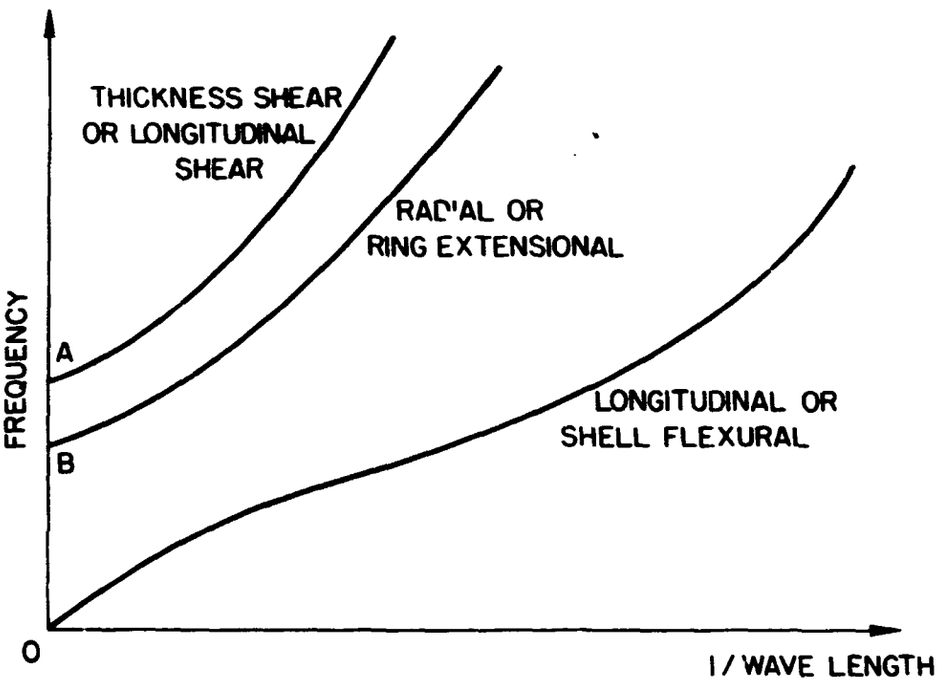

FIGURE IV.3 AXISYMMETRIC VIBRATION MODES OF A CYLINDRICAL SHELL

insight is gained for the asymmetric behavior. Point B corresponds to a pure radial expansion or "breathing" mode. The radial and thickness-shear curves are close together for nearly all sandwich cylinders. In fact, Yu [37] has shown that their relative positions are interchanged for sufficiently low ratios of radius to thickness. Since the radial mode is significant, the determination of the thickness-shear frequencies is also essential in the dynamic analysis of cylindrical sandwich structures.

In both Figure IV.2 and Figure IV.3, the point O represents rigid body translation of the structure as a whole, a motion which is characterized by a zero natural frequency.

IV.4. Examples of Free Vibration Analysis

The finite element analysis has been used to obtain the fundamental frequencies and mode shapes for several beams, plates, and shells. Where results from other sandwich theories are available for comparison, the approximate method provides reasonable agreement for the lower frequencies computed. In this section, three examples are presented: a slender beam, a short beam, and a cylindrical shell. Other configurations, including rotational shells of arbitrary meridian, can be analyzed by the present finite element method. However, it should be re-emphasized that the theory only considers the axisymmetric modes of such structures.

IV.4.1. Simply Supported Slender Beam

Kimel et al. [43] have reported the results of experiments to determine the natural frequencies of a long, slender sandwich beam which is simply supported. They also developed a theory to predict this behavior. The finite element method has been applied to one of their specimens and the results compared to the experiment and theory. The beam has the following properties:

$$h_c = 0.25 \ , \ h_f = 0.016 \ , \ L = 0.282$$

$$E_f = 10.3 \times 10^4 \text{ psi} \ , \ G_f = 3.87 \times 10^6 \text{ psi} \ , \ \kappa_f = 1$$

$$E_c = 2.34 \times 10^4 \text{ psi} \ , \ G_c = 1.17 \times 10^4 \text{ psi} \ , \ \kappa_c = 1$$

$$\text{span, } L = 120" \ , \ \rho_f = 0.0975 \text{ lb./in.}^3 \ , \ \rho_c = 0.00442 \text{ lb./in.}^3$$

The effect of lateral constraint is neglected, i.e., the beam stress-strain relations (III.5a) are used rather than those for the cylindrical shell (III.5b). Hence ν is taken as zero in the theories [43].

The result of calculations is presented in Table IV.1. The theories from References [34] and [43], although somewhat different in concept, agree closely in results. The linear-shear finite element solution matches both theories well. Furthermore, all three theoretical methods provide frequencies within a few percent of the experimental values, better correlation being obtained for lower frequencies.

It is apparent that the inclusion of rotatory inertia has negligible effect on the flexural frequencies for this problem. This is to be expected on the basis of the relatively small effect of rotatory inertia on the flexural vibrations of homogeneous plates [73]. Moreover, by lumping the masses to produce a diagonal mass matrix, the inertial effects have been uncoupled. However, the use of lumped rotatory inertia does provide estimates to the thickness-shear frequency, although for the ten- and twenty- element representations in Table IV.1, the approximations of the thickness-shear cut-off are poor. It is found that the ratio of beam thickness to element length is an important factor in the accuracy of the finite element solutions for thickness shear behavior. Since the thickness-shear cut-off occurs at infinite wave length, it is independent of the span length of the beam. Hence it is possible to estimate the simple thickness-shear frequency by analyzing a simply supported beam of arbitrary length, provided rotatory inertia is included. Figure IV.4 indicates the effect of the thickness to length ratio on the accuracy of the finite element thickness-shear cut-off. The standard of comparison is Yu's determination of this frequency [33,34]. The results shown are independent of the number of elements used. Hence, the finite element analysis can be used to obtain the simple thickness-shear frequency with a sufficiently short one-element representation. This quick and easy calculation

provides an indication of the necessity for including rotatory inertia in the complete analysis. If the cut-off is high with respect to the flexural frequencies, rotatory inertia need not be taken into account.

TABLE IV.1--NATURAL FREQUENCIES OF A SIMPLY SUPPORTED SANDWICH BEAM (CPS)

Mode	Finite Element, Lumped Masses				Yu [34]	Kimel et al [43]	
	Trans. Inertia Only		Rot. & Trans. Inertia		Eq. 2.5	Theory	
	10 elements	20 elements	10 elements	20 elements	$\nu = 0$	$\nu = 0$	Experiment
1	2.5	2.5	2.5	2.5	2.7	2.5	
2	10.1	10.1	10.1	10.1	10.2	10.1	
3	22.6	22.6	22.6	22.6	22.6	22.6	
4	39.9	40.0	39.9	40.0	40.0	39.9	40
5	61.8	62.2	61.8	62.2	62.2	62.1	61
6	87.7	88.7	87.7	88.9	89.0	88.8	90
7	116.3	120.1	116.3	120.1	120.2	120.0	114
8	144.9	155.5	144.9	155.5	155.7	155.4	178
9	167.8	194.8	167.8	194.8	195.2	194.8	201
10		237.8		237.8	238.4	238.0	254
11		284.3		284.2	285.3	284.8	335
12		334.0		333.9	335.4	334.9	353
13		396.7		386.5	388.7	388.1	423
14		441.9		441.7	444.8	444.1	479
15		498.9		498.7	503.4	502.8	532
16		556.3		556.2	564.5	563.8	
17		611.3		611.1	627.7	627.1	
18		658.8		658.6	692.9	692.3	
19		691.8		691.8	759.9	759.3	
TSCO			5100	10200	22900		

TSCO = Thickness-shear cut-off frequency

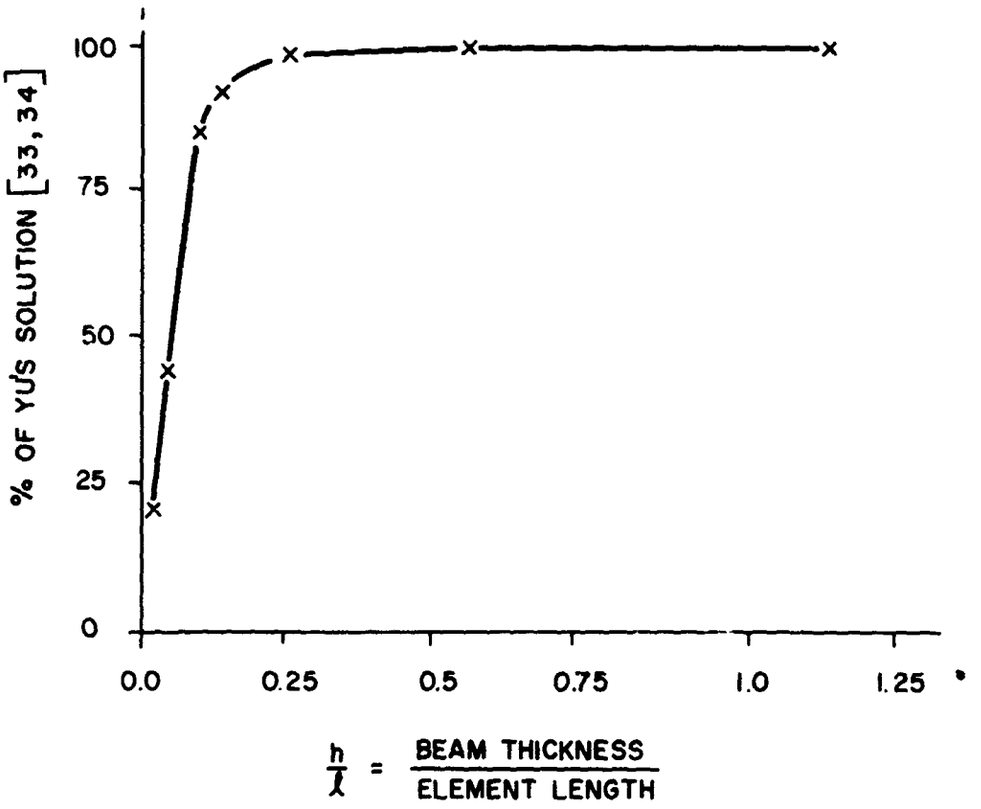

FIGURE IV. 4 ACCURACY OF THICKNESS-SHEAR CUT-OFF FREQUENCY FOR A BEAM

IV.4.1 Simply Supported Short Beam

In order to illustrate a structure for which thickness-shearing modes are important, a short, thick beam is selected with the following properties:

$$h_c = 1.0" \ , \ h_f = 0.05" \ , \ h = 1"$$

$$E_f = 10^7 \text{ psi} \ , \ G_f = 3.84 \times 10^6 \text{ psi} \ , \ \kappa_f = 1$$

$$E_c = 4.26 \times 10^5 \text{ psi} \ , \ G_c = 1.565 \times 10^5 \text{ psi} \ , \ \kappa_c = 1$$

$$\text{span}, \ L = 5.5" \ , \ \rho_f = 0.0975 \text{ lb./in.}^3 \ , \ \rho_c = 0.0469 \text{ lb./in.}^3$$

The beam is represented by 4, 10, and 20 linear-shear finite elements both with and without rotatory inertia; again the results are compared to the theories of References [34] and [43].

The various solutions are given in Table IV.2. The finite element results compare favorably with the theoretical for both flexural and thickness-shear modes. For the various meshes, about 70% of the finite element flexural frequencies are in good agreement with the frequency equation roots. For the higher mode, only about 45% agree with the theoretical solution. That the approximate method will be more accurate for the lower modal branch is not surprising; the finite element displacement models are better able to represent less complex modes of deformation. It should be emphasized that the element mesh is extremely f[illegible]or this particular example. In normal application with a less refined mesh, a smaller proportion of the frequencies for each mode would be accurate to a given tolerance.

TABLE IV.2--NATURAL FREQUENCIES OF A SIMPLY SUPPORTED SANDWICH BEAM (10^5 RAT./SEC.)

Mode		Finite Element Method						Yu [34]	Kimel et al [43]
		Translational Inertia Only			Trans. and Rotatory Inertia			Eq. 2.3	
#	type	4 elems.	10 elems.	20 elems.	4 elems.	10 elems.	20 elems.	$\nu = 0$	$\nu = 0$
1	F	.119	.119	.119	.118	.118	.118	.118	.115
2	F	.324	.326	.327	.321	.324	.325	.325	.323
3	F	.557	.533	.536	.555	.531	.534	.535	.535
4	F		.736	.741		.733	.739	.742	.743
5	F		.939	.943		.937	.941	.946	.949
6	TSCO				.963	.997	1.003	.974	
7	F		1.154	1.143		1.152	1.141	1.150	1.154
8	TS				1.188	1.264	1.275	1.241	
9	F		1.398	1.344		1.396	1.342	1.354	1.359
10	F		1.689	1.546		1.687	1.544	1.559	1.564
11	F		2.001	1.751		2.000	1.749	1.766	1.771
12	TS				1.591	1.815	1.850	1.806	
13	F			1.963			1.961	1.974	1.979
14	F			2.182			2.180	2.185	2.189
15	F			2.414			2.412	2.398	2.401
16	TS				1.890	2.432	2.518	2.469	
17	F			2.622			2.660	2.613	2.616
18	F			2.929			2.927	2.831	2.834
19	F			3.217			3.212	3.052	3.054
20	TS				1.965	3.034	3.214	3.171	
21	F			3.523			3.521	3.276	3.278
22	F			3.831			3.830	3.504	3.504
23	F			4.112			4.111	3.734	3.735
24	TS					3.583	3.905	3.890	

F = Flexural, TSCO = Thickness-Shear Cut-Off, TS = Thickness-Shear

IV.4.3. Simply Supported Cylindrical Shell

The one type of shell for which solutions for natural frequencies are readily available is the cylinder. Yu [37] has derived a three-branched frequency equation for an infinite cylinder in an extension of his theory for sandwich plates [32, 24]. This equation is also applicable to a simply supported shell of finite length. A cylinder with the following properties is now analyzed.

$$h_c = 0.5" \ , \ h_f = 0.025" \ , \ h = 0.55"$$

$$E_f = 10^7 \text{ psi} \ , \ \nu_f = 0.3 \ , \ G_f = 3.85 \times 10^6 \text{ psi} \ , \ \kappa_f = 1$$

$$E_c = 2.6 \times 10^4 \text{ psi} \ , \ \nu_c = 0.3 \ , \ G_c = 10^4 \text{ psi} \ , \ \kappa_c = 1$$

$$\rho_f = 0.1 \text{ lb./in.}^3 \ , \ \rho_c = 0.005 \text{ lb./in.}^3$$

$$\text{radius, } a = 20" \ , \ \text{span, } L = 10"$$

As in the preceding examples, these properties are typical of sandwich construction.

The natural frequencies computed by both methods are presented in Table IV.3. Rotatory inertia is included in all cases and quadratic-shear elements are used. Many more frequencies than would be of practical interest are shown in the table in order to evaluate better the overall effectiveness of the finite element approach. It is noteworthy that the lowest frequencies of each of the three modes are approximated regardless of the number of elements used. The number of frequencies given by the finite element method for each mode depends on the number of degrees of freedom available of the type that are necessary to characterize the particular mode.

For shell structures there is usually more than one branch of the frequency equation that is of engineering importance. Careful study

of the finite element mode shapes must be undertaken in order to identify the frequencies with the appropriate branch. This is especially true in preliminary analyses wherein the frequencies have not yet converged to a predictable pattern.

In the present example, simple supports which preclude translation in any direction are used. Hence the breathing mode or fundamental radial expansion mode is prevented. However, the example has been recomputed with supports that restrain only longitudinal displacements in order to obtain an estimate of the cut-off frequency of this radial mode. Yu's solution [37] for this frequency is 8520 radians/second. The finite element approximations for five, ten, and twenty elements are 8360, 8500 and 8520 radians/second, respectively.

TABLE IV.3--NATURAL FREQUENCIES OF A SIMPLY SUPPORTED SANDWICH CYLINDER (RAD./SEC.)

MODE	TYPE	Yu [34]	Finite Element Method		
		Eq. 29	5 elems.	10 elems.	20 elems.
1	L1	8740	9040	9080	9080
2	L2	11900	11900	12100	12200
3	L3	16300	15500	16700	16800
4	L4	21000	18000	21500	21900
5	L5	25900		26000	27000
6	L6	30800		30000	32300
7	L7	35700		33400	37500
8	L8	40700		35900	42700
9	L9	45700		37400	47700
10	L10	50700			52700
11	R1	53600	5260	53300	53500
12	L11	55700			57400
13	L12	60700			61900
14	L13	65800			66000
15	TSC0	69800	71500	72800	73100
16	L14	70800			69800
17	L15	75800			73100
18	L16	80800			75900
19	L17	85900			78100
20	L18	90900			79700
21	TS1	92500	91200	94100	94900
22	L19	95900			80700
23	L20	101000			
24	L21	106000			
25	R2	107000	99800	105000	107000
32	TS2	140000	128000	138000	141000
37	R3	161000	137000	155000	159000
47	TS3	195000		187000	194000
	R4	214000		200000	211000
	TS4	252000		235000	249000
	R5	268000		241000	261000
	TS5	311000		278000	303000
	R6	321000		275000	309000
	TS7	370000			356000
	R7	375000			356000

L = Longitudinal, R = Radial, TS = Thickness Shear

CHAPTER V: DAMPING BY THE INCLUSION OF VISCOELASTIC LAYERS

V.1. The Complex Modulus Representation

For oscillatory displacements in linear viscoelasticity, the stresses and strains may be related by a complex modulus [135, 136]. This representation of constitutive theory is adopted for the present damping studies. Most of the material in this chapter is therefore formulated in complex algebra. Throughout the chapter, the superscript $*$ indicates a complex quantity and the subscripts 1 and 2 designate the real and imaginary parts of a complex quantity, respectively.

Let a volume of viscoelastic material small enough to neglect spatial variations of stress be subjected to a sinusoidally oscillating stress frequency ω :

$$\sigma_{ij} = \mathrm{Re}\left(\sigma^*_{ij}\, e^{i\omega t}\right) \tag{V.1a}$$

After a time sufficiently long for the effect of initial conditions to be negligible, the steady-state strain response is

$$\varepsilon_{ij} = \mathrm{Re}\left(\varepsilon^*_{ij}\, e^{i\omega t}\right) \tag{V.1b}$$

This formulation presumes that strains are small so that non-linear effects are absent. Then if ε^* corresponding to σ^* can be considered to represent either a deviatoric component or the dilation, the ratio σ^*/ε^* is the "complex modulus"

$$E^*(\omega) = \sigma^*/\varepsilon^* \tag{V.2a}$$

and its reciprocal is the "complex compliance"

$$J^*(\omega) = \varepsilon^*/\sigma^* \quad . \tag{V.2b}$$

These quantities are related by integral transforms to the familiar relaxation modulus $E(t)$ and creep compliance $J(t)$ functions used in quasi-static viscoelasticity.* It should be noted that E is used as a generalized symbol in this section. It can be considered to represent any of the usual moduli (Young's, shear, bulk), depending upon the nature of the "test" in Equations (V.1) and (V.2).

The complex modulus may be written

$$E^* = E_1 + iE_2$$

where i is the square root of -1, E_1 is the modulus of strain which is in phase with the stress and E_2 is the modulus of strain which is 90° out of phase with the stress. Hence, E_1 can be associated with an elastic phenomenon in which energy is stored in a recoverable form and is called the "storage modulus"; conversely, E_2 is associated with viscous behavior in which energy is dissipated and is called the "loss modulus." It is convenient to visualize the stress and strain as a pari of vectors rotating at frequency ω about the origin of the complex plane (Figure V.1). The stresses and strains of Equations (V.1) are the projections of these vectors onto the real axis. Because of the viscous effects, the cyclic strain vector lags behind the cyclic stress vector by an angle θ during the steady state vibration. This angle is between 0° and 90° and is given by

---

*In "quasi-static" viscoelasticity, inertial effects are neglected. The relaxation modulus is obtained from a test at constant strain: $E(t) = \sigma(t)/\varepsilon_o$. Conversely, the creep compliance is ascertained from a constant-stress test: $J(t) = \varepsilon(t)/\sigma_o$.

$$\tan \theta = E_2/E_1 \ .$$

$\tan \theta$ is called the "loss tangent" or "loss factor" of the material since it is a measure of the proportion of energy dissipated in a cycle.

The complex modulus is a function of both temperature and frequency. The nature of this dependence is discussed further in Section V.3. It is assumed in this dissertation that all problems are isothermal; i.e., there are no external thermal effects and the heat generated per unit volume in the damping process either is sufficiently small or is dissipated quickly enough so as not to affect appreciably the material properties. This is a customary approximation in the analysis of structural damping [86, 87]. Often, it is also assumed that the complex material properties are independent of frequency [47]. This is a reasonable assumption for many cases, especially in view of the continual development of new damping materials with favorable damping characteristics over a wide frequency range [97]. However, in Section V.6 a method is proposed wherein the frequency-dependent nature of dissipative materials is taken into account.

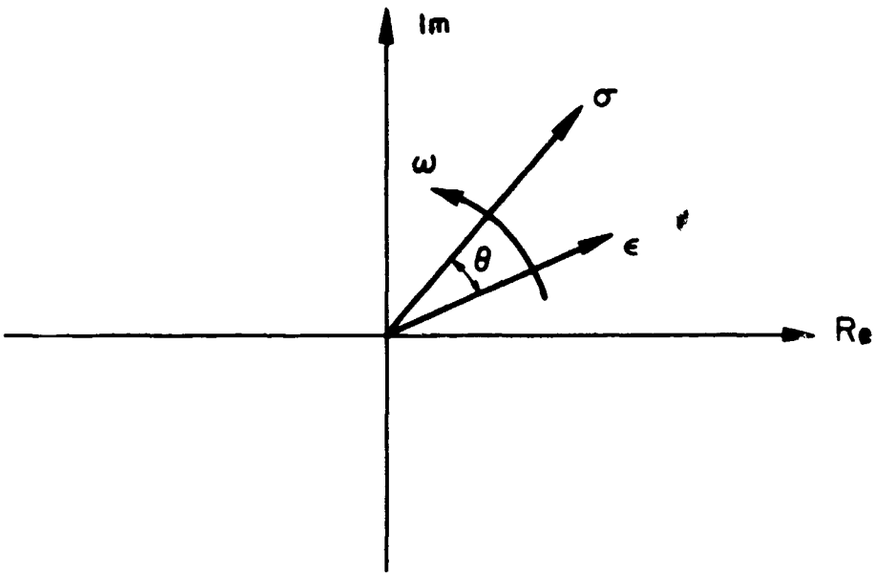

FIGURE V.1 REPRESENTATION OF STRESS AND STRAIN IN THE COMPLEX PLANE

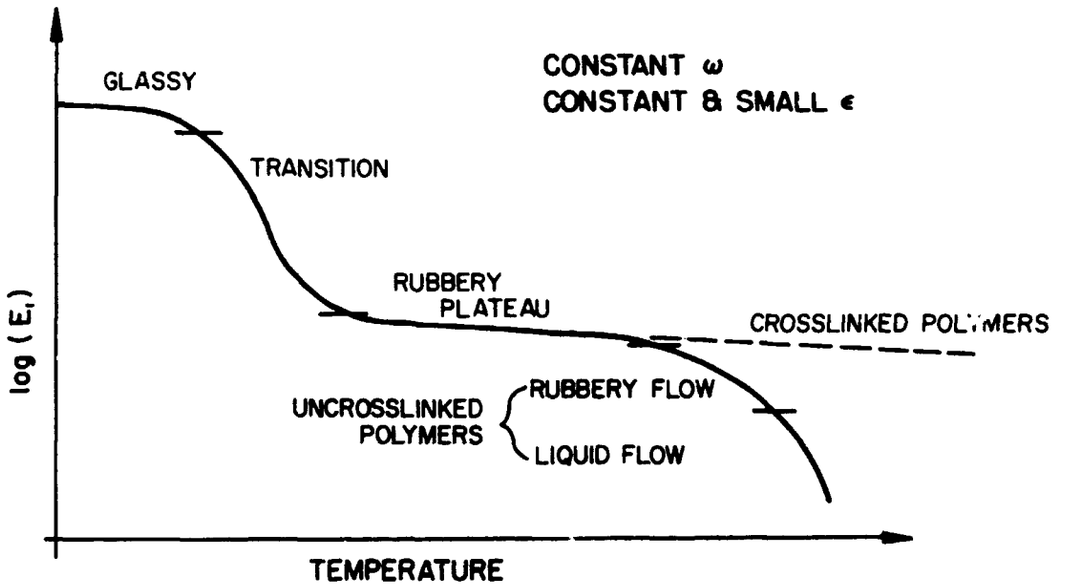

FIGURE V.2 REGIONS OF POLYMER BEHAVIOR

V.2. Correspondence Principle for Linear Dynamic Viscoelasticity

For the case of sinusoidal oscillation problems, Bland [135, p. 67] has stated the following elastic-viscoelastic correspondence principle:

> If the elastic solution for any dependent variable in a particular problem is of the form $f = \mathrm{Re}(f_E^* e^{i\omega t})$ and if the elastic moduli in f_E^* are replaced by the corresponding complex moduli to give f_{VE}^* then the viscoelastic solution for that variable in the corresponding problem is given by $f = \mathrm{Re}(f_{VE}^* e^{i\omega t})$. By "corresponding problem" is meant the identical problem except that the body concerned is viscoelastic instead of elastic. The principle can only be used if (1) the elastic solution is known, (2) no operation in obtaining the elastic solution would have a corresponding operation in the viscoelastic solution which would involve separating the complex moduli into real and imaginary parts, with the exception of the final determination of f from f^* and (3) the boundary conditions for the two cases are identical.

This principle is the basis for the damping studies in this dissertation. The oscillatory problems to which it is applied are the free vibration and the steady-state fixed vibration of the substitute structure composed of an assemblage of finite elements. In this connection, it should be noted that the "elastic solution" mentioned in the principle need not be an exact solution of three-dimensional elasticity. It is valid to apply the principle to an approximate theory of elasticity as well [86, 135, 136].

V.3. Viscoelastic Properties of Polymers

Because the most common materials used to provide damping are polymers, their dynamic viscoelastic properties are now discussed. Only a summary is given in order to provide a perspective on the assumptions used in this dissertation and in other investigations of structural damping. The mechanical properties of polymers is a broad subject and, indeed, several thorough studies have been published [137 - 144]. References [140] and [142] are, in fact, specifically intended for the design engineer.

Polymers are materials composed of extremely long, chain-like molecules. The basic units of these chains are monomers which are usually organic substances. There is not only a great variety of such substances which can be used as constituents, but there is also a multitude of chemical and physical processes which can influence the formation of the final product. Hence, there is effectively an infinite number of possible plastics with widely varying properties and applications. Attempts to describe so diverse a class of materials can be confusing. However, this variability of properties is one of the main advantages of polymers because it permits the technologist to design a material with characteristics suitable for a particular application. Fortunately, some generalizations can be made about the behavior of these substances because such behavior is related to the chain-like molecular structure peculiar to all members of the class.

Elastomers are the polymers of primary interest to engineers concerned with damping. These by definition are materials which exhibit rubber-like behavior in the frequency and temperature ranges of their application and which must be mostly amorphous in the sense that the

molecules are arranged randomly. (However, it should be noted that in some cases there is a small degree of crystallinity, the effect of which is to tie the amorphous regions together.) Like all high polymers, the elastomers possess viscoelastic properties which exhibit a marked dependence upon time and temperature.

V.3.1. Temperature Dependence

The basic behavior of polymers can be ascertained by measuring the viscoelastic properties over a broad range of temperature. Any one of several parameters may be chosen as representative, e.g., the viscosity, creep compliance, relaxation modulus, etc. The same qualitative trends of behavior are detectable from any one of the experiments, although the specific results will depend upon the time (or frequency) of measurement and the method. Figure V.2 shows a schematic plot of the storage modulus of a linear amorphous polymer as a function of temperature. Five regions of viscoelastic behavior are identifiable [137]. Starting at the lowest temperatures, the first is the glassy region in which the polymer is hard and brittle. In this range of temperatures, the molecules are "frozen" in relatively fixed but irregular positions. There is some vibration about this fixed position, but there is essentially no diffusional motion. The second region in which the modulus rapidly changes value is called transition and polymers in this stage are often characterized as leathery. It is theorized that segments (i.e., fractional lengths of the molecules) undergo short-range diffusional motion at these temperatures, although the molecules as a whole are not mobile. The third type of behavior, best described as rubbery, may extend over a fairly broad range of temperatures without much change in modulus (e.g., from -20° C. to +180° C. for sulfur-cured natural rubber

[137]). This region represents behavior most typical of elastomers. Here segmental motion is quite rapid, but the entanglement of the chains retards overall movement of the molecules. If the molecules are linked together, these "entanglements" are permanent. As the temperature is further increased to the region of rubbery flow, the uncrosslinked polymer is still elastic to a degree; but the motion of molecules as a whole becomes important, and actual flow occurs as the chains slip. Crosslinked materials do not exhibit this high-temperature creep, but retain much of this elasticity. Finally, at the highest temperatures, long-range configurational changes of the unlinked molecules occur very rapidly. In this liquid flow region, elastic recovery becomes negligible.

The transition stages and the temperatures at which they occur affect practically all of the mechanical properties of the polymers [140]. In particular, the dynamic mechanical dispersion will be discussed in Section V.3.3. Insofar as elastomeric behavior is concerned, the most significant transition is the glass transition. The rubbery flow transition or melt temperature is also important since it indicates the onset of flow. In addition, there are various less important transitions, for example, those associated with the motion of side branches to the main molecules. Only the first two phenomena are described here. The glass transition occurs over a narrow temperature range (about 10° C.) and can be determined by measuring the specific volume as a function of temperature. In Figure V.3, this transition is indicated by T_g and is associated with a discontinuity in the coefficient of thermal expansion. The crystalline transition temperature, T_m, is less well defined since it does not characterize an abrupt, ideal melting. With increasing temperature, this transition corresponds to a

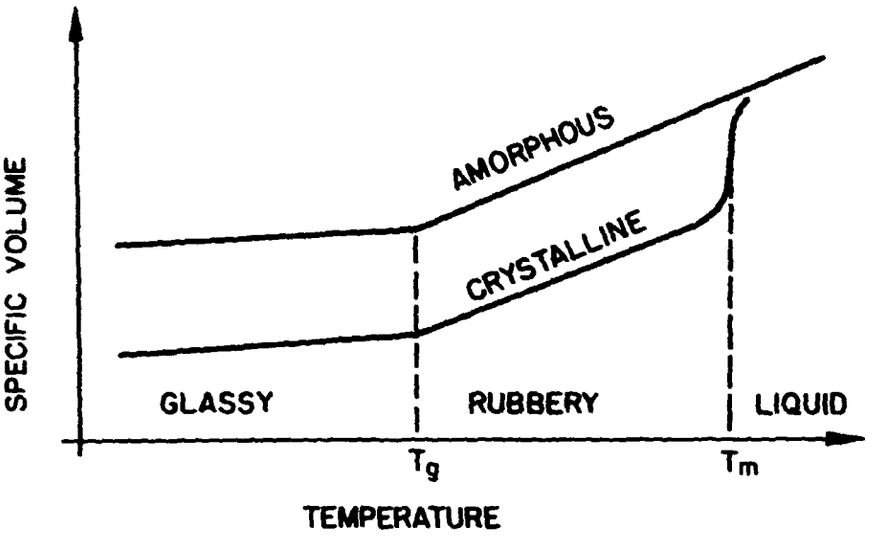

FIGURE V.3 TRANSITION TEMPERATURES OF POLYMERS AFTER NIELSON [140]

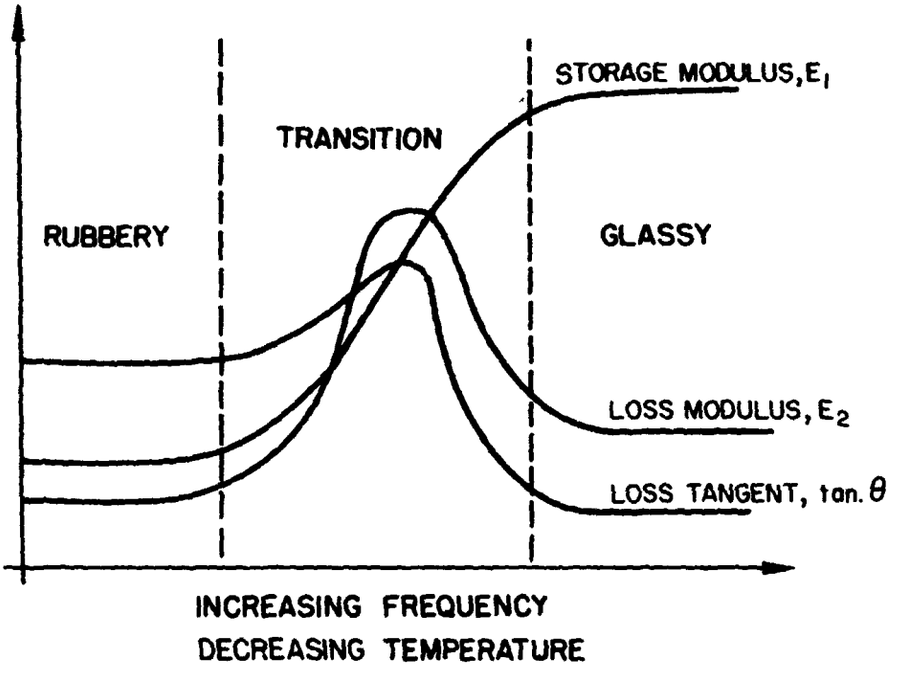

FIGURE V.4 DYNAMIC MECHANICAL DISPERSION

change from a partially crystalline configuration to a completely amorphous one.

V.3.2. Temperature-Frequency Interdependence

Since the behavior of polymers is dependent upon both time and temperature, a complete knowledge of the mechanical properties of a plastic can be obtained from tests conducted at many different temperatures and frequencies. Fortunately, such thorough investigations indicate that there is some analogy between the effects of temperature change and those of frequency change. Hence it has been possible to develop approximate reduction principles which relate these effects. The principles use data obtained at a variety of temperatures and a given frequency to deduce properties at a different frequency and vice versa. These methods are applicable for amorphous polymers and appear to be valid in the temperature range from the glass transition region to the liquid flow region [140]. No details of the reduction principles are given here. For the present purposes, it is sufficient to note that the effect of increasing the temperature or decreasing the frequency is qualitatively the same. Hence, for example, Figure V.2 may be interpreted as a schematic plot in which the abscissa is the inverse of the frequency rather than the temperature.

V.3.3. Dynamic Mechanical Dispersion

The most important effect of a transition insofar as damping is concerned is the mechanical dispersion which occurs near the transition temperatures, especially near T_g. This phenomenon is analogous to optical or dielectric dispersion. The features of the mechanical dispersion associated with the glass transition for an amorphous polymer

are schematically shown in Figure V.4. It is seen that the storage modulus changes from a lower to a higher value over this region while the loss modulus and loss tangent pass through a maximum [144]. As pointed out in Section V.3.2, the molecular mechanism of the damping during this transition is the coiling and uncoiling of chain segments. When maximum damping is required, materials are employed which undergo glass transition in the relevant frequency and temperature range. Highly amorphous polymers are preferred since crystallinity tends to decrease the intensity of the phenomenon. One example of the development of damping compounds with high loss factors over a wide range of temperatures is given in Reference [98]. There several polymers with different glass transition temperatures are mixed to give a blend with more than one T_g and hence a broader range of the favorable damping associated with the dispersion phenomenon. When temperature insensitivity of damping is desired with a single polymer, its elastomeric behavior between T_g and T_m is employed [144] (See Figure V.2). If T_m is approached and if strength is also a concern, polymers with a degree of cross-linking between molecular chains may be used.

V.3.4. Additional Factors Influencing Behavior

Although frequency and temperature are the primary factors affecting the viscoelastic behavior of polymers, there are other physical and chamical effects that must be considered. Crystallinity and cross-linking have already been mentioned. The properties of the final product may also be affected by copolymerization, polyblending, and the addition of plasticizers and fillers [138, 139, 95, 97].

Copolymerization is the formation of polymer molecules from more than one type of monomer. When the constituents occur randomly along

the chains, a new polymer is produced which is unlike any of the polymers composed of the separate monomers. Another type of copolymer occurs when chains made of different monomers are attached either to make one chain (block copolymers) or to make branching molecules (graft co-polymers). These nonuniform or heterogeneous polymers exhibit multiphase properties similar to mechanical mixtures. Each component will retain its own glass transition, so the resulting copolymer will have more than one T_g [139].

Polyblends are merely mechanical mixtures of two or more polymers. The effect of this blending was discussed in the preceding section [98] and the preceding paragraph. In brief, the result of such mixtures is a product whose properties are intermediate to those of the constituents.

A plasticizer is an organic liquid used to dilute the polymer. This dilution increases the chain mobility and lowers the glass transition temperature. Hence, plasticization can be used to adjust the optimal damping to the desired temperature or frequency range [97].

Fillers are inert materials added to the polymer. Because there is no chemical interaction with the plastic, there is usually not a significant influence on the temperature and frequency characteristics [95]. However, for some types of fillers there is sufficient mechanical interaction between the filler particles and the polymer molecules to increase damping efficiency and to broaden the operable temperature and frequency range of the useable damping [97].

In brief, it is apparent that there are several techniques by which polymer technologists can design materials for a specific application. However, despite the ability to adjust the glass transition temperature, it is not always possible to obtain efficient damping from a given polymer. For example, crystalline polymers are nearly always

impractical for damping applications.

V.3.5. Summary

The strong dependence of the viscoelastic properties of polymers on temperature and frequency has been pointed out. As a result, it is seen that the common approximations of temperature- and frequency-independence of structural damping can lead to rather large inaccuracies. However, when applied with care over appropriate ranges of frequency and temperature for a particular damping material, these assumptions can also provide useful results. Finally, there is some justification for the oversimplification of material behavior when real possibilities of designing materials to fit the assumptions exist.

V.4. Measures of Effective Damping

Of the many ways to express the damping of a vibrating structure [87, 94], two primary measures are used here. These are the loss factor, η, and the logarithmic decrement, δ. Damped oscillatory motion of the discretized structure can be written in the following form

$$\{v(t)\} = \mathrm{Re}\left(\{w\}\, e^{i\omega_1 t}\, e^{-\omega_2 t}\right) = \mathrm{Re}\,\{w\}\, e^{i\omega^* t} \tag{V.3}$$

where $\{v(t)\}$ is the vector of nodal displacements, $\{w\}$ is the vector of displacement amplitudes, ω_1 is the frequency and ω_2 is the decay constant. The latter two parameters are combined into a complex modulus, ω^*:

$$\omega^* = \omega_1 + i\omega_2 \tag{V.4}$$

Then the logarithmic decrement is given by [115]

$$\delta = 2\pi\omega_2/\omega_1 \tag{V.5}$$

and the loss factor by [118]

$$\eta = \mathrm{Im}(\omega^{*2})/\mathrm{Re}(\omega^{*2}) \ . \tag{V.6}$$

Since both measures are expressed in terms of the same parameter, they can in turn be related by

$$\eta = \frac{\delta/\pi}{(1 - \delta^2/4\pi^2)}$$

$$\delta = \frac{2\pi}{\eta}\left(\sqrt{1 + \eta^2} - 1\right) \tag{V.7}$$

An alternate, but equivalent definition of the loss factor is useful for

dealing with forced vibrations. In terms of the energy of the vibrating system, it is possible to write

$$\eta = \frac{D}{2\pi W} \tag{V.8}$$

where D is the energy dissipated per cycle and W is the total energy associated with the vibration [94, 145].

V.5. Complex Algebraic Eigenvalue Problems

The information and principles given in the preceding sections are now applied to the damping studies of freely vibrating layered structures using the finite element method. Apparently, the present work is the first such application of the method to structural damping problems. The techniques that are used in this section and the next are not limited to the particular formulation given in Chapters II and III. Rather, the approach can be used for any finite element discretization. However, since an efficient and widely utilized damping mechanism is the shearing of constrained layers [88], the theory developed in this dissertation is particularly appropriate.

For frequency-independent material properties, the elastic-viscoelastic correspondence principle can be applied to the free vibration problem of Equation (IV.2) to give

$$[K^*]\{w_i^*\} = \omega_i^{*2}\,[M]\{w_i^*\} \tag{V.9}$$

Here the complex moduli corresponding to a specific representative frequency are substituted for their real counterparts in the stiffness, and the complex frequency replaces the real frequency. The lumped masses remain real; but since the eigenvalue problem is now complex, the mode shapes may also be complex. Equations (V.9) are reduced to standard form in a manner exactly parallel to that presented in Section IV.2 except that the algebra is no longer real. The computer programs are readily adapted for this change if the particular computer used is capable of accomodating complex arithmetic. Moreover, standard routines are available for the complex algebraic eigenvalue problem.*

---

*Two different SHARE Library subroutines, F2 OR AMAT and F2 NYU EIG4, have been adapted for use in the present investigations. They produce identical eigenvalues although only the former calculates the mode shapes.

As is evident from Equations (V.4) to (V.6), the eigenvalues give both the natural frequency of vibration of the damped system and the effective viscoelastic damping at each natural frequency. The eigenvectors correspond to the decaying mode shapes, and there is no special significance to the fact that these vectors may be complex. The shapes may be obtained from the real parts. Hence, both the free vibration characteristics and the damping behavior are obtained in a single analysis. It should be noted that the computational time is greater than that for the purely elastic free vibration problem. Complex algebra essentially doubles the number of equations, and arithmetic operation* counts are therefore increased by a factor of two to eight, depending upon the procedure being carried out. For example, the solution of simultaneous linear equations has an operation count proportional to the square of the number of equations; for this process, therefore, the number of operations is quadrupled.

Because the frequencies are unknowns in a free vibration problem, it is difficult to account for the frequency-dependence of the complex moduli. An additional complication is that the properties corresponding to only one frequency can be used as input, but several different frequencies are obtained in the solution. If the viscoelastic behavior is relatively insensitive to frequency over the range of the lowest natural frequencies, as is the case for polymers in the rubbery plateau region, it is reasonable to use representative values of the moduli and to assume that these values are frequency-independent. For materials with highly variable properties, the free vibration approach is less satisfactory. When the damping at only a few of the natural

---

*An operation consists of one addition/subtraction and one multiplication/division.

frequencies is of interest, a series of different trial solutions may be worthwhile. The first of these trial solutions would be the elastic case. Since relatively light damping has but slight effect on the natural frequencies, the viscoelastic material properties corresponding to the elastic natural frequencies can be used in subsequent solutions. These procedures can be time-consuming because a separate solution of the entire complex eigenvalue problem is required to obtain an accurate estimate of the damping at each natural frequency of interest (i.e., $[K^*] = [K^*(\omega_j)]$, $j = 1,2, \ldots$).

V.6. Damped Response to Steady-State Harmonic Loading

The steady-state forced vibration problem for a linear viscoelastic structure is now investigated. The solution to such a problem provides both the displacement response and the effective damping for any desired frequency and loading amplitude. An important advantage to this approach is that it takes the frequency dependence of the viscoelastic material properties into account. Because the frequency of the sinusoidal loading is an input to the problem, it is possible to employ correct material properties with respect to frequency in formulating the problem. It should be noted that a similar application of the finite element method to the vibrations of linear viscoelastic solids has been developed simultaneously, but independently, by Murray [146]. However, Murray's work is primarily concerned with the displacement response and does not consider the effective damping of the system.

V.6.1. Formulation of the Problem

If the loads and displacements oscillate at frequency Ω

$$\begin{aligned} \{V(t)\} &= \{P\}\, e^{i\Omega t} \\ \{v(t)\} &= \{w\}\, e^{i\Omega t} \end{aligned} \quad , \tag{V.10}$$

the correspondence principle given in Section V.2 can be applied to Equation (IV.1) to give

$$\left[[K^*] - \Omega^2 [M]\right] \{w^*\} = \{P\} \tag{V.11}$$

Here the frequency Ω is real since there is no decay of the response. Moreover, the vector of load amplitudes $\{P\}$ is real. This vector can be visualized as being directed along the real axis of a complex

co-ordinate system which rotates at constant angular frequency Ω. Then the displacement amplitude vector $\{w^*\}$ must be complex since it lags behind the loads due to the dissipation of energy. This load-displacement relationship is analogous to the stress-strain relationship discussed in Section V.1 and shown in Figure V.1. In the present section, however, the co-ordinate system is assumed to rotate. $[K^*]$ in Equation (V.11) is the stiffness matrix wherein the complex moduli associated with frequency Ω are substituted for the corresponding real moduli.

Bieniek and Freudenthal [47] have utilized an approach similar to the above to study the forced vibrations of cylindrical sandwich panels. However, their application is to a Fourier solution of the closed-form equations rather than to a general discretized system.

The solution of Equations (V.11) presents no difficulty when the appropriate computer programs are transformed to the complex mode. As pointed out in Section V.5, the computational time is about four times greater than for an equivalent real system.

V.6.2. Interpretation of Results

In contrast to the corresponding elastic forced vibration equations which are

$$\left[[K] - \Omega^2[M]\right]\{w\} = \{P\} \quad , \tag{V.12}$$

Equations (V.11) cannot become singular at the natural frequencies of the structure. In other words, although det $([K] - \Omega^2[M])$ may vanish at some values of Ω, det $([K^*] - \Omega^2[M])$ is always non-zero, provided the frequency is real and the system has some non-zero imaginary parts. This lack of singularity points out the effect of energy

dissipation. As a result of the damping, the magnitude of $\{w^*\}$, unlike the magnitude of $\{w\}$, cannot grow without bound at resonance. In fact, the effect of viscoelasticity is to reduce the amplitude of the response at all frequencies.

The actual response of the structure can be determined by taking the absolute value of the elements of $\{w^*\}$. Each such magnitude is then given the sign of the corresponding real part of $\{w^*\}$. In frequency regions near the natural frequency of the structure, it is noted that the sign of the response changes without the displacements becoming zero. This jump in sign is associated with the change in sign which occurs for the real part of det $([K^*] - \Omega^2[M])$ near the natural frequency. Hence, if the response is obtained for a series of frequencies, an estimate of the natural frequencies within this range can be obtained by studying (1) the sign changes of the response and (2) the magnitude of the response. The latter will tend to go through maxima near the natural frequencies.

V.6.3. Determination of Effective Damping

The individual components of the response do not lag behind the load by the same phase angle. Therefore, the most convenient way to compute the effective damping is on the basis of the energies of the vibrating system. The definition of the loss factor given in Equation (V.8) is used for this purpose.

$$\eta = \frac{D}{2\pi W} \qquad (V.8)$$

Here W is taken as the maximum strain energy achieved during any cycle.

In order to compute the various energies, the complex notation that has been used must be discarded. This notation represents the simultaneous treatment of two oscillations which are 90° out of phase [136]. A complex "work" quantity would be meaningless, however, so the method of accomodating the phase difference must be modified. Consider the displacements and associated nodal forces which are harmonic at frequency Ω :

$$\begin{aligned} \{v^*(t)\} &= \{v_o^*\}\, e^{i\Omega t} = \{v_o^*\}\,(\cos \Omega t + i \sin \Omega t) \\ \{V^*(t)\} &= \{V_o^*\}\, e^{i\Omega t} = \{V_o^*\}\,(\cos \Omega t + i \sin \Omega t) \end{aligned} \tag{V.13}$$

These forces and displacements are related by the stiffness equation

$$\{V_o^*\} = [K^*]\{v_o^*\} \tag{V.14a}$$

which may also be written

$$\{V_1 + iV_2\} = [K_1 + iK_2]\,\{v_1 + iv_2\}\ . \tag{V.14b}$$

Hence the real and imaginary parts of the force vector $\{V_o^*\}$ are given by:

$$\{V_1\} = [K_1]\{v_1\} - [K_2]\{v_2\} \tag{V.15}$$

$$\{V_2\} \quad [K_1]\{v_2\} + [K_2]\{v_1\}$$

However, the real parts of the two vectors can also be obtained from Equations (V.13):

$$\begin{aligned} \{V\} &= \mathrm{Re}\,\{V^*\} = \{V_1\}\cos \Omega t - \{V_2\} \sin \Omega t \\ \{v\} &= \mathrm{Re}\,\{v^*\} = \{v_1\}\cos \Omega t - \{v_2\} \sin \Omega t \end{aligned} \tag{V.16}$$

Now, given the real oscillatory displacements

$$\{v\} = \{w_o\} \cos \Omega t \ , \qquad (V.17a)$$

$$\text{i.e., } \{v_1\} = \{w_o\} \text{ and } \{v_2\} = \{0\} \ ,$$

Equations (V.15) and (V.16) can be used to obtain the associated real forces

$$\{V\} = \left[[K_1] \cos \Omega t - [K_2] \sin \Omega t\right]\{w_o\} \qquad (V.17b)$$

Here $\{w_o\}$ is the vector of displacement magnitudes (with appropriate signs) obtained from $\{w^*\}$, the solution of Equations (V.11).

The energy dissipated during a complete period is given by

$$D = \int_0^{2\pi/\Omega} \{\dot{v}\}^T\{V\} \, dt \qquad (V.18a)$$

where

$$\{\dot{v}\} = -\Omega\{w_o\} \sin \Omega t \ . \qquad (V.18b)$$

Substituting Equation (V.17b) into (V.18), the result is

$$D = -\Omega\{w_o\}^T \left[[K_1]\{w_o\} \int_0^{2\pi/\Omega} \sin \Omega t \cos \Omega t \, dt + \right.$$
$$\left. -[K_2]\{w_o\} \int_0^{2\pi/\Omega} \sin^2 \Omega t \, dt \right] \qquad (V.19)$$

The first integral of Equation (V.19) vanishes and is therefore associated with energy stored in a recoverable form. Hence the maximum value of the strain energy achieved during any cycle is given by

$$W = \frac{1}{2} \{w_o\}^T [K_1] \{w_o\} \ . \tag{V.20}$$

The second integral of Equation (V.19) equals π/Ω so the energy dissipated can be written

$$D = \pi \{w_o\}^T [K_2] \{w_o\} \ . \tag{V.21}$$

Equations (V.20) and (V.21) are now substituted into Equation (V.8) to obtain the following expression for the effective loss factor of the structure:

$$\eta = \frac{\{w_o\}^T [K_2] \{w_o\}}{\{w_o\}^T [K_1] \{w_o\}} \tag{V.22}$$

This expression is identical to one derived by Ungar and Kerwin [145] for a lumped-mass system using a different approach. Equation (V.22) is readily incorporated into a computer program. The calculation of the loss factor is particularly efficient if the banded nature of the stiffness matrix is utilized.

V.7. Examples of Damped Vibrations

As in the preceding chapters, the examples in this section are limited by the lack of solutions available for comparison with finite element solutions. Therefore, although the discretized method can be applied to any configuration, the structures analyzed here are of simple shape. In the first example, the free vibrations of two beams are considered. The second problem undertaken is the free vibration of a simply supported cylinder. Finally, the forced vibrations of a beam under three different steady-state harmonic loads is presented.

V.7.1. Damped Free Vibrations of Two Beams

The beams considered in the examples of Sections IV.4.1. and IV.4.2. have been re-analyzed with viscoelastic properties assumed for the core. For each beam, the loss tangent of the core moduli is taken to be 0.1. This is a representative value for moderately efficient damping compounds, although some polymers have loss tangents up to 2.0 for limited ranges of frequency and temperature. All properties are the same as the elastic problem with the exception of the material properties, which are now complex. For the long beam, the moduli are

$$E_f = (E_{f1}, E_{f2}) = (10.3 \times 10^6, 0.0) \text{ psi},$$
$$G_f = (3.87 \times 10^6, 0.0) \text{ psi}$$
$$E_c = (2.34 \times 10^4, 2.34 \times 10^3) \text{ psi}$$
$$G_c = (1.17 \times 10^4, 1.17 \times 10^3) \text{ psi}$$

and the viscoelastic results are presented in Table V.1. For the short beam, the moduli are

$$E_f = (10^7,\ 0.0)\ \text{psi},\quad G_f = (3.8\times 10^6,\ 0.0)\ \text{psi}$$

$$E_c = (4.26 \times 10^5,\ 4.26 \times 10^4)\ \text{psi}$$

$$G_c = (1.565 \times 10^5,\ 1.565 \times 10^4)\ \text{psi}$$

and the frequencies and loss factors are given in Table V.2.*

Comparison with a solution adopted from Yu [115, 34] shows that there is good agreement between the methods, particularly for the lower modes. This is to be expected because the discretized approach cannot accurately approximate the displacement shapes of the higher modes. The tables indicate that a greater proportion of the natural frequencies computed by the finite element method compare favorably with the theoretical values than do the loss factors. A possible explanation for this observation is that the frequencies are less sensitive to the approximations of the mode shape which are inherent in the lumped mass approach. By concentrating the inertia at the nodes, a certain amount of shear "kinking" is introduced at these locations.

By comparing Tables V.1 and V.2 with Tables IV.1 and IV.2, it is evident that the relatively light damping has but slight effect on the natural frequencies.

---

*The real parts of the above complex moduli are the same as the real moduli used in the elastic examples. It should also be noted that the light density for the core of the long beam is realistic for a foamed plastic; however, the core moduli chosen may be atypically high for such a material.

TABLE V.1--NATURAL FREQUENCIES (CPS) AND DAMPING OF A LONG, SIMPLY SUPPORTED SANDWICH BEAM

FLEXURAL MODE NO.	Finite Element Method				Yu [115, 34]	
	10 elements		20 elements			
	ω_1	η	ω_1	η	ω_1	η
1	2.52	.000638	2.52	.000638	2.52	.000638
2	10.1	.000993	10.1	.000994	10.1	.000994
3	22.6	.00157	22.6	.00158	22.6	.00158
4	39.9	.00233	40.0	.00239	40.0	.00239
5	61.8	.00317	62.2	.00340	62.2	.00341
6	87.7	.00385	89.0	.00460	89.0	.00463
7	116	.00396	120	.00594	120	.00603
8	145	.00309	156	.00739	156	.00760
9	168	.00145	195	.00888	195	.00931
10			238	.0103	239	.0112
11			284	.0116	285	.0131
12			334	.0125	336	.0151
13			387	.0131	389	.0172
14			442	.0130	445	.0194
15			499	.0120	504	.0216
16			557	.0100	565	.0238
17			611	.00725	628	.0260
18			658	.00413	694	.0282
19			692	.00156	761	.0304

TABLE V.2--NATURAL FREQUENCIES (RAD./SEC.) AND DAMPING OF A SHORT, SIMPLY SUPPORTED SANDWICH BEAM

MODE NO.	TYPE	Finite Element Method				Yu [115, 34]	
		4 elements		10 elements			
		ω_1	η	ω_1	η	ω_1	η
1	F	11800	0.0427	11800	0.0429	11800	0.0429
2	F	32200	0.0667	32400	0.0706	32600	0.0711
3	F	55600	0.0592	53200	0.0819	53700	0.0835
4	F			73500	0.0856	74400	0.0891
5	F			93800	0.0852	94900	0.0919
6	TSCO	96500	0.0927	99900	0.0987	97700	0.100
7	F			115000	0.0818	115000	0.0933
8	TS	119000	0.0597	126000	0.0667	124000	0.0683
9	F			139000	0.0733	136000	0.0938
10	F			169000	0.0594	156000	0.0941
11	F			200000	0.0397	177000	0.0940
12	TS	196000	0.0113	243000	0.0256	181000	0.0399
16	TS			382000	0.858(?)	247000	0.0247
20	TS			471000	0.0121	317000	0.0216
24	TS			471000	0.0121	388000	0.0185

F = Flexural, TSCO = Thickness-shear cut-off, TS = Thickness shear

V.7.2. Damped Free Vibrations of a Cylindrical Shell

This example is also a recasting of a previously used elastic vibration example so that the effect of viscoelasticity on the natural frequencies can be illustrated. In this case, the simply supported cylinder studied in Section IV.4.3 is re-analyzed with two different sets of core properties. For the first set, a light-damping core with a loss tangent of 0.1 is assumed. Hence the material properties are

$$E_f = (10^7, 0.0) \text{ psi}, \nu_f = 0.3, G_f = (3.85 \times 10^6, 0.0) \text{ psi}$$
$$E_c = (2.6 \times 10^4, 2.6 \times 10^3) \text{ psi}, \nu_c = 0.3, G_c = (10^4, 10^3) \text{ psi}$$

and the results are presented in Table V.3. The second set of material properties includes a more effective dissipative core with a loss tangent of 0.5. The material properties are therefore

$$E_f = (10^7, 0.0) \text{ psi}, \nu_f = 0.3, G_f = (3.85 \times 10^6, 0.0) \text{ psi}$$
$$E_c = (2.6 \times 10^4, 1.3 \times 10^4) \text{ psi}, \nu_c = 0.3$$
$$G_c = (10^4, 5 \times 10^3) \text{ psi}$$

and the solution is given in Table V.4. All other properties and dimensions are the same as were used in Section IV.4.3.*

The natural frequencies and loss factors are contrasted to those obtained by Yu's theory [37, 116]. In general, solutions from the two methods compare well. The quality of the finite element results for the shell is similar to that for the beams given in Section V.7.1 above, and the observations of that example also remain applicable in the present case. In addition, the effect of increasing the dissipative capabilities of the core material can be ascertained by comparing

---

*See the footnote in the previous example.

Table V.4 with Tables V.3 and IV.3. Not only does the core with the higher loss tangent provide more effective damping as expected; but it also has the effect of stiffening the structure somewhat, particularly in the longitudinal or shell flexural modes. Hence, the natural frequencies are higher for the heavily damped case, although the increase is slight (less than 5%). It is interesting to note that an increase in the core loss tangent by a factor of 5 results in approximately five-fold increase in the loss factor at all frequencies.

TABLE V.3--NATURAL FREQUENCIES (RAD./SEC.) AND DAMPING OF A SIMPLY SUPPORTED CYLINDER WITH CORE LOSS TANGENT = 0.1

MODE NO.	MODE TYPE	Finite Element Method				Yu [37, 116]	
		5 elements		10 elements			
		ω_i	η	ω_i	η	ω_i	η
1	L1	9050	.00834	9080	.00770	8740	.00807
2	L2	11900	.0433	12100	.0414	11900	.0412
3	L3	15500	.0687	16700	.0658	16300	.0659
4	L4	18100	.0805	21500	.0783	21000	.0787
5	L5			26000	.0844	25900	.0857
6	L6			30000	.0877	30800	.0898
7	L7			33400	.0894	35800	.0924
8	L8			35900	.0902	40800	.0941
9	L9			37500	.0907	45800	.0953
11	R1	52600	.00288	53300	.00258	53600	.00254
15	TSC0	71600	.09[illegible]	72900	.0988	69900	.100
21	TS1	91300	.05[illegible]	94200	.0586	92500	.0576
25	R2	99900	.00[illegible]5	105000	.00258	107000	.00254
32	TS2	129000	.02[illegible]	138000	.0263	140000	.0257
37	R3	137000	.00304	155000	.00260	161000	.00254
47	TS3			187000	.0133	195000	.0137
	R4			200000	.00261	214000	.00254
	TS4			239000	.00762	252000	.00849
	R5			241000	.00263	268000	.00254

L = Longitudinal, R = Radial, TS = Thickness Shear

TABLE V.4--NATURAL FREQUENCIES (RAD./SEC.) AND DAMPING OF A SIMPLY SUPPORTED CYLINDER WITH CORE LOSS TANGENT = 0.5

MODE NO.	MODE TYPE	Finite Element Method				Yu [37, 116]	
		5 elements		10 elements			
		ω_1	η	ω_1	η	ω_1	η
1	L1	9080	.0388	9120	.0361	8780	.0380
2	L2	12100	.207	12400	.199	12100	.198
3	L3	15900	.334	17100	.321	16600	.322
4	L4	18500	.396	22000	.385	21500	.388
5	L5			26700	.417	26500	.424
6	L6			30800	.435	31600	.446
7	L7			34300	.444	36700	.459
8	L8			36800	.449	41900	.468
9	L9			38400	.451	47000	.475
11	R1	52600	.0141	53300	.0129	53600	.0127
15	TSC0	73800	.472	75000	.493	71900	.500
21	TS1	92300	.273	95200	.293	93400	.288
25	R2	99900	.0144	105000	.0129	107000	.0127
32	TS2	129000	.108	139000	.131	140000	.129
37	R3	137000	.0148	155000	.0129	161000	.0127
47	TS3			188000	.0669	195000	.0685
	R4			200000	.0130	214000	.0127
	TS4			235000	.0381	252000	.0425
	R5			241000	.0131	268000	.0127

L = Longitudinal, R = Radial, TS = Thickness Shear

V.7.3. Steady-State Forced Response of a Beam

In order to illustrate the method proposed in Section V.6, the steady-state forced vibrations of a simply supported beam are now investigated. The short beam used in Examples IV.4.2 and V.7.1 is used with a viscoelastic core. The effect of frequency dependence of the material properties is demonstrated by contrasting the solutions for frequency-dependent and frequency-independent cases. The beam is represented by both four and ten linear shear-strain elements. In general, the results for the two representations are quite similar, indicating a sufficiently fine mesh to obtain convergence. Therefore, to keep the graphs uncluttered, only the ten-element results are shown in the accompanying figures. Rotatory inertia is included.

There are no readily available theoretical solutions with which to compare the results of the present problem. Hence, the frequency-independent properties are taken to be the same as in the viscoelastic free-vibration example of Section V.7.1. It is then possible to have a limited comparison between the free and forced vibration problems. The complex moduli are assumed to be

$$E_f = (10^7,\ 0.0)\ \text{psi},\quad G_f = (3.84 \times 10^6,\ 0.0)\ \text{psi}$$
$$E_c = (4.26 \times 10^5,\ 4.26 \times 10^4)\ \text{psi},$$
$$G_c = (1.565 \times 10^5,\ 1.565 \times 10^4)\ \text{psi}$$

The frequency-dependent core properties are shown in Figure V.5. Although these do not represent actual properties of a specific material, their variation is typical of elastomers near the glass transition temperature [88, 95, 144]. In addition, their magnitude is selected so that the frequency-independent properties are a reasonable approximation

of the variable properties. In particular, the moduli for the two cases are the same at Ω = 10,000 radius/second. It is assumed that the Poisson ratio is real and frequency independent.

The response and damping for three different load cases are shown in Figures V.6 to V.8 for a range of frequencies of the beam. In each case the frequency-dependent and -independent solutions are shown together for ready comparison. The X's in the figures represent the free-vibration solutions for the loss factor (Table V.2). The three different load cases are (1) concentrated loads at all nodes selected to match the inertial loads corresponding to the first fundamental mode, (2) same as case one except chosen to match the second fundamental mode, and (3) a uniformly distributed load of unit magnitude. The displacement response for each of the load cases is given by the magnitude of some characteristic displacement. For the first two load cases, this characteristic displacement is chosen as the transverse displacement at the unit concentrated loads. The mid-point deflection is selected for the third load case.

The loss factors for constant properties in the first two load cases compare favorably with the free vibration loss factors of the respective modes. It is seen from Figures V.6 and V.7 that, for constant material properties, the loss factor varies very little over the frequency range. The first load case causes deformation typical of the first mode at all frequencies; and, similarly, the second load case creates primarily second-mode displacements. Hence it can be concluded that the loss factor depends largely upon the deformation pattern. In fact, when rotatory inertia is neglected, the loss factors for the two cases under consideration are invariant with respect to the forcing grequency. The third load case, in contrast, is not a

"modal" load and thus excites displacements corresponding to various natural modes, particularly the symmetric shapes. Hence, although the response curve in Figure V.8 does not show a noticeable resonance corresponding to the second mode (which is antisymmetric), the loss factor curve does indicate a change in the basic deformation pattern for frequencies in the neighborhood of this mode. Moreover, at the first fundamental frequency, the loss factor matches the free vibration result since the symmetric loading readily excites the related mode shape.

It should be noted that the curves for the loss factors in Figures V.6 to V.8 are smoothed near the natural frequencies of the structure. Using the approximate method of computing loss factors on the basis of energy (Section V.6.3), there are apparently some numerical instabilities in a small neighborhood of frequencies near resonance. This smoothing has been accomplished by discarding at most one data point in such a neighborhood. Since small frequency increments are employed in these regions, it is felt that this procedure is justifiable.

The displacement response curves in Figures V.6 through V.8 are reasonable representations of the behavior that might be expected for a lightly damped structure [47]. If a more effective damping compound were employed, the resonance peaks would be less pronounced. This is evident from the amplitude reduction resulting from the variable material properties, which give greater dissipation at the first fundamental frequency (Figure V.6).

The extent of the possible effects of frequency dependence of the material properties is evident from a comparison between the pairs of curves. It should be granted, however, that the extreme variability of the properties near the glass transition temperature presents a

particularly severe situation. If the frequency range of interest were to correspond to the rubbery plateau of Figure V.2, the properties would be more slowly varying functions of the frequency. Nonetheless, the proposed method of accomodating the variation of properties appears useful for obtaining both the steady-state response and damping of an harmonically loaded viscoelastic structure.

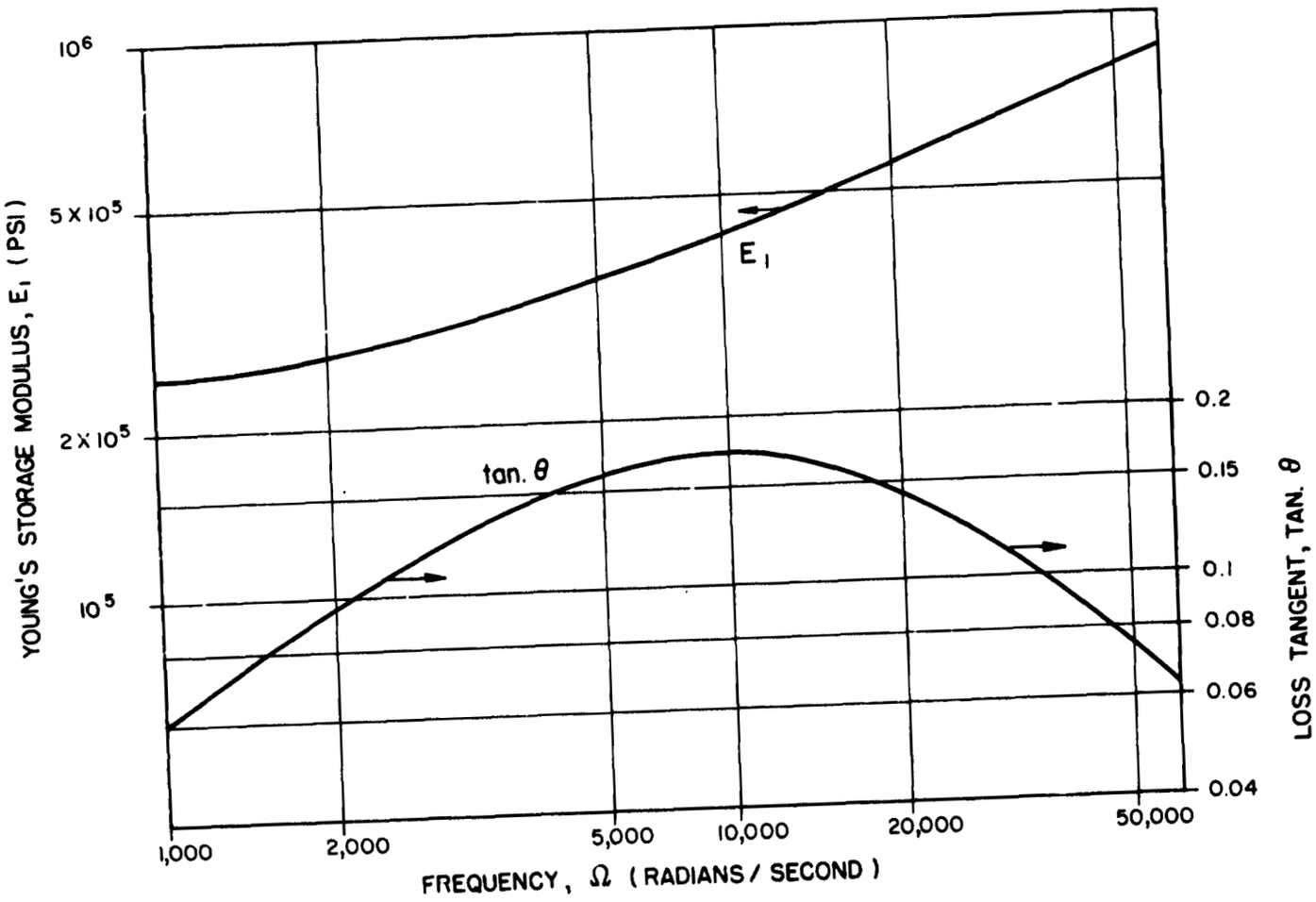

FIGURE V.5 FREQUENCY DEPENDENCE OF MODULUS AND LOSS TANGENT OF CORE FOR EXAMPLE V.7.3

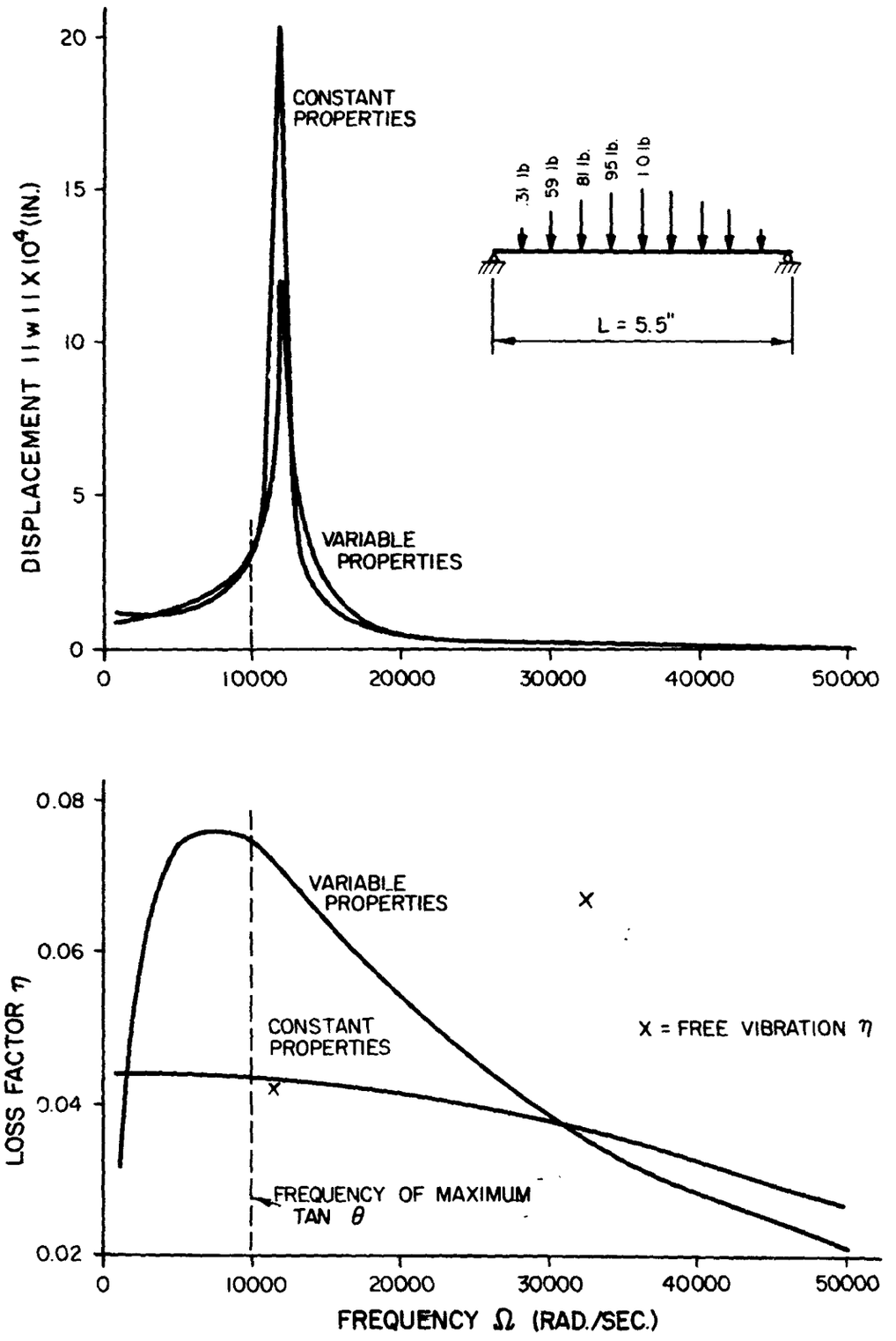

FIGURE V.6 RESPONSE AND DAMPING OF A SANDWICH BEAM FOR LOAD CASE I

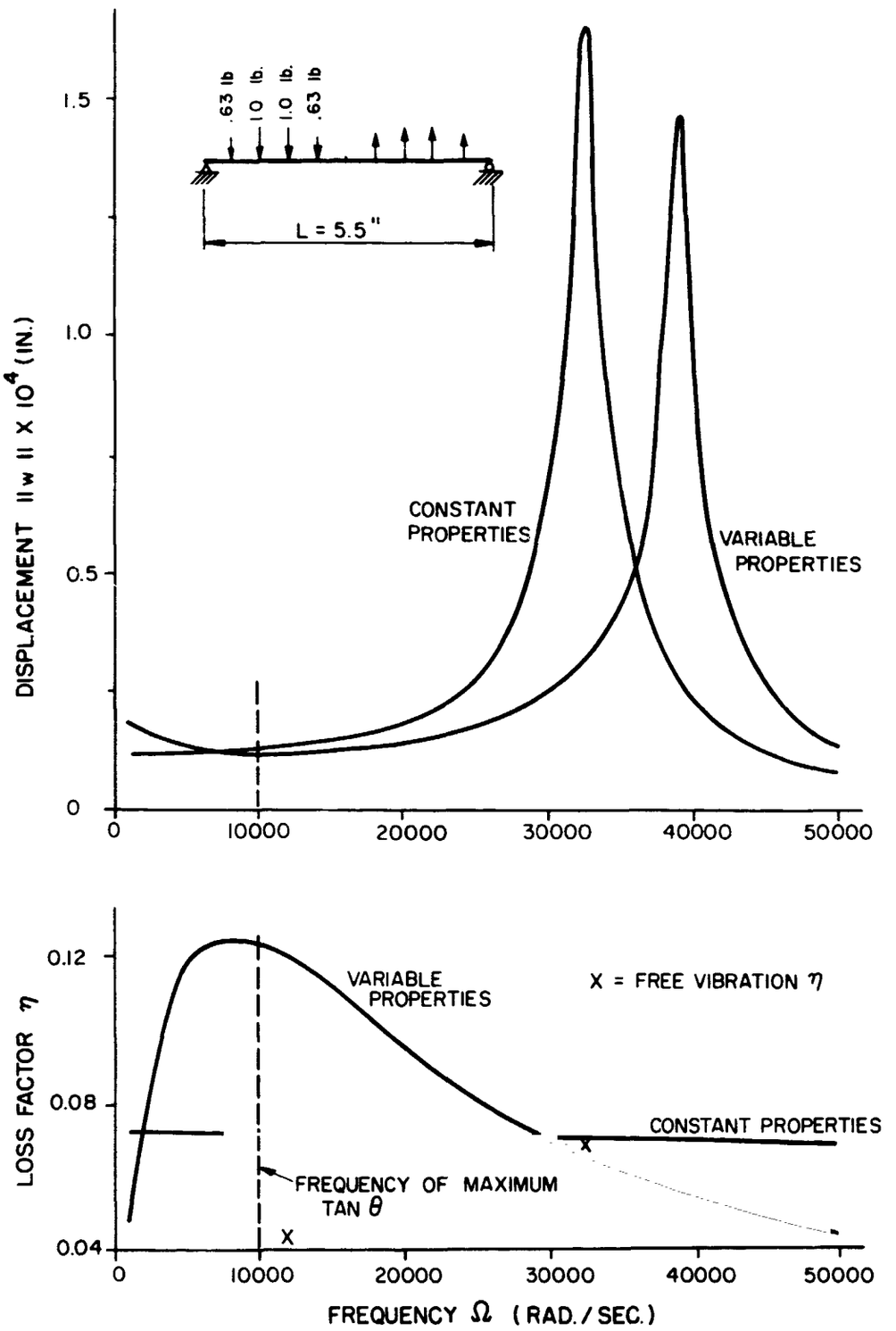

FIGURE V.7 RESPONSE AND DAMPING OF A SANDWICH BEAM FOR LOAD CASE 2

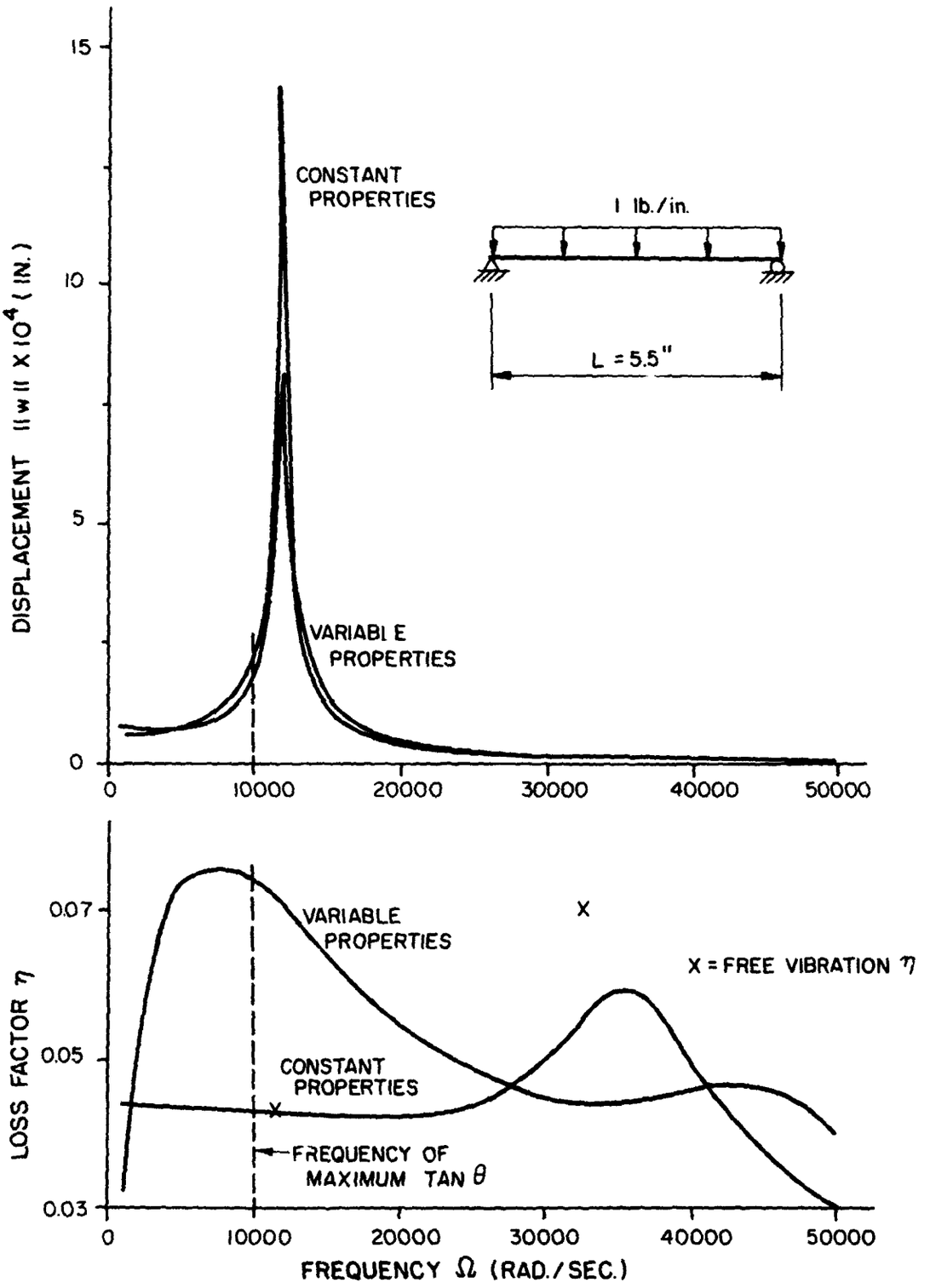

FIGURE V.8 RESPONSE AND DAMPING OF A SANDWICH BEAM FOR LOAD CASE 3

CHAPTER VI. SUMMARY AND CONCLUSIONS

The finite element method has been extended to the refined analysis of multilayer beams, plates and shells. In the theory employed no restriction is placed upon the ratios of the layer thicknesses and properties. The method is applicable to structures wherein shearing deformations are significant, including sandwich construction.

Specific element stiffnesses based on polynomial displacement models have been developed for the linear elastic analysis of beams, circular plates and thin, axisymmetric shells with arbitrary meridians. In each case only the specialized configuration of three-layered construction symmetric about the reference surface has been studied. However, general procedures have also been outlined for developing other types of one- and two-dimensional finite elements.

The method has been applied to the elastic analysis of several beam, plate and shell structures with properties typical of sandwich construction. Examples have been presented for both static and free vibration analysis and the finite element results compare favorably with solutions from other theories and approaches. Generally, the other techniques can only be used for the analysis of sandwich structures with the simplest of configurations. Hence there is a great potential for the application of the finite element method to the solution of sandwiches of arbitrary shape.

One of the features of the formulation developed in this dissertation is the capability of approximating the warping phenomenon. Hence the distribution of the shearing force among the various layers can be determined. Another feature is the use of lumped rotatory

inertia in dynamic analyses. This type of inertia is a prerequisite for the inclusion of the thickness-shear modes of behavior, which are important for some soft-core sandwich structures. A third aspect of the present work is the possibility of neglecting either the shearing, extension or bending of any individual layer. By use of this capability, the effect of various approximations can be evaluated for different geometrical or material properties.

In addition to the elastic analyses, vibration studies for linear viscoelastic materials have been formulated using the complex modulus representation and an elastic-viscoelastic correspondence principle. The effective damping for free vibration and steady-state forced vibration can be obtained as adjuncts of the usual analysis procedures by means of the complex algebra. Apparently, this application of the finite element method is new.

For the viscoelastic free-vibration problem, the material properties are assumed to be independent of both frequency and temperature. A discussion of the characteristics of the most common damping materials, polymers, indicates that these assumptions are often invalid. In the forced-vibration problem, the frequency-dependence of the viscoelastic behavior can be taken into account. However, no attempt has been made to include the thermal effects because of the inherent difficulties of this non-linear, coupled problem. It should be noted that the temperature effects may be important in damped vibrating structures since the energy dissipated into heat disperses very slowly in polymers due to their low thermal conductivity.

The viscoelastic analyses in this dissertation have been carried out on the most elementary level. A logical extension of this research would be the study of initial value problems using a Gurtin-type variational principle for linear dynamic viscoelasticity [147] to formulate directly the stiffness of the structure. An analogous approach has already been used for heat conduction [148], coupled thermoelasticity [149] and quasi-static viscoelastic problems [150] using the finite element method.

REFERENCES

1. Dong, S. B., Matthiesen, R. B., Pister, K. S. and Taylor, R. L., "Analysis of structural laminates," USAF Aeronautical Research Laboratory Report 74, Wright-Patterson AFB, Ohio, Sept. 1961.

2. Taylor, R. L. and Pister, K. S., "Structural laminates literature survey," USAF Aeronautical Research Laboratory Report 75, Wright-Patterson AFB, Ohio, Sept. 1961.

3. Dong, S. B., Pister, K. S. and Taylor, R. L., "On the theory of laminated anisotropic shells and plates," J. Aero.Sci., Vol. 29, No. 8, Aug. 1962, pp. 969-975.

4. Dong, S. B., "Elastic bending of laminated anisotropic shells," Proc. World Conf. on Shell Structures, San Francisco, California, Oct 1962.

5. Ambartsumyan, S. A., "Theory of anisotropic shells," U.S. NASA TT F-118, Washington, D. C., May 1964.

6. Habip, L. M., "A review of recent work on multilayered structures," Int.J.Mech.Sci., Vol. 7, No. 8, Aug. 1965, pp. 589-593.

7. Radkowski, P. P., "Thermal stress analysis of orthotropic thin multi-layered shells of revolution," AIAA Structures Meeting, April 1963.

8. Dong, S. B., "Analysis of laminated shells of revolution," J.Eng.Mechs.Div., Proc. ASCE, Vol. 92, No. EM6, Dec. 1966, pp. 135-155.

9. Foss, J. I., "For the space age: A bibliography of sandwich plates and shells," Douglas Report SM-42883, Dec. 1962, 98 pages.

10. Habip, L. M., "A review of recent Russian work on sandwich structures," Int.J.Mech.Sci., Vol. 6, No. 6, 1964, pp. 483-487.

11. Habip, L. M., "A survey of modern developments in the analysis of sandwich structures," App.Mech.Reviews, Vol. 18, No. 2, Feb. 1965, pp. 93-98.

12. Plantema, F. J., Sandwich Construction: The Bending and Buckling of Sandwich Beams, Plates and Shells, John Wiley & Sons, New York, 1966, 246 pages.

13. Williams, D., Leggett, D. M. A. and Hopkins, H. G., "Flat sandwich panels under compressive end loads," Reports and Memoranda 1987, Aeronautical Research Council, United Kingdom, 1941.

14. Leggett, D. M. A. and Hopkins, H. G., "Sandwich panels and cylinders under compressive end loads," Royal Aircraft Establishment Report SME 320_, Farnborough, United Kingdom, 1942.

15. Reissner, E., "On bending of elastic plates," Quart.App.Math., Vol. 5, No. 1, April 1947, pp. 55-68.

16. Reissner, E., "Small bending and stretching of sandwich-type shells," U. S. NACA TN 1832, March 1949, 89 pages.

17. Hoff, N. J. and Mautner, S. E., "Bending and buckling of sandwich beams," J.Aero.Sci., Vol. 15, No. 12, Dec. 1948, pp. 707-720.

18. Hoff, N. J., "Bending and buckling of rectangular sandwich plates," U. S. NACA TN2225, 1950.

19. Eringen, A. C., "Bending and buckling of rectangular sandwich plates," Proc.First Nat.Cong.App.Mech., ASME, New York, 1952 pp. 381-390.

20. Reissner, E., "Stress-strain relations in the theory of thin elastic shells," J.Math.Physics, Vol. 31, No. 2, July 1952, pp. 109-119.

21. Reissner, E., "Finite deflections of sandwich plates," J.Aero.Sci., Vol. 15, No. 7, July 1948, pp. 435-440 (Erratum in Vol. 17, No. 2, Feb. 1950, p. 125).

22. Schmidt, R., "Sandwich shells of arbitrary shape," J.App.Mech., Vol. 31, No. 2, June 1964, pp. 239-244.

23. Grigolyuk, E. I. and Kiryukhin, Y. P., "Linear theory of three-layered shells with a stiff core," AIAA J., Vol. 1, No. 10, Oct. 1963, pp. 2438-2455.

24. Wempner, G. A. and Baylor, J. L., "A theory of sandwich shells," Developments in Mechanics, Vol. 2, Part 2, Proc. Eighth Mid-western Mechanics Conference, edited by S. Ostrach and R. H. Scanlan, Pergamon Press, 1965, pp. 172-198.

25. Wempner, G. A., "Theory for moderately large deflections of thin sandwich shells," J.App.Mech., Vol. 32, No. 1, March 1965, pp. 76-80.

26. Fulton, R. E., "Non-linear equations for a shallow, unsymmetrical sandwich shell of double curvature," Developments in Mechanics, Vol. 1, 1961, pp. 365-380.

27. Raville, M. E., "Analysis of long cylinders of sandwich construction under uniform external lateral pressure," Forest Product Laboratory Report 1844, USDA Forest Service, Madison, Wisc., Nov. 1954, 28 pages.

28. Raville, M. E., "Analysis of long cylinders of sandwich construction under uniform external lateral pressure. Supplement: Facings of moderate and unequal thickness," Forest Products Laboratory Report 1844-A, USDA Forest Service, Madison, Wisc., Feb. 1955, 30 pages.

29. Reville, M. E., "Buckling of sandwich cylinders of finite length under uniform external lateral pressure," Forest Products Laboratory Report 1844-B, USDA Forest Service, Madison, Wisc., May 1955, 45 pages.

30. Koch, J. E., "Plane-strain bending of sandwich plates," Developments in Mechanics, Vol. 1, 1961, pp. 307-324.

31. Cook, R. D., "On certain approximations in sandwich plate analysis," J.App.Mech., Vol. 33, No. 1, March 1966, pp. 39-44.

32. Yu, Y. Y., "A new theory of elastic sandwich plates--one-dimensional case," J.App.Mech., Vol. 26, No. 3, Sept. 1959, pp. 415-421.

33. Yu, Y. Y., "Simple thickness-shear modes of vibration of infinite sandwich plates," J.App.Mech., Vol. 26, No. 4, Dec. 1959, pp. 679-681.

34. Yu, Y. Y., "Flexural vibrations of elastic sandwich plates," J.Aero.Sci., Vol. 27, No. 4, April 1960, pp. 272-283.

35. Yu, Y. Y., "Simplified vibration analysis of elastic sandwich plates," J.Aero.Sci., Vol. 27, No. 12, Dec. 1960, pp. 894-900.

36. Yu, Y. Y., "Forced flexural vibrations of sandwich plates in plane strain," J.App.Mech., Vol. 27, No. 3, Sept. 1960, pp. 535-540.

37. Yu, Y. Y., "Vibrations of elastic sandwich cylindrical shells," J.App.Mech., Vol. 27, No. 4, Dec. 1960, pp. 653-662.

38. Yu, Y. Y.,"Extensional vibrations of elastic sandwich plates," Proc.Fourth U.S.Nat.Cong.App.Mech., ASME, 1962, pp. 441-447.

39. Koplik, B. and Yu, Y. Y., "Axisymmetric vibrations of homogeneous and sandwich spherical caps," J.App.Mech., Vol. 34, No. 3, Sept. 1967, pp. 667-673.

40. Koplik, B. and Yu, Y. Y., "Approximate solutions for frequencies of axisymmetric vibrations of spherical caps," J.App.Mech., Vol. 34, No. 3, Sept. 1967, pp. 785-787.

41. Yu, Y. Y. and Koplik, B., "Torsional vibrations of homogeneous and sandwich spherical caps and circular plates," J.App.Mech., Vol. 34, No. 3, Sept. 1967, pp. 787-789.

42. Ren, N. and Yu, Y. Y., "Vibrations of two-layered plates," U.S. Air Force Office of Scientific Research AFOSR 65-1423, June 1965, 28 pages.

43. Kimel, W. R., Raville, M. E., Kirmser, P. G. and Patel, M. P., "Natural frequencies of vibration of simply-supported sandwich beams," Proc.Fourth Midwest Conf. on Fluid and Solid Mechs., University of Texas Press, Austin, Texas, Sept. 1959, pp. 441-456.

44. Raville, M. E., Ueng, E. S. and Lei, M. M., "Natural frequencies of vibration of fixed-fixed sandwich beams," J.App.Mech., Vol. 28, No. 3, Sept. 1961, pp. 367-372.

45. Bolotin, V. V., "Vibration of layered elastic plates," Proc. Vibration Problems, (Polska Akad, Nauk, Inst. Podstawowych, Problemov Tech.), Vol. 4, No. 4, 1963, pp. 331-346.

46. Chu, H. N., "Vibrations of honeycomb sandwich cylinders," J.Aero.Sci., Vol. 28, No. 12, Dec. 1961, pp. 930-939, 944.

47. Bieniek, M. P. and Freudenthal, A. M., "Forced vibrations of cylindrical sandwich shells," J.Aero.Sci., Vol. 29, No. 2, Feb. 1962, pp. 180-184.

48. Yu, Y. Y., "Non-linear flexural vibrations of sandwich plates," J.Acous.Soc Amer., Vol. 34, No. 9, Sept. 1962, pp. 1176-1183.

49. Yu, Y. Y., "Application of variational equation of motion to the non-linear vibration analysis of homogeneous and layered plates and shells," J.App.Mech., Vol. 30, No. 1, March 1963, pp. 79-86.

50. Chu, H. N., "Influence of transverse shear on non-linear vibrations of sandwich beams with honeycomb cores," J.Aero.Sci., Vol. 28, No. 5, May 1961, pp. 405-410.

51. Naghdi, P. M., "The effect of transverse shear deformation on the bending of elastic shells of revolution," Quart.App.Math., Vol. 15, No. 1, April 1957, pp 41-52.

52. Rossettos, J. N., "Deflection of shallow spherical sandwich shell under local loading," U. S. NASA TN D-3855, Feb. 1967, 45 pages.

53. Kao, J. S., "Axisymmetric deformation of multilayer circular cylindrical sandwich shells," J.Frank.Inst., Vol. 282, No. 1, July 1966, pp. 31-41.

54. Zienkiewicz, O. C. and Holister, G. S. (editors), Stress Analysis: Recent Developments in Numerical and Experiment al Methods, John Wiley & Sons, New York, 1965, 469 pages.

55. Zienkiewicz, O. C. and Cheung, Y. K., The Finite Element Method in Structural and Continuum Mechanics, McGraw-Hill, London, 1967, 272 pages.

56. Przemieniecki, J. S., The Theory of Matrix Structural Analysis, McGraw-Hill, New York, 1968, 468 pages.

57. Felippa, C. A., "Refined finite element analysis of linear and nonlinear two-dimensional structures," Ph.D. Dissertation, University of California, Berkeley, California, 1966.

58. Felippa, C. A., "Refined finite element analysis of linear and nonlinear two-dimensional structures," SESM Report 66-22, Department of Civil Engineering, University of California, Berkeley, California, Oct. 1966.

59. Felippa, C. A., "Analysis of plate bending problems by the finite element method," SESM Report 68-4, Department of Civil Engineering, University of California, Berkeley, California, 1968.

60. Felippa, C. A. and Clough, R. W., "The finite element method in solid mechanics," Symposium on Numerical Solutions of Field Problems in Continuum Mechanics, American Mathematical Society, Durham, N.C., April 5-6, 1968.

61. Argyris, J. H., Energy Theorems and Structural Analysis, Butterworth's, London, 1960 (reprinted from Aircraft Engineering, 1954-1955).

62. Turner, M. J., Clough, R. W., Martin, H. C. and Topp, L. J., "Stiffness and deflection analysis of complex structures," J.Aero.Sci., Vol. 23, No. 9, Sept. 1956, pp. 805-823.

63. Turner, M. J., "The direct stiffness method of structural analysis," AGARD Meeting, Aachen, Germany, 1959.

64. Fraeijs de Veubeke, B., "Upper and lower bounds in matrix structural analysis," in Matrix Methods of Structural Analysis, AGARDograph 72, edited by B. Fraeijs de Veubeke, MacMillan, 1964, 343 pages.

65. Irons, B. H. R. and Draper, K. J., "Inadequacy of nodal connections in a stiffness solution for plate bending," AIAA J., Vol. 3, No. 5, May 1965, p. 961.

66. Clough, R. W. and Tocher, J. L., "Finite element stiffness matrices for analysis of plate bending," Proc.Conf.on Matrix Methods in Structural Mechanics, AFIT, Wright-Patterson AFB, Ohio, 1965, pp. 515-541.

67. Adini, A. and Clough, R. W., "Analysis of plate bending by the finite element method," NSF Report, Grant G7337, 1960.

68. Melosh, R. J., "Basis for derivation of matrices for the direct stiffness method," AIAA J., Vol. 1, No. 7, July 1963, pp. 1631-1637.

69. Melosh, R. J., "A stiffness matrix for the analysis of thin plates in bending," J.Aero.Sci., Vol. 28, No. 1, Jan. 1961, pp. 34-42.

70. Papenfuss, S. W., "Lateral plate deflection by stiffness matrix methods with application to a marquee," M.S. Dissertation, Department of Civil Engineering, University of Washington, Seattle, 1959.

71. Timoshenko, S. P., "On the correction for shear of differential equation for transverse vibrations of prismatic bars," Philosophical Mag., Vol. 41, Series 6, 1921, pp. 744-746.

72. Timoshenko, S. P., "On the transverse vibration of bars of uniform cross-section," Philosophical Mag., Vol. 42, Series 6, 1922, pp. 125-131.

73. Mindlin, R. D., "Influence of rotatory inertia on shear and flexural motions of isotropic elastic plates," J.App.Mech., Vol. 18, No. 1, March 1951, pp. 31-38.

74. Clough, R. W. and Johnson, C. P., "A finite element approximation for the analysis of thin shells," Int'l.J.Solids Structures, Vol. 4, No. 1, Jan. 1968, pp. 43-60.

75. Carr, A. J., "A refined finite element analysis of thin shells including dynamic loads," Ph.D. Dissertation, Department of Civil Engineering, University of California, Berkeley, California, 1967 (also published as SESM Report 67-9).

76. Johnson, C. P., "The analysis of thin shells by a finite element procedure," Ph.D. Dissertation, Department of Civil Engineering, University of California, Berkeley, California, 1967 (also published as SESM Report 67-22).

77. Meyer, R. R. and Harmon, M. B., "Conical segment method for analyzing open crown shells of revolution for edge loading," AIAA J., Vol. 1, No. 4, April 1963, pp. 886-891.

78. Popov, E. P., Penzien, J., and Lu, Z. A., "Finite element solution for axisymmetric shells," J.of Eng.Mechs.Div., Proc. ASCE, Vol. 90, No. EM5, Oct. 1964, pp. 119-145.

79. Grafton, P. E. and Strome, D. R., "Analysis of axisymmetrical shells by the direct stiffness method," AIAA J., Vol. 1, No. 10, Oct. 1963, pp. 2342-2347.

80. Percy, J. H., Pian, T. H. H., Klein, S. and Navaratna, D. R., "Application of matrix displacement method to linear elastic analysis of shells of revolution," AIAA J., Vol. 3, No. 11, Nov. 1965, pp. 2138-2145.

81. Jones, R. E. and Strome, D. R., "A survey of the analysis of shells by the displacement method," Proc.Conf. on Matrix Methods in Structural Mechanics, AFIT, Wright-Patterson AFB, Ohio, 1965, pp. 205-229.

82. Jones, R. E. and Strome, D. R., "Direct stiffness method analysis of shells of revolution utilizing curved elements," AIAA J., Vol. 4, No. 9, Sept. 1966, pp. 1519-1525.

83. Striklin, J. A., Navaratna, D. R. and Pian, T. H. H., "Improvements on the analysis of shells of revolution by the matrix displacement method," AIAA J., Vol. 4, No. 11, Nov. 1966, pp. 2069-2072.

84. Khojasteh-Bakht, M., "Analysis of elastic-plastic shells of revolution under axisymmetric loading by the finite element method," Ph.D. Dissertation, Department of Civil Engineering, University of California, Berkeley, California, 1967 (also published as SESM Report 67-8).

85. Archer, J. S., "Consistent matrix formulations for structural analysis using finite element techniques," AIAA J., Vol. 3, No. 10, Oct. 1965, pp. 1910-1918.

86. Ruzicka, J. E., (editor), Structural Damping, ASME, New York, 1959.

87. Lazan, B. J., "Energy dissipation mechanisms in structures, with particular reference to material damping," pp. 1-34 of Reference 86.

88. Ross, D., Ungar, E. E. and Kerwin, E. M. Jr., "Damping of plate flexural vibrations by means of viscoelastic laminae," pp. 49-87 of Reference 86.

89. Hertelendy, P., "Eigenvalue approximations for elastic bodies and the effect of damping due to internal dissipation or to a surface membrane coating," Ph.D. Dissertation, Department of Mechanical Engineering, University of California, Berkeley, California, 1965.

90. Nelson, F. C., "The use of viscoelastic material to damp vibration in buildings and large structures," AISC Engineering Journal, April 1968, pp. 72-78.

91. Blanchflower, R., "Damping properties of engineering and viscoelastic materials," Environmental Engineering, No. 19, March 1966, pp. 19-25.

92. Kerwin, E. M. Jr., "Macromechanisms of damping in composite structures," Internal Friction, Damping and Cyclic Plasticity, ASTM STP-378, Philadelphia, Pennsylvania, 1964, pp. 125-147.

93. James, R. R., "Reduction of ships' noise by viscoelastic damping," (abstract) J.Acous.Soc.Amer., Vol. 37, No. 6, June 1965, p. 1207.

94. Lazan, B. J., "Damping properties of material and material composites," App.Mechs.Rev., Vol. 15, No. 2, Feb. 1962, pp. 81-88.

95. Ungar, E. E. and Hatch, D. K., "Your selection guide to high damping materials," Prod.Eng., Vol. 32, No. 16, April 17, 1961, pp. 44-56.

96. Oberst, H., Bohn, L. and Linhardt, F., "Schwingungdämpfende Kunststoffe in der Lärmbekämpfung," Kunststoffe, Vol. 51, No. 9, Sept. 1961, pp. 495-502.

97. Ball, G. L. III and Salyer, I. O., "Development of a viscoelastic composition having superior vibration-damping capability," J.Acous. Soc.Amer., Vol. 39, No. 4, April 1966, pp. 663-673.

98. Owens, F. S., "Elastomers for damping over wide temperature ranges," NRL Shock and Vibration Bull., No. 36, Part 4, Jan. 1967, pp. 25-35.

99. Oberst, H. and Frankenfeld, K., "Über die Dämpfung der Biegeschwingungen dünner Bleche durch fest haftende Beilage--I," Acustica, Akustische Beihefte, Vol. 2, No. 4, 1952, pp. AB181-AB194.

100. Oberst, H. and Becker, G. W., "Über die Dämpfung der Biegeschwingungen dünner Bleche durch fest haftende Beilage--II," Acustica, Vol. 4, No. 1, 1954, pp. 433-444.

101. Liénard, P., "Etude d'une méthode de mesure du frottement intérieur de revetements plastiques travaillant en flexion," La Recherche Aéronautique, No. 20, March-April 1951, pp. 11-22.

102. Schwarzl, F., "Forced bending and extensional vibrations of a two-layered compound linear viscoelastic beam," Acustica, Vol. 8, No. 3, 1958, pp. 164-172.

103. Ungar, E. E., "Damping tapes for vibration control," Prod.Eng., Vol. 31, No. 4, Jan. 25, 1960, pp. 57-62.

104. Ungar, E. E. and Ross, D., "Damping of flexural vibrations by alternate viscoelastic and elastic layers," Proc. Fourth Midwestern Conf. on Fluid and Solid Mech., University of Texas Press, Austin, Texas, 1959, pp. 468-487.

105. Kerwin, E. M. Jr., "Damping of flexural waves by a constrained viscoelastic layer," J.Acous.Soc.Amer., Vol. 31, No. 7, July 1959, pp. 952-962.

106. Plass, H. J. Jr., "Damping of vibrations in elastic rods and sandwich structures by incorporation of additional viscoelastic material," Proc. Third Midwestern Conf. on Solid Mechs., 1957, pp. 48-71.

107. Ungar, E. E., "Loss factors of viscoelastically damped beam structures," J.Acous.Soc.Amer., Vol. 34, No. 8, August 1962, pp. 1082-1089.

108. Mead, D. J., "Damped sandwich plate for vibration control," Environmental Engineering, No. 9, March 1964, pp. 11-15.

109. DiTaranto, R. A., "Theory of vibratory bending for elastic and viscoelastic finite-length beams," J.App.Mech., Vol. 32, No. 4, Dec. 1965, pp. 881-886.

110. DiTaranto, R. A. and Blasingame, W., "Effect of end conditions on the damping of laminated beams," J.Acous.Soc.Amer., Vol. 39, No. 2, Feb. 1966, pp. 405-407.

111. DiTaranto, R. A. and Blasingame, W., "Composite loss factors of selected laminated beams," J.Acous.Soc.Amer., Vol. 40, No. 1, July 1966, pp. 187-194.

112. DiTaranto, R. A. and Blasingame, W., "Composite damping of vibrating sandwich beams," Paper No. 67-Vibr-6, ASME Vibrations Conference, Boston, Massachusetts, March 29-31, 1967.

113. Bert, C. W., Wilkins, D. J. Jr. and Crisman, W. C., "Damping in sandwich beams with shear flexible cores," Paper No. 67-Vibr.-11, ASME Vibrations Conf., Boston, Massachusetts, March 29-31, 1967.

114. Ruzicka, J. E., Derby, T. F., Schubert, D. W. and Pepi, J. S., "Damping of structural composites with viscoelastic shear-damping mechanisms," U. S. NASA CR-742, Washington, D. C., March 1967, 176 pages.

115. Yu, Y. Y., "Damping of flexural vibrations of sandwich plates," J.Aero.Sci., Vol. 29, No. 7, July 1962, pp. 790-803.

116. Yu, Y. Y. "Viscoelastic damping of vibrations of sandwich plates and shells," Proc.IASS Symp. on Non-Classical Shell Probs., North-Holland Pub. Co., Amsterdam, and Polish Scientific Publications, Warsaw, 1964, pp. 551-571.

117. Yu, Y. Y. and Ren, N., "Damping parameters of layered plates and shells," Accoustical Fatigue in Aerospace Structures, Proc. Second Int. Conf. Acous. Fatigue, Trapp, W. J. and Forney, D. R. Jr. (editors), Syracuse University Press, Syracuse, New York, 1965, pp. 555-584.

118. Hertelendy, P. and Goldsmith, W., "Flexural vibrations of elastic plates with two symmetric viscoelastic coatings," J.App.Mech., Vol. 34, No. 1, March 1967, pp. 187-194.

119. Nicholas, T. and Heller, R. A., "Determination of the complex shear modulus of a filled elastomer from a vibrating sandwich beam," Exp.Mechs., Vol. 7, No. 3, March 1967, pp. 110-116.

120. Nashif, A. D., "New method for determining damping properties of viscoelastic materials," NRL Shock and Vibration Bull., Jan. 1967, pp. 37-47.

121. Love, A. E. H., A Treatise on the Mathematical Theory of Elasticity, Fourth Edition, Dover Pubs., New York, 1944, 643 pages.

122. Novozhilov, V. V., The Theory of Thin Elastic Shells, translated from the Russian by P. G. Lowe, edited by J. R. M. Radok, P. Noordhoff Ltd., Groningen, The Netherlands, 1959.

123. Cowper, G. R., "The shear coefficient in Timoshenko's beam theory," J.App.Mech., Vol. 33, No. 2, June 1966., pp. 335-340.

124. Reissner, E., "The effect of transverse shear deformation on the bending of elastic plates," J.App.Mech., Vol. 12, No. 2, June 1945, pp. A69-A77.

125. Nordby, G. M., Crisman, W. C. and Bert, C. W., "Dynamic elastic, damping and fatigue characteristics of fibreglass reinforced sandwich structure," U. S. Army Aviation Material Laboratories, Technical Report 65-60, Oct. 1965.

126. Clough, R. W., "The finite element method in structural mechanics," Chapter 7, pp. 85-119 of Reference 54.

127. Turner, M. J., Martin, R. C. and Weikel, R. C., "Further developments and applications of the stiffness method," in AGARDograph 72, cited in Reference 64.

128. Fraeijs de Veubeke, B., "Displacement and equilibrium models in the finite element method," Chapter 9, pp. 145-197 of Reference 54.

129. Timoshenko, S. P., Strength of Materials, Third Edition, Vol. I, D. Van Nostrand Co., Princeton, New Jersey, 1956, Section 39, pp. 170-175.

130. March, H. W., "Sandwich construction in the elastic range," Symposium on Structural Sandwich Construction, ASTM Special Technical Publication No. 118, Philadelphia, Pennsylvania, 1951, pp. 32-45.

131. Abramowitz, M. and Stegun, I. A. (editors), Handbook of Mathematical Functions with Formulas, Graphs and Mathematical Tables, National Bureau of Standards, App. Math Series No. 55, 1964, (also Dover, New York, 1965), pp. 887-89, 916-917.

132. Timoshenko, S. P. and Woinowsky-Krieger, S., Theory of Plates and Shells, McGraw-Hill, New York, 1960, 580 pages.

133. Flügge, W., Stresses in Shells, Springer-Verlag, Berlin, 1961, 499 pages.

134. Wilkinson, J. P. D., "Natural frequencies of closed spherical sandwich shells," J.Ac.Soc.Amer., Vol. 40, No. 4, Oct. 1966, pp. 801-806.

135. Bland, D. R., The Theory of Linear Viscoelasticity, Pergamon Press, New York, 1960, 125 pages.

136. Flügge, W., Viscoelasticity, Blaisdell Publishing Co., Waltham, Massachusetts, 1967, 127 pages.

137. Tobolsky, A. V., Properties and Structure of Polymers, John Wiley & Sons, New York, 1960, 331 pages.

138. Ferry, J. D., Viscoelastic Properties of Polymers, John Wiley & Sons, New York, 1961, 482 pages.

139. Bueche, F., Physical Properties of Polymers, Interscience Publishers, New York, 1962, 354 pages.

140. Nielson, L. E., Mechanical Properties of Polymers, Reinhold Publishing Co., New York, 1962, 274 pages.

141. Ritchie, P. D. (editor), Physics of Plastics, D. Van Nostrand Co., Princeton, New Jersey, 1965, 447 pages.

142. Baer, E. (editor), Engineering Design for Plastics, Reinhold Publishing Co., New York, 1964, 1202 pages.

143. Sharma, M. G., Viscoelasticity and Mechanical Properties of Polymers, Summer Institute on Applied Mechanics and Materials Science, Department of Engineering Mechanics, The Pennsylvania State University, University Park, Pennsylvania, 1964, 280 pages.

144. Kaelble, D. H., "Micromechanisms and phenomenology of damping in polymers," Internal Friction, Damping and Cyclic Plasticity, ASTM STP-378, Philadelphia, Pennsylvania, 1964, pages 109-124.

145. Ungar, E. E. and Kerwin, E. M. Jr., "Loss factors of viscoelastic systems in terms of energy concepts," J.Ac.Soc.Amer., Vol. 34, No. 7, July 1962, pages 954-957.

146. Murray, R. C., "Steady state vibrations of linear viscoelastic solids," Graduate Student Research Report No. 331, SESM Division, Department of Civil Engineering, University of California, Berkeley, California, 1968.

147. Leitmann, M. J., "Variational principles in the linear dynamic theory of viscoelasticity," Quart.App.Math., Vol. 24, No. 1, April 1966, pp. 37-46.

148. Wilson, E. L. and Nickell, R. E., "Application of the finite element method to heat conduction analysis," Nuc.Eng.and Design, Vol. 4, No. 3, Oct. 1966, pp. 276-286.

149. Nickell, R. E. and Sackman, J. L., "Variational principles for linear coupled thermoelasticity," Quart.App.Math., Vol. 26, No.1, April 1968, pp. 11-26.

150. Chang, T. Y., "Approximate solutions in linear viscoelasticity," SESM Report 66-8, Department of Civil Engineering, University of California, Berkeley, California, 1966.

APPENDIX A: MATRICES FOR SANDWICH BEAMS

The matrices that follow are for a three-layer sandwich beam element of unit width and length ℓ. The facing layers are of equal thickness and are composed of the same material. Further details are given in Section III.1.

A.1. Linear Variation of Shear Strain

The relevant vectors for the stiffness analysis are defined as follows:

$$\{u(\xi)\}^T = \langle w(\xi)\ \chi(\xi)\ \gamma_c(\xi)\ \gamma_f(\xi)\rangle$$

$$\{q\}^T = \langle u(o)\ \vdots\ u(1)\rangle = \langle u_i\ \vdots\ u_j\rangle$$

$$\{\varepsilon(\xi)\}^T = \langle \kappa_{xc}\ \gamma_{xzc}\ \varepsilon^{ot}_{xf}\ \kappa^{t}_{xf}\ \gamma^{t}_{xzf}\ \varepsilon^{ob}_{xf}\ \kappa^{b}_{xf}\ \gamma^{b}_{xzf}\rangle$$

$$\{\in(\xi,z)\}^T = \langle \varepsilon_{xc}\ \gamma_{xzc}\ \varepsilon^{t}_{xf}\ \gamma^{t}_{xzf}\ \varepsilon^{b}_{xf}\ \gamma^{b}_{xzf}\rangle$$

$$\{\sigma(\xi,z)\}^T = \langle \sigma_{xc}\ \tau_{xzc}\ \sigma^{t}_{xf}\ \tau^{t}_{xzf}\ \sigma^{b}_{xf}\ \tau^{b}_{xzf}$$

$$\{r\}^T = \langle w_i\ \chi_{bi}\ \gamma_i\ w_j\ \chi_{bj}\ \gamma_j\ \vdots\ \gamma_{fi}\ \gamma_{fj}\rangle$$

A.1.1. $[\Phi(\xi)]$ of Equation (II.19)

$$\left[\begin{array}{cccc|cccc}
(1-3\xi^2+2\xi^3) & \ell\xi(1-2\xi+\xi^2) & 0 & 0 & \xi^2(3-2\xi) & \ell\xi^2(\xi-1) & 0 & 0 \\
6\xi(\xi-1)/\ell & (1-4\xi+3\xi^2) & 0 & 0 & 6\xi(1-\xi)/\ell & \xi(3\xi-2) & 0 & 0 \\
0 & 0 & (1-\xi) & 0 & 0 & 0 & \xi & 0 \\
0 & 0 & 0 & (1-\xi) & 0 & 0 & 0 & \xi
\end{array}\right]$$

A.1.2 [ ] of Equation (II.20)

$$\left[\begin{array}{cccc|cccc}
\frac{6}{\ell^2}(1-2\xi) & \frac{2}{\ell}(2-3\xi) & -\frac{1}{\ell} & 0 & \frac{6}{\ell^2}(2\xi-1) & \frac{2}{\ell}(1-3\xi) & \frac{1}{\ell} & 0 \\
0 & 0 & (1-\xi) & 0 & 0 & 0 & \xi & 0 \\
\frac{3d}{\ell^2}(2\xi-1) & \frac{d}{\ell}(3\xi-2) & \frac{h_c}{2\ell} & \frac{h_f}{2\ell} & \frac{3d}{\ell^2}(1-2\xi) & \frac{d}{\ell}(3\xi-1) & -\frac{h_c}{2\ell} & -\frac{h_f}{2\ell} \\
\frac{6}{\ell^2}(1-2\xi) & \frac{2}{\ell}(2-3\xi) & 0 & -\frac{1}{\ell} & \frac{6}{\ell^2}(2\xi-1) & \frac{2}{\ell}(1-3\xi) & 0 & \frac{1}{\ell} \\
0 & 0 & 0 & (1-\xi) & 0 & 0 & 0 & \xi \\
\frac{3d}{\ell^2}(1-2\xi) & \frac{d}{\ell}(2-3\xi) & -\frac{h_c}{2\ell} & -\frac{h_f}{2\ell} & \frac{3d}{\ell^2}(2\xi-1) & \frac{d}{\ell}(1-3\xi) & \frac{h_c}{2\ell} & \frac{h_f}{2\ell} \\
\frac{6}{\ell^2}(1-2\xi) & \frac{2}{\ell}(2-3\xi) & 0 & -\frac{1}{\ell} & \frac{6}{\ell^2}(2\xi-1) & \frac{2}{\ell}(1-3\xi) & 0 & \frac{1}{\ell} \\
0 & 0 & 0 & (1-\xi) & 0 & 0 & 0 & \xi
\end{array}\right]$$

A.1.3. [Z] of Equation (II.21)

$$\begin{bmatrix}
z_c & 0 & 0 & 0 & 0 & 0 & 0 & 0 \\
0 & 1 & 0 & 0 & 0 & 0 & 0 & 0 \\
0 & 0 & 1 & z_f & 0 & 0 & 0 & 0 \\
0 & 0 & 0 & 0 & 1 & 0 & 0 & 0 \\
0 & 0 & 0 & 0 & 0 & 1 & z_f & 0 \\
0 & 0 & 0 & 0 & 0 & 0 & 0 & 1
\end{bmatrix}$$

A.1.4. [C] of Equation (II.22)

$$\begin{bmatrix}
E_c & & & & & & & \\
 & \kappa_c G_c & & & & & & \\
 & & E_f & & & & & \\
 & & & \kappa_f G_f & & & & \\
 & & & & E_f & & & \\
 & & & & & \kappa_f G_f & &
\end{bmatrix}$$

A.1.5. [G] of Equation (II.27)

$$\begin{bmatrix} E_c I_c & & & & & & & & & & & \\ & \kappa_c G_c A_c & & & & & & & & & & \\ & & E_f A_f & & & & & & & & & \\ & & & E_f I_f & & & & & & & & \\ & & & & \kappa_f G_f A_f & & & & & & & \\ & & & & & E_f A_f & & & & & & \\ & & & & & & E_f I_f & & & & & \\ & & & & & & & \kappa_f G_f A_f & & & & \\ & & & & & & & & E_f A_f & & & \\ & & & & & & & & & E_f I_f & & \\ & & & & & & & & & & \kappa_f G_f A_f & \\ & & & & & & & & & & & \searrow \end{bmatrix}$$

A.1.6. $[k_q]$ of Equations (II.29) and (III.9)

$$[k_c^Q] = \frac{\kappa_c A_c G_c \ell}{6} \left[\begin{array}{cccc|cccc} 0 & 0 & 0 & 0 & 0 & 0 & 0 & 0 \\ & 0 & 0 & 0 & 0 & 0 & 0 & 0 \\ & & 2 & 0 & 0 & 0 & 1 & 0 \\ & & & 0 & 0 & 0 & 0 & 0 \\ \hline & & & & 0 & 0 & 0 & 0 \\ & & & & & 0 & 0 & 0 \\ \text{symmetric} & & & & & & 2 & 0 \\ & & & & & & & 0 \end{array}\right]$$

$$[k_c^M] = \frac{E_c I_c}{\ell^3} \left[\begin{array}{cccc|cccc} 12 & 6\ell & 0 & 0 & -12 & 6\ell & 0 & 0 \\ & 4\ell^2 & -\ell^2 & 0 & -6\ell & 2\ell^2 & \ell^2 & 0 \\ & & \ell^2 & 0 & 0 & \ell^2 & -\ell^2 & 0 \\ & & & 0 & 0 & 0 & 0 & 0 \\ \hline & & & & 12 & -6\ell & 0 & 0 \\ & & & & & 4\ell^2 & -\ell^2 & 0 \\ \text{symmetric} & & & & & & \ell^2 & 0 \\ & & & & & & & 0 \end{array}\right]$$

$$[k_f^Q] = \frac{\kappa_f A_f G_f \ell}{3}$$

$$\left[\begin{array}{cccc|cccc} 0 & 0 & 0 & 0 & 0 & 0 & 0 & 0 \\ & 0 & 0 & 0 & 0 & 0 & 0 & 0 \\ & & 0 & 0 & 0 & 0 & 0 & 0 \\ & & & 2 & 0 & 0 & 0 & 1 \\ \hline & & & & 0 & 0 & 0 & 0 \\ & & & & & 0 & 0 & 0 \\ & & & & & & 0 & 0 \\ \text{symmetric} & & & & & & & 2 \end{array}\right]$$

$$[k_f^M] = \frac{2E_f I_f}{\ell^3}$$

$$\left[\begin{array}{cccc|cccc} 12 & 6\ell & 0 & 0 & -12 & 6\ell & 0 & 0 \\ & 4\ell^2 & 0 & -\ell^2 & -6\ell & 2\ell^2 & 0 & \ell^2 \\ & & 0 & 0 & 0 & 0 & 0 & 0 \\ & & & \ell^2 & 0 & \ell^2 & 0 & -\ell^2 \\ \hline & & & & 12 & -6\ell & 0 & 0 \\ & & & & & 4\ell^2 & 0 & -\ell^2 \\ & & & & & & 0 & 0 \\ \text{symmetric} & & & & & & & \ell^2 \end{array}\right]$$

$$[k_f^N] = \frac{E_f A_f}{2\ell^3}$$

$$\left[\begin{array}{cccc|cccc} 12d^2 & 6\ell i^2 & 0 & 0 & -12d^2 & 6\ell d^2 & 0 & 0 \\ & 4\ell^2 d & -h_c \ell^2 d & -h_f \ell^2 d & -6\ell d^2 & 2\ell^2 d^2 & h_c \ell^2 d & h_f \ell^2 d \\ & & h_c^2 \ell^2 & h_c h_f \ell^2 & 0 & h_c \ell^2 d & -h_c^2 \ell^2 & -h_c h_f \ell^2 \\ & & & h_f^2 \ell^2 & 0 & h_f \ell^2 d & -h_c h_f \ell^2 & -h_f^2 \ell^2 \\ \hline & & & & 12d^2 & -6\ell d^2 & 0 & 0 \\ & & & & & 4\ell^2 d^2 & -h_c \ell^2 d & -h_f \ell^2 d \\ & & & & & & -h_c^2 \ell^2 & h_c h_f \ell^2 \\ \text{symmetric} & & & & & & & h_f \ell^2 \end{array}\right]$$

A.1.7. Transformation matrix [T] = [$\underline{T}$] of Equation (II.31)

$$\left[\begin{array}{cccccc|cc}
1 & 0 & 0 & 0 & 0 & 0 & 0 & 0 \\
0 & 1 & h_c/d & 0 & 0 & 0 & 1 & 0 \\
0 & 0 & 1 & 0 & 0 & 0 & 1 & 0 \\
0 & 0 & 0 & 0 & 0 & 0 & 1 & 0 \\
\hline
0 & 0 & 0 & 1 & 0 & 0 & 0 & 0 \\
0 & 0 & 0 & 0 & 1 & h_c/d & 0 & 1 \\
0 & 0 & 0 & 0 & 0 & 0 & 0 & 1 \\
0 & 0 & 0 & 0 & 0 & 0 & 0 & 1
\end{array}\right]$$

A.1.8. Consistent load vector in global co-ordinates from Equations (II.29) and (II.33).

$$\{R\}^T = \frac{p_z \ell}{2} \left\langle 1 \; \frac{\ell}{6} \; \frac{h_c \ell}{6} \; 1 \; \frac{-\ell}{6} \; \frac{-h_c \ell}{6} \; \middle| \; \frac{\ell}{6} \; \frac{-\ell}{6} \right\rangle$$

A.2. Quadratic Variation of Shear Strain

The relevant vectors for the stiffness analysis are defined as follows:

$$\{q\}^T = \langle w_i \; X_i \; \gamma_{ci} \; \gamma_{fi} \; | \; w_j \; X_j \; \gamma_{cj} \; \gamma_{fj} \; | \; \gamma_{co} \; \gamma_{fo} \rangle$$

$$\{r\}^T = \langle w_i \; X_{bi} \; \gamma_i \; w_j \; X_{bj} \; \gamma_j \; | \; \gamma_{fi} \; \gamma_{fj} \; \gamma_{co} \; \gamma_{fo} \rangle$$

The vectors $\{u\}$, $\{\varepsilon\}$, $\{\epsilon\}$ and $\{\sigma\}$ remain the same as given in Appendix A.1. [Z], [C] and [G] are also unchanged.

A.2.1. $[\Phi(\xi)]$ of Equation (II.19)

$$\left[\begin{array}{cccc|cccc}
(1-3\xi^2+2\xi^3) & \ell\xi(1-2\xi+\xi^2) & 0 & 0 & \xi^2(3-2\xi) & \ell\xi^2(\xi-1) & 0 & 0 \\
6\xi(\xi-1)/\ell & (1-4\xi+3\xi^2) & 0 & 0 & 6\xi(1-\xi)/\ell & \xi(3\xi-2) & 0 & 0 \\
0 & 0 & (1-3\xi+2\xi^2) & 0 & 0 & 0 & \xi(2\xi-1) & 0 \\
0 & 0 & 0 & (1-3\xi+2\xi^2) & 0 & 0 & 0 & \xi(2\xi-1)
\end{array}\right.$$

$$\left.\begin{array}{cc}
0 & 0 \\
0 & 0 \\
4\xi(1-\xi) & 0 \\
0 & 4\xi(1-\xi)
\end{array}\right]$$

A.2.2. $[B(\xi)]$ of Equation (II.20)

$$\left[\begin{array}{cccc|cccc}
\frac{6}{\ell^2}(1-2\xi) & \frac{2}{\ell}(2-3\xi) & \frac{1}{\ell}(4\xi-3) & 0 & \frac{6}{\ell^2}(2\xi-1) & \frac{2}{\ell}(1-3\xi) & \frac{1}{\ell}(4\xi-1) & 0 \\
0 & 0 & (1-3\xi+2\xi^2) & 0 & 0 & 0 & \xi(2\xi-1) & 0 \\
\frac{3d}{\ell^2}(2\xi-1) & \frac{d}{\ell}(3\xi-2) & \frac{h_c}{2\ell}(3-4\xi) & \frac{h_f}{2\ell}(3-4\xi) & \frac{3d}{\ell^2}(1-2\xi) & \frac{d}{\ell}(3\xi-1) & \frac{h_c}{2\ell}(1-4\xi) & \frac{h_f}{2\ell}(1-4\xi) \\
\frac{6}{\ell^2}(1-2\xi) & \frac{2}{\ell}(2-3\xi) & 0 & \frac{1}{\ell}(4\xi-3) & \frac{6}{\ell^2}(2\xi-1) & \frac{2}{\ell}(1-3\xi) & 0 & \frac{1}{\ell}(4\xi-1) \\
0 & 0 & 0 & (1-3\xi+2\xi^2) & 0 & 0 & 0 & \xi(2\xi-1) \\
\frac{3d}{\ell^2}(1-2\xi) & \frac{d}{\ell}(2-3\xi) & \frac{h_c}{2\ell}(4\xi-3) & \frac{h_f}{2\ell}(4\xi-3) & \frac{3d}{\ell^2}(2\xi-1) & \frac{d}{\ell}(1-3\xi) & \frac{h_c}{2\ell}(4\xi-1) & \frac{h_f}{2\ell}(4\xi-1) \\
\frac{6}{\ell^2}(1-2\xi) & \frac{2}{\ell}(2-3\xi) & 0 & \frac{1}{\ell}(3-4\xi) & \frac{6}{\ell^2}(2\xi-1) & \frac{2}{\ell}(1-3\xi) & 0 & \frac{1}{\ell}(1-4\xi) \\
0 & 0 & 0 & (1-3\xi+2\xi^2) & 0 & 0 & 0 & \xi(2\xi-1)
\end{array}\right.$$

$$\left.\begin{array}{cc}
\frac{4}{\ell}(1-2\xi) & 0 \\
4\xi(1-\xi) & 0 \\
\frac{2h_c}{\ell}(2\xi-1) & \frac{2h_f}{\ell}(2\xi-1) \\
0 & \frac{4}{\ell}(1-2\xi) \\
0 & 4\xi(1-\xi) \\
\frac{2h_c}{\ell}(1-2\xi) & \frac{2h_f}{\ell}(1-2\xi) \\
0 & \frac{4}{\ell}(1-2\xi) \\
0 & 4\xi(1-\xi)
\end{array}\right]$$

A.2.3. $[k_q]$ of Equations (II.29) and (III.9)

$$[k_c^Q] = \frac{\kappa_c A_c G_c \ell}{30}$$

$$\begin{bmatrix}
0 & 0 & 0 & 0 & 0 & 0 & 0 & 0 & 0 & 0 \\
 & 0 & 0 & 0 & 0 & 0 & 0 & 0 & 0 & 0 \\
 & & 4 & 0 & 0 & 0 & -1 & 0 & 2 & 0 \\
 & & & 0 & 0 & 0 & 0 & 0 & 0 & 0 \\
 & & & & 0 & 0 & 0 & 0 & 0 & 0 \\
 & & & & & 0 & 0 & 0 & 0 & 0 \\
 & & & & & & 4 & 0 & 2 & 0 \\
 & & & & & & & 0 & 0 & 0 \\
 & & & & & & & & 1\ell & 0 \\
\text{symmetric} & & & & & & & & & 0
\end{bmatrix}$$

$$[k_c^M] = \frac{E_c I_c}{\ell^3}$$

$$\begin{bmatrix}
12 & 6\ell & -4\ell & 0 & -12 & 6\ell & -4\ell & 0 & 8\ell & 0 \\
 & 4\ell^2 & -3\ell^2 & 0 & -6\ell & 2\ell^2 & -\ell^2 & 0 & 4\ell^2 & 0 \\
 & & 7\ell^2/3 & 0 & 4\ell & -\ell^2 & \ell^2/3 & 0 & -8\ell^2/3 & 0 \\
 & & & 0 & 0 & 0 & 0 & 0 & 0 & 0 \\
 & & & & 12 & -6\ell & 4\ell & 0 & -8\ell & 0 \\
 & & & & & 4\ell^2 & -3\ell^2 & 0 & 4\ell^2 & 0 \\
 & & & & & & 7\ell^3/3 & 0 & -8\ell^2/3 & 0 \\
 & & & & & & & 0 & 0 & 0 \\
 & & & & & & & & 16\ell^2/3 & 0 \\
\text{symmetric} & & & & & & & & & 0
\end{bmatrix}$$

$$[k_f^Q] = \frac{\kappa_f A_f G_f \ell}{15}$$

$$\begin{bmatrix}
0 & 0 & 0 & 0 & 0 & 0 & 0 & 0 & 0 & 0 \\
 & 0 & 0 & 0 & 0 & 0 & 0 & 0 & 0 & 0 \\
 & & 0 & 0 & 0 & 0 & 0 & 0 & 0 & 0 \\
 & & & 4 & 0 & 0 & 0 & -1 & 0 & 2 \\
 & & & & 0 & 0 & 0 & 0 & 0 & 0 \\
 & & & & & 0 & 0 & 0 & 0 & 0 \\
 & & & & & & 0 & 0 & 0 & 0 \\
\text{symmetric} & & & & & & & 4 & 0 & 2 \\
 & & & & & & & & 0 & 0 \\
 & & & & & & & & & 16
\end{bmatrix}$$

$$[k_f^M] = \frac{2E_f I_f}{\ell^3}$$

$$\begin{bmatrix}
12 & 6\ell & 0 & -4\ell & -12 & 6\ell & 0 & -4\ell & 0 & 8\ell \\
 & 4\ell^2 & 0 & -3\ell^2 & -6\ell & 4\ell^2 & 0 & -\ell^2 & 0 & 4\ell^2 \\
 & & 0 & 0 & 0 & 0 & 0 & 0 & 0 & 0 \\
 & & & 7\ell^2/3 & 4\ell & -\ell^2 & 0 & \ell^2/3 & 0 & -8\ell^2/3 \\
 & & & & 12 & -6\ell & 0 & 4\ell & 0 & -8\ell \\
 & & & & & 4\ell^2 & 0 & -3\ell^2 & 0 & 4\ell^2 \\
 & & & & & & 0 & 0 & 0 & 0 \\
 & & & & & & & -7\ell^3/3 & 0 & -8\ell^3/3 \\
\text{symmetric} & & & & & & & & 0 & 0 \\
 & & & & & & & & & 16\ell^2/3
\end{bmatrix}$$

$$[k_f^N] = \frac{E_f A_f}{\ell^3}$$

$$\begin{bmatrix}
6d^2 & 3d^2\ell & -2h_c d\ell & -2h_f d\ell & -6d^2 & 3d^2\ell & -2h_c d\ell & -2h_f d\ell & 4h_c d\ell & 4h_f d\ell \\
 & 2d^2\ell^2 & -3h_c d\ell^2/2 & -3h_f d\ell^2/2 & -3d^2\ell & d^2\ell^2 & -h_c d\ell^2/2 & -h_f d\ell^2/2 & 2h_c d\ell^2 & 2h_f d\ell^2 \\
 & & 7h_c^2\ell^2/6 & 7h_c h_f \ell^2/6 & 2h_c d\ell & -h_c d\ell^2/2 & h_c^2\ell^2/6 & h_c h_f \ell^2/6 & -4h_c^2\ell^2/6 & -4h_c h_f \ell^2/3 \\
 & & & 7h_f^2\ell^2/6 & 2h_f d\ell & -h_f d\ell^2/2 & h_c h_f \ell^2/6 & h_f^2\ell^2/6 & -4h_c h_f \ell^2/3 & -4h_f^2\ell^2/3 \\
 & & & & 6d^2 & -3d^2\ell & 2h_c d\ell & 2h_f d\ell & -4h_c h_f \ell^2/3 & -4h_f d\ell \\
 & & & & & 2d^2\ell & -3h_c d\ell^2/2 & -3h_f d\ell^2/2 & 2h_c d\ell^2 & 2h_f d\ell^2 \\
 & & & & & & 7h_c^2\ell^2/6 & 7h_c h_f \ell^2/6 & -4h_c^2\ell^2/3 & -4h_c h_f \ell^2/3 \\
 & & & & & & & 7h_f^2\ell^2/6 & -4h_c h_f \ell^2/3 & -4h_f^2\ell^2/3 \\
\text{symmetric} & & & & & & & & 8h_c^2\ell^2/3 & 8h_f h_c \ell^2/3 \\
 & & & & & & & & & 8h_f^2\ell^2/3
\end{bmatrix}$$

A.2.4 Transformation matrix $[T] = [\underline{T}]$ of Equation (II.31)

$$\begin{bmatrix}
1 & 0 & 0 & 0 & 0 & 0 & 0 & 0 & 0 & 0 \\
0 & 1 & h_c/d & 0 & 0 & 0 & 1 & 0 & 0 & 0 \\
0 & 0 & 1 & 0 & 0 & 0 & 1 & 0 & 0 & 0 \\
0 & 0 & 0 & 0 & 0 & 0 & 1 & 0 & 0 & 0 \\
0 & 0 & 0 & 1 & 0 & 0 & 0 & 0 & 0 & 0 \\
0 & 0 & 0 & 0 & 1 & h_c/d & 0 & 1 & 0 & 0 \\
0 & 0 & 0 & 0 & 0 & 1 & 0 & 1 & 0 & 0 \\
0 & 0 & 0 & 0 & 0 & 0 & 0 & 1 & 0 & 0 \\
0 & 0 & 0 & 0 & 0 & 0 & 0 & 0 & 1 & 0 \\
0 & 0 & 0 & 0 & 0 & 0 & 0 & 0 & 0 & 1
\end{bmatrix}$$

A.2.5. Consistent load vector in global co-ordinates from Equations (II.29) and (II.33)

$$\{R\}^T = \frac{p_z \ell}{2} < 1 \; \frac{\ell}{6} \; \frac{h_c \ell}{6} \; 1 \; \frac{-\ell}{6} \; \frac{-h_c \ell}{6} \; | \; \frac{\ell}{6} \; \frac{-\ell}{6} \; 0 \; 0 >$$

APPENDIX B: MATRICES FOR AXISYMMETRIC SANDWICH PLATES

The matrices that follow are for a three-layered axisymmetric sandwich plate element of radial length ℓ. The facing layers are of equal thickness and are composed of the same material. Further details are given in Section III.2.

The following vectors and matrices apply for all of the elements for which specialized matrices are given below

$$\{u(\xi)\}^T = \langle w \; \chi_b \; \gamma \; \gamma_f \rangle$$

$$\{\varepsilon(\xi)\}^T = \langle \gamma_{rzc} \; \kappa_{rc} \; \kappa_{\theta c} \; \varepsilon^{ot}_{rf} \; \varepsilon^{ot}_{\theta f} \; \gamma^t_{rzf} \; \kappa^t_{rf} \; \kappa^t_{\theta f} \; \varepsilon^{ob}_{rf} \; \varepsilon^{ob}_{\theta f} \; \gamma^b_{rzf} \; \kappa^b_{rf} \; \kappa^b_{\theta f} \rangle$$

$$\{\epsilon(\xi)\}^T = \langle \varepsilon_{rc} \; \varepsilon_{\theta c} \; \gamma_{rzc} \; \varepsilon^t_{rf} \; \varepsilon^t_{\theta f} \; \gamma^t_{rzf} \; \varepsilon^b_{rf} \; \varepsilon^b_{\theta f} \; \gamma^b_{rzf} \rangle$$

$$\{\sigma(\xi)\}^T = \langle \sigma_{rc} \; \sigma_{\theta c} \; \tau_{rzc} \; \sigma^t_{rf} \; \sigma^t_{\theta f} \; \tau^t_{rzf} \; \sigma^b_{rf} \; \sigma^b_{\theta f} \; \tau^b_{rzf} \rangle$$

$$[C]_{9\times 9} = \begin{bmatrix} C_c & 0 & 0 \\ 0 & C_f & 0 \\ 0 & 0 & C_f \end{bmatrix} \quad \text{where}$$

$$[C_i]_{3\times 3} = \begin{bmatrix} E_i/(1-\nu_i^2) & \nu_i E_i/(1-\nu_i^2) & 0 \\ \nu_i E_i/(1-\nu_i^2) & E_i/(1-\nu_i^2) & 0 \\ 0 & 0 & \kappa_i G_i \end{bmatrix} \quad i = c,f$$

$$[Z]_{9\times 13} = \begin{bmatrix} Z_c & 0 & 0 \\ 0 & Z_f & 0 \\ 0 & 0 & Z_f \end{bmatrix} \quad \text{where}$$

$$[Z] = \begin{matrix} 0 & z_c & 0 \\ 0 & 0 & z_c \\ 1 & 0 & 0 \end{matrix}, \qquad [Z_f] = \begin{matrix} 1 & 0 & 0 & z_f & 0 \\ 0 & 1 & 0 & 0 & z_f \\ 0 & 0 & 1 & 0 & 0 \end{matrix}$$

$$[G]_{13\times13} = \begin{matrix} F_c & 0 & 0 \\ 0 & F_f & 0 \\ 0 & 0 & F_f \end{matrix} \quad \text{where}$$

$$[F_c] = \begin{matrix} \kappa_c G_c h_c & 0 & 0 \\ 0 & D_c & \nu_c D_c \\ 0 & \nu_c D_c & D_c \end{matrix}, \qquad [F_f] = \begin{matrix} B_f & \nu_f B_f & 0 & 0 & 0 \\ \nu_f B_f & B_f & 0 & 0 & 0 \\ 0 & 0 & \kappa_f G_f h_f & 0 & 0 \\ 0 & 0 & 0 & D_f & \nu_f D_f \\ 0 & 0 & 0 & \nu_f D_f & D_f \end{matrix}$$

$$B_i = \frac{E_i h_i}{(1-\nu_i^2)}, \qquad D_i = \frac{E_i h_i^3}{12(1-\nu_i^2)}, \qquad i = c,f$$

B.1. Annular Element with Linear Shear

The nodal displacement vectors are chosen as follows

$$\{q\}^T = \{r\}^T = \langle w_i \; \chi_{bi} \; \gamma_i \; w_j \; \chi_{bj} \; \gamma_j \quad \gamma_{fi} \; \gamma_{fj} \rangle$$

B.1.1. $[\Phi(\xi)]$ of Equation (II.19)

$$\begin{matrix} 1 & \xi & \xi^2 & \xi^3 & 0 & 0 & 0 & 0 \\ & 1/\ell & 2\xi/\ell & 3\xi^2/\ell & -h_c/d & -h_c\xi/d & -h_f/d & -h_f\xi/d \\ 0 & 0 & 0 & 0 & 1 & \xi & -1 & -\xi \\ 0 & 0 & 0 & 0 & 0 & 0 & 1 & \xi \end{matrix}$$

B.1.2. [B(ξ)] of Equation (II.20)

$$
\begin{bmatrix}
0 & 0 & 0 & 0 & 1 & \xi & 0 & 0 \\
0 & 0 & -2/\ell^2 & -6\xi/\ell^2 & 0 & 1/\ell & 0 & 0 \\
0 & -1/r\ell & -2\xi/r\ell & -3\xi^2/r\ell & 1/r & \xi/r & 0 & 0 \\
0 & 0 & d/\ell^2 & 3d\xi/\ell^2 & 0 & -h_c/2\ell & 0 & -h_f/2\ell \\
0 & d/2r\ell & d\xi/r\ell & 3d\xi^2/2r\ell & -h_c/2r & -h_c\xi/2r\ell & -h_f/2r & -h_f\xi/2r\ell \\
0 & 0 & 0 & 0 & 0 & 0 & 1 & \xi \\
0 & 0 & -2/\ell^2 & -6\xi/\ell^2 & 0 & 0 & 0 & 1/\ell \\
0 & -1/r\ell & -\xi/r\ell & -3\xi^2/r\ell & 0 & 0 & 1/r & \xi/r \\
0 & 0 & -d/\ell^2 & -3d\xi/\ell^2 & 0 & h_c/2\ell & 0 & h_f/2\ell \\
0 & -d/2r\ell & -d\xi/r\ell & -3d\xi^2/2r\ell & h_c/2r & h_c\xi/2r\ell & h_f/2r & h_f\xi/2r\ell \\
0 & 0 & 0 & 0 & 0 & 0 & 1 & \xi \\
0 & 0 & -2/\ell^2 & -6\xi/\ell^2 & 0 & 0 & 0 & 1/\ell \\
0 & -1/r\ell & -2\xi/r\ell & -3\xi^2/r\ell & 0 & 0 & 1/r & \xi/r
\end{bmatrix}
$$

B.1.3. [A] of Equation (II.30)

$$
\begin{bmatrix}
1 & 0 & 0 & 0 & 0 & 0 & 0 & 0 \\
0 & 1/\ell & 0 & 0 & -h_c/d & 0 & -h_f/d & 0 \\
0 & 0 & 0 & 0 & 1 & 0 & -1 & 0 \\
1 & 1 & 1 & 1 & 0 & 0 & 0 & 0 \\
0 & 1/\ell & 2/\ell & 3/\ell & -h_c/d & -h_c/d & -h_f/d & -h_f/d \\
0 & 0 & 0 & 0 & 1 & 1 & -1 & -1 \\
0 & 0 & 0 & 0 & 0 & 0 & 1 & 0 \\
0 & 0 & 0 & 0 & 0 & 0 & 1 & 1
\end{bmatrix}
$$

B.1.4 $[A^{-1}] = [\underline{T}]$ of Equations (II.30) and (II.33)

$$
\begin{bmatrix}
1 & 0 & 0 & 0 & 0 & 0 & 0 & 0 \\
0 & \ell & h_c\ell/d & 0 & 0 & 0 & \ell & 0 \\
-3 & -2\ell & -2h_c\ell/d & 3 & -\ell & -h_c\ell/d & -2\ell & -\ell \\
2 & \ell & h_c\ell/d & -2 & \ell & h_c\ell/d & \ell & \ell \\
0 & 0 & -1 & 0 & 0 & 0 & 1 & 0 \\
0 & 0 & -1 & 0 & 0 & 0 & -1 & 1 \\
0 & 0 & 0 & 0 & 0 & 0 & 1 & 0 \\
0 & 0 & 0 & 0 & 0 & 0 & -1 & 1
\end{bmatrix}
$$

B.1.5. $\{Q_\alpha\}$ of Equations (III.20) and (III.21) for linear variation of transverse distributed load.

$$\{Q_\alpha\}^T = 2\pi\ell < Q_1\ Q_2\ Q_3\ Q_4\ 0\ 0\ 0\ 0 >$$

$$Q_1 = (r_i/3 + \ell/6)p_i + (r_i/2 + \ell/3)p_j$$

$$Q_2 = (r_i/6 + \ell/12)p_i + (r_i/3 + \ell/4)p_j$$

$$Q_3 = (r_i/12 + \ell/20)p_i + (r_i/4 + \ell/5)p_j$$

$$Q_4 = (r_i/20 + \ell/30)p_i + (r_i/5 + \ell/6)p_j$$

B.1.6. $\{R\}$ of Equation (II.33)

$$
\{R\} \quad 2\pi\ell
\begin{bmatrix}
Q_1 - 3Q_3 + 2Q_4 \\
\ell(Q_2 - 2Q_3 + Q_4) \\
h_c\ell(Q_2 - 2Q_3 + Q_4)/d \\
3Q_3 - 2Q_4 \\
-\ell(Q_3 - Q_4) \\
-h_c\ell(Q_3 - Q_4)/d \\
\ell(Q_2 - 2Q_3 + Q_4) \\
-\ell(Q_3 - Q_4)
\end{bmatrix}
$$

B.2. Annular Element with Quadratic Shear

The nodal displacement vector is

$$\{q\}^T = \{r\}^T = < w_i \; \chi_{bi} \; \gamma_i \; w_j \; \chi_{bj} \; \gamma_j \quad \gamma_{fi} \; \gamma_{fj} \; \gamma_{co} \; \gamma_{fo} >$$

B.2.1. $[\Phi(\xi)]$ of Equation (II.19)

$$\begin{matrix}
1 & \xi & \xi^2 & \xi^3 & 0 & 0 & 0 & 0 & 0 & 0 \\
0 & 1/\ell & 2\xi/\ell & 3\xi^2/\ell & -h_c/d & -h_c\xi/d & -h_f/d & -h_f\xi/d & -h_c\xi^2/d & -h_f\xi^2/d \\
0 & 0 & 0 & 0 & 1 & \xi & -1 & -\xi & \xi^2 & -\xi^2 \\
0 & 0 & 0 & 0 & 0 & 0 & 1 & \xi & 0 & \xi^2
\end{matrix}$$

B.2.2. $[B(\xi)]$ of Equation (II.20)

The first eight columns of $[B]$ are the same as $[B]$ given in Appendix

B.1.2. The transpose of the two additional columns is:

$$\begin{matrix}
\xi & 2\xi/\ell & \xi^2/r & -h_c\xi/\ell & -h_c\xi^2/2r & 0 & 0 & 0 & h_c\xi/\ell & h_c\xi^2/2r & 0 & 0 & 0 \\
0 & 0 & 0 & -h_f\xi/\ell & -h_f\xi^2/2r & \xi^2 & 2\xi/\ell & \xi^2/r & h_f\xi/\ell & h_f\xi^2/2r & \xi^2 & 2\xi/\ell & \xi^2/r
\end{matrix}$$

B.2.3. $[A]$ of Equation (II.30)

$$\begin{matrix}
1 & 0 & 0 & 0 & 0 & 0 & 0 & 0 & 0 & 0 \\
0 & 1/\ell & 0 & 0 & -h_c/d & 0 & -h_f/d & 0 & 0 & 0 \\
0 & 0 & 0 & 0 & 1 & 0 & -1 & 0 & 0 & 0 \\
1 & 1 & 1 & 1 & 0 & 0 & 0 & 0 & 0 & 0 \\
0 & 1/\ell & 2/\ell & 3/\ell & -h_c/d & -h_c/d & -h_f/d & -h_f/d & -h_c/d & -h_f/d \\
0 & 0 & 0 & 0 & 1 & 1 & -1 & -1 & 1 & -1 \\
0 & 0 & 0 & 0 & 0 & 0 & 1 & 0 & 0 & 0 \\
0 & 0 & 0 & 0 & 0 & 0 & 1 & 1 & 0 & 1 \\
0 & 0 & 0 & 0 & 1 & 1/2 & 0 & 0 & 1/4 & 0 \\
0 & 0 & 0 & 0 & 0 & 0 & 1 & 1/2 & 0 & 1/4
\end{matrix}$$

B.2.4. $[A^{-1}] = [\underline{T}]$ of Equations (II.30) and (II.33)

$$\begin{array}{cccccccccc}
1 & 0 & 0 & 0 & 0 & 0 & 0 & 0 & 0 & 0 \\
0 & \ell & h_c\ell/d & 0 & 0 & 0 & \ell & 0 & 0 & 0 \\
-3 & -2\ell & -2h_c\ell/d & 3 & -\ell & -h_c\ell/d & -2\ell & \ell & 0 & 0 \\
2 & \ell & h_c\ell/d & -2 & \ell & h_c\ell/d & \ell & -\ell & 0 & 0 \\
0 & 0 & 1 & 0 & 0 & 0 & 1 & 0 & 0 & 0 \\
0 & 0 & -3 & 0 & 0 & -1 & -3 & -1 & 4 & 0 \\
0 & 0 & 0 & 0 & 0 & 0 & 1 & 0 & 0 & 0 \\
0 & 0 & 0 & 0 & 0 & 0 & -3 & -1 & 0 & 4 \\
0 & 0 & 2 & & 0 & 2 & 2 & 2 & -4 & 0 \\
0 & 0 & 0 & 0 & 0 & 0 & 2 & 2 & 0 & -4
\end{array}$$

B.2.5. $\{Q_\alpha\}$ of Equations (III.20) and (III.21) for linear variation of transverse loads. The notation of B.1.5 applies.

$$\{Q_\alpha\}^T = 2\pi\ell < Q_1 \quad Q_2 \quad Q_3 \quad Q_4 \quad 0 \quad 0 \quad 0 \quad 0 \quad 0 \quad 0 >$$

B.2.6. $\{R\}$ of Equation (II.33) is the same as in B.1.6 except for the addition of two zero elements to make the vector 10×1.

B.3. Disc Element with Linear Shear

When $r_i = 0$, the nodal displacement vectors are chosen as follows

$$\{q\}^T = \{r\}^T = < w_i \quad 0 \quad 0 \quad w_j \quad \chi_{bj} \quad \gamma_j \quad 0 \quad \gamma_{fj} >$$

B.3.1 [illegible] of Equation (II.19)

$$\begin{array}{cccccccc}
0 & 0 & 0 & 1 & \xi^2 & \xi^3 & 0 & 0 \\
0 & 0 & 0 & 0 & 2\xi/\ell & 3\xi^2/\ell & -h_c\xi/d & -h_f\xi/d \\
0 & 0 & 0 & 0 & 0 & 0 & \xi & -\xi \\
0 & 0 & 0 & 0 & 0 & 0 & 0 & \xi
\end{array}$$

B.3.2. $[B(\xi)]$ of Equation (II.20) (Note: $r/\ell = \xi$)

$$
\begin{bmatrix}
0 & 0 & 0 & 0 & 0 & 0 & \xi & 0 \\
0 & 0 & 0 & 0 & -2/\ell^2 & -6\xi/\ell^2 & 1/\ell & 0 \\
0 & 0 & 0 & 0 & -2/\ell^2 & -3\xi/\ell^2 & 1/\ell & 0 \\
0 & 0 & 0 & 0 & d/\ell^2 & 3d\xi/\ell^2 & -h_c/2\ell & -h_f/2\ell \\
0 & 0 & 0 & 0 & d/\ell^2 & 3d\xi/2\ell^2 & -h_c/2\ell & -h_f/2\ell \\
0 & 0 & 0 & 0 & 0 & 0 & 0 & \xi \\
0 & 0 & 0 & 0 & -2/\ell^2 & -6\xi/\ell^2 & 0 & 1/\ell \\
0 & 0 & 0 & 0 & -2/\ell^2 & -3\xi/\ell^2 & 0 & 1/\ell \\
0 & 0 & 0 & 0 & -d/\ell^2 & -3d\xi/\ell^2 & h_c/2\ell & h_f/2\ell \\
0 & 0 & 0 & 0 & -d/\ell^2 & -3d\xi/2\ell^2 & h_c/2\ell & h_f/2\ell \\
0 & 0 & 0 & 0 & 0 & 0 & 0 & \xi \\
0 & 0 & 0 & 0 & -2/\ell^2 & -6\xi/\ell^2 & 0 & 1/\ell \\
0 & 0 & 0 & 0 & -2/\ell^2 & -3\xi/\ell^2 & 0 & 1/\ell
\end{bmatrix}
$$

B.3.3. $[A]$ of Equation (II.30)

$$
\begin{bmatrix}
0 & 0 & 0 & 1 & 0 & 0 & 0 & 0 \\
0 & 0 & 0 & 0 & 0 & 0 & 0 & 0 \\
0 & 0 & 0 & 0 & 0 & 0 & 0 & 0 \\
0 & 0 & 0 & 1 & 1 & 1 & 0 & 0 \\
0 & 0 & 0 & 0 & 2/\ell & 3/\ell & -h_c/d & -h_c/d \\
0 & 0 & 0 & 0 & 0 & 0 & 1 & -1 \\
0 & 0 & 0 & 0 & 0 & 0 & 0 & 0 \\
0 & 0 & 0 & 0 & 0 & 0 & 0 & 1
\end{bmatrix}
$$

B.3.4. $[A^{-1}] = [\underline{T}]$ of Equations (II.30) and (II.33)

$$\begin{matrix} 0 & 0 & 0 & 0 & 0 & 0 & 0 & 0 \\ 0 & 0 & 0 & 0 & 0 & 0 & 0 & 0 \\ 0 & 0 & 0 & 0 & 0 & 0 & 0 & 0 \\ 1 & 0 & 0 & 0 & 0 & 0 & 0 & 0 \\ -3 & 0 & 0 & 3 & -\ell & -h_c\ell/d & 0 & -\ell \\ 2 & 0 & 0 & -2 & \ell & h_c\ell/d & 0 & \ell \\ 0 & 0 & 0 & 0 & 0 & 1 & 0 & 1 \\ 0 & 0 & 0 & 0 & 0 & 0 & 0 & 1 \end{matrix}$$

B.3.5. $\{Q_\alpha\}$ of Equations (III.20) and (III.21) for linear variation of transverse distributed loads. The notation of B.1.5 applies.

$$\{Q_\alpha\}^T = 2\pi\ell < 0 \quad 0 \quad 0 \quad Q_1 \quad Q_3 \quad Q_4 \quad 0 \quad 0 >$$

B.3.6. $\{R\}$ of Equation (II.33)

$$\{R\} = 2\pi\ell \begin{matrix} Q_1 - 3Q_3 + 2Q_4 \\ 0 \\ 0 \\ 3Q_3 - 2Q_4 \\ -\ell(Q_3 - Q_4) \\ h_c\ell(Q_3 - Q_4)/d \\ 0 \\ -\ell(Q_3 - Q_4) \end{matrix}$$

B.4. Disc Element with Quadratic Shear

When $r_i = 0$, the nodal displacement vectors are chosen as follows:

$$\{q\}^T = \{r\}^T = < w_i \quad 0 \quad 0 \quad w_j \quad \chi_{bj} \quad \gamma_j \quad 0 \quad \gamma_{fj} \quad \gamma_{co} \quad \gamma_{fo} >$$

B.4.1. $[\Phi(\xi)]$ of Equation (II.19)

$$\begin{bmatrix}
0 & 0 & 0 & 1 & \xi^2 & \xi^3 & 0 & 0 & 0 & 0 \\
0 & 0 & 0 & 0 & 2\xi/\ell & 3\xi^2/\ell & -h_c\xi/d & -h_f\xi/d & -h_c\xi^2/d & -h_f\xi^2/d \\
0 & 0 & 0 & 0 & 0 & 0 & \xi & -\xi & \xi^2 & -\xi^2 \\
0 & 0 & 0 & 0 & 0 & 0 & 0 & \xi & 0 & \xi^2
\end{bmatrix}$$

B.4.2. $[B(\xi)]$ of Equation (II.20)

The first eight columns of $[B]$ are the same as $[B]$ given in Appendix B.3.2. The transpose of the two additional columns is the same as that given in Appendix B.2.2 with r/ξ replaced by ℓ.

B.4.3. $[A]$ of Equation (II.30)

$$\begin{bmatrix}
0 & 0 & 0 & 1 & 0 & 0 & 0 & 0 & 0 & 0 \\
0 & 0 & 0 & 0 & 0 & 0 & 0 & 0 & 0 & 0 \\
0 & 0 & 0 & 0 & 0 & 0 & 0 & 0 & 0 & 0 \\
0 & 0 & 0 & 1 & 1 & 1 & 0 & 0 & 0 & 0 \\
0 & 0 & 0 & 0 & 2/\ell & 3/\ell & -h_c/d & -h_f/d & -h_c/d & -h_f/d \\
0 & 0 & 0 & 0 & 0 & 0 & 1 & -1 & 1 & -1 \\
0 & 0 & 0 & 0 & 0 & 0 & 0 & 0 & 0 & 0 \\
0 & 0 & 0 & 0 & 0 & 0 & 0 & 1 & 0 & 1 \\
0 & 0 & 0 & 0 & 0 & 0 & 1/2 & 0 & 1/4 & 0 \\
0 & 0 & 0 & 0 & 0 & 0 & 0 & 1/2 & 0 & 1/4
\end{bmatrix}$$

B.4.4 $[A^{-1}] = [\underline{T}]$ of Equations (II.30) and (II.33)

0	0	0	0	0	0	0	0	0	0
0	0	0	0	0	0	0	0	0	0
0	0	0	0	0	0	0	0	0	0
1	0	0	0	0	0	0	0	0	0
-3	0	0	3	$-\ell$	$-h_c\ell/d$	0	$-\ell$	0	0
2	0	0	-2	ℓ	$h_c\ell/d$	0	ℓ	0	0
0	0	0	0	0	-1	0	-1	4	0
0	0	0	0	0	0	0	-1	0	4
0	0	0	0	0	2	0	2	-4	0
0	0	0	0	0	0	0	2	0	-4

B.4.5 $\{Q_\alpha\}$ of Equations (III.20) and (III.21) for linear variation of transverse loads. The notation of B.1.5 applies.

$$\{Q_\alpha\}^T = 2\pi\ell < 0 \quad 0 \quad 0 \quad Q_1 \quad Q_2 \quad Q_3 \quad 0 \quad 0 \quad 0 \quad 0 \quad 0 >$$

B.4.6. $\{R\}$ of Equation (II.33) is the same as in B.3.6 except for the addition of two zero elements to make the vector 10×1.

APPENDIX C: MATRICES FOR AXISYMMETRIC SANDWICH SHELLS

The matrices that follow are for a three-layer axisymmetric sandwich shell element with chord length ℓ (see Section III.3). The facing layers are of equal thickness and are composed of the same material. Further details are given in Section III.4.

The following vectors and matrices apply for all of the elements for which specialized matrices are given below:

$$\{u(\xi)\}^T = < w \quad \chi_b \quad \gamma \quad \gamma_f >$$

$$\{\varepsilon(\xi)\}^T = < \varepsilon^\circ_{sc} \quad \varepsilon^\circ_{\theta c} \quad \gamma_{s\zeta c} \quad \kappa_{rc} \quad \kappa_{\theta c}$$
$$\varepsilon^{\circ t}_{sf} \quad \varepsilon^{\circ t}_{\theta f} \quad \gamma^t_{s\zeta f} \quad \kappa^t_{sf} \quad \kappa^t_{\theta f} \quad \varepsilon^b_{sf} \quad \varepsilon^b_{\theta f} \quad \gamma^b_{s\zeta f} \quad \kappa^b_{sf} \quad \kappa^b_{\theta f} >$$

$$\{\boldsymbol{\epsilon}(\xi)\}^T = < \varepsilon_{sc} \quad \varepsilon_{\theta c} \quad \gamma_{s\zeta c} \quad \varepsilon^t_{sf} \quad \varepsilon^t_{\theta f} \quad \gamma^t_{s\zeta f} \quad \varepsilon^b_{sf} \quad \varepsilon^b_{\theta f} \quad \gamma^b_{s\zeta f} >$$

$$\{\sigma(\xi)\}^T = < \sigma_{sc} \quad \sigma_{\theta c} \quad \tau_{s\zeta c} \quad \sigma^t_{sf} \quad \sigma^t_{\theta f} \quad \tau^t_{s\zeta f} \quad \sigma^b_{sf} \quad \sigma^b_{\theta f} \quad \tau^b_{s\zeta f} >$$

$$[C]_{9\times 9} = \begin{bmatrix} C_c & 0 & 0 \\ 0 & C_f & 0 \\ 0 & 0 & C_f \end{bmatrix} \quad \text{where}$$

$$[C_i]_{3\times 3} = \begin{bmatrix} E_i/(1-\nu_i^2) & \nu_i E_i/(1-\nu_i^2) & 0 \\ \nu_i E_i/(1-\nu_i^2) & E_i/(1-\nu_i^2) & 0 \\ 0 & 0 & \kappa_i G_i \end{bmatrix}, \quad i = c,f.$$

$$[Z]_{9\times 15} = \begin{bmatrix} Z_c & 0 & 0 \\ 0 & Z_f & 0 \\ 0 & 0 & Z_f \end{bmatrix} \quad \text{where}$$

$$[Z_i] = \begin{bmatrix} 1 & 0 & 0 & \zeta_i & 0 \\ 0 & 1 & 0 & 0 & \zeta_i \\ 0 & 0 & 1 & 0 & 0 \end{bmatrix}, \quad i = c,f.$$

$$[G] = \begin{bmatrix} F_c & 0 & 0 \\ 0 & F_f & 0 \\ 0 & 0 & F_f \end{bmatrix} \quad \text{where}$$

$$[F_i] = \begin{bmatrix} B_i & \nu_i B_i & 0 & 0 & 0 \\ \nu_i B_i & B_i & 0 & 0 & 0 \\ 0 & 0 & \kappa_i G_i h_i & 0 & 0 \\ 0 & 0 & 0 & D_i & \nu_i D_i \\ 0 & 0 & 0 & \nu_i D_i & D_i \end{bmatrix}, \quad i = c,f.$$

and $B_i = \dfrac{E_i h_i}{(1-\nu_i^2)}$, $D_i = \dfrac{E_i h_i^3}{12(1-\nu_i^2)}$, $i = c,f.$

C.1. Frustrum Element with Linear Shear

The nodal displacement vectors are chosen as follows:

$$\{q\}^T = < u_{1i}\ u_{2i}\ \chi_{bi}\ \gamma_i\ \gamma_{fi}\ \ u_{1j}\ \ u_{2j}\ \ \chi_{bj}\ \ \gamma_j\ \ \gamma_{fj} >$$

$$\{r\}^T = < u_i\ \ w_i\ \ \chi_{bi}\ \ \gamma_i\ \ u_j\ \ w_j\ \ \chi_{bj}\ \ \gamma_j\ \ \gamma_{fi}\ \ \gamma_{fj} >$$

C.1.1. $[\Phi(\xi)]$ of Equation (II.19)

$$\begin{bmatrix} 1 & \xi & 0 & 0 & 0 & 0 & 0 & 0 & 0 & 0 \\ 0 & 0 & 1 & \xi & \xi^2 & \xi^3 & 0 & 0 & 0 & 0 \\ 0 & \cos^2\beta\tan\beta/\ell & 0 & -\cos^2\beta/\ell & -2\xi\cos^2\beta/\ell & +3\xi^2\cos^2\beta/\ell & h_c/d & -h_c\xi/d & -h_f/d & -h_f\xi/d \\ 0 & 0 & 0 & 0 & 0 & 0 & 1 & \xi & -1 & -\xi \\ 0 & 0 & 0 & 0 & 0 & 0 & 0 & 0 & 1 & \xi \end{bmatrix}$$

C.1.2. [B(ξ)] of Equation (II.20)

$$
\begin{array}{cccccc}
0 & \cos^2\beta/\ell & 0 & b_7 & 2\xi b_7 & 3\xi^3 b_7 \\
\sin\psi/r & \xi\sin\psi/r & \cos\psi/r & \xi\cos\psi/r & \xi^2\cos\psi/r & \xi^3\cos\psi/r \\
0 & 0 & 0 & 0 & 0 & 0 \\
0 & b_1 & 0 & b_2 & 2b_2\xi+2b_3 & 3b_2\xi^2+6b_3\xi \\
0 & b_4 & 0 & b_5 & 2b_5\xi & 3b_5\xi^2
\end{array}
$$

$$
\left.
\begin{array}{l}
B_{ij} = B_{(i-5)j} + \frac{d}{2} B_{(i-2)j}, \quad i=6,7 \\
B_{ij} = B_{(i-5)j}, \quad i=8,9,10
\end{array}
\right\} j=1,\ldots,6
$$

$$
\begin{array}{cccc}
0 & -h_c\cos\beta/2\ell & 0 & -h_f\cos\beta/2\ell \\
-h_c b_6/2 & -h_c b_6\xi/2 & -h_f b_6/2 & -h_f b_6\xi/2 \\
0 & 0 & 1 & \xi \\
0 & 0 & 0 & \cos\beta/\ell \\
0 & 0 & b_6 & b_6\xi
\end{array}
$$

$$
\left.
\begin{array}{l}
B_{ij} = B_{(i-10)j} - \frac{d}{2} B_{(i-7)j}, \quad i=11,12 \\
B_{ij} = B_{(i-10)j}, \quad i=13,14,15
\end{array}
\right\} j=1,\ldots,6
$$

$$
\begin{array}{cccc}
0 & h_c\cos\beta/2\ell & 0 & h_f\cos\beta/2\ell \\
h_c b_6/2 & h_c b_6\xi/2 & h_f b_6/2 & h_f b_6\xi/2 \\
0 & 0 & 1 & \xi \\
0 & 0 & 0 & \cos\beta/\ell \\
0 & 0 & b_6 & b_6\zeta
\end{array}
$$

where

$b_1 = -\eta''\cos^5\beta(1-\tan^2\beta)/\ell^2$

$b_2 = -2\eta''\tan\beta\ \cos^5\beta/\ell^2$

$b_3 = \cos^3\beta/\ell^2$

$b_4 = -\cos^3\beta\tan\beta(\sin\psi+\cos\psi\tan\beta)/r\ell$

$b_5 = -b_4/\tan\beta$

$b_6 = -\ell b_5/\cos^2\beta$

$b_7 = \cos^2\beta\tan\beta/\ell$

C.1.3. [A] of Equation (II.30)

$$\begin{bmatrix}
1 & 0 & 0 & 0 & 0 & 0 & 0 & 0 & 0 & 0 \\
0 & 0 & 1 & 0 & 0 & 0 & 0 & 0 & 0 & 0 \\
0 & a_1\tan\beta_i & 0 & -a_1 & 0 & 0 & -h_c/d & 0 & -h_f/d & 0 \\
0 & 0 & 0 & 0 & 0 & 0 & 1 & 0 & -1 & 0 \\
0 & 0 & 0 & 0 & 0 & 0 & 0 & 0 & 1 & 0 \\
1 & 1 & 0 & 0 & 0 & 0 & 0 & 0 & 0 & 0 \\
0 & 0 & 1 & 1 & 1 & 1 & 0 & 0 & 0 & 0 \\
0 & a_2\tan\beta_j & 0 & -a_2 & -2a_2 & -3a_2 & -h_c/d & -h_c/d & -h_f/d & -h_f/d \\
0 & 0 & 0 & 0 & 0 & 0 & 1 & 1 & -1 & -1 \\
0 & 0 & 0 & 0 & 0 & 0 & 0 & 0 & 1 & 1
\end{bmatrix}$$

where $a_1 = \cos^2\beta_i/\ell$

$a_2 = \cos^2\beta_j/\ell$

C.1.4. $[A^{-1}]$ of Equation (II.30)

$$\begin{bmatrix}
1 & 0 & 0 & 0 & 0 & 0 & 0 & 0 & 0 & 0 \\
-1 & 0 & 0 & 0 & 0 & 1 & 0 & 0 & 0 & 0 \\
0 & 1 & 0 & 0 & 0 & 0 & 0 & 0 & 0 & 0 \\
-\tan\beta_i & 0 & -1/a_1 & -h_c/da_1 & -1/a_1 & \tan\beta_i & 0 & 0 & 0 & 0 \\
a_3 & -3 & 2/a_1 & 2h_c/da_1 & 2/a_1 & -a_3 & 3 & 1/a_2 & h_c/da_2 & 1/a_2 \\
-a_4 & 2 & -1/a_1 & -h_c/da_1 & -1/a_1 & a_4 & -2 & -1/a_2 & -h_c/da_2 & -1/a_2 \\
0 & 0 & 0 & 1 & 1 & 0 & 0 & 0 & 0 & 0 \\
0 & 0 & 0 & -1 & -1 & 0 & 0 & 0 & 1 & 1 \\
0 & 0 & 0 & 0 & 1 & 0 & 0 & 0 & 0 & 0 \\
0 & 0 & 0 & 0 & -1 & 0 & 0 & 0 & 0 & 1
\end{bmatrix}$$

where $a_3 = 2\tan\beta_i + \tan\beta_j$

$a_4 = \tan\beta_i + \tan\beta_j$

C.1.5. $[T]_{(s,\theta,\zeta)}$ of Equation (II.31) and Section III.4.4.

$$\begin{bmatrix}
\cos\beta_i & \sin\beta_i & 0 & 0 & 0 & 0 & 0 & 0 & 0 & 0 \\
\sin\beta_i & -\cos\beta_i & 0 & 0 & 0 & 0 & 0 & 0 & 0 & 0 \\
0 & 0 & 1 & 0 & 0 & 0 & 0 & 0 & 0 & 0 \\
0 & 0 & 0 & 1 & 0 & 0 & 0 & 0 & 0 & 0 \\
0 & 0 & 0 & 0 & 0 & 0 & 0 & 0 & 1 & 0 \\
0 & 0 & 0 & 0 & \cos\beta_j & \sin\beta_j & 0 & 0 & 0 & 0 \\
0 & 0 & 0 & 0 & \sin\beta_j & -\cos\beta_j & 0 & 0 & 0 & 0 \\
0 & 0 & 0 & 0 & 0 & 0 & 1 & 0 & 0 & 0 \\
0 & 0 & 0 & 0 & 0 & 0 & 0 & 1 & 0 & 0 \\
0 & 0 & 0 & 0 & 0 & 0 & 0 & 0 & 0 & 1
\end{bmatrix}$$

C.1.6. $[T]_{(r,\theta,z)}$ of Equation (II.31) and Section III.4.4.

$[T]_{(r,\theta,z)}$ is the same as $[T]_{(s,\theta,\zeta)}$ except that each of the 2×2 sub-matrices corresponding to the translations is replaced by

$$\begin{matrix} \sin\psi & \cos\psi \\ \cos\psi & -\sin\psi \end{matrix}$$

Note that in $\{r\}$, u changes to u_r and w to u_z.

C.2. Frustrum Element with Quadratic Shear

The model displacement vectors are chosen as follows:

$$\{q\}^T = < u_{1i} \;\; u_{2i} \;\; \chi_{bi} \;\; \gamma_i \;\; \gamma_{fi} \;\; u_{1j} \;\; u_{2j} \;\; \chi_{bj} \;\; \gamma_j \;\; \gamma_{fj} \;\; \gamma_{co} \;\; \gamma_{fo} >$$

$$\{r\}^T = < u_i \;\; w_i \;\; \chi_{bi} \;\; \gamma_i \;\; u_j \;\; w_j \;\; \chi_{bj} \;\; \gamma_j \;\; \gamma_{fi} \;\; \gamma_{fj} \;\; \gamma_{co} \;\; \gamma_{fo} >$$

C.2.1. $[\Phi(\xi)]$ of Equation (II.19)

The first ten columns of $[\Phi]$ are the same as in Section C.1.1. The additional two columns are

$$\begin{matrix} 0 & 0 \\ 0 & 0 \\ -h_c\xi^2/d & -h_c\xi^2/d \\ \xi^2 & -\xi^2 \\ 0 & \xi^2 \end{matrix}$$

C.2.2. $[B(\xi)]$ of Equation (II.20)

The first ten columns of $[B]$ are the same as in Section C.1.2. The transpose of the additional two columns is

$$\begin{matrix} 0 & 0 & \xi^2 & \frac{2\xi\cos\beta}{\ell} & b_6\xi^2 & \frac{-h_c\xi\cos\beta}{\ell} & \frac{-h_c\xi^2 b_6}{2} & 0 & 0 & 0 \\ 0 & 0 & 0 & 0 & 0 & \frac{-h_f\xi\cos\beta}{\ell} & \frac{-h_f\xi^2 b_6}{2} & \xi^2 & \frac{2\xi\cos\beta}{\ell} & b_6\xi^2 \\ & & & & & \frac{h_c\xi\cos\beta}{\ell} & \frac{h_c\xi^2 b_6}{2} & 0 & 0 & 0 \\ & & & & & \frac{h_f\xi\cos\beta}{\ell} & \frac{h_f\xi^2 b_6}{2} & \xi^2 & \frac{2\xi\cos\beta}{\ell} & b_6\xi^2 \end{matrix}$$

C.2.3. [A] of Equation (II.30)

1	0	0	0	0	0	0	0	0	0	0	0
0	0	1	0	0	0	0	0	0	0	0	0
0	$a_1\tan\beta_i$	0	$-a_1$	0	0	$-h_c/d$	0	$-h_f/d$	0	0	0
0	0	0	0	0	0	1	0	-1	0	0	0
0	0	0	0	0	0	0	0	1	0	0	0
1	1	0	0	0	0	0	0	0	0	0	0
0	0	1	1	1	1	0	0	0	0	0	0
0	$a_2\tan\beta_j$	0	$-a_2$	$-2a_2$	$-3a_2$	$-h_c/d$	$-h_c/d$	$-h_f/d$	$-h_f/d$	$-h_c/d$	$-h_f/d$
0	0	0	0	0	0	1	1	-1	-1	1	-1
0	0	0	0	0	0	0	0	1	1	0	1
0	0	0	0	0	0	1	1/2	0	0	1/4	0
0	0	0	0	0	0	0	0	1	1/2	0	1/4

C.2.4 $[A^{-1}]$ of Equation (II.30)

1	0	0	0	0	0	0	0	0	0	0	0
-1	0	0	0	0	1	0	0	0	0	0	0
0	1	0	0	0	0	0	0	0	0	0	0
$-\tan\beta_i$	0	$\frac{-1}{a_1}$	$\frac{-h_c}{da_1}$	$\frac{-1}{a_1}$	$\tan\beta_i$	0	0	0	0	0	0
a_3	-3	$\frac{2}{a_1}$	$\frac{2h_c}{da_1}$	$\frac{-2}{a_1}$	$-a_3$	3	$\frac{1}{a_2}$	$\frac{h_c}{da_2}$	$\frac{1}{a_2}$	0	0
	2	$\frac{-1}{a_1}$	$\frac{-h_c}{da_1}$	$\frac{-1}{a_1}$	a_4	-2	$\frac{-1}{a_2}$	$\frac{-h_c}{da_2}$	$\frac{-1}{a_2}$	0	0
	0	0	1	1	0	0	0	0	0	0	0
	0	0	-3	-3	0	0	0	-1	-1	4	0
	0	0	0	1	0	0	0	0	0	0	0
	0	0	0	-3	0	0	0	0	-1	0	4
	0	0	2	2	0	0	0	2	2	-4	0
	0	0	0	2	0	0	0	0	2	0	-4

where a_1 through a_4 are defined in Section C.1.

C.2.5. $[T]_{(s,\theta,\zeta)}$ of Equation (II.31) and Section III.4.4.

$$
\begin{bmatrix}
\cos\beta_i & \sin\beta_i & 0 & 0 & 0 & 0 & 0 & 0 & 0 & 0 & 0 & 0 \\
\sin\beta_i & -\cos\beta_i & 0 & 0 & 0 & 0 & 0 & 0 & 0 & 0 & 0 & 0 \\
0 & 0 & 1 & 0 & 0 & 0 & 0 & 0 & 0 & 0 & 0 & 0 \\
0 & 0 & 0 & 1 & 0 & 0 & 0 & 0 & 0 & 0 & 0 & 0 \\
0 & 0 & 0 & 0 & 0 & 0 & 0 & 0 & 1 & 0 & 0 & 0 \\
0 & 0 & 0 & 0 & \cos\beta_j & \sin\beta_j & 0 & 0 & 0 & 0 & 0 & 0 \\
0 & 0 & 0 & 0 & \sin\beta_j & -\cos\beta_j & 0 & 0 & 0 & 0 & 0 & 0 \\
0 & 0 & 0 & 0 & 0 & 0 & 1 & 0 & 0 & 0 & 0 & 0 \\
0 & 0 & 0 & 0 & 0 & 0 & 0 & 1 & 0 & 0 & 0 & 0 \\
0 & 0 & 0 & 0 & 0 & 0 & 0 & 0 & 0 & 1 & 0 & 0 \\
0 & 0 & 0 & 0 & 0 & 0 & 0 & 0 & 0 & 0 & 1 & 0 \\
0 & 0 & 0 & 0 & 0 & 0 & 0 & 0 & 0 & 0 & 0 & 1
\end{bmatrix}
$$

C.2.6. $[T]_{(r,\theta,z)}$ of Equation (II.31) and Section III.4.4.

$[T]_{(r,\theta,z)}$ is the same as $[T]_{(s,\theta,\zeta)}$ except that each of the 2×2 submatrices corresponding to the translations is replaced by

$$
\begin{bmatrix}
\sin\psi & \cos\psi \\
\cos\psi & -\sin\psi
\end{bmatrix}
$$

Note that in $\{\,\}$, u changes to u_r and w to u_z.

C.3. Cap Element with Linear Shear

The nodal displacement vectors are chosen as follows:

$$\{q\}^T = < 0 \quad u_{zi} \quad 0 \quad 0 \quad 0 \quad u_{1j} \quad u_{2j} \quad \chi_{bj} \quad \gamma_j \quad \gamma_{fj} >$$

$$\{r\}^T = < 0 \quad u_{zi} \quad 0 \quad 0 \quad u_j \quad w_j \quad \chi_{bj} \quad \gamma_j \quad 0 \quad \gamma_{fj} >$$

C.3.1. $[\Phi(\xi)]$ of Equation (II.19)

$$
\begin{array}{cccccccccc}
0 & 0 & 0 & 0 & -\cos\psi & \xi & 0 & 0 & 0 & 0 \\
0 & 0 & 0 & 0 & \sin\psi & \xi\tan\beta_i & \xi^2 & \xi^3 & 0 & 0 \\
0 & 0 & 0 & 0 & 0 & \dfrac{(\tan\beta-\tan\beta_i)\cos^2\beta}{\ell} & \dfrac{-2\xi\cos^2\beta}{\ell} & \dfrac{-3\xi^2\cos^2\beta}{\ell} & \dfrac{-h_c\xi}{d} & \dfrac{-h_f\xi}{d} \\
0 & 0 & 0 & 0 & 0 & 0 & 0 & 0 & \xi & -\xi \\
0 & 0 & 0 & 0 & 0 & 0 & 0 & 0 & 0 & \xi
\end{array}
$$

C.3.2. $[B(\xi)]$ of Equation (II.20)

$$
\begin{array}{cccccccccc}
0 & 0 & 0 & 0 & 0 & b_8 & 2\xi b_7 & 3\xi^2 b_7 & 0 & 0 \\
0 & 0 & 0 & 0 & 0 & b_9 & \dfrac{\xi\cos\psi}{\bar{r}} & \dfrac{\xi^2\cos\psi}{\bar{r}} & 0 & 0 \\
0 & 0 & 0 & 0 & 0 & 0 & 0 & 0 & \xi & 0 \\
0 & 0 & 0 & 0 & 0 & b_1+b_2\tan\beta_i & 2b_2\xi+2b_3 & 3b_2\xi^2+6b_3\xi & \dfrac{\cos\beta}{\ell} & 0 \\
0 & 0 & 0 & 0 & 0 & b_{10} & b_{11} & b_{12} & b_{13} & 0 \\
 & & & & & & & & \dfrac{-h_c\cos\beta}{2\ell} & \dfrac{-h_f\cos\beta}{2\ell} \\
 & & & & & & & & \dfrac{-h_c}{2}\,b_{13} & \dfrac{-h_f}{2}\,b_{13} \\
 & & & & & & & & 0 & \xi \\
 & & & & & & & & 0 & \dfrac{\cos\beta}{\ell} \\
 & & & & & & & & 0 & b_{13} \\
 & & & & & & & & \dfrac{h_c\cos\beta}{2\ell} & \dfrac{h_f\cos\beta}{2\ell} \\
 & & & & & & & & \dfrac{h_c}{2}\,b_{13} & \dfrac{h_f}{2}\,b_{13} \\
 & & & & & & & & 0 & \xi \\
 & & & & & & & & 0 & \dfrac{\cos\beta}{\ell} \\
 & & & & & & & & 0 & b_{13}
\end{array}
$$

(ditto) (See Section C.1.2.)

(ditto) (See Section C.1.2.)

where b_1 through b_7 are defined in Section C.1.2. and

$$b_8 = (1+\tan\beta_i\tan\beta)\cos^2\beta/\ell$$

$$b_9 = (\sin\psi+\tan\beta_i\cos\psi)/\bar{r}$$

$$b_{10} = \frac{\cos^3\beta}{\bar{r}\,\ell}\, b_{14}[5a_4\xi^2+4(a_3-a_4)\xi^2+3(a_2-a_3)\xi+2(a_2-a_1)]$$

$$b_{11} = 2b_{14}\cos^3\beta/\bar{r}\,\ell$$

$$b_{12} = 3b_{11}\xi/2$$

$$b_{13} = b_{14}\cos\beta/\bar{r}$$

$$b_{14} = \sin\psi+\cos\psi\tan\beta$$

$$\bar{r} = r/\xi = \ell(\sin\psi+\bar{\eta}\cos\psi)$$

$$\bar{\eta} = \eta/\xi$$

and a_1 through a_4 are defined in Section III.3.

C.3.3. [A] of Equation (II.30)

0	0	0	0	0	0	0	0	0	0
0	0	0	0	-1	0	0	0	0	0
0	0	0	0	0	0	0	0	0	0
0	0	0	0	0	0	0	0	0	0
0	0	0	0	0	0	0	0	0	0
0	0	0	0	$-\cos\psi$	1	0	0	0	0
0	0	0	0	$\sin\psi$	$\tan\beta_i$	1	1	0	0
0	0	0	0	0	$(\tan\beta_j-\tan\beta_i)a_2$	$-2a_2$	$-3a_2$	$-h_c/d$	$-h_f/d$
0	0	0	0	0	0	0	0	1	-1
0	0	0	0	0	0	0	0	0	1

where $a_2 = \cos^2\beta_j/\ell$.

C.3.4. $[A^{-1}]$ of Equation (II.30)

0	0	0	0	0	0	0	0	0	0
0	0	0	0	0	0	0	0	0	0
0	0	0	0	0	0	0	0	0	0
0	0	0	0	0	0	0	0	0	0
0	-1	0	0	0	0	0	0	0	0
0	$-\cos\psi$	0	0	0	1	0	0	0	0
0	a_5	0	0	0	$-a_3$	3	$1/a_2$	h_c/da_2	$1/a_2$
0	a_6	0	0	0	a_4	2	$-1/a_2$	$-h_c/da_2$	$-1/a_2$
0	0	0	0	0	0	0	0	1	1
0	0	0	0	0	0	0	0	0	1

where $a_2 = \cos^2\beta_j/\ell$

$a_3 = 2\tan\beta_i+\tan\beta_j$

$a_4 = \tan\beta_i+\tan\beta_j$

$a_5 = a_3\cos\psi+3\sin\psi$

$a_6 = -a_4\cos\psi-2\sin\psi$

C.3.5. $[T]_{(s,\theta,\zeta)}$ of Equation (II.31) and Section III.4.4.

0	0	0	0	0	0	0	0	0	0
0	1	0	0	0	0	0	0	0	0
0	0	0	0	0	0	0	0	0	0
0	0	0	0	0	0	0	0	0	0
0	0	0	0	0	0	0	0	0	0
0	0	0	0	$\cos\beta_j$	$\sin\beta_j$	0	0	0	0
0	0	0	0	$\sin\beta_j$	$-\cos\beta_j$	0	0	0	0
0	0	0	0	0	0	1	0	0	0
0	0	0	0	0	0	0	1	0	0
0	0	0	0	0	0	0	0	0	1

page no. 206 follows

C.3.6. $[T]_{(r,\theta,z)}$ of Equation (II.31) and Section III.4.4.

$(T]_{(r,\theta,z)}$ is the same as $[T]_{(s,\theta,\zeta)}$ except

$$\begin{matrix} \cos\beta_j & \sin\beta_j \\ \sin\beta_j & -\cos\beta_j \end{matrix} \quad \text{is replaced by} \quad \begin{matrix} \sin\psi & \cos\psi \\ \cos\psi & -\sin\psi \end{matrix}$$

Note that in $\{r\}$, u changes to u_r and w to u_z.

C.4. Cap Element with Quadratic Shear

The nodal displacement vectors are chosen as follows:

$$\{q\}^T = < 0 \quad u_{zi} \quad 0 \quad 0 \quad 0 \quad u_{1j} \quad u_{2j} \quad \chi_{bj} \quad \gamma_j \quad \gamma_{fj} \quad \gamma_{co} \quad \gamma_{fo} >$$

$$\{r\}^T = < 0 \quad u_{zi} \quad 0 \quad 0 \quad u_j \quad w_j \quad \chi_{bj} \quad \gamma_j \quad 0 \quad \gamma_{fj} \quad \gamma_{co} \quad \gamma_{fo} >$$

C.4.1. $[\Phi(\xi)]$ of Equation (II.19)

See Section C.2.1.

C.4.2. $[B(\xi)]$ of Equation (II.20)

Same as Section C.2.2 except ξb_6 is replaced by b_{13}.

C.4.3. [A] of Equation (II.30)

0	0	0	0	0	0	0	0	0	0	0	0
0	0	0	0	-1	0	0	0	0	0	0	0
0	0	0	0	0	0	0	0	0	0	0	0
0	0	0	0	0	0	0	0	0	0	0	0
0	0	0	0	0	0	0	0	0	0	0	0
0	0	0	0	$-\cos\psi$	1	0	0	0	0	0	0
0	0	0	0	$\sin\psi$	$\tan\beta_i$	1	1	0	0	0	0
0	0	0	0	0	$(\tan\beta_j-\tan\beta_i)a_2$	$-2a_2$	$-3a_2$	$-h_c/d$	$-h_f/d$	$-h_c/d$	$-h_f/d$
0	0	0	0	0	0	0	0	1	-1	1	-1
0	0	0	0	0	0	0	0	0	1	0	1
0	0	0	0	0	0	0	0	1/2	0	1/4	0
0	0	0	0	0	0	0	0	0	1/2	0	1/4

C.4.4. $[A^{-1}]$ of Equation (II.30)

0	0	0	0	0	0	0	0	0	0	0	0
0	0	0	0	0	0	0	0	0	0	0	0
0	0	0	0	0	0	0	0	0	0	0	0
0	0	0	0	0	0	0	0	0	0	0	0
0	-1	0	0	0	0	0	0	0	0	0	0
0	$-\cos\psi$	0	0	0	1	0	0	0	0	0	0
0	a_5	0	0	0	$-a_3$	3	$1/a_2$	h_c/da_2	$1/a_2$	0	0
0	a_6	0	0	0	a_4	-2	$-1/a_2$	$-h_c/da_2$	$-1/a_3$	0	0
0	0	0	0	0	0	0	0	-1	-1	4	0
0	0	0	0	0	0	0	0	0	-1	0	4
0	0	0	0	0	0	0	0	2	2	-4	0
0	0	0	0	0	0	0	0	0	2	0	-4

where a_2 through a_6 are defined in Section C.3.4.

C.4.5. $[T]_{(s,\theta,\zeta)}$ of Equation (II.31) and Section III.4.4.

0	0	0	0	0	0	0	0	0	0	0	0
0	1	0	0	0	0	0	0	0	0	0	0
0	0	0	0	0	0	0	0	0	0	0	0
0	0	0	0	0	0	0	0	0	0	0	0
0	0	0	0	0	0	0	0	0	0	0	0
0	0	0	0	$\cos\beta_j$	$\sin\beta_j$	0	0	0	0	0	0
0	0	0	0	$\sin\beta_j$	$-\cos\beta_j$	0	0	0	0	0	0
0	0	0	0	0	0	1	0	0	0	0	0
0	0	0	0	0	0	0	1	0	0	0	0
0	0	0	0	0	0	0	0	0	1	0	0
0	0	0	0	0	0	0	0	0	0	1	0
0	0	0	0	0	0	0	0	0	0	0	1

C.4.6. $[T]_{(r,\theta,z)}$ of Equation (II.31) and Section III.4.4.

See Section C.3.6.

APPENDIX D.. COMPUTER PROGRAM FOR STATIC ANALYSIS OF ELASTIC AXISYMMETRIC SANDWICH SHELLS (FORTRAN IV)

```
      PROGRAM AXSNSHL(INPUT,OUTPUT,TAPE1,TAPE2,TAPE3)
C
C     ANALYSIS OF THIN SANDWICH ROTATIONAL SHELL WITH AXISYMMETRIC LOAD-
C     ING.  CONSTANT THICKNESS SHELL WITH TWICE CONTINUOUS MERIDIAN.
C     MATERIAL PROPERTIES MAY NOT VARY IN THE MERIDIONAL DIRECTION FOR
C     THE PRESENT PROGRAM, ALTHOUGH MODIFICATION FOR THIS CAPABILITY
C     MAY BE READILY ACHIEVED.  NO RESTRICTION ON RATIOS OF LAYER THICK-
C     NESSES OR LAYER PROPERTIES.  NODES ARE NUMBERED CONSECUTIVELY
C     ALONG THE MERIDIAN AND IF A NODE IS LOCATED ON THE AXIS OF SYM-
C     METRY NUMBERING MUST BEGIN AT THIS NODE.  ELEMENTS ARE NUMBERED
C     SUCH THAT THE ELEMENT NUMBER IS THE SAME AS THE SMALLER ADJACENT
C     NODE NUMBER.
C     STORAGE FOR 100 NODES (AND THUS FOR 99 ELEMENTS).
C     SHEAR STRAIN AND CURVATURE MODELS VARY LINEARLY ALONG CHORD LENGTH
C
C***********************************************************************
C     DATA CARDS FOR AXSNSHL
C***********************************************************************
C
C     1 CARD.. I10  NUMBER OF SHELLS TO BE ANALYZED
C     THEN, FOR EACH SHELL, ALL OF THE FOLLOWING..
C
C     1 CARD..  COLS. 2-72  TITLE
C
C     1 CARD.. 3I10
C                 NUMBER OF NODES, NN
C                 NUMBER OF LOAD CASES, NLC
C                 NUMBER OF NODES WITH RESTRAINTS, NBC
C
C     1 CARD..  5F10.0
C                 THICKNESS OF 1 FACING (IN.)
C                 YOUNGS MODULUS OF FACINGS (PSI)
C                 POISSON RATIO OF FACINGS
C                 SHEAR MODULUS OF FACINGS (PSI)
C                 SHEAR STRESS CORRECTION FACTOR FOR FACINGS
C     1 CARD..  5F10.0
C                 THICKNESS OF CORE (IN.)
C                 YOUNGS MODULUS OF CORE (PSI)
C                 POISSON RATIO OF CORE
C                 SHEAR MODULUS OF CORE (PSI)
C                 SHEAR STRESS CORRECTION FACTOR FOR COR
C     (NOTE..  SHEARING MAY BE NEGLECTED BY SETTING G TO >     99999)
C
C     NN CARDS.. I10,3F10.0
C                 NODE NUMBER
C                 R, ABSCISSA OF NODE (IN.)
C                 Z, ORDINATE OF NODE (IN.)
C                 PHI, LATITUDE ANGLE OF NODE (DEGREES)
C
C     NN-1 CARDS.. 2F10.0
```

```
C                   CURVATURE AT NODE I OF ELEMENT (1/IN.)
C                   CURVATURE AT NODE J OF ELEMENT (1/IN.)
C
C     NBC CARDS.. 5I10
C                   NODE NUMBER
C                   TANGENTIAL DISPLACEMENT INDEX (0=FREE, 1=CONSTRAINED)
C                   RADIAL DISPLACEMENT INDEX ( DITTO )
C                   BENDING ROTATION INDEX ( DITTO )
C                   SHEAR WARPING INDEX ( DITTO )
C
C      FOR EACH LOAD CASE, THE FOLLOWING..
C     1 CARD.. 2I10,L10
C                   NUMBER OF LOADED ELEMENTS, NLE
C                   NUMBER OF LOADED NODES, NLN
C                   UNIFORM LOAD INDEX, LUL (T IF SAME DISTRIBUTED LOAD
C                        ON NLE ADJACENT ELEMENTS, F OTHERWISE)
C     NLE CARDS.. I10,6F10.0 (IF LUL IS T, THEN ONLY 1 CARD FOR FIRST
C                        LOADED ELEMENT IS NEEDED)
C                   ELEMENT NUMBER
C                   TANGENTIAL LOAD INTENSITY AT END I (PSI)
C                   RADIAL LOAD INTENSITY AT END I (PSI)
C                   MOMENT LOAD INTENSITY AT END I (IN.-LB./IN**2)
C                   TANGENTIAL LOAD INTENSITY AT END J (PSI)
C                   RADIAL LOAD INTENSITY AT END J (PSI)
C                   MOMENT LOAD INTENSITY AT END J (IN.-LB./IN**2)
C                  (NOTE.. LINEAR INTERPOLATION OF DISTRIBUTED LOADS
C                   IS USED ALONG THE CHORD LENGTH OF THE ELEMENT.)
C     NLN CARDS..  I10,3F10.0
C                   NODE NUMBER
C                   TANGENTIAL CONCENTRATED LOAD AT NODE (LB./IN.)
C                   RADIAL CONCENTRATED LOAD AT NODE (LB./IN.)
C                   CONCENTRATED MOMENT AT NODE (I   -LB./IN.)
C
      COMMON /   / NN,NE,NLC,NDOF,NBC,NRD,NLE,NLN
      PI = 3.14159265358979
      READ 1000, NSHELLS
      DO 100 N = 1,NSHELLS
      CALL SETUP
      CALL BCS
      DO 100 I = 1,NLC
      CALL LOADS(I)
  100 CALL SOLVE(I)
 1000 FORMAT(I10
      STOP
      END




      SUBROUTINE SETUP
C     THIS SUBROUTINE READS THE GEOMETRICAL AND MATERIAL PROPERTIES OF
C     THE SHELL AND SETS UP THE FOLLOWING.. (1) OVERALL STIFFNESS MATRIX
C     UNMODIFIED FOR BOUNDARY CONDITIONS (2) ELEMENT TRANSFORMATION
```

```
C     MATRICES ST  ED ON TAPE 1 (3) NODAL STRESS RESULTANT MATRICES
C     STORED ON TAPE 2 (4) CONSISTENT LOAD INTEGRATION MATRICES STORED
C     ON TAPE 3.
C     SHEAR STRAIN AND CURVATURE MODELS VARY LINEARLY ALONG CHORD LE'GTH
      REAL NUF,NUC,KF,KC
      COMMON /   / NN,NE,NLC,NDOF,NBC,NRD,NLE,NLN,PI
      COMMON /ARRAY/ S(400,8),ST(99,10,2),IBC(50),RL(400),RC(200),U(990)
      COMMON /PROPS/ H,D,HF,HC,EF,NUF,GF,EC,NUC,GC,BF,DF,BC,DC
      COMMON /XGEOM/ YP,YPP,RX,COSB,YBAR
      COMMON /ELGEOM/ R(100),Z(100),                    EL,SPSI,CPSI,
     1 TBI,TBJ,CBI,CBJ,SBI,SBJ,A1,A2,A3,A4
      COMMON /INTEG/ X(12),W(10)
      COMMON /STMATS/ SEL(10,10),B(12,10),DB(12,10),T(10,10)
      DIMENSION CPHI(100),SPHI(100),P(10,10,3),P1(10),P2(10),P3(10),
     1 PHI(100)
      EQUIVALENCE (CPHI(1),RL(1)), (SPHI(1),RL(101)), (P(1),U(1)),
     1 (P1(1),U(301)), (P2(1),U(311)), (P3(1),U(321))
      DATA  X  /  0.0, 0.013046735741414, 0.067468316655507,
     1 0.160295215850488, 0.283302302935376, 0.425562830509184,
     2 0.574437169490816, 0.716697697064624, 0.839704784149512,
     3 0.932531683344493, 0.986953264258586, 1.0  /
      DATA  W  /  0.066671344308688, 0.149451349150581,
     1 0.219086362515982, 0.269266719309996,   0.295524224714753,
     2 0.295524224714753, 0.269266719309996, 0.219086362515982,
     3  0.149451349150581, 0.066671344308688  /
      PRINT 2000
      READ 1000
      PRINT 1000
      READ 1001, NN,NLC,NBC
      READ 1002, HF,EF,NUF,GF,KF
      READ 1002, HC,EC,NUC,GC,KC
      PRINT 2001, NN,NLC,NBC, HF,HC, EF,NUF,GF,KF,  EC,NUC,GC,KC
      IF(NN.GT.100) GO TO 900
      IF(GF.GE.9999999998.0) GF = 1.0E+20
      IF(GC.GE.9999999998.0) GC = 1.0E+20
      H = HC + 2.0*HF
      D = HC + HF
      NE = NN - 1
      NDOF = 4*NN
      EF = EF/(1.0 - NUF*NUF)
      EC = EC/(1.0 - NUC*NUC)
      BF = EF*HF
      BC = EC*HC
      GF = GF*HF*KF
      GC = GC*HC*KC
      DF = BF*HF*HF/12.0
      DC = BC*HC*HC/12.0
      DO 100 I = 1,NDOF
      DO 100 J = 1,8
  100 S(I,J) = 0.0
      JK = 0
      PRINT 2002
      DR = 180.0/PI
      DO 110 I = 1,NN
      READ 1003, I,R(I),Z(I),PHI(I)
```

```
      PRINT 2003,I,R(I),Z(I),PHI(I)
      PHI(I) = PHI(I)/DR
      SPHI(I) = SIN(PHI(I))
  110 CPHI(I) = COS(PHI(I))
      REWIND 1
      REWIND 2
      REWIND 3
      PRINT 2004
      DO 500 I = 1,NE
      DR = R(I+1) - R(I)
      DZ = Z(I+1) - Z(I)
      EL = SQRT(DR*DR + DZ*DZ)
      SPSI = DR/EL
      CPSI = DZ/EL
      SBI = CPHI(I)*CPSI - SPHI(I)*SPSI
      CBI = SPHI(I)*CPSI + CPHI(I)*SPSI
      TBI = SBI/CBI
      SBJ = CPHI(I+1)*CPSI - SPHI(I+1)*SPSI
      CBJ = SPHI(I+1)*CPSI + CPHI(I+1)*SPSI
      TBJ = SBJ/CBJ
      READ 2004, CURVI,CURVJ
      PRINT 2005, I,CURVI,CURVJ,EL,SPSI,CPSI,TBI,TBJ
      YPPI = -EL*CURVI/CBI**3
      YPPJ = -EL*CURVJ/CBJ**3
      A1 = TBI
      A2 = TBI + 0.5*YPPI
      A3 = -(5.0*TBI + 4.0*TBJ) + 0.5*YPPJ - YPPI
      A4 = 3.0*(TBI + TBJ) + 0.5*(YPPI - YPPJ)
      DO 150 J = 1,10
      DO 150 K = 1,10
  150 SEL(J,K) = 0.0
C     COMPUTE AND STORE ELEMENT TRANSFORMATION MATRIX  (A**-1)*T
      CALL TMAT(I)
      WRITE(1) ((T(K,L),L=1,10),K=1,10)
      DO 400 J = 1,12
      YBAR = (1.0 - X(J))*(A1 + X(J)*(A2 + X(J)*(A3 + X(J)*A4)))
      YP = A1*(1.0 - 2.0*X(J))+ X(J)*(A2*(2.0 - 3.0*X(J)) + X(J)*(A3*
     1 (3.0 - 4.0*X(J)) + A4*X(J)*(4.0 - 5.0*X(J))))
      YPP = 2.0*(-A1 + A2*(1.0 - 3.0*X(J)))+ X(J)*(A3*(6.0 - 12.0*X(J))
     1 + A4*X(J)*(12.0 - 20.0*X(J)))
      RX = R(I) + X(J)*EL*(SPSI + YBAR*CPSI)
      COSB = 1.0/(SQRT(1.0 + YP*YP))
C     EVALUATE B(,) AT NODES AND INTEGRATION POINTS
      CALL BMAT(I,J)
      IF(J.EQ.1.OR.J.EQ.12) GO TO 200
C     ADD CONTRIBUTION TO ELEMENT STIFFNESS INTEGRATION
      C = PI*EL*RX*W(J-1)/COSB
      CALL SELA(C)
C     COMPUTE MATRICES FOR INTEGRATION OF DISTRIBUTED LOADS
      CALL PHITMAT(I,J)
      P1(J-1) = C
      P2(J-1) = YP
      P3(J-1) = COSB
      GO TO 400
  200 CONTINUE
```

```
C     STORE MATRICES NEEDED TO RECOVER STRESS RESULTANTS AT NODES
      CALL STRESS
      WRITE(2) ((B(K,L),L=1,10),K=1,12)
  400 CONTINUE
C     STORE INFORMATION FOR INTEGRATION OF DISTRIBUTED LOADS
      WRITE (3) (((P(J,K,L),L=1,3),K=1,10),J=1,10),(P1(J),P2(J),P3(J),
     1 J=1,10)
C     TRANSFORM 10X10 ELEMENT STIFFNESS TO GLOBAL CO-ORDINATES AND CON-
C     DENSE TO 8X8
      CALL SELR(I)
C     STORE MULTIPLIERS AND PIVOTS
      DO 420 J = 1,2
      IJ = J + 8
      DO 420 K = 1,10
  420 ST(I,K,J) = SEL(IJ,K)
C     ADD 8X8 ELEMENT STIFFNESS TO OVERALL STIFFNESS
      DO 450 J = 1,8
      IJ = JK + J
      DO 450 K = J,8
      IK = K - J + 1
  450 S(IJ,IK) = S(IJ,IK) + SEL(J,K)
  500 JK = JK + 4
      END FILE 1
      END FILE 2
      END FILE 3
      RETURN
  900 PRINT 2900
      STOP
 1000 FORMAT(72H
     1                                                    )
 1001 FORMAT(3I10)
 1002 FORMAT(5F10.0)
 1003 FORMAT(I10,3F10.0)
 1004 FORMAT(2F10.0)
 2000 FORMAT(1H1)
 2001 FORMAT(10X,28HNUMBER OF NODES                  ,I3/
     1 10X,28HNUMBER OF LOAD CASES                   ,I3/
     2 10X,28HNUMBER OF RESTRAINED NODES             ,I3//
     3 10X,16HFACE THICKNESS =,F10.6/
     4 10X,16HCORE THICKNESS =,F10.6//
     5 10X,8HFACE E =,F13.1/
     6 10X,9HFACE NU =,F12.5/
     7 10X,8HFACE G =,F13.1/
     7 10X,10HFACE KAP =,F11.5//
     8 10X,8HCORE E =,F13.1/
     9 10X,9HCORE NU =,F12.5/
     1 10X,8HCORE G =,F13.1/
     1 10X,10HCORE KAP =,F11.5//
     2 39H ALL QUANTITIES IN INCHES AND/OR POUNDS  /)
 2002 FORMAT(//11HONODAL DATA /
     9       2X,4HNODE,7X,11HABSCISSA, R,8X,12H ORDINATE, Z,6X,
     1 14HLATITUDE ANGLE/
     2 15X,5H(IN.),15X,5H(IN.),13X,8H(DEGREE)/)
 2003 FORMAT(I4,3F20.8)
 2004 FORMAT(/18H0ELEMENT GEOMETRY /
```

```
     1 8H ELEMENT,10X,7HCURV(I),10X,7HCURV(J),5X,12HCHORD LENGTH,10X,
     2 7HSIN PSI,10X,7HCOS PSI,6X,11HTAN BETA(I),6X,11HTAN BETA(J)/
     3 18X,7H(1/IN.),10X,7H(1/IN.),12X,5H(IN.))
 2005 FORMAT(I8,7F17.9)
 2900 FORMAT(/////41HONUMBER OF NODES EXCEEDS ALLOWABLE   STOP     )
      END




      SUBROUTINE TMAT(I)
C     THIS SUBROUTINE EVALUATES THE CO-ORDINATE TRANSFORMATION MATRIX
C     (A**-1)*T FOR ELEMENT I.
C     GLOBAL CO-ORDINATES ARE  S  AND  XI  (MERIDIONAL AND RADIAL), AND
C     THUS CAN BE APPLIED ONLY TO SHELLS WITH TWICE CONTINUOUS MERIDIANS
C     SHEAR STRAIN AND CURVATURE MODELS VARY LINEARLY ALONG CHORD LENGTH
      REAL NUC,NUF
      COMMON /PROPS/ H,D,HF,HC,EF,NUF,GF,EC,NUC,GC,BF,DF,BC,DC
      COMMON /STMATS/ SEL(10,10),B(12,10),DB(12,10),T(10,10)
      COMMON /ELGEOM/ R(100),Z(100),                    EL,SPSI,CPSI,
     1 TBI,TBJ,CBI,CBJ,SBI,SBJ,A1,A2,A3,A4
      DO 100 J = 1,10
      DO 100 K = 1,10
  100 B(J,K) = 0.0
      IF(R(I).EQ.0.0) GO TO 500
C     MATRIX FOR OPEN-ENDED ELEMENT
      B(1,1) = B(3,2) = B(2,6) = 1.0
      B(7,4) = B(7,5) = B(9,5) = 1.0
      B(8,9) = B(8,10) = B(10,10) = 1.0
      B(2,1) = B(8,4) = B(8,5) = B(10,5) = -1.0
      B(4,1) = -TBI
      B(4,6) = TBI
      B(6,6) = TBI + TBJ
      B(6,1) = - B(6,6)
      B(5,1) = B(6,6) + TBI
      B(5,6) = -B(5,1)
      B(5,2) = -3.0
      B(6,2) = 2.0
      B(5,7) = 3.0
      B(6,7) = -2.0
      B(4,3) = B(6,3) = -EL/CBI/CBI
      B(5,3) = -2.0*B(4,3)
      B(4,4) = B(6,4) = HC*B(4,3)/D
      B(5,4) = -2.0*B(4,4)
      B(4,5) = B(6,5) = B(4,3)
      B(5,5) = -2.0*B(4,5)
      B(5,8) = EL/CBJ/CBJ
      B(6,8) = -B(5,8)
      B(5,9) = HC*B(5,8)/D
      B(6,9) = -B(5,9)
      B(5,10) = B(5,8)
      B(6,10) = -B(5,10)
      DO 200 J = 1,10
```

```
      T(J,1) = CBI*B(J,1) + SBI*B(J,2)
      T(J,2) = SBI*B(J,1) - CBI*B(J,2)
      T(J,3) = B(J,3)
      T(J,4) = B(J,4)
      T(J,5) = CBJ*B(J,6) + SBJ*B(J,7)
      T(J,6) = SBJ*B(J,6) - CBJ*B(J,7)
      T(J,7) = B(J,8)
      T(J,8) = B(J,9)
      T(J,9) = B(J,5)
  200 T(J,10) = B(J,10)
      GO TO 1000
C     MATRIX FOR CAP
  500 B(5,2) = -1.0
      B(6,6) = B(9,9) = B(9,10) = B(10,10) = 1.0
      B(7,7) = 3.0
      B(8,7) = -2.0
      B(6,2) = -CPSI
      B(7,2) = (2.0*TBI + TBJ)*CPSI + 3.0*SPSI
      B(8,2) = -B(7,2) + TBI*CPSI + SPSI
      B(7,6) = -2.0*TBI - TBJ
      B(8,6) = TBI + TBJ
      B(7,8) = EL/CBJ/CBJ
      B(8,8) = -B(7,8)
      B(7,9) = HC*B(7,8)/D
      B(8,9) = -B(7,9)
      B(7,10) = B(7,8)
      B(8,10) =-B(7,10)
      DO 700 J = 1,10
      T(J,1) = T(J,3) = T(J,4) = T(J,9) = 0.0
      T(J,2) = B(J,2)
      T(J,5) = CBJ*B(J,6) + SBJ*B(J,7)
      T(J,6) = SBJ*B(J,6) - CBJ*B(J,7)
      T(J,7) = B(J,8)
      T(J,8) = B(J,9)
  700 T(J,10) = B(J,10)
 1000 RETURN
      END
```

```
      SUBROUTINE BMAT(I,J)
C     THIS SUBROUTINE EVALUATES THE MATRIX B FOR ELEMENT I AT POINT X(J)
C     SHEAR STRAIN AND CURVATURE MODELS VARY LINEARLY ALONG CHORD LENGTH
      REAL NUF,NUC
      COMMON /PROPS/ H,D,HF,HC,EF,NUF,GF,EC,NUC,GC,BF,DF,BC,DC
      COMMON /XGEOM/ YP,YPP,RX,COSB,YBAR
      COMMON /ELGEOM/ R(100),Z(100),                    EL,SPSI,CPSI,
     1 TBI,TBJ,CBI,CBJ,SBI,SBJ,A1,A2,A3,A4
      COMMON /STMATS/ SFL(10,10),B(12,10),DB(12,10),T(10,10)
      COMMON /INTEG/ X(12),W(10)
      DO 100 K = 1,12
      DO 100 L = 1,10
```

```
  100 B(K,L) = 0.0
      B1 = -YPP*COSB**5*(1.0 - YP*YP)/(EL*EL)
      B3 = COSB**3/(EL*EL)
      B2 = -2.0*YPP*YP*B3*COSB*COSB
      IF(R(I).EQ.0.0) GO TO 400
      B4 = -EL*B3*YP*(SPSI + CPSI*YP)/RX
      B5 = EL*B3*(SPSI + CPSI*YP)/RX
      B6 = COSB*(SPSI + CPSI*YP)/RX
C     MATRIX FOR OPEN-ENDED ELEMENT
      B(2,1) = B(7,1) = B(12,1) = SPSI/RX
      B(2,3) = B(7,3) = B(12,3) = CPSI/RX
      B(2,2) =                    B(12,1)*X(J)
      B(2,4) =                    B(12,3)*X(J)
      B(2,5) = B(2,4)*X(J)
      B(2,6) = B(2,5)*X(J)
      B(4,8) = B(9,10)  =            COSB/EL
      B(1,2) =                    COSB*B(9,10)
      B(1,4) = B(1,2)*YP
      B(1,5) = 2.0*X(J)*B(1,4)
      B(1,6) = 1.5*X(J)*B(1,5)
      B(3,7) = B(8,9) = 1.0
      B(3,8) = B(8,10) = X(J)
      B(4,2) = B(9,2) = B1
      B(4,4) = B(9,4) = B2
      B(5,2) = B(10,2) = B4
      B(5,4) = B(10,4) = B5
      B(5,7) = B(10,9) = B6
      B(5,8) = B(10,10) =            B6*X(J)
      B(4,5) = B(9,5) =           2.0*B2*X(J)  + 2.0*B3
      B(4,6) = B(9,6) =           (3.0*B2*X(J) + 6.0*B3)*X(J)
      B(5,5) = B(10,5) =           2.0*B5*X(J)
      B(5,6) = B(10,6) =           3.0*B5*X(J)*X(J)
      B(6,2) = B(1,2) - D*B1/2.0
      B(11,2) =  B(1,2) + D*B1/2.0
      B(6,4) = B(1,4) - D*B2/2.0
      B(11,4) =  B(1,4) + D*B2/2.0
      B(6,5) = B(1,5) - D*B(4,5)/2.0
      B(11,5) = B(6,5) + D*B(4,5)
      B(6,6) = B(1,6) - D*B(4,6)/2.0
      B(11,6) = B(6,6) + D*B(4,6)
      B(6,8) = -HC*B(4,8)/2.0
      B(11,8) = -B(6,8)
      B(6,10) = -HF*B(4,8)/2.0
      B(11,10) = -B(6,10)
      B(7,2) = B(2,2) - D*B4/2.0
      B(12,2) =  B(7,2) + D*B4
      B(7,4) = B(2,4) - D*B5/2.0
      B(12,4) =  B(7,4) + D*B5
      B(7,5) = B(2,5) - D*B(5,5)/2.0
      B(12,5) = B(7,5) + D*B(5,5)
      B(7,6) = B(2,6) - D*B(5,6)/2.0
      B(12,6) = B(7,6) + D*B(5,6)
      B(7,7) = -HC*B6/2.0
      B(12,7) = -B(7,7)
      B(7,8) = B(7,7)*X(J)
```

```
      B(12,8) = -B(7,8)
      B(7,9) = -HF*B6/2.0
      B(12,9) = -B(7,9)
      B(7,10) = B(7,9)*X(J)
      B(12,10) = -B(7,10)
      GO TO 1000
C     MATRIX FOR CAP ELEMENT
  400 B6 = EL*(SPSI + YBAR*CPSI)
      B5 = COSB**3*(SPSI + YP*CPSI)/(B6*EL)
      B4 = COSB*(SPSI + CPSI*YP)/B6
      B(3,9) = B(8,10) = X(J)
      B(4,9) = B(9,10) = COSB/EL
      B(4,6) = B(9,6) =            B1 + TBI*B2
      B(4,7) = B(9,7) =            2.0*B2*X(J) + 2.0*B3
      B(4,8) = B(9,8) =            (3.0*B2*X(J) + 6.0*B3)*X(J)
      B(5,6) = B(10,6) =B5*(((5.0*A4*X(J) + 4.0*(A3 - A4))*X(J) +
     1 3.0*(A2 - A3))*X(J) + 2.0*(A1 - A2))
      B(5,7) = B(10,7) =            2.0*B5
      B(5,8) = B(10,8) =            3.0*B5*X(J)
      B(5,9) = B(10,10) = B4
      B(1,6) = COSB*B(4,9)*(1.0+ TBI*YP)
      B(1,7) = 2.0*X(J)*COSB*B(4,9)*YP
      B(1,8) = 1.5*X(J)*B(1,7)
      B(2,6) = (SPSI + CPSI*TBI)/B6
      B(2,7) = X(J)*CPSI/B6
      B(2,8) = X(J)*B(2,7)
      B(6,6) = B(1,6) - D*B(4,6)/2.0
      B(11,6) = B(6,6) + D*B(4,6)
      B(6,7) = B(1,7) - D*B(4,7)/2.0
      B(11,7) = B(6,7) + D*B(4,7)
      B(6,8) = B(1,8) - D*B(4,8)/2.0
      B(11,8) = B(6,8) + D*B(4,8)
      B(6,9) = -HC*B(4,9)/2.0
      B(11,9) = -B(6,9)
      B(6,10) = -HF*B(4,9)/2.0
      B(11,10) = -B(6,10)
      B(7,6) = B(2,6) - D*B(5,6)/2.0
      B(12,6) = B(7,6) + D*B(5,6)
      B(7,7) = B(2,7) - D*B5
      B(12,7) = B(2,7) + D*B5
      B(7,8) = B(2,8) - D*B(5,8)/2.0
      B(12,8) = B(7,8) + D*B(5,8)
      B(7,9) = -HC*B4/2.0
      B(12,9) = -B(7,9)
      B(7,10) = -HF*B4/2.0
      B(12,10) = -B(7,10)
 1000 RETURN
      END
```

```
      SUBROUTINE PHITMAT(I,J)
C     THIS SUBROUTINE EVALUATES THE TRANSFORM OF THE MATRIX PHI FOR
C     ELEMENT I AT POINT XI(J)
C     SHEAR STRAIN AND CURVATURE MODELS VARY LINEARLY ALONG CHORD LENGTH
      REAL NUF,NUC
      COMMON /PROPS/ H,D,HF,HC,EF,NUF,GF,EC,NUC,GC,BF,DF,BC,DC
      COMMON /XGEOM/ YP,YPP,RX,COSB,YBAR
      COMMON /ELGEOM/ R(100),Z(100),                    EL,SPSI,CPSI,
     1 TBI,TBJ,CBI,CBJ,SBI,SBJ,A1,A2,A3,A4
      COMMON /ARRAY/ S(400,8),ST(99,10,2),IBC(50),RL(400),RC(200),U(990)
      COMMON /INTEG/ X(12),W(10)
      COMMON /STMATS/ SEL(10,10),B(12,10),DB(12,10),T(10,10)
      DIMENSION PH(10,10,3)
      EQUIVALENCE (PH(1),U(1))
      K = J - 1
      DO 100 M = 1,10
      DO 100 L = 1,3
  100 PH(K,M,L) = 0.0
      IF(R(I).EQ.0.0) GO TO 500
C     MATRIX FOR OPEN-ENDED ELEMENT
      PH(K,1,1) = PH(K,3,2) = 1.0
      PH(K,2,1) = PH(K,4,2) = X(J)
      PH(K,5,2) = X(J)*X(J)
      PH(K,6,2) = X(J)*PH(K,5,2)
      PH(K,2,3) = COSB*YP*COSB/EL
      PH(K,4,3) = -COSB*COSB/EL
      PH(K,5,3) = 2.0*X(J)*PH(K,4,3)
      PH(K,6,3) = 1.5*X(J)*PH(K,5,3)
      PH(K,7,3) = -HC/D
      PH(K,8,3) = X(J)*PH(K,7,3)
      PH(K,9,3) = -HF/D
      PH(K,10,3) = X(J)*PH(K,9,3)
      GO TO 1000
C     MATRIX FOR CAP
  500 PH(K,5,1) = -CPSI
      PH(K,5,2) = SPSI
      PH(K,6,1) = X(J)
      PH(K,6,2) = X(J)*TBI
      PH(K,7,2) = X(J)*X(J)
      PH(K,8,2) = X(J)**3
      PH(K,6,3) = (YP - TBI)*COSB*COSB/EL
      PH(K,7,3) = -2.0*X(J)*COSB*COSB/EL
      PH(K,8,3) = 1.5*X(J)*PH(K,7,3)
      PH(K,9,3) = -HC*X(J)/D
      PH(K,10,3) = -HF*X(J)/D
 1000 RETURN
      END
```

```
      SUBROUTINE SELA(C)
C     THIS SUBROUTINE COMPUTES A TERM IN THE GAUSS INTEGRATION FOR THE
C     STIFFNESS MATRIX IN GENERALIZED CO-ORDINATES
C     SHEAR STRAIN AND CURVATURE MODELS VARY LINEARLY ALONG CHORD LENGTH
      REAL NUF,NUC
      COMMON /PROPS/ H,D,HF,HC,EF,NUF,GF,EC,NUC,GC,BF,DF,BC,DC
      COMMON /STMATS/ SEL(10,10),B(12,10),DB(12,10),T(10,10)
      DO 100 K = 1,10
      DB(1,K) = BC*(B(1,K) + NUC*B(2,K))*C
      DB(2,K) = BC*(B(2,K) + NUC*B(1,K))*C
      DB(3,K) = GC*B(3,K)*C
      DB(4,K) = DC*(B(4,K) + NUC*B(5,K))*C
      DB(5,K) = DC*(B(5,K) + NUC*B(4,K))*C
      DB(6,K) = BF*(B(6,K) + NUF*B(7,K))*C
      DB(7,K) = BF*(B(7,K) + NUF*B(6,K))*C
      DB(8,K) = GF*B(8,K)*C*2.0
      DB(9,K) = DF*(B(9,K)+ NUF*B(10,K))*C*2.0
      DB(10,K) = DF*(B(10,K) + NUF*B(9,K))*C*2.0
      DB(11,K) = BF*(B(11,K) + NUF*B(12,K))*C
  100 DB(12,K) = BF*(B(12,K) + NUF*B(11,K))*C
      DO 200 K = 1,10
      DO 200 L = 1,10
      DO 200 M = 1,12
  200 SEL(K,L) = SEL(K,L) + B(M,K)*DB(M,L)
      RETURN
      END
```

```
      SUBROUTINE STRESS
C     THIS SUBROUTINE EVALUATES THE MATRIX E*B*T AT THE NODES OF THE
C     ELEMENT FOR LATER CALCULATION OF THE STRESS RESULTANTS.
C     SHEAR STRAIN AND CURVATURE MODELS VARY LINEARLY ALONG CHORD LENGTH
      REAL NUF,NUC
      COMMON /PROPS/ H,D,HF,HC,EF,NUF,GF,EC,NUC,GC,BF,DF,BC,DC
      COMMON /STMATS/ SEL(10,10),B(12,10),DB(12,10),T(10,10)
      DO 150 I = 1,10
      DB(1,I) = BC*(B(1,I) + NUC*B(2,I))
      DB(2,I) = BC*(B(2,I) + NUC*B(1,I))
      DB(3,I) = GC*B(3,I)
      DB(4,I) = DC*(B(4,I) + NUC*B(5,I))
      DB(5,I) = DC*(B(5,I) + NUC*B(4,I))
      DO 100 J = 5,10,5
      DB(J+1,I) = BF*(B(J+1,I) + NUF*B(J+2,I))
  100 DB(J+2,I) = BF*(B(J+2,I) + NUF*B(J+1,I))
      DB(8,I) = GF*B(8,I)
      DB(9,I) = DF*(B(9,I) + NUF*B(10,I))
  150 DB(10,I) = DF*(B(10,I) + NUF*B(9,I))
      DO 200 I = 1,12
      DO 200 J = 1,10
      B(I,J) = 0.0
      DO 200 K = 1,10
```

```
  200 B(I,J) = B(I,J) + DB(I,K)*T(K,J)
      RETURN
      END



      SUBROUTINE SELR(L)
C     THIS SUBROUTINE TRANSFORMS THE ELEMENT STIFFNESS FROM GENERALIZED
C     TO GLOBAL CO-ORDINATES AND CONDENSES IT FROM 10X10 TO 8X8 USING
C     STATIC CONDENSATION.
C     SHEAR STRAIN AND CURVATURE MODELS VARY LINEARLY ALONG CHORD LENGTH
      COMMON /ELGEOM/ R(100),Z(100),                    EL,SPSI,CPSI,
     1 TBI,TBJ,CBI,CBJ,SBI,SBJ,A1,A2,A3,A4
      COMMON /STMATS/ SEL(10,10),B(12,10),DB(12,10),T(10,10)
C     SYMMETRIZE ELEMENT STIFFNESS IN GENERALIZED CO-ORDINATES
      DO 50 I = 1,9
      IJ = I + 1
      DO 50 J = IJ,10
      IF(SEL(I,J).EQ.0.0.OR.SEL(J,I).EQ.0.0) GO TO 45
      SEL(I,J) = 0.5*(SEL(I,J) + SEL(J,I))
      GO TO 50
   45 SEL(I,J) = 0.0
   50 SEL(J,I) = SEL(I,J)
C      TRANSFORM TO GLOBAL CO-ORDINATES
      DO 100 I = 1,10
      DO 100 J = 1,10
      DB(I,J) = 0.0
      DO 100 K = 1,10
  100 DB(I,J) = DB(I,J) + SEL(I,K)*T(K,J)
      DO 200 I = 1,10
      DO 200 J = 1,10
      SEL(I,J) = 0.0
      DO 200 K = 1,10
  200 SEL(I,J) = SEL(I,J) + T(K,I)*DB(K,J)
      IF(R(L).NE.0.0) GO TO 250
      SEL(1,1) = SEL(3,3) = SEL(4,4) = SEL(9,9) = 1.0
C     CONDENSE TO 8X8 ELEMENT STIFFNESS
  250 DO 300 J = 1,2
      IJ = 10 - J
      IK = IJ + 1
      PIVOT = SEL(IK,IK)
      DO 300 K = 1,IJ
      C = SEL(IK,K)/PIVOT
      SEL(IK,K) = C
      DO 300 I = K,IJ
      SEL(I,K) = SEL(I,K) - C*SEL(I,IK)
  300 SEL(K,I) = SEL(I,K)
      RETURN
      END
```

```
      SUBROUTINE BCS
C     THIS SUBROUTINE READS THE BOUNDARY CONDITION DATA, MODIFIES THE
C     OVERALL STIFFNESS MATRIX ACCORDINGLY AND THEN TRIANGULARIZES THE
C     STIFFNESS FOR READY SOLUTION
C     SHEAR STRAIN AND CURVATURE MODELS VARY LINEARLY ALONG CHORD LENGTH
      COMMON /   / NN,NE,NLC,NDOF,NBC,NRD,NLE,NLN,PI
      COMMON /ARRAY/ S(400,8),ST(99,10,2),IBC(50),RL(400),RC(200),U(990)
      COMMON /ELGEOM/ R(100),Z(100),                    EL,SPSI,CPSI,
     1 TBI,TBJ,CBI,CBJ,SBI,SBJ,A1,A2,A3,A4
      DIMENSION NR(4)
      NRD = 0
      IF(R(1).NE.0.0) GO TO 100
      NRD = 3
      IBC(1) = 1
      IBC(2) = 3
      IBC(3) = 4
  100 PRINT 2000
C     READ KINEMATIC CONSTRAINTS AND MODIFY OVERALL STIFFNESS
      DO 300 I = 1,NBC
      READ 1001, N,(NR(J),J=1,4)
      PRINT 2001, N,(NR(J),J = 1,4)
      IJ = 4*N - 4
      DO 300 J = 1,4
      IF(NR(J).EQ.0) GO TO 300
      NRD = NRD + 1
      IK = IJ + J
      IBC(NRD) = IK
      S(IK,1) = 1.0
      DO 200 K = 2,8
      S(IK,K) = 0.0
      L = IK - K + 1
      IF(L.LE.0) GO TO 200
      S(L,K) = 0.0
  200 CONTINUE
  300 CONTINUE
      IF(NRD.GT.50) GO TO 999
C     TRIANGULARIZE STIFFNESS MATRIX
      CALL BANSOL(1,RL,S,400,8,NDOF,8)
      RETURN
  999 PRINT 2999,NRD
      STOP
 1001 FORMAT(5I10)
 2000 FORMAT(//59H0KINEMATIC CONSTRAINTS (0 = UNCONSTRAINED, 1 = CONSTRA
     1INED) /
     2 6X,4HNODE,5X,10HMERIDIONAL,9X,6HRADIAL,7X,8HROTATION,
     3 8X,7HWARPING/)
 2001 FORMAT(I10,4I15)
 2999 FORMAT(/////38HONUMBER OF CONSTRAINED DISPLACEMENTS =,I4,
     1 28H EXCEEDS ALLOWABLE 50   STOP   )
      END
```

```
      SUBROUTINE LOADS(I)
C     THIS SUBROUTINE READS THE LOADING DATA, INTEGRATES TO OBTAIN
C     THE CONSISTENT LOADS, REDUCES THE LOADS BY STATIC CONDENSATION
C     AND ASSEMBLES THE OVERALLL LOAD VECTOR WITH MODIFICATION FOR KINE-
C     MATIC CONSTRAINTS.
C     SHEAR STRAIN AND CURVATURE MODELS VARY LINEARLY ALONG CHORD LENGTH
      COMMON /   / NN,NE,NLC,NDOF,NBC,NRD,NLE,NLN,PI
      COMMON /ARRAY/ S(400,8),ST(99,10,2),IBC(50),RL(400),RC(200),U(990)
      COMMON /INTEG/ X(12),W(10)
      COMMON /STMATS/ SEL(10,10),B(12,10),DB(12,10),T(10,10)
      COMMON /ELGEOM/ R(100),Z(100),                    EL,SPSI,CPSI,
     1 TBI,TBJ,CBI,CBJ,SBI,SBJ,A1,A2,A3,A4
      DIMENSION P(10),PV(11),PR(10), PH(10,10,3),P1(10),P2(10),P3(10),
     1 CL(500)
      EQUIVALENCE (P(1),SEL(1)), (PR(1),SEL(11)),(PV(1),SEL(21)),
     1 (PH(1),U(1)), (P1(1),U(301)), (P2(1),U(311)), (P3(1),U(321)),
     2 (CL(1),U(331))
      LOGICAL LUL
      REWIND 1
      REWIND 3
      N = NDOF/2
      DO 50 J = 1,N
      IJ = N + J
   50 RL(J) = RL(IJ) = RC(J) = 0.0
      N = N/2 + NDOF
      DO 60 J = 1,N
   60 CL(J) = 0.0
      READ 1000, NLE,NLN,LUL
      PRINT 2000, I,NE,NLE,NLN,LUL
      IF(NLE.EQ.0) GO TO 600
      PRINT 2001
      IT = 1
      DO 500 J = 1,NLE
      DO 100 K = 1,10
  100 PR(K) = 0.0
C     READ VALUE OF DISTRIBUTED LO.        CODES OF LOADED ELEMENTS
      IF(LUL.AND.J.GT.1) GO TO 155
      READ 1001, IE,(PV(K),K=6,11)
C     PREPARE TAPES FOR ELEMENT IE
      IF(IE-IT) 120,160,140
  120 N = IT - IE
      DO 130 K = 1,N
      BACKSPACE 1
  130 BACKSPACE 3
      GO TO 160
  140 N = IE - IT
      DO 150 K = 1,N
      READ (1)
  150 READ (3)
      GO TO 160
  155 IE = IE + 1
  160 PRINT 2002,IE,(PV(K),K=6,11)
C     INTEGRATE LOAD VECTOR OVER XI
      READ (3)  (((PH(K,L,M),M=1,3),L=1,10),K=1,10), (P1(K),P2(K),P3(K),
```

```
     1 K=1,10)
      DO 200 K = 1,10
      C = P1(K)
      YP = P2(K)
      COSB = P3(K)
      PV(4) = PV(6) + X(K+1)*(PV(9) - PV(6))
      PV(5) = PV(7) + X(K+1)*(PV(10) - PV(7))
      PV(1) = C*COSB*(PV(4) + YP*PV(5))
      PV(2) = C*COSB*(YP*PV(4) - PV(5))
      PV(3) = C*(PV(8) + X(K+1)*(PV(11) - PV(8)))
      DO 200 L = 1,10
      DO 200 M = 1,3
  200 PR(L) = PR(L) + PH(K,L,M)*PV(M)
C     TRANSFORM ELEMENT LOAD VECTOR TO GLOBAL CO-ORDINATES
      READ (1)  ((T(M,L),L=1,10),M=1,10)
      DO 300 K = 1,10
      P(K) = 0.0
      DO 300 L = 1,10
  300 P(K) = P(K) + T(L,K)*PR(L)
      IJ = 5*IE - 5
      C1 = 2.0*PI*R(IE)
      IF(R(IE).EQ.0.0) C1 = 1.0
      C2 = 2.0*PI*R(IE+1)
      DO 325 K = 1,4
      IK = IJ + K
      CL(IK) = CL(IK) + P(K)/C1
      IK = IK + 5
  325 CL(IK) = CL(IK) + P(K+4)/C2
      CL(IJ+5) = CL(IJ+5) + P(9)/C1
      CL(IJ+10) = CL(IJ+10) + P(10)/C2
C     CONDENSE LOAD VECTOR TO 8X1
      DO 400 K = 1,2
      IJ = 10 - K
      JK = IJ + 1
      IK = JK - 8
      DO 350 L = 1,IJ
  350 P(L) = P(L) - ST(IE,L,IK)*P(JK)
  400 P(JK) = P(JK)/ST(IE,JK,IK)
C     ASSEMBLE CONDENSED AND REDUCED LOADS
      IJ = 4*IE - 4
      DO 450 K = 1,8
      JK = IJ + K
  450 RL(JK) = RL(JK) + P(K)
      IK = 2*IE - 2
      RC(IK+1) = P(9)
      RC(IK +2) = P(10)
  500 IT = IE + 1
      PRINT 2005, (J,CL(5*J-4),CL(5*J-3),CL(5*J-2),CL(5*J-1),CL(5*J),
     1 J = 1,NN)
  600 IF(NLN.EQ.0) GO TO 800
      PRINT 2003
C     READ AND ASSEMBLE CONCENTRATED NODAL LOADS
      DO 700 J = 1,NLN
      READ 1002, N,(P(K),K=1,3)
      PRINT 2004,N,(P(K),K=1,3)
```

```
      IF(R(N).EQ.0.0) PRINT 2900
      RL(4*N-3) = 2.0*PI*P(1)*R(N) + RL(4*N-3)
      RL(4*N-2) = 2.0*PI*P(2)*R(N) + RL(4*N-2)
  700 RL(4*N-1) = 2.0*PI*P(3)*R(N) + RL(4*N-1)
C     MODIFY LOAD VECTOR FOR KINEMATIC CONSTRAINTS
  800 CONTINUE
      DO 900 J = 1,NRD
      K = IBC(J)
  900 RL(K) = 0.0
      IF(R(1).EQ.0.0) RC(1) = 0.0
      RETURN
 1000 FORMAT(2I10,L10)
 1001 FORMAT(I10,6F10.0)
 1002 FORMAT(I10,3F10.0)
 2000 FORMAT(20H1LOADING CASE NUMBER ,I5/
     1 5X,18HNUMBER OF ELEMENTS , I10/
     2 5X,25HNUMBER OF LOADED ELEMENTS ,I3/
     3 5X,22HNUMBER OF LOADED NODES ,I6/
     4 5X,29HSAME LOADING ON ALL ELEMENTS  ,L3/)
 2001 FORMAT(57H0DISTRIBUTED LOAD ORDINATES AT NODES OF ELEMENTS (IN PSI
     1) /
     2 8H ELEMENT,3X,17HMERIDIONAL, PS(I),7X,13HRADIAL, PZ(I),7X,
     3 13HMOMENT, MS(I),3X,17HMERIDIONAL, PS(J),7X,13HRADIAL, PZ(J),7X,
     4 13HMOMENT, MS(J) )
     4 13HMOMENT, MS(J) )
 2002 FORMAT(I8,6F20.5)
 2003 FORMAT(56H0CONCENTRATED LOADS AT NODES (PER UNIT OF CIRCUMFERENCE)
     1/4X,4HNODE,6X,14HMERIDIONAL, PS,10X,10HRADIAL, PZ,10X,
     2 10HMOMENT, MS )
 2004 FORMAT(I8,3F20.5)
 2005 FORMAT(//54H0CONSISTENT LOAD VECTOR (LOADS PER UNIT CIRCUMFERENCE)
     1/10X,4HNODE,16X,4HP(S),16X,4HP(Z),16X,4HM(S),14X,6HM(GAM),13X,
     2 7HM(GAMF) //     (I14,5E20.8))
 2900 FORMAT(77H0LOADING ON PREVIOUS NODE IGNORED (THEORY DOES NOT ACCOM
     1ODATE LOADS AT APEX)  /)
      END
```

```
      SUBROUTINE SOLVE(I)
C     THIS SUBROUTINE SOLVES FOR THE NODAL DISPLACEMENTS, RECOVERS THE
C     CONDENSED DISPLACEMENTS, PRINTS THE ELEMENT DISPLACEMENTS AND
C     CALCULATES AND PRINTS THE NODAL STRESS RESULTANTS.
C     SHEAR STRAIN AND CURVATURE MODELS VARY LINEARLY ALONG CHORD LENGTH
      REAL NUF,NUC
      COMMON /PROPS/ H,D,HF,HC,EF,NUF,GF,EC,NUC,GC,BF,DF,BC,DC
      COMMON /  / NN,NE,NLC,NDOF,NBC,NRD,NLE,NLN,PI
      COMMON /ARRAY/ S(400,8),ST(99,10,2),IBC(50),RL(400),RC(200),U(990)
      COMMON /ELGEOM/ R(100),Z(100),                    EL,SPSI,CPSI,
     1 TBI,TBJ,CBI,CBJ,SBI,SBJ,A1,A2,A3,A4
      COMMON /STMATS/ SEL(10,10),B(12,10),DB(12,10),T(10,10)
      DIMENSION SRI(21),SRJ(21),ASR(100,21)
```

```
      EQUIVALENCE (SRI(1),SEL(1)), (SRJ(1),SEL(31))
C     SOLVE FOR NODAL DISPLACEMENTS
      CALL BANSOL(2,RL,S,400,8,NDOF,8)
      PRINT 2000, I
      DO 300 J = 1,NE
      IJ = 10*J - 10
      IL = 4*J - 4
      DO 100 K = 1,8
      IK = IL + K
      JK = IJ + K
  100 U(JK) = RL(IK)
C     RECOVER CONDENSED DISPLACEMENTS
      IL = 2*J - 2
      DO 200 K = 1,2
      JK = K + 8
      IK = JK - 1
      II = IJ + JK
      M = IL + K
      U(II) = RC(M)
      DO 200 L = 1,IK
      M = IJ + L
  200 U(II) = U(II) - ST(J,L,K)*U(M)
C     COMPUTE ADDITIONAL DISPLACEMENTS OF INTEREST AND PRINT
      GAMCI = U(IJ+4) + U(IJ+9)
      GAMCJ = U(IJ+8) + U(IJ+10)
      CHISI = (HC*GAMCI + HF*U(IJ+9))/D
      CHISJ = (HC*GAMCJ + HF*U(IJ+10))/D
      CHII  = U(IJ+3) + CHISI
      CHIJ  = U(IJ+7) + CHISJ
  300 PRINT 2001, J,R(J),Z(J),
     1 U(IJ+1),U(IJ+2),CHII,U(IJ+3), CHISI,U(IJ+4),GAMCI,U(IJ+9),
     2 U(IJ+5),U(IJ+6),CHIJ,U(IJ+7), CHISJ,U(IJ+8),GAMCJ,U(IJ+10)
      PRINT 2002, R(NN),Z(NN)
      PRINT 2003, I
C     COMPUTE STRESS RESULTANTS AT NODES
      DO 350 J = 1,NN
      DO 350 K = 1,20
  350 ASR(J,K) = 0.0
      REWIND 2
      DO 500 J = 1,NE
      CALL RESULTS(J)
      SRI(21) = SRJ(21) = 1.0E+10
      IF(ABS(SRI(8)).GE.1.0E-16) SRI(21) = SRI(3)/SRI(8)
      IF(ABS(SRJ(8)).GE.1.0E-16) SRJ(21) = SRJ(3)/SRJ(8)
      C1 = 0.5
      C2 = 0.5
      IF(J.EQ.1) C1 = 1.0
      IF(J.EQ.NE) C2 = 1.0
      DO 400 K = 1,20
      ASR(J,K) = ASR(J,K) + C1*SRI(K)
  400 ASR(J+1,K) = ASR(J+1,K) + C2*SRJ(K)
  500 PRINT 2004, J,R(J),Z(J),
     1                (SRI(K),K=6,10), (SRI(K),K=1,5), (SRI(K),K=11,21),
     2 J,R(J+1),Z(J+1),
     3    (SRJ(K),K=6,10), (SRJ(K),K=1,5), (SRJ(K),K=11,21)
```

```
      PRINT 2005, I
      IF(NLN.GT.0) PRINT 2008
      PRINT 2007
      DO 600 J = 1,NN
      ASR(J,21) = 1.0E+10
      IF(ABS(ASR(J,8)).GE.1.0E-16) ASR(J,21) = ASR(J,3)/ASR(J,8)
  600 PRINT 2006, J,R(J),Z(J),
     1 (ASR(J,K),K=6,10), (ASR(J,K),K=1,5), (ASR(J,K),K=11,21)
      RETURN
 2000 FORMAT(38H1NODAL DISPLACEMENTS FOR LOADING CASE ,I3/
     1 5H NODE,2X,13HMERIDIONAL, U,6X,9HRADIAL, W,2X,13HROTATION, CHI,
     2 9X,6HCHI(B),9X,6HCHI(S),3X,12HWARPING, GAM,7X,8HGAMMA(C),7X,
     3 8HGAMMA(F)/)
 2001 FORMAT(8H ELEMENT,I3,39X,7H(R,Z) =, F9.4,1H,,F9.4 /
     1 4X,1HI,8E15.7/
     2 4X,1HJ,8E15.7/)
 2002 FORMAT(50X,7H(R,Z) =,F9.4,1H,,F9.4 )
 2003 FORMAT(56H1STRESS RESULTANTS AT ENDS OF ELEMENTS FOR LOADING CASE
     9 ,I3/
     17H  LAYER,16X,4HN(S),12X,8HN(THETA),16X,4HQ(S),16X,4HM(S),12X,
     2 8HM(THETA),7X,13HQ(S,C)/Q(S,F))
 2004 FORMAT(8H ELEMENT,I3,8H, NODE I,31X,7H(R,Z) =,F9.4,1H,,F9.4 /
     1 7H    TOP,5F20.8/
     2 7H   CORE,5F20.8/
     3 7H BOTTOM,5F20.8/
     4 7H  TOTAL,5F20.8,F20.5/
     5 8H ELEMENT,I3,8H, NODE J,31X,7H(R,Z) =,F9.4,1H,,F9.4 /
     6 7H    TOP,5F20.8/
     7 7H   CORE,5F20.8/
     8 7H BOTTOM,5F20.8/
     9 7H  TOTAL,5F20.8,F20.5/)
 2005 FORMAT(52H1AVERAGE STRESS RESULTANTS AT NODES FOR LOADING CASE ,
     9 I3/ )
 2006 FORMAT(5H NODE,I4,41X,7H(R,Z) =,F9.4,1H,,F9.4/
     1' 7H    TOP,5F20.8/
     2 7H   CORE,5F20.8/
     3 7H BOTTOM,5F20.8/
     4 7H  TOTAL,5F20.8,F20.5/ )
 2007 FORMAT(
     17H  LAYER,16X,4HN(S),12X,8HN(THETA),16X,4HQ(S),16X,4HM(S),12X,
     2 8HM(THETA),7X,13HQ(S,C)/Q(S,F))
 2008 FORMAT(5X,117HNOTE..  AT NODES WHERE CONCENTRATED TRANSVERSE LOADS
     1 OCCUR, ELEMENT SHEAR-STRESS RESULTANTS ARE MORE ACCURATE THAN   /
     2 13X,36HAVERAGE SHEAR-STRESS RESULTANTS            /)
      END




      SUBROUTINE RESULTS(J)
C     THIS SUBROUTINE EVALUATES THE NODAL STRESS RESULTANTS FOR ELE-
C     MENT J
C     SHEAR STRAIN AND CURVATURE MODELS VARY LINEARLY ALONG CHORD LENGTH
```

```
      REAL NUF,NUC
      COMMON /PROPS/ H,D,HF,HC,EF,NUF,GF,EC,NUC,GC,BF,DF,BC,DC
      COMMON /ARRAY/ S(400,8),ST(99,10,2),IBC(50),RL(400),RC(200),U(990)
      COMMON /STMATS/ SEL(10,10),B(12,10),DB(12,10),T(10,10)
      DIMENSION SRI(21),SRJ(21)
      EQUIVALENCE (SRI(1),SEL(1)), (SRJ(1),SEL(31))
      IJ = 10*J - 10
      READ (2) ((B(K,L),L=1,10),K=1,12)
      READ(2) ((DB(K,L),L=1,10),K=1,12)
C     COMPUTE NODAL STRESS RESULTANTS IN THE LAYERS
      DO 100 L = 1,12
      SRI(L) = SRJ(L) = 0.0
      DO 100 K = 1,10
      IK = IJ + K
      SRI(L) = SRI(L) + B(L,K)*U(IK)
  100 SRJ(L) = SRJ(L) + DB(L,K)*U(IK)
      DO 150 L = 13,15
      SRI(L) = SRI(L-5)
  150 SRJ(L) = SRJ(L-5)
C     COMPUTE THE TOTAL NODAL STRESS RESULTANTS
      DO 200 L = 16,20
      SRI(L) = SRJ(L) = 0.0
      DO 200 K = 1,11,5
      IK = K + L - 16
      SRI(L) = SRI(L) + SRI(IK)
  200 SRJ(L) = SRJ(L) + SRJ(IK)
      SRI(19) = SRI(19) + 0.5*D*(SRI(11) - SRI(6))
      SRI(20) = SRI(20) + 0.5*D*(SRI(12) - SRI(7))
      SRJ(19) = SRJ(19) + 0.5*D*(SRJ(11) - SRJ(6))
      SRJ(20) = SRJ(20) + 0.5*D*(SRJ(12) - SRJ(7))
      RETURN
      END




      SUBROUTINE BANSOL(KKK, B, A, ND, MD, NN, MM)
C      SYMMETRIC BAND MATRIX EQUATION SOLVER
C      -----
C      KKK = 1 TRIANGULARIZES A
C      KKK = 2 SOLVES FOR VECTOR B, SOLUTION VECTOR RETURNS IN B
C
C     PROGRAMMED BY C. A. FELIPPA.
C
      DIMENSION B(1), A(ND,MD)
      NRS = NN - 1
      NR = NN
      IF (KKK-1) 100,100,200
  100 DO 120  N = 1,NRS
      M = N - 1
      MR = MIN0(MM,NR-M)
      PIVOT = A(N,1)
      DO 120  L = 2,MR
```

```
      C = A(N,L)/PIVOT
      I = M + L
      J = 0
      DO 110  K = L,MR
      J = J + 1
  110 A(I,J) = A(I,J) - C*A(N,K)
  120 A(N,L) = C
      GO TO 400
  200 DO 220  N = 1,NRS
      M = N - 1
      MR = MIN0(MM,NR-M)
      C = B(N)
      B(N) = C/A(N,1)
      DO 220  L = 2,MR
      I = M + L
  220 B(I) = B(I) - A(N,L)*C
      B(NR) = B(NR)/A(NR,1)
      DO 320  I = 1,NRS
      N = NR - I
      M = N - 1
      MR = MIN0(MM,NR-M)
      DO 320  K = 2,MR
      L = M + K
  320 B(N) = B(N) - A(N,K)*B(L)
  400 RETURN
      END
```

APPENDIX E.. COMPUTER PROGRAM FOR FREE VIBRATION ANALYSIS OF ELASTIC AXISYMMETRIC SANDWICH SHELLS (FORTRAN IV)

```
      PROGRAM AXSSFVQ(INPUT,OUTPUT,TAPE1=INPUT,TAPE2=OUTPUT)
C
C     FREE AXISYMMETRIC VIBRATION ANALYSIS OF THIN ROTATIONAL SANDWICH
C     SHELL WITH CONSTANT THICKNESS AND TWICE CONTINUOUS MERIDIAN.
C     MATERIAL PROPERTIES MAY NOT VARY IN THE MERIDIONAL DIRECTION FOR
C     THE PRESENT PROGRAM. ALTHOUGH MODIFICATION FOR THIS CAPABILITY
C     MAY BE READILY ACHIEVED.  NO RESTRICTION ON RATIOS OF LAYER THICK-
C     NESSES OR LAYER PROPERTIES.  NODES ARE NUMBERED CONSECUTIVELY
C     ALONG THE MERIDIAN AND IF A NODE IS LOCATED ON THE AXIS OF SYM-
C     METRY NUMBERING MUST BEGIN AT THIS NODE.  ELEMENTS ARE NUMBERED
C     SUCH THAT THE ELEMENT NUMBER IS THE SAME AS THE SMALLER ADJACENT
C     NODE NUMBER.
C     STORAGE FOR  35 NODES (AND THUS FOR 34 ELEMENTS).
C     SHEAR STRAIN AND CURVATURE MODELS VARY QUADRATICALLY AND LINEARLY
C     ALONG THE CHORD LENGTH, RESPECTIVELY.
C
C*********************************************************************
C     DATA CARDS FOR AXSSFVQ
C*********************************************************************
C
C     1 CARD.. I10  NUMBER OF SHELLS TO BE ANALYZED
C     THEN, FOR EACH SHELL, ALL OF THE FOLLOWING..
C
C     1 CARD..  COLS. 2-72  TITLE
C
C     1 CARD.. 3I10,L10
C                 NUMBER OF NODES, NN
C                 NUMBER OF MODE SHAPES, NMS
C                 NUMBER OF NODES WITH RESTRAINTS, NBC
C                 ROTATORY INERTIA INDEX (T IF LUMPED ROTATORY INERTIA
C                      INCLUDED, F OTHERWISE)
C
C     1 CARD..  6F10.0
C                 THICKNESS OF 1 FACING (IN.)
C                 YOUNGS MODULUS OF FACINGS (PSI)
C                 POISSON RATIO OF FACINGS
C                 SHEAR MODULUS OF FACINGS (PSI)
C                 SHEAR STRESS CORRECTION FACTOR FOR FACING
C                 DENSITY OF FACINGS (LB./IN.**3)
C     1 CARD..  6F10.0
C                 THICKNESS OF CORE (IN.)
C                 YOUNGS MODULUS OF CORE (PSI)
C                 POISSON RATIO OF CORE
C                 SHEAR MODULUS OF CORE (PSI)
C                 SHEAR STRESS CORRECTION FACTOR FOR CORE
C                 DENSITY OF CORE (LB./IN.**3)
C     (NOTE..  SHEARING MAY BE NEGLECTED BY SETTING G TO 9999999999)
C
C     NN CARDS.. I10,3F10.0
C                 NODE NUMBER
```

```
C                   R, ABSCISSA OF NODE (IN.)
C                   Z, ORDINATE OF NODE (IN.)
C                   PHI, LATITUDE ANGLE OF NODE (DEGREES)
C
C     NN-1 CARDS.. 2F10.0
C                   CURVATURE AT NODE I OF ELEMENT (1/IN.)
C                   CURVATURE AT NODE J OF ELEMENT (1/IN.)
C
C     NBC CARDS.. 5I10
C                   NODE NUMBER
C                   TANGENTIAL DISPLACEMENT INDEX (0=FREE, 1=CONSTRAINED)
C                   RADIAL DISPLACEMENT INDEX ( DITTO )
C                   BENDING ROTATION INDEX ( DITTO )
C                   SHEAR WARPING INDEX ( DITTO )
C
      LOGICAL LRI
      COMMON /  / NN,NE,NMS,NDOF,NBC,NLM,LRI,PI
      PI = 3.14159265358979
      READ 1000, NSHELLS
      DO 100 N = 1,NSHELLS
      CALL SETUP
      CALL BCS
      CALL EIGEN
      IF(NMS.NE.0) CALL SHAPES
  100 CONTINUE
 1000 FORMAT(I10)
      STOP
      END




      SUBROUTINE SETUP
C     THIS SUBROUTINE READS THE GEOMETRICAL AND MATERIAL PROPERTIES OF
C     THE SHELL AND SETS UP THE OVERALL STIFFNESS MATRIX AND THE DIAGON-
C     AL MASS MATRIX, BOTH UNMODIFIED FOR BOUNDARY CONDITIONS.
C     SHEAR STRAIN AND CURVATURE MODELS VARY QUADRATICALLY AND LINEARLY
C     ALONG CHORD LENGTH, RESPECTIVELY.
      REAL NUF,NUC,KF,KC
      LOGICAL LRI
      COMMON /  / NN,NE,NMS,NDOF,NBC,NLM,LRI,PI
      COMMON /ARRAY/ S(140,8),ST(34,12,4),XM(140),A(105,105),E(105),
     1 V(105,105),IV(105),DUM(140)
      COMMON /PROPS/ H,D,HF,HC,EF,NUF,GF,EC,NUC,GC,BF,DF,BC,DC
      COMMON /XGEOM/ YP,YPP,RX,COSB,YBAR,X(10)
      COMMON /ELGEOM/ EL,SPSI,CPSI,TBI,TBJ,CBI,CBJ,SBI,SBJ,A1,A2,A3,A4
      COMMON /NODGEO/ R(35),Z(35)
      COMMON /STMATS/ SEL(12,12),B(12,12),DB(12,12),T(12,12)
      DIMENSION CPHI(35),SPHI(35),W(10),Y(10),WM(10),AN(35),PHI(35)
      EQUIVALENCE (CPHI(1),A(1)), (SPHI(1),A(101)), (PHI(1),A(201)),
     1 (AN(1),A(301))
      DATA  X  /       0.013046735741414, 0.067468316655507,
     1 0.160295215850488, 0.283302302935376, 0.425562830509184,
```

```
     2 0.574437169490816, 0.716697697064624, 0.839704784149512,
     3 0.932531683344493, 0.986953264258586   /
      DATA  W  /  0.066671344308688, 0.149451349150581,
     1 0.219086362515982, 0.269266719309996,   0.295524224714753,
     2 0.295524224714753, 0.269266719309996, 0.219086362515982,
     3  0.149451349150581, 0.066671344308688  /
      DATA  Y  /  0.023455038515334, 0.115382672473579,
     1 0.25, 0.384617327526421, 0.476544961484666, 0.523455038515334,
     2 0.615382672473579, 0.75, 0.884617327526421, 0.976544961484666  /
      DATA  WM  / 0.236926885056189, 0.478628670499366,
     1 0.568888888888889, 0.478628670499366, 0.236926885056189,
     2 0.236926885056189, 0.478628670499366, 0.568888888888889,
     3 0.478628670499366, 0.236926885056189  /
      WRITE (2,2000)
      READ (1,1000)
      WRITE (2,1000)
      READ (1,1001) NN,NMS,NBC,LRI
      READ (1,1002) HF,EF,NUF,GF,KF,RHOF
      READ (1,1002) HC,EC,NUC,GC,KC,RHOC
      WRITE (2,2001) NN,NMS,NBC, HF,HC, EF,NUF,GF,KF,RHOF, EC,NUC,GC,KC,
     1 RHOC, LRI
      IF(NN.GT. 35) GO TO 900
      IF(GF.GE.9999999998.0) GF = 1.0E+20
      IF(GC.GE.9999999998.0) GC = 1.0E+20
      H = HC + 2.0*HF
      D = HC + HF
      NE = NN - 1
      NDOF = 4*NN
      NLM = 2*NN
      IF(LRI) NLM = 3*NN
      EF = EF/(1.0 - NUF*NUF)
      EC = EC/(1.0 - NUC*NUC)
      BF = EF*HF
      BC = EC*HC
      GF = GF*HF*KF
      GC = GC*HC*KC
      DF = BF*HF*HF/12.0
      DC = BC*HC*HC/12.0
      RHO = (HC*RHOC + 2.0*HF*RHOF)/386.088
      AMOM = (RHOC*HC**3 + RHOF*(H**3 - HC**3))/(12.0*386.088)
      DO 100 I = 1,NDOF
      X1(I) = 0.0
      DO 100 J = 1,8
  100 S(I,J) = 0.0
      JK = 0
      WRITE (2,2002)
      DR = 180.0/PI
      DO 110 I = 1,NN
      AN(I) = 0.0
      READ (1,1003) I,R(I),Z(I),PHI(I)
      WRITE (2,2003) I,R(I),Z(I),PHI(I)
      PHI(I) = PHI(I)/DR
      SPHI(I) = SIN(PHI(I))
  110 CPHI(I) = COS(PHI(I))
      WRITE (2,2004)
```

```
      DO 500 I = 1,NE
      DR = R(I+1) - R(I)
      DZ = Z(I+1) - Z(I)
      EL = SQRT(DR*DR + DZ*DZ)
      SPSI = DR/EL
      CPSI = DZ/EL
      SBI = CPHI(I)*CPSI - SPHI(I)*SPSI
      CBI = SPHI(I)*CPSI + CPHI(I)*SPSI
      TBI = SBI/CBI
      SBJ = CPHI(I+1)*CPSI - SPHI(I+1)*SPSI
      CBJ = SPHI(I+1)*CPSI + CPHI(I+1)*SPSI
      TBJ = SBJ/CBJ
      READ (1,1004) CURVI,CURVJ
      WRITE (2,2005) I,CURVI,CURVJ,EL,SPSI,CPSI,TBI,TBJ
      YPPI = -EL*CURVI/CBI**3
      YPPJ = -EL*CURVJ/CBJ**3
      A1 = TBI
      A2 = TBI + 0.5*YPPI
      A3 = -(5.0*TBI + 4.0*TBJ) + 0.5*YPPJ - YPPI
      A4 = 3.0*(TBI + TBJ) + 0.5*(YPPI - YPPJ)
      DO 150 J = 1,12
      DO 150 K = 1,12
  150 SEL(J,K) = 0.0
C     COMPUTE ELEMENT TRANSFORMATION MATRIX (A**-1)*T
      CALL TMAT(I)
      DO 400 J = 1,10
      YBAR = (1.0 - X(J))*(A1 + X(J)*(A2 + X(J)*(A3 + X(J)*A4)))
      YP = A1*(1.0 - 2.0*X(J))+ X(J)*(A2*(2.0 - 3.0*X(J)) + X(J)*(A3*
     1 (3.0 - 4.0*X(J)) + A4*X(J)*(4.0 - 5.0*X(J))))
      YPP = 2.0*(-A1 + A2*(1.0 - 3.0*X(J)))+ X(J)*(A3*(6.0 - 12.0*X(J))
     1 + A4*X(J)*(12.0 - 20.0*X(J)))
      RX = R(I) + X(J)*EL*(SPSI + YBAR*CPSI)
      COSB = 1.0/(SQRT(1.0 + YP*YP))
C     EVALUATE B(,) AT INTEGRATION POINTS
      CALL BMAT(I,J)
C     ADD CONTRIBUTION TO ELEMENT STIFFNESS INTEGRATION
      C = PI*EL*RX*W(J)  /COSB
      CALL SELA(C)
      YBAR = (1.0 - Y(J))*(A1 + Y(J)*(A2 + Y(J)*(A3 + Y(J)*A4)))
      YP = A1*(1.0 - 2.0*Y(J))+ Y(J)*(A2*(2.0 - 3.0*Y(J)) + Y(J)*(A3*
     1 (3.0 - 4.0*Y(J)) + A4*Y(J)*(4.0 - 5.0*Y(J))))
      RX = R(I) + Y(J)*EL*(SPSI + YBAR*CPSI)
      COSB = 1.0/(SQRT(1.0 + YP*YP))
      C = PI*EL*RX*WM(J)/COSB/2.0
      IF(J.GT.5) GO TO 200
      AN(I) = AN(I) + C
      GO TO 400
  200 AN(I+1) =AN(I+1) + C
  400 CONTINUE
C     TRANSFORM 12X12 ELEMENT STIFFNESS TO GLOBAL CO-ORDINATES AND CON-
C     DENSE TO 8X8
      CALL SELR(I)
C     STORE MULTIPLIERS AND PIVOTS
      DO 420 J = 1,4
      IJ = J + 8
```

```
      DO 420 K = 1,12
  420 ST(I,K,J) = SEL(IJ,K)
C     ADD 8X8 ELEMENT STIFFNESS TO OVERALL STIFFNESS
      DO 450 J = 1,8
      IJ = JK + J
      DO 450 K = J,8
      IK = K - J + 1
  450 S(IJ,IK) = S(IJ,IK) + SEL(J,K)
  500 JK = JK + 4
C     CONSTRUCT DIAGONAL MASS MATRIX
      DO 600 I = 1,NN
      IJ = 4*I - 3
      XM(IJ) = XM(IJ+1) = SQRT(RHO*AN(I))
      IF(.NOT.LRI) GO TO 600
      XM(IJ+2) = SQRT(AMOM*AN(I))
  600 CONTINUE
      RETURN
  900 WRITE (2,2900)
      STOP
 1000 FORMAT(72H
     1
 1001 FORMAT(3I10,L10)
 1002 FORMAT(6F10.0)
 1003 FORMAT(I10,3F10.0)
 1004 FORMAT(2F10.0)
 2000 FORMAT(1H1)
 2001 FORMAT(10X,28HNUMBER OF NODES                    ,I3/
     1 10X,28HNUMBER OF MODE SHAPES                    ,I3/
     2 10X,28HNUMBER OF RESTRAINED NODES               ,I3//
     3 10X,16HFACE THICKNESS =,F10.6/
     4 10X,16HCORE THICKNESS =,F10.6//
     5 10X,8HFACE E =,F13.1/
     6 10X,9HFACE NU =,F12.5/
     7 10X,8HFACE G =,F13.1/
     6 10X,10HFACE KAP =,F11.5/
     7 10X,10HFACE RHO =,F11.6//
     8 10X,8HCORE E =,F13.1/
     9 10X,9HCORE NU =,F12.5/
     1 10X,8HCORE G =,F13.1/
     2 10X,10HCORE KAP =,F11.5/
     3 10X,10HCORE RHO =,F11.6//
     4 44H ROTATORY INERTIA INCLUDED (T = YES, F = NO) ,L5 //
     5 45H ALL QUANTITIES IN INCHES, POUNDS AND SECONDS  /)
 2002 FORMAT(//11HONODAL DATA /
     9        2X,4HNODE,7X,11HABSCISSA, R,8X,12H ORDINATE, Z,6X,
     1 14HLATITUDE ANGLE/
     2 15X,5H(IN.),15X,5H(IN.),13X,8H(DEGREE)/)
 2003 FORMAT(I4,3F20.8)
 2004 FORMAT(/18HOELEMENT GEOMETRY /
     1 8H ELEMENT,10X,7HCURV(I),10X,7HCURV(J),5X,12HCHORD LENGTH,10X,
     2 7HSIN PSI,10X,7HCOS PSI,6X,11HTAN BETA(I),6X,11HTAN BETA(J)/
     3 18X,7H(1/IN.),10X,7H(1/IN.),12X,5H(IN.))
 2005 FORMAT(I8,7F17.8)
 2900 FORMAT(/////41HONUMBER OF NODES EXCEEDS ALLOWABLE   STOP     )
      END
```

```
      SUBROUTINE TMAT(I)
C     THIS SUBROUTINE EVALUATES THE CO-ORDINATE TRANSFORMATION MATRIX
C     (A**-1)*T FOR ELEMENT I.
C     GLOBAL CO-ORDINATES ARE  S  AND  XI  (MERIDIONAL AND RADIAL), AND
C     THUS CAN BE APPLIED ONLY TO SHELLS WITH TWICE CONTINUOUS MERIDIANS
C     SHEAR STRAIN AND CURVATURE MODELS VARY QUADRATICALLY AND LINEARLY
C     ALONG CHORD LENGTH, RESPECTIVELY.
      REAL NUC,NUF
      COMMON /PROPS/ H,D,HF,HC,EF,NUF,GF,EC,NUC,GC,BF,DF,BC,DC
      COMMON /STMATS/ SEL(12,12),B(12,12),DB(12,12),T(12,12)
      COMMON /NODGEO/ R(35),Z(35)
      COMMON /ELGEOM/ EL,SPSI,CPSI,TBI,TBJ,CBI,CBJ,SBI,SBJ,A1,A2,A3,A4
      DO 100 J = 1,12
      DO 100 K = 1,12
  100 B(J,K) = 0.0
      IF(R(I).EQ.0.0) GO TO 500
C     MATRIX FOR OPEN-ENDED ELEMENT
      B(1,1) = B(3,2) = B(2,6) = 1.0
      B(7,4) = B(7,5) = B(9,5) = 1.0
      B(8,9) = B(8,10) = B(10,10) = B(2,1) = -1.0
      B(4,1) = -TBI
      B(4,6) = TBI
      B(6,6) = TBI + TBJ
      B(6,1) = - B(6,6)
      B(5,1) = B(6,6) + TBI
      B(5,6) = -B(5,1)
      B(5,2) = B(8,4) = B(8,5) = B(10,5) = -3.0
      B(6,2) = B(11,4) = B(11,5) = B(12,5) = 2.0
      B(11,9) = B(11,10) = B(12,10) = 2.0
      B(5,7) = 3.0
      B(6,7) = -2.0
      B(8,11) = B(10,12) = 4.0
      B(11,11) = B(12,12) = -4.0
      B(4,3) = B(6,3) = -EL/CBI/CBI
      B(5,3) = -2.0*B(4,3)
      B(4,4) = B(6,4) = HC*B(4,3)/D
      B(5,4) = -2.0*B(4,4)
      B(4,5) = B(6,5) = B(4,3)
      B(5,5) = -2.0*B(4,5)
      B(5,8) = EL/CBJ/CBJ
      B(6,8) = -B(5,8)
      B(5,9) = HC*B(5,8)/D
      B(6,9) = -B(5,9)
      B(5,10) = B(5,8)
      B(6,10) = -B(5,10)
      DO 200 J = 1,12
      T(J,1) = CBI*B(J,1) + SBI*B(J,2)
      T(J,2) = SBI*B(J,1) - CBI*B(J,2)
      T(J,3) = B(J,3)
      T(J,4) = B(J,4)
      T(J,5) = CBJ*B(J,6) + SBJ*B(J,7)
      T(J,6) = SBJ*B(J,6) - CBJ*B(J,7)
      T(J,7) = B(J,8)
      T(J,8) = B(J,9)
      T(J,9) = B(J,5)
```

```
      T(J,10) = B(J,10)
      T(J,11) = B(J,11)
  200 T(J,12) = B(J,12)
      GO TO 1000
C     MATRIX FOR CAP
  500 B(5,2) = -1.0
      B(9,9) = B(9,10) = B(10,10) = -1.0
      B(6,6) = 1.0
      B(7,7) = 3.0
      B(11,9) = B(11,10) = B(12,10) = 2.0
      B(8,7) = -2.0
      B(9,11) = B(10,12) = 4.0
      B(11,11) = B(12,12) = -4.0
      B(6,2) = -CPSI
      B(7,2) = (2.0*TBI + TBJ)*CPSI + 3.0*SPSI
      B(8,2) = -B(7,2) + TBI*CPSI + SPSI
      B(7,6) = -2.0*TBI - TBJ
      B(8,6) = TBI + TBJ
      B(7,8) = EL/CBJ/CBJ
      B(8,8) = -B(7,8)
      B(7,9) = HC*B(7,8)/D
      B(8,9) = -B(7,9)
      B(7,10) = B(7,8)
      B(8,10) =-B(7,10)
      DO 700 J = 1,12
      T(J,1) = T(J,3) = T(J,4) = T(J,9) = 0.0
      T(J,2) = B(J,2)
      T(J,5) = CBJ*B(J,6) + SBJ*B(J,7)
      T(J,6) = SBJ*B(J,6) - CBJ*B(J,7)
      T(J,7) = B(J,8)
      T(J,8) = B(J,9)
      T(J,10) = B(J,10)
      T(J,11) = B(J,11)
  700 T(J,12) = B(J,12)
 1000 RETURN
      END
```

```
      SUBROUTINE BMAT(I,J)
C     THIS SUBROUTINE EVALUATES THE MATRIX B FOR ELEMENT I AT POINT X(J)
C     SHEAR STRAIN AND CURVATURE MODELS VARY QUADRATICALLY AND LINEARLY
C     ALONG CHORD LENGTH, RESPECTIVELY.
      REAL NUF,NUC
      COMMON /PROPS/ H,D,HF,HC,EF,NUF,GF,EC,NUC,GC,BF,DF,BC,DC
      COMMON /STMATS/ SEL(12,12),B(12,12),DB(12,12),T(12,12)
      COMMON /ELGEOM/ EL,SPSI,CPSI,TBI,TBJ,CBI,CBJ,SBI,SBJ,A1,A2,A3,A4
      COMMON /NODGEO/ R(35),Z(35)
      COMMON /XGEOM/ YP,YPP,RX,COSB,YBAR,X(10)
      DO 100 K = 1,12
      DO 100 L = 1,12
  100 B(K,L) = 0.0
```

```
      B1 = -YPP*COSB**5*(1.0 - YP*YP)/(EL*EL)
      B3 = COSB**3/(EL*EL)
      B2 = -2.0*YPP*YP*B3*COSB*COSB
      IF(R(I).EQ.0.0) GO TO 400
      B4 = -EL*B3*YP*(SPSI + CPSI*YP)/RX
      B5 = EL*B3*(SPSI + CPSI*YP)/RX
      B6 = COSB*(SPSI + CPSI*YP)/RX
C     MATRIX FOR OPEN-ENDED ELEMENT
      B(2,1) = B(7,1) = B(12,1) = SPSI/RX
      B(2,3) = B(7,3) = B(12,3) = CPSI/RX
      B(2,2) =                    B(12,1)*X(J)
      B 2,4) =                    B(12,3)*X(J)
      B(2,5) = B(2,4)*X(J)
      B(2,6) = B(2,5)*X(J)
      B(4,8) = B(9,10)  =            COSB/EL
      B(4,11) = B(9,12) = 2.0*X(J)*B(4,8)
      B(1,2) =                    COSB*B(9,10)
      B(1,4) = B(1,2)*YP
      B(1,5) = 2.0*X(J)*B(1,4)
      B(1,6) = 1.5*X(J)*B(1,5)
      B(3,7) = B(8,9) = 1.0
      B(3,8) = B(8,10) = X(J)
      B(3,11) = B(8,12) = X(J)*X(J)
      B(4,2) = B(9,2) = B1
      B(4,4) = B(9,4) = B2
      B(5,2) = B(10,2) = B4
      B(5,4) = B(10,4) = B5
      B(5,7) = B(10,9) = B6
      B(5,8) = B(10,10) =            B6*X(J)
      B(5,11) = B(10,12) = X(J)*B(5,8)
      B(4,5) = B(9,5) =           2.0*B2*X(J)  + 2.0*B3
      B(4,6) = B(9,6) =           (3.0*B2*X(J) + 6.0*B3)*X(J)
      B(5,5) = B(10,5) =           2.0*B5*X(J)
      B(5,6) = B(10,6) =           3.0*B5*X(J)*X(J)
      B(6,2) = B(1,2) - D*B1/2.0
      B(11,2) =  B(1,2) + D*B1/2.0
      B(6,4) = B(1,4) - D*B2/2.0
      B(11,4) =  B(1,4) + D*B2/2.0
      B(6,5) = B(1,5) - D*B(4,5)/2.0
      B(11,5) = B(6,5) + D*B(4,5)
      B(6,6) = B(1,6) - D*B(4,6)/2.0
      B(11,6) = B(6,6) + D*B(4,6)
      B(6,8) = -HC*B(4,8)/2.0
      B(11,8) = -B(6,8)
      B(6,10) = -HF*B(4,8)/2.0
      B(11,10) = -B(6,10)
      B(6,11) = 2.0*X(J)*B(6,8)
      B(11,11) = -B(6,11)
      B(6,12) = 2.0*X(J)*B(6,10)
      B(11,12) = -B(6,12)
      B(7,2) = B(2,2) - D*B4/2.0
      B(12,2) =  B(7,2) + D*B4
      B(7,4) = B(2,4) - D*B5/2.0
      B(12,4) =  B(7,4) + D*B5
      B(7,5) = B(2,5) - D*B(5,5)/2.0
```

```
      B(12,5) = B(7,5) + D*B(5,5)
      B(7,6) = B(2,6) - D*B(5,6)/2.0
      B(12,6) = B(7,6) + D*B(5,6)
      B(7,7) = -HC*B6/2.0
      B(12,7) = -B(7,7)
      B(7,8) = B(7,7)*X(J)
      B(12,8) = -B(7,8)
      B(7,9) = -HF*B6/2.0
      B(12,9) = -B(7,9)
      B(7,10) = B(7,9)*X(J)
      B(12,10) = -B(7,10)
      B(7,11) = X(J)*B(7,8)
      B(12,11) = -B(7,11)
      B(7,12) = X(J)*B(7,10)
      B(12,12) = -B(7,12)
      GO TO 1000
C     MATRIX FOR CAP ELEMENT
  400 B6 = EL*(SPSI + YBAR*CPSI)
      B5 = COSB**3*(SPSI + YP*CPSI)/(B6*EL)
      B4 = COSB*(SPSI + CPSI*YP)/B6
      B(3,9) = B(8,10) = X(J)
      B(3,11) = B(8,12) = X(J)*X(J)
      B(4,9) = B(9,10) = COSB/EL
      B(4,11) = B(9,12) = 2.0*X(J)*B(4,9)
      B(4,6) = B(9,6) =            B1 + TBI*B2
      B(4,7) = B(9,7) =            2.0*B2*X(J) + 2.0*B3
      B(4,8) = B(9,8) =            (3.0*B2*X(J) + 6.0*B3)*X(J)
      B(5,6) = B(10,6) =B5*(((5.0*A4*X(J) + 4.0*(A3 - A4))*X(J) +
     1 3.0*(A2 - A3))*X(J) + 2.0*(A1 - A2))
      B(5,7) = B(10,7) =            2.0*B5
      B(5,8) = B(10,8) =            3.0*B5*X(J)
      B(5,9) = B(10,10) = B4
      B(5,11) = B(10,12) = X(J)*B4
      B(1,6) = COSB*B(4,9)*(1.0+ TBI*YP)
      B(1,7) = 2.0*X(J)*COSB*B(4,9)*YP
      B(1,8) = 1.5*X(J)*B(1,7)
      B(2,6) = (SPSI + CPSI*TBI)/B6
      B(2,7) = X(J)*CPSI/B6
      B(2,8) = X(J)*B(2,7)
      B(6,6) = B(1,6) - D*B(4,6)/2.0
      B(11,6) = B(6,6) + D*B(4,6)
      B(6,7) = B(1,7  - D*B(4,7)/2.0
      B(11,7) = B(6,7) + D*B(4,7)
      B(6,8) = B(1,8) - D*B(4,8)/2.0
      B(11,8) = B(6,8) + D*B(4,8)
      B(6,9) = -HC*B(4,9)/2.0
      B(11,9) = -B(6,9)
      B(6,10) = -HF*B(4,9)/2.0
      B(11,10) = -B(6,10)
      B(6,11) = 2.0*X(J)*B(6,9)
      B(11,11) = -B(6,11)
      B(6,12) = 2.0*X(J)*B(6,10)
      B(11,12) = -B(6,12)
      B(7,6) = B(2,6) - D*B(5,6)/2.0
      B(12,6) = B(7,6) + D*B(5,6)
```

```
      B(7,7) = B(2,7) - D*B5
      B(12,7) = B(2,7) + D*B5
      B(7,8) = B(2,8) - D*B(5,8)/2.0
      B(12,8) = B(7,8) + D*B(5,8)
      B(7,9) = -HC*B4/2.0
      B(12,9) = -B(7,9)
      B(7,10) = -HF*B4/2.0
      B(12,10) = -B(7,10)
      B(7,11) = X(J)*B(7,9)
      B(12,11) = -B(7,11)
      B(7,12) = X(J)*B(7,10)
      B(12,12) = -B(7,12)
 1000 RETURN
      END
```

```
      SUBROUTINE SELA(C)
C     THIS SUBROUTINE COMPUTES A TERM IN THE GAUSS INTEGRATION FOR THE
C     STIFFNESS MATRIX IN GENERALIZED CO-ORDINATES
C     SHEAR STRAIN AND CURVATURE MODELS VARY QUADRATICALLY AND LINEARLY
C     ALONG CHORD LENGTH, RESPECTIVELY.
      REAL NUF,NUC
      COMMON /PROPS/ H,D,HF,HC,EF,NUF,GF,EC,NUC,GC,BF,DF,BC,DC
      COMMON /STMATS/ SEL(12,12),B(12,12),DB(12,12),T(12,12)
      DO 100 K = 1,12
      DB(1,K) = BC*(B(1,K) + NUC*B(2,K))*C
      DB(2,K) = BC*(B(2,K) + NUC*B(1,K))*C
      DB(3,K) = GC*B(3,K)*C
      DB(4,K) = DC*(B(4,K) + NUC*B(5,K))*C
      DB(5,K) = DC*(B(5,K) + NUC*B(4,K))*C
      DB(6,K) = BF*(B(6,K) + NUF*B(7,K))*C
      DB(7,K) = BF*(B(7,K) + NUF*B(6,K))*C
      DB(8,K) = GF*B(8,K)*C*2.0
      DB(9,K) = DF*(B(9,K)+ NUF*B(10,K))*C*2.0
      DB(10,K) = DF*(B(10,K) + NUF*B(9,K))*C*2.0
      DB(11,K) = BF*(B(11,K) + NUF*B(12,K))*C
  100 DB(12,K) = BF*(B(12,K) + NUF*B(11,K))*C
      DO 200 K = 1,12
      DO 200 L = 1,12
      DO 200 M = 1,12
  200 SEL(K,L) = SEL(K,L) + B(M,K)*DB(M,L)
      RETURN
      END
```

```
      SUBROUTINE SELR(L)
C     THIS SUBROUTINE TRANSFORMS THE ELEMENT STIFFNESS FROM GENERALIZED
C     TO GLOBAL CO-ORDINATES AND CONDENSES IT FROM 12X12 TO 8X8 USING
C     STATIC CONDENSATION.
C     SHEAR STRAIN AND CURVATURE MODELS VARY QUADRATICALLY AND LINEARLY
C     ALONG CHORD LENGTH, RESPECTIVELY.
      COMMON /NODGEO/ R(35),Z(35)
      COMMON /STMATS/ SEL(12,12),B(12,12),DB(12,12),T(12,12)
C     SYMMETRIZE ELEMENT STIFFNESS IN GENERALIZED CO-ORDINATES
      DO 50 I = 1,11
      IJ = I + 1
      DO 50 J = IJ,12
      IF(SEL(I,J).EQ.0.0.OR.SEL(J,I).EQ.0.0) GO TO 45
      SEL(I,J) = 0.5*(SEL(I,J) + SEL(J,I))
      GO TO 50
   45 SEL(I,J) = 0.0
   50 SEL(J,I) = SEL(I,J)
C      TRANSFORM TO GLOBAL CO-ORDINATES
      DO 100 I = 1,12
      DO 100 J = 1,12
      DB(I,J) = 0.0
      DO 100 K = 1,12
  100 DB(I,J) = DB(I,J) + SEL(I,K)*T(K,J)
      DO 200 I = 1,12
      DO 200 J = 1,12
      SEL(I,J) = 0.0
      DO 200 K = 1,12
  200 SEL(I,J) = SEL(I,J) + T(K,I)*DB(K,J)
      IF(R(L).NE.0.0) GO TO 250
      SEL(1,1) = SEL(3,3) = SEL(4,4) = SEL(9,9) = 1.0
C     CONDENSE TO 8X8 ELEMENT STIFFNESS
  250 DO 300 J = 1,4
      IJ = 12 - J
      IK = IJ + 1
      PIVOT = SEL(IK,IK)
      DO 300 K = 1,IJ
      C = SEL(IK,K)/PIVOT
      SEL(IK,K) = C
      DO 300 I = K,IJ
      SEL(I,K) = SEL(I,K) - C*SEL(I,IK)
  300 SEL(K,I) = SEL(I,K)
      RETURN
      END
```

```
      SUBROUTINE BCS
C     THIS SUBROUTINE READS THE BOUNDARY CONDITION DATA, MODIFIES THE
C     OVERALL STIFFNESS MATRIX AND MASS MATRIX ACCORDINGLY AND THEN
C     TRIANGULARIZES THE STIFFNESS FOR READY SOLUTION.
C     SHEAR STRAIN AND CURVATURE MODELS VARY QUADRATICALLY AND LINEARLY
C     ALONG CHORD LENGTH, RESPECTIVELY.
```

```
      LOGICAL LRI
      COMMON /   / NN,NE,NMS,NDOF,NBC,NLM,LRI,PI
      COMMON /ARRAY/ S(140,8),ST(34,12,4),XM(140),A(105,105),E(105),
     1 V(105,105),IV(105),W(140)
      COMMON /NODGEO/ R(35),Z(35)
      DIMENSION NR(4)
      IF(R(1).NE.0.0) GO TO 100
      NLM = NLM - 1
      XM(1) = 0.0
      IF(.NOT.LRI) GO TO 100
      NLM = NLM - 1
      XM(3) = 0.0
  100 WRITE (2,2000)
C     READ KINEMATIC CONSTRAINTS AND MODIFY OVERALL STIFFNESS AND MASS
      DO 300 I = 1,NBC
      READ (1,1001)  N,(NR(J),J=1,4)
      WRITE (2,2001) N,(NR(J),J=1,4)
      IJ = 4*N - 4
      DO 300 J = 1,4
      IF(NR(J).EQ.0) GO TO 300
      IK = IJ + J
      S(IK,1) = 1.0
      DO 200 K = 2,8
      S(IK,K) = 0.0
      L = IK - K + 1
      IF(L.LE.0) GO TO 200
      S(L,K) = 0.0
  200 CONTINUE
      IF(J.EQ.4) GO TO 300
      IF(J.EQ.3.AND..NOT.LRI)GO TO 300
      NLM = NLM - 1
      XM(IK) = 0.0
  300 CONTINUE
      IF (NMS.GT.NLM) NMS = NLM
C     TRIANGULARIZE STIFFNESS MATRIX
      CALL DYBSOL(NDOF,8,140,S, W,1,1)
      RETURN
 1001 FORMAT(5I10)
 2000 FORMAT(//59H0KINEMATIC CONSTRAINTS (0 = UNCONSTRAINED, 1 = CONSTRA
     1INED) /
     2 6X,4HNODE,5X,10HMERIDIONAL,9X,6HRADIAL,7X,8HROTATION,
     3 8X,7HWARPING/)
 2001 FORMAT(I10,4I15)
      END




      SUBROUTINE EIGEN
C     THIS SUBROUTINE TRANSFORMS THE EIGENVALUE PROBLEM FROM
C          K(,)*U() = OM**2*M(,)*U()
C     TO
C          A(,)*V() = V()/OM**2
```

```
C      WHERE
C           K(,) = STIFFNESS MATRIX
C           M(,) = DIAGONAL MASS MATRIX
C           A(,) = M(,)**0.5*F(,)*M(,)**0.5
C           F(,) = FLEXIBILITY MATRIX AFTER CONDENSATION ON DEGREES OF
C                  FREEDOM NOT CORRESPONDING TO LUMPED MASSES
C           V() = M(,)**0.5*U()
C      THE EIGENVALUES AND NMS OF THE EIGENVECTORS ARE THEN COMPUTED.
       LOGICAL LRI
       COMMON /  / NN,NE,NMS,NDOF,NBC,NLM,LRI,PI
       COMMON /ARRAY/ S(140,8),ST(34,12,4),XM(140),A(105,105),E(105),
      1 V(105,105),IV(105),W(140)
       COMMON /STMATS/ SEL(12,12),B(12,12),DB(12,12),T(12,12)
       DIMENSION G(105),R(105),P(105),Q(105),INT(105)
       EQUIVALENCE (G(1),SEL(1)), (R(1),SEL(106)), (P(1),B(67)),
      1 (Q(1),DB(28)), (INT(1),DB(133))
C      COMPUTE INDEX VECTOR OF LUMPED MASSES
       N = 1
       DO 100 I = 1,NLM
    50 IF(XM(N).NE.0.0) GO TO 60
       N = N+1
       GO TO 50
    60 IV(I) = N
   100 N = N+1
C      ASSEMBLE MATRIX A(,)
       DO 300 I = 1,NLM
       DO 200 J = 1,NDOF
   200 W(J) = 0.0
       N = IV(I)
       W(N) = 1.0
       CALL DYBSOL(NDOF,8,140,S,W,2,N)
       DO 300 J = I,NLM
       L = IV(J)
       A(J,I) = XM(L)*W(L)*XM(N)
   300 A(I,J) = A(J,I)
C      COMPUTE EIGENVALUES AND EIGENVECTORS
       CALL HQRW(NLM,105,NMS,A,E,V,G,R,P,Q,W,INT)
C      COMPUTE AND PRINT NATURAL FREQUENCIES
       WRITE (2,2000)
       DO 400 I = 1,NLM
       E(I) = 1.0/SQRT(E(I))
       PER = 2.0*PI/E(I)
       FREQ = 1.0/PER
   400 WRITE (2,2001) I,E(I),FREQ,PER
       RETURN
  2000 FORMAT(21H1NATURAL FREQUENCIES  //
      1 10H  MODE NO.,15X,5HOMEGA,10X,10HOMEGA/2*PI,14X,6HPERIOD /
      2 21X,9H(RAD/SEC),11X,9H(CYC/SEC),15X,5H(SEC) /)
  2001 FORMAT(I10,3E20.8)
       END
```

```
      SUBROUTINE SHAPES
C     THIS SUBROUTINE RECOVERS AND PRINTS THE COMPLETE MODE SHAPES.
      LOGICAL LRI
      REAL NUC,NUF
      COMMON /   / NN,NE,NMS,NDOF,NBC,NLM,LRI,PI
      COMMON /ARRAY/ S(140,8),ST(34,12,4),XM(140),A(105,105),E(105),
     1 V(105,105),IV(105),W(140)
      COMMON /NODGEO/ R(35),Z(35)
      COMMON /PROPS/ H,D,HF,HC,EF,NUF,GF,EC,NUC,GC,BF,DF,BC,DC
      DIMENSION U(12)
      EQUIVALENCE (U(1),A(1))
      WRITE (2,2003)
      DO 800 I = 1,NMS
      C = E(I)*E(I)
      DO 100 J = 1,NDOF
  100 W(J) = 0.0
      DO 200 K = 1,NLM
      L = IV(K)
  200 W(L) = C*XM(L)*V(K,I)
      CALL DYBSOL(NDOF,8,140,S,W,2,1)
      WRITE (2,2000) I
      DO 700 J = 1,NE
      IL = 4*J - 4
      DO 300 K = 1,8
      IK = IL + K
  300 U(K) = W(IK)
C     RECOVER CONDENSED DISPLACEMENTS
      DO 400 K = 1,4
      JK = K + 8
      IK = JK - 1
      U(JK) = 0.0
      DO 400 L = 1,IK
  400 U(JK) = U(JK) - ST(J,L,K)*U(L)
C     COMPUTE ADDITIONAL DISPLACEMENTS OF INTEREST AND PRINT
      GAMCI = U(4) + U(9)
      GAMCJ = U(8) + U(10)
      CHISI = (HC*GAMCI + HF*U(9))/D
      CHISJ = (HC*GAMCJ + HF*U(10))/D
      CHII = U(3) + CHISI
      CHIJ = U(7) + CHISJ
      GAMO = U(11) - U(12)
      CHISO = (HC*U(11) + HF*U(12))/D
  700 WRITE (2,2001) J,R(J),Z(J),
     1 U(1),U(2),CHII,U(3),CHISI,U(4),GAMCI,U(9),
     2 CHISO,GAMO,U(11),U(12),
     3 U(5),U(6),CHIJ,U(7),CHISJ,U(8),GAMCJ,U(10)
  800 WRITE (2,2002) R(NN),Z(NN)
      RETURN
 2000 FORMAT(/18H0MODE SHAPE NUMBER ,I3/
     1 5H NODE,2X,13HMERIDIONAL, U,6X,9HRADIAL, W,2X,13HROTATION, CHI,
     2 9X,6HCHI(B),9X,6HCHI(S),3X,12HWARPING, GAM,7X,8HGAMMA(C),7X,
     3 8HGAMMA(F)/)
 2001 FORMAT(8H ELEMENT,I3,39X,7H(R,Z) =, F9.4,1H,,F9.4 /
     1 4X,1HI,8E15.7/
```

```
     2 4X,1HO,60X,4E15.7/
     3 4X,1HJ,8E15.7/)
 2002 FORMAT(50X,7H(R,Z) =,F9.4,1H,,F9.4 )
 2003 FORMAT(16H1VIBRATION MODES  /)
      END




      SUBROUTINE DYBSOL (NN,MM,NDIM,A,B,KKK,LIM)
C     DYBSOL IS AN SPECIAL IN-CORE BAND SOLVER FOR DYNAMIC PROBLEMS
C     INVOLVING CONDENSATION OF ROTATIONAL DEGREES OF FREEDOM.
C     PROGRAMMED BY C. A. FELIPPA.
C
      DIMENSION A(NDIM,1), B(1)
      NR = NN - 1
      IF (KKK.GT.1)  GO TO 300
C
C     DECOMPOSITION OF BAND MATRIX A WITH SEMI-BANDWIDTH MM
C
      DO 200  N = 1,NR
      M = N - 1
      PIVOT = A(N,1)
      IF (PIVOT.EQ.0.)  PIVOT = 1.0E-08
      MR = MIN0 (MM,NN-M)
      DO 200  L = 2,MR
      C = A(N,L)/PIVOT
      IF (C.EQ.0.)  GO TO 200
      I = M + L
      J = 0
      DO 180  K = L,MR
      J = J + 1
  180 A(I,J) = A(I,J) - C*A(N,K)
      A(N,L) = C
  200 CONTINUE
      GO TO 500
C
C     FORWARD REDUCTION OF VECTOR B FROM B(LIM) TO B(N)
C     AND BACKSUBSTITUTION FROM B(N) TO B(LIM)
C
  300 DO 350  N = LIM,NR
      M = N - 1
      MR = MIN0 (MM,NN-M)
      C = B(N)
      B(N) = C/A(N,1)
      DO 350  L = 2,MR
      I = M + L
  350 B(I) = B(I) - A(N,L)*C
      B(NN) = B(NN)/A(NN,1)
      NS = NN - LIM + 1
      DO 400  K = 2,NS
      M = NN - K
      N = M + 1
```

```
      MR = MIN0 (MM,K)
      DO 400  L = 2,MR
      I = M + L
  400 B(N) = B(N) - A(N,L)*B(I)
  500 RETURN
      END
```

```
      SUBROUTINE HQRW (N,NM,M,G,E,V,A,B,P,W,Q,INT)
C
C * * * * * * * * * * * * * * * * * * * * * * * * * * * * * * * * * * * *
C     SUBROUTINE TO COMPUTE EIGENVALUES AND EIGENVECTORS OF A
C     SYMMETRIC REAL MATRIX STORED AS A TWO-DIMENSIONAL ARRAY.
C * * * * * * * * * * * * * * * * * * * * * * * * * * * * * * * * * * * *
C     PROGRAMMED BY C. A. FELIPPA, FEB. 1967
C
C
C  INPUTS
C
C       N     MATRIX ORDER, MUST NOT EXCEED NM.
C
C       NM    DIMENSION OF INPUT MATRIX G IN THE CALLING PROGRAM.
C
C       M     NVEC = IABS(M)  IS THE NUMBER OF EIGENVECTORS DESIRED
C             (0 TO N). ITS SIGN SPECIFIES THE ORDERING OF THE
C             EIGENVALUES   E(1) ..... E(N)  AS FOLLOWS
C               IF M LT 0 OR -0, BY INCREASING ALGEBRAIC VALUE
C               IF M GT 0 OR +0, BY DECREASING ALGEBRAIC VALUE.
C             CALCULATED EIGENVECTORS (IF ANY) WILL CORRESPOND TO
C             E(1), E(2) ... E(NVEC)
C
C       G     INPUT SYMMETRIC SQUARE MATRIX (RETURNS UNALTERED).
C
C
C  OUTPUTS
C
C       E     VECTOR OF EIGENVALUES, ARRANGED AS EXPLAINED ABOVE.
C
C       V     NORMALIZED EIGENVECTORS, STORED AS COLUMNS OF V.
C             IF NVEC=0, V MAY BE A DUMMY VARIABLE.
C
C       A     DIAGONAL OF REDUCED TRIDIAGONAL FORM.
C
C       B     FIRST OFF-DIAGONAL OF REDUCED TRIDIAGONAL FORM.
C
C
C  WORKING SPACE
C
C       P,W,Q,INT     WORKING VECTORS OF LENGTH AT LEAST N,N+1,N AND N
C                     RESPECTIVELY. IF NVEC=0, Q AND INT MAY BE
C                     DUMMY VARIABLES.
```

```
C
C
C      MINIMUM DIMENSIONS IN THE CALLING PROGRAM SHOULD BE
C     G(NM,N), E(N), V(NM,NVEC), A(N), B(N), P(N), W(N+1), Q(N), INT(N)
C      BUT V,Q AND INT CAN BE DUMMIES IF NVEC=0 (NO EIGENVECTORS).
C
C
C * * * * * * * * * * * * * * * * * * * * * * * * * * * * * * * * * * * *
C     THE FOLLOWING PARAMETERS ARE MACHINE-DEPENDENT AND SHOULD
C     BE PRE-SET AS FOLLOWS
C
C      PRECS = 10.**(-NDIG)    WHERE NDIG IS THE NUMBER OF SIGNIFICAN.
C              DECIMAL DIGITS CARRIED OUT BY THE MACHINE IN FLOATING
C              POINT ARITHMETIC.
C      BASE =  THE BASE NUMBER OF THE MACHINE, IN FLOATING POINT.
C      ILIM =  TO BE CHOSEN SO THAT BASE**(ILIM+4) IS OF THE ORDER
C              (BUT DOES NOT EXCEED) THE MACHINE OVERFLOW LIMIT.
C      HOV  =  BASE**(ILIM/2)
C
C     THIS VERSION IS FOR THE CDC 6400 (NDIG=15, BASE=2., ILIM=1000)
C * * * * * * * * * * * * * * * * * * * * * * * * * * * * * * * * * * * *
C
      DIMENSION  G(NM,1), E(1), V(NM,1), A(1), B(1), P(1), W(1), Q(1)
      REAL LAMBDA
      LOGICAL INT(1)
      IF (N.LE.0.OR.N.GT.NM)  GO TO 1000
      PRECS = 1.0E-15
      BASE = 2.0
      ILIM = 1000
      HOV = BASE**500
      B(1) = 0.
      SQRT2 = SQRT(2.)
      N1 = N - 1
      DO 100  I = 1,N
  100 E(I) = G(I,I)
      IF  (N-2)  900,280,110
C
C * * * * * * * * * * * * * * * * * * * * * * * * * * * * * * * * * * * *
C     TRI-DIAGONALIZE MATRIX G BY HOUSEHOLDER'S PROCEDURE
C * * * * * * * * * * * * * * * * * * * * * * * * * * * * * * * * * * * *
C
  110 DO 250  K = 2,N1
      K1 = K - 1
      KJ = K + 1
      Y = G(K,K1)
      SUM = 0.0
      DO 120  I = KJ,N
  120 SUM = SUM + G(I,K1)**2
      IF (SUM.EQ.0.)  GO TO 230
      S = SQRT(SUM+Y**2)
      B(K) = SIGN(S,-Y)
      W(K) = SQRT(1.+ABS(Y)/S)
      X = SIGN(1./(S*W(K)),Y)
      DO 150  I = K,N
      IF (I.GT.K)  W(I) = X*G(I,K1)
```

```
      P(I) = 0.
  150 G(I,K1) = W(I)
      DO 180  I = K,N
      Y = W(I)
      IF (Y EQ.0.)  GO TO 180
      I1 = I + 1
      DO 160  J = K,I
  160 P(J) = P(J) + Y*G(I,J)
      IF (I1.GT.N)  GO TO 180
      DO 170  J = I1,N
  170 P(J) = P(J) + Y*G(J,I)
  180 CONTINUE
  190 X = 0.
      DO 200  J = K,N
  200 X = X + W(J)*P(J)
      X = 0.5*X
      DO 210  J = K,N
  210 P(J) = X*W(J) - P(J)
      DO 220  J = K,N
      DO 220  I = J,N
  220 G(I,J) = G(I,J) + P(I)*W(J) + P(J)*W(I)
      GO TO 250
  230 G(K,K1) = SQRT2
      B(K) = -Y
      DO 240  I = KJ,N
  240 G(I,K) = -G(I,K)
  250 CONTINUE
  280 DO 290  I = 1,N
      A(I) = G(I,I)
  290 G(I,I) = E(I)
      B(N) = G(N,N1)
C
C * * * * * * * * * * * * * * * * * * * * * * * * * * * * * * * * * * * * *
C     GET EIGENVALUES OF TRIDIAGONAL FORM BY KAHAN-VARAH Q-R METHOD
C * * * * * * * * * * * * * * * * * * * * * * * * * * * * * * * * * * * * *
C
      TOL = PRECS/(10.*FLOAT(N))
      BMAX = 0.
      TMAX = 0.
      W(N+1) = 0.
      DO 300  I = 1,N
      BMAX = AMAX1(BMAX,ABS(B(I)))
  300 TMAX = AMAX1(BMAX,ABS(A(I)),TMAX)
      SCALE = 1.0
      IF (BMAX.EQ.0.)  GO TO 520
      DO 310  I = 1,ILIM
      IF (SCALE*TMAX.GT.HOV)  GO TO 320
  310 SCALE = SCALE*BASE
  320 DO 330  I = 1,N
      E(I) = A(I)*SCALE
  330 W(I) = (B(I)*SCALE)**2
      DELTA = TMAX*SCALE*TOL
      EPS = DELTA**2
      K = N
  350 L = K
```

```
      IF (L.LE.0)  GO TO 460
      L1 = L - 1
      DO 360  I = 1,L
      K1 = K
      K = K - 1
  360 IF (W(K1).LT.EPS)  GO TO 380
  380 IF (K1.NE.L)  GO TO 400
      W(L) = 0.
      GO TO 350
  400 T = E(L) - E(L1)
      X = W(L)
      Y = 0.5*T
      S = SQRT(X)
      IF (ABS(T).GT.DELTA)  S = (X/Y)/(1.+SQRT(1.+X/Y**2))
      E1 = E(L) + S
      E2 = E(L1)- S
      IF (K1.NE.L1)  GO TO 430
      E(L)  = E1
      E(L1) = E2
      W(L1) = 0.
      GO TO 350
  430 LAMBDA = E1
      IF (ABS(T).LT.DELTA.AND.ABS(E2).LT.ABS(E1))  LAMBDA = E2
      S = 0.
      C = 1.
      GG = E(K1)-LAMBDA
      GO TO 450
  440 C = F/T
      S = X/T
      A = GG
      GG = C*(E(K1)-LAMBDA) - S*X
      E(K) = (X-GG) + E(K1)
      IF (ABS(GG).LT.DELTA) GG = GG + SIGN(C*DELTA,GG)
      F = GG**2/C
      K = K1
      K1 = K   1
      X = W(K1)
      T = X + F
      W(K) = S*T
      IF (K.LT.L)  GO TO 440
      E(K) = GG + LAMBDA
      GO TO 350
  460 DO 470  I = 1,N
  470 E(I) = E(I)/SCALE
      Y =  ISIGN(1,M)
      DO 500  L = 1,N1
      K = N - L
      DO 500  I = 1,K
      IF (Y*(E(I)-E(I+1)).GT.0.)  GO TO 500
      X = E(I)
      E(I) = E(I+1)
      E(I+1) = X
  500 CONTINUE
  520 IF (M.EQ.0)  GO TO 1000
C
```

```
C * * * * * * * * * * * * * * * * * * * * * * * * * * * * * * * * * * * * *
C     COMPUTE EIGENVECTORS BY INVERSE ITERATION
C * * * * * * * * * * * * * * * * * * * * * * * * * * * * * * * * * * * * *
C
      NVEC = IABS(M)
      IF (NVEC.GT.N)  NVEC = N
      F = SCALE/HOV
      IF (BMAX*F.LT.PRECS)  GO TO 830
      DO 530  I = 1,N
      A(I) = A(I)*F
  530 B(I) = B(I)*F
      SEP = 25.*TMAX*PRECS
      X1 = 0.
      X2 = SQRT2
      DO 800  NV = 1,NVEC
      IF (NV.GT.1.AND.ABS(E(NV)-E(NV-1)).LT.SEP)  GO TO 550
      DO 540  I = 1,N
  540 W(I) = 1.0
      GO TO 570
  550 DO 560  I = 1,N
      X = AMOD(X1+X2,2.0)
      X1 = X2
      X2 = X
  560 W(I) = X - 1.0
  570 EV = E(NV)*F
      X = A(1) - EV
      Y = B(2)
      J = N1
      DO 600  I = 1,N1
      C = A(I+1) - EV
      S = B(I+1)
      IF (ABS(X).GE.ABS(S))  GO TO 580
      P(I) = S
      Q(I) = C
      INT(I) = .TRUE.
      Z = -X/S
      X = Y + Z*C
      IF (I.LT.N1)  Y = Z*B(I+2)
      GO TO 600
  580 IF (ABS(X).LT.TOL)  X = TOL
      P(I) = X
      Q(I) = Y
      INT(I) = .FALSE.
      Z = -S/X
      X = C + Z*Y
      Y = B(I+2)
  600 V(I,NV) = Z
      IF (ABS(X).LT.TOL)  X = TOL
      NITER = 0
  620 NITER = NITER + 1
      W(N) = W(N)/X
      SUM = W(N)**2
      DO 640  L = 1,N1
      I = N - L
      Y = W(I) - Q(I)*W(I+1)
```

```
      IF (INT(I))  Y = Y - B(I+2)*W(I+2)
      W(I) = Y/P(I)
  640 SUM = SUM + W(I)**2
      S = SQRT(SUM)
      DO 660  I = 1,N
  660 W(I) = W(I)/S
      IF (NITER.GE.2)  GO TO 760
      DO 700  I = 1,N1
      Z = V(I,NV)
      IF (INT(I))  GO TO 680
      W(I+1) = W(I+1) + Z*W(I)
      GO TO 700
  680 Y = W(I)
      W(I) = W(I+1)
      W(I+1) = Y + Z*W(I)
  700 CONTINUE
      GO TO 620
  730 L = J
      J = J - 1
      X = 0.
      DO 740  I = L,N
  740 X = X + G(I,J)*W(I)
      DO 750  I = L,N
  750 W(I) = W(I) - X*G(I,J)
  760 IF (J.GT.1)  GO TO 730
      DO 800  I = 1,N
  800 V(I,NV) = W(I)
      DO 820  I = 1,N
      A(I) = A(I)/F
  820 B(I) = B(I)/F
      GO TO 860
  830 DO 850  NV = 1,NVEC
      DO 840  I = 1,N
  840 V(I,NV) = 0.
  850 V(NV,NV) = 1.0
  860 DO 880  I = 2,N
      K = I - 1
      DO 880  J = 1,K
  880 G(I,J) = G(J,I)
      GO TO 1000
  900 V(1,1) = 1.0
      A(1) = E(1)
 1000 RETURN
      END
```

APPENDIX F.. COMPUTER PROGRAM FOR FREE VIBRATION ANALYSIS OF VISCOELASTIC AXISYMMETRIC SANDWICH SHELLS (FORTRAN IV)

```
      PROGRAM ASVEFVQ(INPUT,OUTPUT,TAPE1=INPUT,TAPE2=OUTPUT)
C
C     FREE AXISYMMETRIC VIBRATION ANALYSIS OF THIN ROTATIONAL SANDWICH
C     SHELL WITH CONSTANT THICKNESS AND TWICE CONTINUOUS MERIDIAN.
C     INCLUDES DETERMINATION OF EFFECTIVE DAMPING DUE TO LINEAR VISCO-
C     ELASTIC MATERIALS.  (LIMITED TO MATERIALS WITH REAL POISSON RATIO)
C     MATERIAL PROPERTIES MAY NOT VARY IN THE MERIDIONAL DIRECTION FOR
C     THE PRESENT PROGRAM, ALTHOUGH MODIFICATION FOR THIS CAPABILITY
C     MAY BE READILY ACHIEVED.  NO RESTRICTION ON RATIOS OF LAYER THICK-
C     NESSES OR LAYER PROPERTIES.  NODES ARE NUMBERED CONSECUTIVELY
C     ALONG THE MERIDIAN AND IF A NODE IS LOCATED ON THE AXIS OF SYM-
C     METRY NUMBERING MUST BEGIN AT THIS NODE.  ELEMENTS ARE NUMBERED
C     SUCH THAT THE ELEMENT NUMBER IS THE SAME AS THE SMALLER ADJACENT
C     NODE NUMBER.
C     STORAGE FOR  20 NODES (AND THUS FOR 19 ELEMENTS).
C     SHEAR STRAIN AND CURVATURE MODELS VARY QUADRATICALLY AND LINEARLY
C     ALONG THE CHORD LENGTH, RESPECTIVELY.
C
C*********************************************************************
C     DATA CARDS FOR ASVEFVQ
C*********************************************************************
C
C     1 CARD.. I10  NUMBER OF SHELLS TO BE ANALYZED
C     THEN, FOR EACH SHELL, ALL OF THE FOLLOWING..
C
C     1 CARD..  COLS. 2-72  TITLE
C
C     1 CARD.. 3I10,L10
C                 NUMBER OF NODES, NN
C                 NUMBER OF MODE SHAPES, NMS
C                 NUMBER OF NODES WITH RESTRAINTS, NBC
C                 ROTATORY INERTIA INDEX (T IF LUMPED ROTATORY INERTIA
C                      INCLUDED, F OTHERWISE)
C
C     1 CARD..  8F10.0
C                 THICKNESS OF 1 FACING (IN.)
C                 YOUNGS MODULUS OF FACINGS (PSI) (RE AND IM PARTS)
C                 POISSON RATIO OF FACINGS
C                 SHEAR MODULUS OF FACINGS (PSI) (RE AND IM PARTS)
C                 SHEAR STRESS CORRECTION FACTOR FOR FACING
C                 DENSITY OF FACINGS (LB./IN.**3)
C     1 CARD..  8F10.0
C                 THICKNESS OF CORE (IN.)
C                 YOUNGS MODULUS OF CORE (PSI) (RE AND IM PARTS)
C                 POISSON RATIO OF CORE
C                 SHEAR MODULUS OF CORE (PSI) (RE AND IM PARTS)
C                 SHEAR STRESS CORRECTION FACTOR FOR CORE
C                 DENSITY OF CORE (LB./IN.**3)
C     (NOTE..  SHEARING MAY BE NEGLECTED BY SETTING REAL PART OF G TO
C                 9999999999)
```

```
C
C     NN CARDS.. I10,3F10.0
C                NODE NUMBER
C                R, ABSCISSA OF NODE (IN.)
C                Z, ORDINATE OF NODE (IN.)
C                PHI, LATITUDE ANGLE OF NODE (DEGREES)
C
C     NN-1 CARDS.. 2F10.0
C                CURVATURE AT NODE I OF ELEMENT (1/IN.)
C                CURVATURE AT NODE J OF ELEMENT (1/IN.)
C
C     NBC CARDS.. 5I10
C                NODE NUMBER
C                TANGENTIAL DISPLACEMENT INDEX (0=FREE, 1=CONSTRAINED)
C                RADIAL DISPLACEMENT INDEX ( DITTO )
C                BENDING ROTATION INDEX ( DITTO )
C                SHEAR WARPING INDEX ( DITTO )
C
      LOGICAL LRI
      COMMON /  / NN,NE,NMS,NDOF,NBC,NLM,LRI,PI
      PI = 3.14159265358979
      READ 1000, NSHELLS
      DO 100 N = 1,NSHELLS
      CALL SETUP
      CALL BCS
      CALL EIGEN
      IF(NMS.NE.0) CALL SHAPES
  100 CONTINUE
 1000 FORMAT(I10)
      STOP
      END




      SUBROUTINE SETUP
C     THIS SUBROUTINE READS THE GEOMETRICAL AND MATERIAL PROPERTIES OF
C     THE SHELL AND SETS UP THE OVERALL STIFFNESS MATRIX AND THE DIAGON-
C     AL MASS MATRIX, BOTH UNMODIFIED FOR BOUNDARY CONDITIONS.
C     SHEAR STRAIN AND CURVATURE MODELS VARY QUADRATICALLY AND LINEARLY
C     ALONG CHORD LENGTH, RESPECTIVELY.
C     COMPLEX ARITHMETIC FOR LINEAR VISCOELASTIC MATERIALS.
      REAL NUF,NUC,KF,KC
      LOGICAL LRI
      COMPLEX S,ST,A,E,V
      COMPLEX EC,GC,EF,GF,BF,DF,BC,DC
      COMPLEX SEL,DB
      COMMON /  / NN,NE,NMS,NDOF,NBC,NLM,LRI,PI
      COMMON /ARRAY/ S(80,8),ST(19,12,4),XM(80),A(60,60),E(60),IV(60),
     1 V(80)
      COMMON /PROPS/ H,D,HF,HC,EF,NUF,GF,EC,NUC,GC,BF,DF,BC,DC
      COMMON /XGEOM/ YP,YPP,RX,COSB,YBAR,X(10)
      COMMON /ELGEOM/ EL,SPSI,CPSI,TBI,TBJ,CBI,CBJ,SBI,SBJ,A1,A2,A3,A4
```

```
      COMMON /NODGEO/ R(35),Z(35)
      COMMON /STMATS/ SEL(12,12),B(12,12),DB(12,12),T(12,12)
      DIMENSION CPHI(35),SPHI(35),W(10),Y(10),WM(10),AN(35),PHI(35)
      EQUIVALENCE (CPHI(1),A(1)), (SPHI(1),A(101)), (PHI(1),A(201)),
     1 (AN(1),A(301))
      DATA  X  /       0.013046735741414, 0.067468316655507,
     1 0.160295215850488, 0.283302302935376, 0.425562830509184,
     2 0.574437169490816, 0.716697697064624, 0.839704784149512,
     3 0.932531683344493, 0.986953264258586   /
      DATA  W  /  0.066671344308688, 0.149451349150581,
     1 0.219086362515982, 0.269266719309996,   0.295524224714753,
     2 0.295524224714753, 0.269266719309996, 0.219086362515982,
     3  0.149451349150581, 0.066671344308688  /
      DATA  Y  /  0.023455038515334, 0.115382672473579,
     1 0.25, 0.384617327526421, 0.476544961484666, 0.523455038515334,
     2 0.615382672473579, 0.75, 0.884617327526421, 0.976544961484666  /
      DATA  WM  / 0.236926885056189, 0.478628670499366,
     1 0.568888888888889, 0.478628670499366, 0.236926885056189,
     2 0.236926885056189, 0.478628670499366, 0.568888888888889,
     3 0.478628670499366, 0.236926885056189  /
      WRITE (2,2000)
      READ (1,1000)
      WRITE (2,1000)
      READ (1,1001) NN,NMS,NBC,LRI
      READ (1,1002) HF,EF,NUF,GF,KF,RHOF
      READ (1,1002) HC,EC,NUC,GC,KC,RHOC
      WRITE (2,2001) NN,NMS,NBC, HF,HC, EF,NUF,GF,KF,RHOF, EC,NUC,GC,KC,
     1 RHOC, LRI
      IF(NN.GT. 20) GO TO 900
      IF(REAL(GF).GE.9999999998.0) GF = (1.0E+20, 0.0)
      IF(REAL(GC).GE.9999999998.0) GC = (1.0E+20, 0.0)
      H = HC + 2.0*HF
      D = HC + HF
      NE = NN - 1
      NDOF = 4*NN
      NLM = 2*NN
      IF(LRI) NLM = 3*NN
      EF = EF/(1.0 - NUF*NUF)
      EC = EC/(1.0 - NUC*NUC)
      BF = EF*HF
      BC = EC*HC
      GF = GF*HF*KF
      GC = GC*HC*KC
      DF = BF*HF*HF/12.0
      DC = BC*HC*HC/12.0
      RHO = (HC*RHOC + 2.0*HF*RHOF)/386.088
      AMOM = (RHOC*HC**3 + RHOF*(H**3 - HC**3))/(12.0*386.088)
      DO 100 I = 1,NDOF
      XM(I) = 0.0
      DO 100 J = 1,8
  100 S(I,J) = (0.0,0.0)
      JK = 0
      WRITE (2,2002)
      DR = 180.0/PI
      DO 110 I = 1,NN
```

```
      AN(I) = 0.0
      READ (1,1003) I,R(I),Z(I),PHI(I)
      WRITE (2,2003) I,R(I),Z(I),PHI(I)
      PHI(I) = PHI(I)/DR
      SPHI(I) = SIN(PHI(I))
  110 CPHI(I) = COS(PHI(I))
      WRITE (2,2004)
      DO 500 I = 1,NE
      DR = R(I+1) - R(I)
      DZ = Z(I+1) - Z(I)
      EL = SQRT(DR*DR + DZ*DZ)
      SPSI = DR/EL
      CPSI = DZ/EL
      SBI = CPHI(I)*CPSI - SPHI(I)*SPSI
      CBI = SPHI(I)*CPSI + CPHI(I)*SPSI
      TBI = SBI/CBI
      SBJ = CPHI(I+1)*CPSI - SPHI(I+1)*SPSI
      CBJ = SPHI(I+1)*CPSI + CPHI(I+1)*SPSI
      TBJ = SBJ/CBJ
      READ (1,1004) CURVI,CURVJ
      WRITE (2,2005) I,CURVI,CURVJ,EL,SPSI,CPSI,TBI,TBJ
      YPPI = -EL*CURVI/CBI**3
      YPPJ = -EL*CURVJ/CBJ**3
      A1 = TBI
      A2 = TBI + 0.5*YPPI
      A3 = -(5.0*TBI + 4.0*TBJ) + 0.5*YPPJ - YPPI
      A4 = 3.0*(TBI + TBJ) + 0.5*(YPPI - YPPJ)
      DO 150 J = 1,12
      DO 150 K = 1,12
  150 SEL(J,K) = (0.0,0.0)
C     COMPUTE ELEMENT TRANSFORMATION MATRIX (A**-1)*T
      CALL TMAT(I)
      DO 400 J = 1,10
      YBAR = (1.0 - X(J))*(A1 + X(J)*(A2 + X(J)*(A3 + X(J)*A4)))
      YP = A1*(1.0 - 2.0*X(J))+ X(J)*(A2*(2.0 - 3.0*X(J)) + X(J)*(A3*
     1 (3.0 - 4.0*X(J)) + A4*X(J)*(4.0 - 5.0*X(J))))
      YPP = 2.0*(-A1 + A2*(1.0 - 3.0*X(J)))+ X(J)*(A3*(6.0 - 12.0*X(J))
     1 + A4*X(J)*(12.0 - 20.0*X(J)))
      RX = R(I) + X(J)*EL*(SPSI + YBAR*CPSI)
      COSB = 1.0/(SQRT(1.0 + YP*YP))
C     EVALUATE B(,) AT INTEGRATION POINTS
      CALL BMAT(I,J)
C     ADD CONTRIBUTION TO ELEMENT STIFFNESS INTEGRATION
      C = PI*EL*RX*W(J)  /COSB
      CALL SELA(C)
      YBAR = (1.0 - Y(J))*(A1 + Y(J)*(A2 + Y(J)*(A3 + Y(J)*A4)))
      YP = A1*(1.0 - 2.0*Y(J))+ Y(J)*(A2*(2.0 - 3.0*Y(J)) + Y(J)*(A3*
     1 (3.0 - 4.0*Y(J)) + A4*Y(J)*(4.0 - 5.0*Y(J))))
      RX = R(I) + Y(J)*EL*(SPSI + YBAR*CPSI)
      COSB = 1.0/(SQRT(1.0 + YP*YP))
      C = PI*EL*RX*WM(J)/COSB/2.0
      IF(J.GT.5) GO TO 200
      AN(I) = AN(I) + C
      GO TO 400
  200 AN(I+1) =AN(I+1) + C
```

```
  400 CONTINUE
C     TRANSFORM 12X12 ELEMENT STIFFNESS TO GLOBAL CO-ORDINATES AND CON-
C     DENSE TO 8X8
      CALL SELR(I)
C     STORE MULTIPLIERS AND PIVOTS
      DO 420 J = 1,4
      IJ = J + 8
      DO 420 K = 1,12
  420 ST(I,K,J) = SEL(IJ,K)
C     ADD 8X8 ELEMENT STIFFNE    TO OVERALL STIFFNESS
      DO 450 J = 1,8
      IJ = JK + J
      DO 450 K = J,8
      IK = K - J + 1
  450 S(IJ,IK) = S(IJ,IK) + SEL(J,K)
  500 JK = JK + 4
C     CONSTRUCT DIAGONAL MASS MATRIX
      DO 600 I = 1,NN
      IJ = 4*I - 3
      XM(IJ) = XM(IJ+1) = SQRT(RHO*AN(I))
      IF(.NOT.LRI) GO TO 600
      XM(IJ+2) = SQRT(AMOM*AN(I))
  600 CONTINUE
      RETURN
  900 WRITE (2,2900)
      STOP
 1000 FORMAT(72H
     1                                                    )
 1001 FORMAT(3I10,L10)
 1002 FORMAT(8F10.0)
 1003 FORMAT(I10,3F10.0)
 1004 FORMAT(2F10.0)
 2000 FORMAT(1H1)
 2001 FORMAT(10X,28HNUMBER OF NODES                  ,I3/
     1 10X,28HNUMBER OF MODE SHAPES                  ,I3/
     2 10X,28HNUMBER OF RESTRAINED NODES             ,I3//
     3 10X,16HFACE THICKNESS =,F10.6/
     4 10X,16HCORE THICKNESS =,F10.6//
     5 10X,8HFACE E =,F13.1,1H,,F14.3/
     6 10X,9HFACE NU =,F12.5/
     7 10X,8HFACE G =,F13.1,1H,,F14.3/
     6 10X,10HFACE KAP =,F11.5/
     7 10X,10HFACE RHO =,F11.6//
     8 10X,8HCORE E =,F13.1,1H,,F14.3/
     9 10X,9HCORE NU =,F12.5/
     1 10X,8HCORE G = F13.1,1H,,F14.3/
     2 10X,10HCORE KAP =,F11.5/
     3 10X,10HCORE RHO =,F11.6//
     4 44H ROTATORY INERTIA INCLUDED (T = YES, F = NO) ,L5 //
     5 45H ALL QUANTITIES IN INCHES, POUNDS AND SECONDS  /)
 2002 FORMAT(//11HONODAL DATA /
     9        2X,4HNODE,7X,11HABSCISSA, R,8X,12H ORDINATE, Z,6X,
     1 14HLATITUDE ANGLE/
     2 15X,5H(IN.),15X,5H(IN.),13X,8H(DEGREE)/)
 2003 FORMAT(I4,3F20.8)
```

```
 2004 FORMAT(/18HOELEMENT GEOMETRY /
     1 8H ELEMENT,10X,7HCURV(I),10X,7HCURV(J),5X,12HCHORD LENGTH,10X,
     2 7HSIN PSI,10X,7HCOS PSI,6X,11HTAN BETA(I),6X,11HTAN BETA(J)/
     3 18X,7H(1/IN.),10X,7H(1/IN.),12X,5H(IN.))
 2005 FORMAT(I8,7F17.8)
 2900 FORMAT(/////41HONUMBER OF NODES EXCEEDS ALLOWABLE   STOP     )
      END




      SUBROUTINE TMAT(I)
C     THIS SUBROUTINE EVALUATES THE CO-ORDINATE TRANSFORMATION MATRIX
C     (A**-1)*T FOR ELEMENT I.
C     GLOBAL CO-ORDINATES ARE  S  AND  XI  (MERIDIONAL AND RADIAL), AND
C     THUS CAN BE APPLIED ONLY TO SHELLS WITH TWICE CONTINUOUS MERIDIANS
C     SHEAR STRAIN AND CURVATURE MODELS VARY QUADRATICALLY AND LINEARLY
C     ALONG CHORD LENGTH, RESPECTIVELY.
C     COMPLEX ARITHMETIC FOR LINEAR VISCOELASTIC MATERIALS.
      REAL NUC,NUF
      COMPLEX EC,GC,EF,GF,BF,DF,BC,DC
      COMPLEX SEL,DB
      COMMON /PROPS/ H,D,HF,HC,EF,NUF,GF,EC,NUC,GC,BF,DF,BC,DC
      COMMON /STMATS/ SEL(12,12),B(12,12),DB(12,12),T(12,12)
      COMMON /NODGEO/ R(35),Z(35)
      COMMON /ELGEOM/ EL,SPSI,CPSI,TBI,TBJ,CBI,CBJ,SBI,SBJ,A1,A2,A3,A4
      DO 100 J = 1,12
      DO 100 K = 1,12
  100 B(J,K) = 0.0
      IF(R(I).EQ.0.0) GO TO 500
C     MATRIX FOR OPEN-ENDED ELEMENT
      B(1,1) = B(3,2) = B(2,6) = 1.0
      B(7,4) = B(7,5) = B(9,5) = 1.0
      B(8,9) = B(8,10) = B(10,10) = B(2,1) = -1.0
      B(4,1) = -TBI
      B(4,6) = TBI
      B(6,6) = TBI + TBJ
      B(6,1) = - B(6,6)
      B(5,1) = B(6,6) + TBI
      B(5,6) = -B(5,1)
      B(5,2) = B(8,4) = B(8,5) = B(10,5) = -3.0
      B(6,2) = B(11,4) = B(11,5)   B(12,5) = 2.0
      B(11,9) = B(11,10) = B(12,10) = 2.0
      B(5,7) = 3.0
      B(6,7) = -2.0
      B(8,11) = B(10,12) = 4.0
      B(11,11) = B(12,12) = -4.0
      B(4,3) = B(6,3) = -EL/CBI/CBI
      B(5,3) = -2.0*B(4,3)
      B(4,4) = B(6,4) = HC*B(4,3)/D
      B(5,4) = -2.0*B(4,4)
      B(4,5) = B(6,5) = B(4,3)
      B(5,5) = -2.0*B(4,5)
```

```
      B(5,8) = EL/CBJ/CBJ
      B(6,8) = -B(5,8)
      B(5,9) = HC*B(5,8)/D
      B(6,9) = -B(5,9)
      B(5,10) = B(5,8)
      B(6,10) = -B(5,10)
      DO 200 J = 1,12
      T(J,1) = CBI*B(J,1) + SBI*B(J,2)
      T(J,2) = SBI*B(J,1) - CBI*B(J,2)
      T(J,3) = B(J,3)
      T(J,4) = B(J,4)
      T(J,5) = CBJ*B(J,6) + SBJ*B(J,7)
      T(J,6) = SBJ*B(J,6) - CBJ*B(J,7)
      T(J,7) = B(J,8)
      T(J,8) = B(J,9)
      T(J,9) = B(J,5)
      T(J,10) = B(J,10)
      T(J,11) = B(J,11)
  200 T(J,12) = B(J,12)
      GO TO 1000
C     MATRIX FOR CAP
  500 B(5,2) = -1.0
      B(9,9) = B(9,10) = B(10,10) = -1.0
      B(6,5) = 1.0
      B(7,7) = 3.0
      B(11,9) = B(11,10) = B(12,10) = 2.0
      B(8,7) = -2.0
      B(9,11) = B(10,12) = 4.0
      B(11,11) = B(12,12) = -4.0
      B(6,2) = -CPSI
      B(7,2) = (2.0*TBI + TBJ)*CPSI + 3.0*SPSI
      B(8,2) = -B(7,2) + TBI*CPSI + SPSI
      B(7,6) = -2.0*TBI - TBJ
      B(8,6) = TBI + TBJ
      B(7,8) = EL/CBJ/CBJ
      B(8,8) = -B(7,8)
      B(7,9) = HC*B(7,8)/D
      B(8,9) = -B(7,9)
      B(7,10) = B(7,8)
      B(8,10) =-B(7,10)
      DO 700 J = 1,12
      T(J,1) = T(J,3) = T(J,4) = T(J,9) = 0.0
      T(J,2) = B(J,2)
      T(J,5) = CBJ*B(J,6) + SBJ*B(J,7)
      T(J,6) = SBJ*B(J,6) - CBJ*B(J,7)
      T(J,7) = B(J,8)
      T(J,8) = B(J,9)
      T(J,10) = B(J,10)
      T(J,11) = B(J,11)
  700 T(J,12) = B(J,12)
 1000 RETURN
      END
```

```
      SUBROUTINE BMAT(I,J)
C     THIS SUBROUTINE EVALUATES THE MATRIX B FOR ELEMENT I AT POINT X(J)
C     SHEAR STRAIN AND CURVATURE MODELS VARY QUADRATICALLY AND LINEARLY
C     ALONG CHORD LENGTH, RESPECTIVELY.
C     COMPLEX ARITHMETIC FOR LINEAR VISCOELASTIC MATERIALS.
      REAL NUF,NUC
      COMPLEX EC,GC,EF,GF,BF,DF,BC,DC
      COMPLEX SEL,DB
      COMMON /PROPS/ H,D,HF,HC,EF,NUF,GF,EC,NUC,GC,BF,DF,BC,DC
      COMMON /STMATS/ SEL(12,12),B(12,12),DB(12,12),T(12,12)
      COMMON /ELGEOM/ EL,SPSI,CPSI,TBI,TBJ,CBI,CBJ,SBI,SBJ,A1,A2,A3,A4
      COMMON /NODGEO/ R(35),Z(35)
      COMMON /XGEOM/ YP,YPP,RX,COSB,YBAR,X(10)
      DO 100 K = 1,12
      DO 100 L = 1,12
  100 B(K,L) = 0.0
      B1 = -YPP*COSB**5*(1.0 - YP*YP)/(EL*EL)
      B3 = COSB**3/(EL*EL)
      B2 = -2.0*YPP*YP*B3*COSB*COSB
      IF(R(I).EQ.0.0) GO TO 400
      B4 = -EL*B3*YP*(SPSI + CPSI*YP)/RX
      B5 = EL*B3*(SPSI + CPSI*YP)/RX
      B6 = COSB*(SPSI + CPSI*YP)/RX
C     MATRIX FOR OPEN-ENDED ELEMENT
      B(2,1) = B(7,1) = B(12,1) = SPSI/RX
      B(2,3) = B(7,3) = B(12,3) = CPSI/RX
      B(2,2) =                    B(12,1)*X(J)
      B(2,4) =                    B(12,3)*X(J)
      B(2,5) = B(2,4)*X(J)
      B(2,6) = B(2,5)*X(J)
      B(4,8) = B(9,10)  =            COSB/EL
      B(4,11) = B(9,12) = 2.0*X(J)*B(4,8)
      B(1,2) =                    COSB*B(9,10)
      B(1,4) = B(1,2)*YP
      B(1,5) = 2.0*X(J)*B(1,4)
      B(1,6) = 1.5*X(J)*B(1,5)
      B(3,7) = B(3,9) = 1.0
      B(3,8) = B(8,10) = X(J)
      B(3,11) = B(8,12) = X(J)*X(J)
      B(4,2) = B(9,2) = B1
      B(4,4) = B(9,4) = B2
      B(5,2) = B(10,2) = B4
      B(5,4) = B(10,4) = B5
      B(5,7) = B(10,9) = B6
      B(5,8) = B(10,10) =            B6*X(J)
      B(5,11) = B(10,12) = X(J)*B(5,8)
      B(4,5) = B(9,5) =            2.0*B2*X(J)  + 2.0*B3
      B(4,6) = B(9,6) =            (3.0*B2*X(J) + 6.0*B3)*X(J)
      B(5,5) = B(10,5) =            2.0*B5*X(J)
      B(5,6) = B(10,6) =            3.0*B5*X(J)*X(J)
      B(6,2) = B(1,2) - D*B1/2.0
      B(11,2) =  B(1,2) + D*B1/2.0
      B(6,4) = B(1,4) - D*B2/2.0
      B(11,4) =  B(1,4) + D*B2/2.0
      B(6,5) = B(1,5) - D*B(4,5)/2.0
```

```
      B(11,5) = B(6,5) + D*B(4,5)
      B(6,6) = B(1,6) - D*B(4,6)/2.0
      B(11,6) = B(6,6) + D*B(4,6)
      B(6,8) = -HC*B(4,8)/2.0
      B(11,8) = -B(6,8)
      B(6,10) = -HF*B(4,8)/2.0
      B(11,10) = -B(6,10)
      B(6,11) = 2.0*X(J)*B(6,8)
      B(11,11) = -B(6,11)
      B(6,12) = 2.0*X(J)*B(6,10)
      B(11,12) = -B(6,12)
      B(7,2) = B(2,2) - D*B4/2.0
      B(12,2) =  B(7,2) + D*B4
      B(7,4) = B(2,4) - D*B5/2.0
      B(12,4) =  B(7,4) + D*B5
      B(7,5) = B(2,5) - D*B(5,5)/2.0
      B(12,5) = B(7,5) + D*B(5,5)
      B(7,6) = B(2,6) - D*B(5,6)/2.0
      B(12,6) = B(7,6) + D*B(5,6)
      B(7,7) = -HC*B6/2.0
      B(12,7) = -B(7,7)
      B(7,8) = B(7,7)*X(J)
      B(12,8) = -B(7,8)
      B(7,9) = -HF*B6/2.0
      B(12,9) = -B(7,9)
      B(7,10) = B(7,9)*X(J)
      B(12,10) = -B(7,10)
      B(7,11) = X(J)*B(7,8)
      B(12,11) = -B(7,11)
      B(7,12) = X(J)*B(7,10)
      B(12,12) = -B(7,12)
      GO TO 1000
C     MATRIX FOR CAP ELEMENT
  400 B6 = EL*(SPSI + YBAR*CPSI)
      B5 = COSB**3*(SPSI + YP*CPSI)/(B6*EL)
      B4 = COSB*(SPSI + CPSI*YP)/B6
      B(3,9) = B(8,10) = X(J)
      B(3,11) = B(8,12) = X(J)*X(J)
      B(4,9) = B(9,10) = COSB/EL
      B(4,11) = B(9,12) = 2.0*X(J)*B(4,9)
      B(4,6) = B(9,6) =            B1 + TBI*B2
      B(4,7) = B(9,7) =            2.0*B2*X(J) + 2.0*B3
      B(4,8) = B(9,8) =            (3.0*B2*X(J) + 6.0*B3)*X(J)
      B(5,6) = B(10,6) = .5*(((5.0*A4*X(J) + 4.0*(A3 - A4))*X(J) +
     1 3.0*(A2 - A3))*X(J) + 2.0*(A1 - A2))
      B(5,7) = B(10,7) =            2.0*B5
      B(5,8) = B(10,8) =            3.0*B5*X(J)
      B(5,9) = B(10,10) = B4
      B(5,11) = B(10,12) = X(J)*B4
      B(1,6) = COSB*B(4,9)*(1.0+ TBI*YP)
      B(1,7) = 2.0*X(J)*COSB*B(4,9)*YP
      B(1,8) = 1.5*X(J)*B(1,7)
      B(2,6) = (SPSI + CPSI*TBI)/B6
      B(2,7) = X(J)*CPSI/B6
      B(2,8) = X(J)*B(2,7)
```

```
      B(6,6) = B(1,6) - D*B(4,6)/2.0
      B(11,6) = B(6,6) + D*B(4,6)
      B(6,7) = B(1,7) - D*B(4,7)/2.0
      B(11,7) = B(6,7) + D*B(4,7)
      B(5,8) = B(1,8) - D*B(4,8)/2.0
      B(11,8) = B(6,8) + D*B(4,8)
      B(6,9) = -HC*B(4,9)/2.0
      B(11,9) = -B(6,9)
      B(5,10) = -HF*B(4,9)/2.0
      B(11,10) = -B(6,10)
      B(5,11) = 2.0*X(J)*B(6,9)
      B(11,11) = -B(6,11)
      B(6,12) = 2.0*X(J)*B(6,10)
      B(11,12) = -B(6,12)
      B(7,6) = B(2,6) - D*B(5,6)/2.0
      B(12,6) = B(7,6) + D*B(5,6)
      B(7,7) = B(2,7) - D*B5
      B(12,7) = B(2,7) + D*B5
      B(7,8) = B(2,8) - D*B(5,8)/2.0
      B(12,8) = B(7,8) + D*B(5,8)
      B(7,9) = -HC*B4/2.0
      B(12,9) = -B(7,9)
      B(7,10) = -HF*B4/2.0
      B(12,10) = -B(7,10)
      B(7,11) = X(J)*B(7,9)
      B(12,11) = -B(7,11)
      B(7,12) = X(J)*B(7,10)
      B(12,12) = -B(7,12)
 1000 RETURN
      END
```

```
      SUBROUTINE SELA(C)
C     THIS SUBROUTINE COMPUTES A TERM IN THE GAUSS INTEGRATION FOR THE
C     STIFFNESS MATRIX IN GENERALIZED CO-ORDINATES
C     SHEAR STRAIN AND CURVATURE MODELS VARY QUADRATICALLY AND LINEARLY
C     ALONG CHORD LENGTH, RESPECTIVELY.
C     COMPLEX ARITHMETIC FOR LINEAR VISCOELASTIC MATERIALS.
      REAL NUF,NUC
      COMPLEX EC,GC,EF,GF,BF,DF,BC,DC
      COMPLEX SEL,DB
      COMMON /PROPS/ H,D,HF,HC,EF,NUF,GF,EC,NUC,GC,BF,DF,BC,DC
      COMMON /STMATS/ SEL(12,12),B(12,12),DB(12,12),T(12,12)
      DO 100 K = 1,12
      DB(1,K) = BC*(B(1,K) + NUC*B(2,K))*C
      DB(2,K) = BC*(B(2,K) + NUC*B(1,K))*C
      DB(3,K) = GC*B(3,K)*C
      DB(4,K) = DC*(B(4,K) + NUC*B(5,K))*C
      DB(5,K) = DC*(B(5,K) + NUC*B(4,K))*C
      DB(6,K) = BF*(B(6,K) + NUF*B(7,K))*C
      DB(7,K) = BF*(B(7,K) + NUF*B(6,K))*C
```

```
      DB(8,K) = GF*B(8,K)*C*2.0
      DB(9,K) = DF*(B(9,K)+ NUF*B(10,K))*C*2.0
      DB(10,K) = DF*(B(10,K) + NUF*B(9,K))*C*2.0
      DB(11,K) = BF*(B(11,K) + NUF*B(12,K))*C
  100 DB(12,K) = BF*(B(12,K) + NUF*B(11,K))*C
      DO 200 K = 1,12
      DO 200 L = 1,12
      DO 200 M = 1,12
  200 SEL(K,L) = SEL(K,L) + B(M,K)*DB(M,L)
      RETURN
      END



      SUBROUTINE SELR(L)
C     THIS SUBROUTINE TRANSFORMS THE ELEMENT STIFFNESS FROM GENERALIZED
C     TO GLOBAL CO-ORDINATES AND CONDENSES IT FROM 12X12 TO 8X8 USING
C     STATIC CONDENSATION.
C     SHEAR STRAIN AND CURVATURE MODELS VARY QUADRATICALLY AND LINEARLY
C     ALONG CHORD LENGTH, RESPECTIVELY.
C     COMPLEX ARITHMETIC FOR LINEAR VISCOELASTIC MATERIALS.
      COMPLEX SEL,DB
      COMPLEX PIVOT, C
      COMMON /NODGEO/ R(35),Z(35)
      COMMON /STMATS/ SEL(12,12),B(12,12),DB(12,12),T(12,12)
C     SYMMETRIZE ELEMENT STIFFNESS IN GENERALIZED CO-ORDINATES
      DO 50 I = 1,11
      IJ = I + 1
      DO 50 J = IJ,12
      IF(CABS(SEL(I,J)).EQ.0.0.OR.CABS(SEL(J,I)).EQ.0.0) GO TO 45
      SEL(I,J) = 0.5*(SEL(I,J) + SEL(J,I))
      GO TO 50
   45 SEL(I,J) = (0.0,0.0)
   50 SEL(J,I) = SEL(I,J)
C      TRANSFORM TO GLOBAL CO-ORDINATES
      DO 100 I = 1,12
      DO 100 J = 1,12
      DB(I,J) = (0.0,0.0)
      DO 100 K = 1,12
  100 DB(I,J) = DB(I,J) + SEL(I,K)*T(K,J)
      DO 200 I = 1,12
      DO 200 J = 1,12
      SEL(I,J) = (0.0,0.0)
      DO 200 K = 1,12
  200 SEL(I,J) = SEL(I,J) + T(K,I)*DB(K,J)
      IF(R(L).NE.0.0) GO TO 250
      SEL(1,1) = SEL(3,3) = SEL(4,4) = SEL(9,9) = (1.0,0.0)
C     CONDENSE TO 8X8 ELEMENT STIFFNESS
  250 DO 300 J = 1,4
      IJ = 12 - J
      IK = IJ + 1
      PIVOT = SEL(IK,IK)
```

```
      DO 300 K = 1,IJ
      C = SEL(IK,K)/PIVOT
      SEL(IK,K) = C
      DO 300 I = K,IJ
      SEL(I,K) = SEL(I,K) - C*SEL(I,IK)
  300 SEL(K,I) = SEL(I,K)
      RETURN
      END




      SUBROUTINE BCS
C     THIS SUBROUTINE READS THE BOUNDARY CONDITION DATA, MODIFIES THE
C     OVERALL STIFFNESS MATRIX AND MASS MATRIX ACCORDINGLY AND THEN
C     TRIANGULARIZES THE STIFFNESS FOR READY SOLUTION.
C     SHEAR STRAIN AND CURVATURE MODELS VARY QUADRATICALLY AND LINEARLY
C     ALONG CHORD LENGTH, RESPECTIVELY.
C     COMPLEX ARITHMETIC FOR LINEAR VISCOELASTIC MATERIALS.
      COMPLEX S,ST,A,E,V
      LOGICAL LRI
      COMMON /   / NN,NE,NMS,NDOF,NBC,NLM,LRI,PI
      COMMON /ARRAY/ S(80,8),ST(19,12,4),XM(80),A(60,60),E(60),IV(60),
     1 V(80)
      COMMON /NODGEO/ R(35),Z(35)
      DIMENSION NR(4)
      IF(R(1).NE.0.0) GO TO 100
      NLM = NLM - 1
      XM(1) = 0.0
      IF(.NOT.LRI) GO TO 100
      NLM = NLM - 1
      XM(3) = 0.0
  100 WRITE (2,2000)
C     READ KINEMATIC CONSTRAINTS AND MODIFY OVERALL STIFFNESS AND MASS
      DO 300 I = 1,NBC
      READ (1,1001)  N,(NR(J),J=1,4)
      WRITE (2,2001) N,(NR(J),J=1,4)
      IJ = 4*N - 4
      DO 300 J = 1,4
      IF(NR(J).EQ.0) GO TO 300
      IK = IJ + J
      S(IK,1) = (1.0,0.0)
      DO 200 K = 2,8
      S(IK,K) = (0.0,0.0)
      L = IK - K + 1
      IF(L.LE.0) GO TO 200
      S(L,K) = (0.0,0.0)
  200 CONTINUE
      IF(J.EQ.4) GO TO 300
      IF(J.EQ.3.AND..NOT.LRI)GO TO 300
      NLM = NLM - 1
      XM(IK) = 0.0
  300 CONTINUE
```

```
      IF (NMS.GT.NLM) NMS = NLM
C     TRIANGULARIZE STIFFNESS MATRIX
      CALL DYBSLC(NDOF,8,80,S,V,1,1)
      RETURN
 1001 FORMAT(5I10)
 2000 FORMAT(//59HOKINEMATIC CONSTRAINTS (0 = UNCONSTRAINED, 1 = CONSTRA
     1INED) /
     2 6X,4HNODE,5X,10HMERIDIONAL,9X,6HRADIAL,7X,8HROTATION,
     3 8X,7HWARPING/)
 2001 FORMAT(I10,4I15)
      END




      SUBROUTINE EIGEN
C     THIS SUBROUTINE TRANSFORMS THE EIGENVALUE PROBLEM FROM
C          K(,)*U() = OM**2*M(,)*U()
C     TO
C          A(,)*V() = V()/OM**2
C     WHERE
C          K(,) = STIFFNESS MATRIX
C          M(,) = DIAGONAL MASS MATRIX
C          A(,) = M(,)**0.5*F(,)*M(,)**0.5
C          F(,) = FLEXIBILITY MATRIX AFTER CONDENSATION ON DEGREES OF
C                 FREEDOM NOT CORRESPONDING TO LUMPED MASSES
C          V() = M(,)**0.5*U()
C     THE EIGENVALUES AND NMS OF THE EIGENVECTORS ARE THEN COMPUTED.
C     COMPLEX ARITHMETIC FOR LINEAR VISCOELASTIC MATERIALS.
      LOGICAL LRI
      COMPLEX S,ST,A,E,V
      COMMON /   / NN,NE,NMS,NDOF,NBC,NLM,LRI,PI
      COMMON /ARRAY/ S(80,8),ST(19,12,4),XM(80),A(60,60),E(60),IV(60),
     1 V(80)
C     COMPUTE INDEX VECTOR OF LUMPED MASSES
      N = 1
      DO 100 I = 1,NLM
   50 IF(XM(N).NE.0.0) GO TO 60
      N = N+1
      GO TO 50
   60 IV(I) = N
  100 N = N+1
C     ASSEMBLE MATRIX A(,)
      DO 300 I = 1,NLM
      DO 200 J = 1,NDOF
  200 V(J) = (0.0,0.0)
      N = IV(I)
      V(N) = (1.0,0.0)
      CALL DYBSLC(NDOF,8,80,S,V,2,N)
      DO 300 J = I,NLM
      L = IV(J)
      A(J,I) = XM(L)*V(L)*XM(N)
  300 A(I,J) = A(J,I)
```

```
C     COMPUTE EIGENVALUES AND EIGENVECTORS
      CALL ALLMAT(A,E,NLM,60,NCAL,NMS)
C     COMPUTE AND PRINT NATURAL FREQUENCIES
      WRITE (2,2000)
      IF(NCAL.EQ.0) GO TO 500
      DO 400 I = 1,NCAL
      E(I) = 1.0/E(I)
      ETA = AIMAG(E(I))/REAL(E(I))
      E(I) = CSQRT(E(I))
      DEC = AIMAG(E(I))*2.0*PI/REAL(E(I))
      PER = 2.0*PI/REAL(E(I))
      FREQ = 1.0/PER
  400 WRITE (2,2001) I,E(I),FREQ,PER,DEC,ETA
  500 IF(NCAL.LT.NLM) WRITE (2,2002) NCAL,NLM
      IF(NMS.GT.NCAL) NMS = NCAL
      RETURN
 2000 FORMAT(50H1FUNDAMENTAL FREQUENCIES AND CORRESPONDING DAMPING //
     1 9H      MODE,11X,5HOMEGA,4X,12HDECAY CONST.,6X,10HOMEGA/2*PI,10X,
     2 6HPERIOD,7X,9HLOG. DEC.,5X,11HLOSS FACTOR /
     3 16X,9H(RAD/SEC),8X,8H(1/SEC.),7X,9H(CYC/SEC),10X,6H(SEC.))
 2001 FORMAT(I9,6E16.8)
 2002 FORMAT(///5X,28HNOTE..  CONVERGENCE FOR ONLY,I3,3H OF,I3,
     1 21H POSSIBLE FREQUENCIES    )
      END




      SUBROUTINE SHAPES
C     THIS SUBROUTINE RECOVERS AND PRINTS THE COMPLETE MODE SHAPES.
C     COMPLEX ARITHMETIC FOR LINEAR VISCOELASTIC MATERIALS.
      LOGICAL LRI
      REAL NUC,NUF
      COMPLEX S,ST,A,E,V
      COMPLEX EC,GC,EF,GF,BF,DF,BC,DC
      COMPLEX C,W(12)
      COMMON /   / NN,NE,NMS,NDOF,NBC,NLM,LRI,PI
      COMMON /ARRAY/ S(80,8),ST(19,12,4),XM(80),A(60,60),E(60),IV(60),
     1 V(80)
      COMMON /NODGEO/ R(35),Z(35)
      COMMON /PROPS/ H,D,HF,HC,EF,NUF,GF,EC,NUC,GC,BF,DF,BC,DC
      DIMENSION U(12)
      WRITE (2,2003)
      DO 800 I = 1,NMS
      C = E(I)*E(I)
      DO 100 J = 1,NDOF
  100 V(J) = (0.0,0.0)
      DO 200 K = 1,NLM
      L = IV(K)
  200 V(L) = C*XM(L)*A(K,I)
      CALL DYBSLC(NDOF,8,80,S,V,2,1)
      WRITE (2,2000) I
      DO 700 J = 1,NE
```

```
      IL = 4*J - 4
      DO 300 K = 1,8
      IK = IL + K
  300 W(K) = V(IK)
C     RECOVER CONDENSED DISPLACEMENTS
      DO 400 K = 1,4
      JK = K + 8
      IK = JK - 1
      W(JK) = (0.0,0.0)
      DO 400 L = 1,IK
  400 W(JK) = W(JK) - ST(J,L,K)*W(L)
      DO 500 K = 1,12
      IF(REAL(W(K)).EQ.0.0) GO TO 450
      U(K) = REAL(W(K))*CABS(W(K))/ABS(REAL(W(K)))
      GO TO 500
  450 U(K) = CABS(W(K))
  500 CONTINUE
C     COMPUTE ADDITIONAL DISPLACEMENTS OF INTEREST AND PRINT
      GAMCI = U(4) + U(9)
      GAMCJ = U(8) + U(10)
      CHISI = (HC*GAMCI + HF*U(9))/D
      CHISJ = (HC*GAMCJ + HF*U(10))/D
      CHII = U(3) + CHISI
      CHIJ = U(7) + CHISJ
      GAMO = U(11) - U(12)
      CHISO = (HC*U(11) + HF*U(12))/D
  700 WRITE (2,2001) J,R(J),Z(J),
     1 U(1),U(2),CHII,U(3),CHISI,U(4),GAMCI,U(9),
     2 CHISO,GAMO,U(11),U(12),
     3 U(5),U(6),CHIJ,U(7),CHISJ,U(8),GAMCJ,U(10)
  800 WRITE (2,2002) R(NN),Z(NN)
      RETURN
 2000 FORMAT(/18HOMODE SHAPE NUMBER ,I3/
     1 5H NODE,2X,13HMERIDIONAL, U,6X,9HRADIAL, W,2X,13HROTATION, CHI,
     2 9X,6HCHI(B),9X,6HCHI(S),3X,12HWARPING, GAM,7X,8HGAMMA(C),7X,
     3 8HGAMMA(F)/)
 2001 FORMAT(8H ELEMENT,I3,39X,7H(R,Z) =, F9.4,1H,,F9.4 /
     1 4X,1HI,8E15.7/
     2 4X,1HO,60X,4E15.7/
     3 4X,1HJ,8E15.7/)
 2002 FORMAT(50X,7H(R,Z) =,F9.4,1H,,F9.4 )
 2003 FORMAT(16H1VIBRATION MODES  /)
      END




      SUBROUTINE DYBSLC (NN,MM,NDIM,A,B,KKK,LIM)
C
C     DYBSLC IS AN SPECIAL IN-CORE BAND SOLVER FOR DYNAMIC PROBLEMS
C     INVOLVING CONDENSATION OF ROTATIONAL DEGREES OF FREEDOM.
C     SOLUTION IS IN COMPLEX MODE.
C
```

```
C     ADAPTED FROM A PROGRAM BY C. A. FELIPPA.
C
      COMPLEX A(NDIM,1), B(1), PIVOT, C
      NR = NN - 1
      IF (KKK.GT.1)  GO TO 300
C
C     DECOMPOSITION OF BAND MATRIX A
C
      DO 200  N = 1,NR
      M = N - 1
      PIVOT = A(N,1)
      IF(CABS(PIVOT).EQ.0.0) PIVOT = (1.0E-08, 0.0)
      MR = MIN0 (MM,NN-M)
      DO 200  L = 2,MR
      C = A(N,L)/PIVOT
      IF(CABS(C).EQ.0.0) GO TO 200
      I = M + L
      J = 0
      DO 180  K = L,MR
      J = J + 1
  180 A(I,J) = A(I,J) - C*A(N,K)
      A(N,L) = C
  200 CONTINUE
      GO TO 500
C
C     FORWARD REDUCTION OF VECTOR B FROM B(LIM) TO B(N)
C     AND BACKSUBSTITUTION FROM B(N) TO B(LIM)
C
  300 DO 350  N = LIM,NR
      M = N - 1
      MR = MIN0 (MM,NN-M)
      C = B(N)
      B(N) = C/A(N,1)
      DO 350  L = 2,MR
      I = M + L
  350 B(I) = B(I) - A(N,L)*C
      B(NN) = B(NN)/A(NN,1)
      NS = NN - LIM + 1
      DO 400  K = 2,NS
      M = NN - K
      N = M + 1
      MR = MIN0 (MM,K)
      DO 400  L = 2,MR
      I = M + L
  400 B(N) = B(N) - A(N,L)*B(I)
  500 RETURN
      END
```

```
      SUBROUTINE ALLMAT(A,LAMBDA,M,IA,NCAL,IVEC)
C
C PROG.AUTHORS JOHN RINZEL,R.E.FUNDERLIC,UNION CARBIDE CORP.
C NUCLEAR DIVISION,CENTRAL DATA PROCESSING FACILITY,
C OAK RIDGE TENNESSEE
C
C     SHARE LIBRARY PROGRAM  $F2 OR AMAT  WITH MODIFICATIONS
C
C     A = INPUT MATRIX OF ORDER AT LEAST M X M WHICH UPON RETURN CON-
C          TAINS THE EIGENVECTORS OF THE INPUT MATRIX.
C     LAMDA = VECTOR OF EIGENVALUES WHERE LAMDA(I) CORRESPONDS TO
C          EIGENVECTOR STORED IN A(,I).  ARRANGED BY DECREASING ORDER
C          OF ABSOLUTE VALUE.
C     M = ORDER OF PROBLEM TO BE SOLVED.
C     IA = FIRST DIMENSION OF A(,) IN THE CALLING PROGRAM.
C     NCAL = INTEGER CONTAINING UPON RETURN THE NUMBER OF EIGENVALUES
C          CALCULATED.  (THIS VALUE WILL BE LESS THAN M IF CONVERGENCE
C          IS NOT OBTAINED FOR ONE OR MORE EIGENVALUES.)
C     IVEC = INTEGER WHOSE VALUE IS THE NUMBER OF EIGENVECTORS TO BE
C            CALCULATED.  THESE CORRESPOND TO THE EIGENVALUES OF LOWEST
C            MODULUS.
C
      COMPLEX A(IA,1),H(60,60),HL(60,60),LAMBDA(1),VECT(60),
     1MULT(60),SHIFT(3),TEMP,SIN,COS,TEMP1,TEMP2
      LOGICAL INTH(60),TWICE
      INTEGER INT(60),R,RP1,RP2
      NCAL = 0
      IF(M.GT.60) GO TO 57
      N=M
      NCAL=N
      IF(N.NE.1)GO TO 1
      LAMBDA(1)=A(1,1)
      A(1,1)=1.
      GO TO 57
    1 ICOUNT=0
      SHIFT=0.
      IF(N.NE.2)GO TO 4
    2 TEMP=(A(1,1)+A(2,2)+CSQRT((A(1,1)+A(2,2))**2-
     14.*(A(2,2)*A(1,1)-A(2,1)*A(1,2))))/2.
      IF(REAL(TEMP).NE.0..OR.AIMAG(TEMP).NE.0.)GO TO 3
      LAMBDA(M)=SHIFT
      LAMBDA(M-1)=A(1,1)+A(2,2)+SHIFT
      GO TO 137
    3 LAMBDA(M)=TEMP+SHIFT
      LAMBDA(M-1)=(A(2,2)*A(1,1)-A(2,1)*A(1,2))/(LAMBDA(M)-SHIFT)+SHIFT
      GO TO 137
C
C     REDUCE MATRIX A TO HESSENBERG FORM
C
    4 NM2=N-2
      DO 15 R=1,NM2
      RP1=R+1
      RP2=R+2
      ABIG=0.
      INT(R)=RP1
```

```
      DO 5 I=RP1,N
      ABSSQ=REAL(A(I,R))**2+AIMAG(A(I,R))**2
      IF(ABSSQ.LE.ABIG)GO TO 5
      INT(R)=I
      ABIG=ABSSQ
    5 CONTINUE
      INTER=INT(R)
      IF(INTER.EQ.RP1)GO TO 8
      IF(ABIG.EQ.0.)GO TO 15
      DO 6 I=R,N
      TEMP=A(RP1,I)
      A(RP1,I)=A(INTER,I)
    6 A(INTER,I)=TEMP
      DO 7 I=1,N
      TEMP=A(I,RP1)
      A(I,RP1)=A(I,INTER)
    7 A(I,INTER)=TEMP
    8 DO 9 I=RP2,N
      MULT(I)=A(I,R)/A(RP1,R)
    9 A(I,R)=MULT(I)
      DO 11 I=1,RP1
      TEMP=0.
      DO 10 J=RP2,N
   10 TEMP=TEMP+A(I,J)*MULT(J)
   11 A(I,RP1)=A(I,RP1)+TEMP
      DO 13 I=RP2,N
      TEMP=0.
      DO 12 J=RP2,N
   12 TEMP=TEMP+A(I,J)*MULT(J)
   13 A(I,RP1)=A(I,RP1)+TEMP-MULT(I)*A(RP1,RP1)
      DO 14 I=RP2,N
      DO 14 J=RP2,N
   14 A(I,J)=A(I,J)-MULT(I)*A(RP1,J)
   15 CONTINUE
C
C     CALCULATE EPSILON
C
      EPS=0.
      DO 16 I=1,N
   16 EPS=EPS+CABS(A(1,I))
      DO 18 I=2,N
      SUM=0.
      IM1=I-1
      DO 17 J=IM1,N
   17 SUM=SUM+CABS(A(I,J))
   18 IF(SUM.GT.EPS)EPS=SUM
      EPS=SQRT(FLOAT(N))*EPS*1.E-12
      IF(EPS.EQ.0.)EPS=1.E-12
      DO 19 I=1,N
      DO 19 J=1,N
   19 H(I,J)=A(I,J)
   20 IF(N.NE.1)GO TO 21
      LAMBDA(M)=A(1,1)+SHIFT
      GO TO 137
   21 IF(N.EQ.2)GO TO 2
```

```
   22 MN1=M-N+1
      IF(REAL(A(N,N)).NE.0..OR.AIMAG(A(N,N)).NE.0.)
     1 IF(ABS(REAL(A(N,N-1)/A(N,N)))+ABS(AIMAG(A(N,N-1)/A(N,N)))-1.E-9)
     2 24,24,23
   23 IF(ABS(REAL(A(N,N-1)))+ABS(AIMAG(A(N,N-1))).GE.EPS)GO TO 25
   24 LAMBDA(MN1)=A(N,N)+SHIFT
      ICOUNT=0
      N=N-1
      GO TO 21
C
C     DETERMINE SHIFT
C
   25 SHIFT(2)=(A(N-1,N-1)+A(N,N)+CSQRT((A(N-1,N-1)+A(N,N))**2
     1 -4.*(A(N,N)*A(N-1,N-1)-A(N,N-1)*A(N-1,N))))/2.
      IF(REAL(SHIFT(2)).NE.0..OR.AIMAG(SHIFT(2)).NE.0.)GO TO 26
      SHIFT(3)=A(N-1,N-1)+A(N,N)
      GO TO 27
   26 SHIFT(3)=(A(N,N)*A(N-1,N-1)-A(N,N-1)*A(N-1,N))/SHIFT(2)
   27 IF(CABS(SHIFT(2)-A(N,N)).LT.CABS(SHIFT(3)-A(N,N)))GO TO 28
      INDEX=3
      GO TO 29
   28 INDEX=2
   29 IF(CABS(A(N-1,N-2)).GE.EPS)GO TO 30
      LAMBDA(MN1)=SHIFT(2)+SHIFT
      LAMBDA(MN1+1)=SHIFT(3)+SHIFT
      ICOUNT=0
      N=N-2
      GO TO 20
   30 SHIFT=SHIFT+SHIFT(INDEX)
      DO 31 I=1,N
   31 A(I,I)=A(I,I)-SHIFT(INDEX)
C
C     PERFORM GIVENS ROTATIONS, QR ITERATES
C
      IF(ICOUNT.LE.10)GO TO 32
      NCAL=M-N
      GO TO 137
   32 NM1=N-1
      TEMP1=A(1,1)
      TEMP2=A(2,1)
      DO 36 R=1,NM1
      RP1=R+1
      RHO=SQRT(REAL(TEMP1)**2+AIMAG(TEMP1)**2+
     1 REAL(TEMP2)**2+AIMAG(TEMP2)**2)
      IF(RHO.EQ.0.)GO TO 36
      COS=TEMP1/RHO
      SIN=TEMP2/RHO
      INDEX=MAX0(R-1,1)
      DO 33 I=INDEX,N
      TEMP=CONJG(COS)*A(R,I)+CONJG(SIN)*A(RP1,I)
      A(RP1,I)=-SIN*A(R,I)+COS*A(RP1,I)
   33 A(R,I)=TEMP
      TEMP1=A(RP1,RP1)
      TEMP2=A(R+2,R+1)
      DO 34 I=1,R
```

```
      TEMP=COS*A(I,R)+SIN*A(I,RP1)
      A(I,RP1)=-CONJG(SIN)*A(I,R)+CONJG(COS)*A(I,RP1)
   34 A(I,R)=TEMP
      INDEX=MIN0(R+2,N)
      DO 35 I=RP1,INDEX
      A(I,R)=SIN*A(I,RP1)
   35 A(I,RP1)=CONJG(COS)*A(I,RP1)
   36 CONTINUE
      ICOUNT=ICOUNT+1
      GO TO 22
C
C     ARRANGE EIGENVALUES ACCORDING TO DESCENDING ABSOLUTE VALUE
C
  137 NCALM = NCAL - 1
      DO 139 I = 1,NCALM
      TEMP  = LAMBDA(I)
      K = I
      L = I + 1
      DO 138 J = L,NCAL
      IF(CABS(TEMP).GE.CABS(LAMBDA(J))) GO TO 138
      TEMP = LAMBDA(J)
      K = J
  138 CONTINUE
      IF(K.EQ.I) GO TO 139
      LAMBDA(K) = LAMBDA(I)
      LAMBDA(I) = TEMP
  139 CONTINUE
C
C     CALCULATE VECTORS
C
   37 IF(NCAL.EQ.0)GO TO 57
      IF(IVEC.EQ.0) GO TO 57
      IF(IVEC.GT.NCAL) IVEC = NCAL
      N=M
      NM1=N-1
      IF(N.NE.2)GO TO 38
      EPS=AMAX1(CABS(LAMBDA(1)),CABS(LAMBDA(2)))*1.E-8
      IF(EPS.EQ.0.)EPS=1.E-12
      H(1,1)=A(1,1)
      H(1,2)=A(1,2)
      H(2,1)=A(2,1)
      H(2,2)=A(2,2)
   38 DO 56 L=1,IVEC
      DO 40 I=1,N
      DO 39 J=1,N
   39 HL(I,J)=H(I,J)
   40 HL(I,I)=HL(I,I)-LAMBDA(L)
      DO 44 I=1,NM1
      MULT(I)=0.
      INTH(I)=.FALSE.
      IP1=I+1
      IF(CABS(HL(I+1,I)).LE.CABS(HL(I,I)))GO TO 42
      INTH(I)=.TRUE.
      DO 41 J=I,N
      TEMP=HL(I+1,J)
```

```
      HL(I+1,J)=HL(I,J)
   41 HL(I,J)=TEMP
   42 IF(REAL(HL(I,I)).EQ.0..AND.AIMAG(HL(I,I)).EQ.0.)GO TO 44
      MULT(I)=-HL(I+1,I)/HL(I,I)
      DO 43 J=IP1,N
   43 HL(I+1,J)=HL(I+1,J)+MULT(I)*HL(I,J)
   44 CONTINUE
      DO 45 I=1,N
   45 VECT(I)=1.
      TWICE=.FALSE.
   46 IF(REAL(HL(N,N)).EQ.0..AND.AIMAG(HL(N,N)).EQ.0.)HL(N,N)=EPS
      VECT(N)=VECT(N)/HL(N,N)
      DO 48 I=1,NM1
      K=N-I
      DO 47 J=K,NM1
   47 VECT(K)=VECT(K)-HL(K,J+1)*VECT(J+1)
      IF(REAL(HL(K,K)).EQ.0..AND.AIMAG(HL(K,K)).EQ.0.)HL(K,K)=EPS
   48 VECT(K)=VECT(K)/HL(K,K)
      BIG=0.
      DO 49 I=1,N
      SUM=ABS(REAL(VECT(I)))+ABS(AIMAG(VECT(I)))
   49 IF(SUM.GT.BIG)BIG=SUM
      DO 50 I=1,N
   50 VECT(I)=VECT(I)/BIG
      IF(TWICE)GO TO 52
      DO 51 I=1,NM1
      IF(.NOT.INTH(I))GO TO 51
      TEMP=VECT(I)
      VECT(I)=VECT(I+1)
      VECT(I+1)=TEMP
   51 VECT(I+1)=VECT(I+1)+MULT(I)*VECT(I)
      TWICE=.TRUE.
      GO TO 46
   52 IF(N.EQ.2)GO TO 55
      NM2=N-2
      DO 54 I=1,NM2
      N1I=N-1-I
      NI1=N-I+1
      DO 53 J=NI1,N
   53 VECT(J)=H(J,N1I)*VECT(N1I+1)+VECT(J)
      INDEX=INT(N1I)
      TEMP=VECT(N1I+1)
      VECT(N1I+1)=VECT(INDEX)
   54 VECT(INDEX)=TEMP
   55 DO 56 I=1,N
   56 A(I,L)=VECT(I)
   57 RETURN
      END
```